DEVELOPMENT OF A NOVEL ANTIBACTERIAL PEPTIDE PAM-5 VIA COMBINATION OF PHAGE DISPLAY SELECTION AND COMPUTER-ASSISTED MODIFICATION

By

YUEN HAWK LEONG

A thesis submitted to the Department of Allied Health Sciences,
Faculty of Science,
Universiti Tunku Abdul Rahman,
in partial fulfillment of the requirements for the degree of
Doctor of Philosophy in Science
May 2020

ABSTRACT

**DEVELOPMENT OF AN NOVEL ANTIBACTERIAL PEPTIDE PAM-5
VIA COMBINATION OF PHAGE DISPLAY SELECTION AND
COMPUTER-ASSISTED MODIFICATION**

Yuen Hawk Leong

The rapid acquisition and dissemination of antibiotic-resistance among
pathogenic bacteria has been regarded as the major obstacle to effective
treatment of bacterial infections. Therefore, development of alternative
antibacterial agents is indeed an urgent need. Accumulating evidence have
strongly proposed that antibacterial peptides (ABPs) are potential alternative
antibacterial agents due to their unique features. However, isolation of these
compounds from natural resources can be tedious and the yield is not ensuing.
Moreover, certain natural ABPs were found toxic to mammalian cells, thus
restricting their clinical use. Therefore, the objective of this study was to develop
a potent ABP with minimal toxicity via phage-display selection followed by
computer-assisted modification. Briefly, a 12-mer phage-displayed peptide
library was used to identify peptides that bound to the cell surface of
Pseudomonas aeruginosa (*P. aeruginosa*) with high affinity. The affinity-
selected peptide with the highest selection frequency was modified to PAM-5
(KWKWRPLKRKLVLRM) with enhanced antibacterial features by using
online peptide database. Using *in vitro* microbroth dilution assay, PAM-5 was
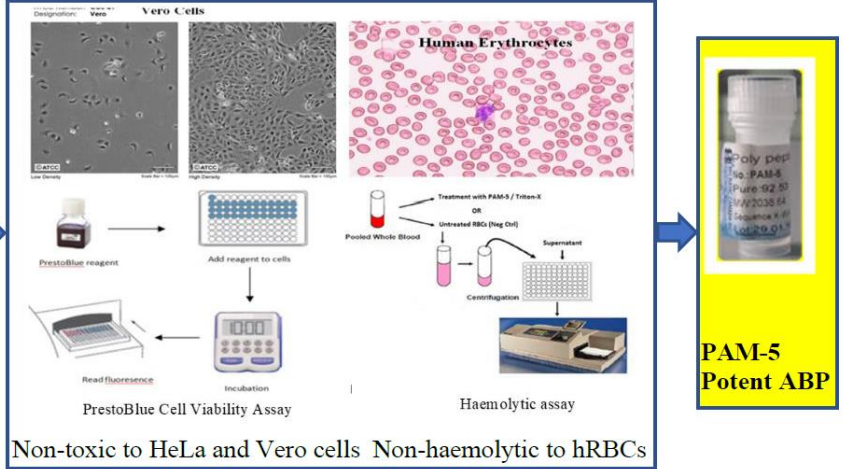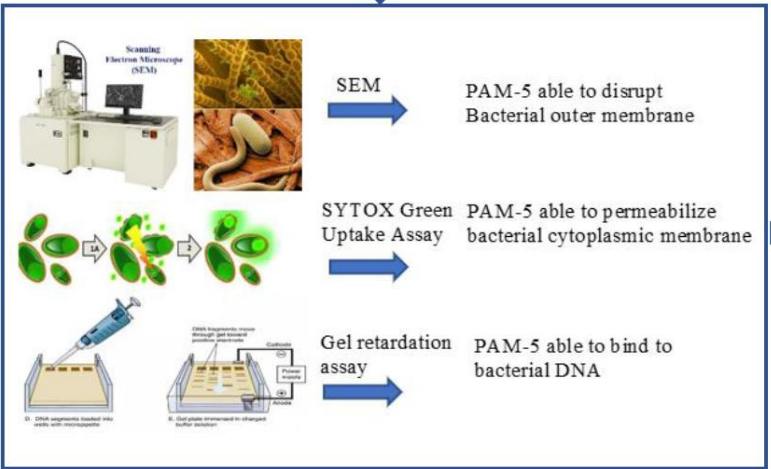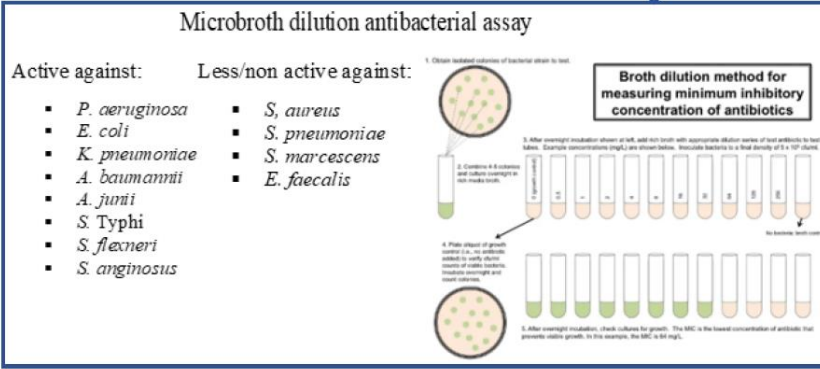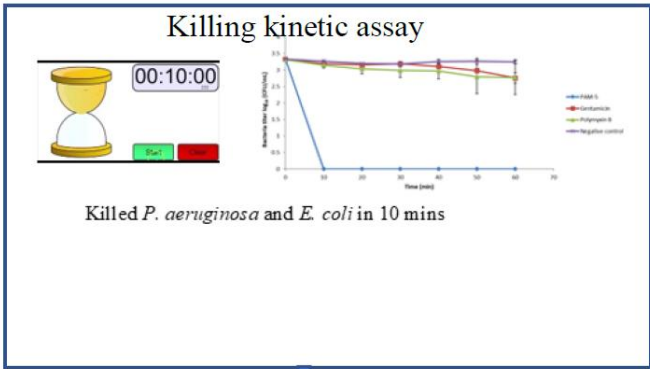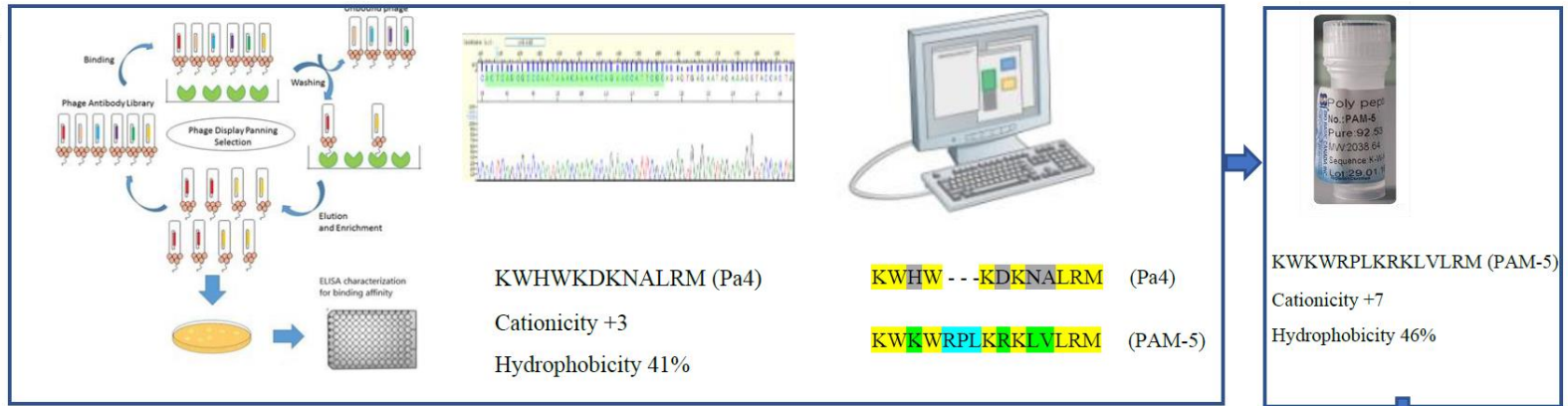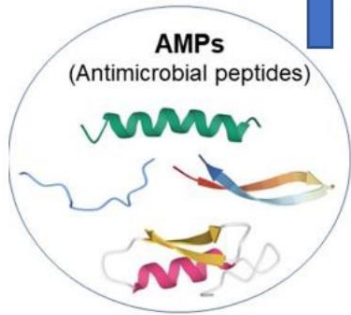shown active against a panel of Gram-negative bacteria and selected Gram-

positive bacteria. Interestingly, the peptide also exhibited similar bactericidal effect in *ex vivo* assay which was set up in human plasma. Scanning electron microscopy and SYTOX Green uptake assay revealed that PAM-5 was able to cause outer membrane disruption and inner membrane permeabilization to the bacteria, respectively. Additionally, the peptide was also able to bind to bacterial DNA as demonstrated by gel retardation assay. In time-kill assay, PAM-5 was shown able to cause complete bacterial elimination in 10 minutes. More importantly, PAM-5 was non-cytotoxic to Vero and HeLa cells and non-haemolytic to human erythrocytes at all concentrations tested for the antibacterial assays. Thus, this study showed that the combination of phage display screening and computer-assisted modification could be used to develop potent novel ABPs, and PAM-5 derived from these approaches is worth to be further elucidated for its potential clinical use.

ABSTRACT FLOWCHART

Emergence and dissemination of antibiotic-resistant bacteria

High morbidity and mortality rate of bacterial infections

Urgent need to explore new antibacterial agents with novel antibacterial mechanisms of action

AMPs (Antimicrobial peptides)

KWHWKDKNALRM (Pa4)
Cationicity +3
Hydrophobicity 41%

KWHW - - -KDKNALRM (Pa4)

KWKWRPLKRKLVLRM (PAM-5)

KWKWRPLKRKLVLRM (PAM-5)
Cationicity +7
Hydrophobicity 46%

Killing kinetic assay

00:10:00

Killed *P. aeruginosa* and *E. coli* in 10 mins

Microbroth dilution antibacterial assay

Active against:
- *P. aeruginosa*
- *E. coli*
- *K. pneumoniae*
- *A. baumannii*
- *A. junii*
- *S.* Typhi
- *S. flexneri*
- *S. anginosus*

Less/non active against:
- *S. aureus*
- *S. pneumoniae*
- *S. marcescens*
- *E. faecalis*

Broth dilution method for measuring minimum inhibitory concentration of antibiotics

SEM — PAM-5 able to disrupt Bacterial outer membrane

SYTOX Green Uptake Assay — PAM-5 able to permeabilize bacterial cytoplasmic membrane

Gel retardation assay — PAM-5 able to bind to bacterial DNA

PrestoBlue Cell Viability Assay   Haemolytic assay

Non-toxic to HeLa and Vero cells   Non-haemolytic to hRBCs

PAM-5 Potent ABP

iv

ACKNOWLEDGEMENT

First and foremost, I would like to express my sincere gratitude to my honourable supervisor, Dr. Kho Chiew Ling, for relentlessly supporting and imparting words of wisdom which had guided me well throughout the entire length of the research project from title's selection to thesis writing. I am truly humbled and thankful for all guidance, valuable advices and the endless inspiration that I have received.

Besides my supervisor, I would like to thank my project co-supervisor, Dr. Tan Gim Cheong for his patience, motivation and constructive suggestion that helped me to complete this project and thesis. His words had indeed incented me to widen my research from various perspectives.

I would like to deliver my sincere appreciation to the committee members of my work completion seminar: Dr. Sit Nam Weng, Dr. Eddy Cheah Seong Guan, and Dr Chee Huei Phing for their insightful comments and encouragement. Their recommendations for the corrective actions to my research were undoubtedly helpful to improve my thesis writing.

Furthermore, I would like to express my utmost gratitude to the laboratory officers Mr. Mr. Saravanan, Mr. Tie Shin Wei, Mr Gwee Siew Meng, Mr. Nicholas Ooh Keng Fei and Ms. Fatin for their valuable assistance in providing

technical support in terms of laboratory materials and instrumentation throughout the bench work during the entire project. Additionally, they had made my access simpler to the research facilities and laboratory. Without their support, it is impossible to obtain most of the important data for this study.

I would always remember my fellow labmates for the stimulating discussions, continuous moral supports and all the fun we have had in the last few years. Special thanks to Chan Szn Yi, Eveiyn Phoon Weng Yan, Ding Yi En, Ng Wei Nee, Tan Kai Xian, Lai Kah Nyin, Tham Mun Wei and Gwee Chin Piaw who have been working relentlessly with me for many sleepless nights to achieve numerous objectives before deadlines throughout these years. You all had shown me the important meaning of teamwork.

Lastly, I would like to convey my sincere gratitude towards my beloved parents and family for their unconditional love, patience and faith throughout the entire journey. They have been giving me enough moral support, encouragement and motivation to accomplish my personal goals so that I only pay attention to the studies without any obstacle on the way. Without them, I'm nothing. Thank you.

DECLARATION

I hereby declare that the dissertation is based on my original work except for quotations and citations which have been duly acknowledged. I also declare that it has not been previously or concurrently submitted for any other degree at UTAR or other institutions.

Name _Yuen Hawk Leong_

Date ____27 May 2020___

APPROVAL SHEET

This dissertation/thesis entitled "**DEVELOPMENT OF A NOVEL ANTIBACTERIAL PEPTIDE PAM-5 VIA COMBINATION OF PHAGE DISPLAY SELECTION AND COMPUTER-ASSISTED MODIFICATION"** was prepared by YUEN HAWK LEONG and submitted as partial fulfillment of the requirements for the degree of Doctor of Philosophy in Science at Universiti Tunku Abdul Rahman.

Approved by:

_____
(Dr. KHO CHIEW LING)   Date:…………………..
Supervisor
Department of Biological Science
Faculty of Science
Universiti Tunku Abdul Rahman

_____
(Dr. TAN GIM CHEONG)   Date:…………………..
Co-supervisor
Department of Allied Health Sciences
Faculty of Science
Universiti Tunku Abdul Rahman

TABLE OF CONTENTS

xiv

LIST OF TABLES

LIST OF FIGURES

LIST OF ABBREVIATIONS/GLOSSARY OF TERMS

A	Alanine
ABPs	Antibacterial peptides
ABTS	2,2'-azino-bis (3-ethylbenzothiazoline-6-sulfonic acid) diammonium
AFPs	Antifungal peptides
AMPs	Antimicrobial peptides
AMR	Antimicrobial Resistance
APD	Antimicrobial Peptide Database
APPs	Anti-parasitic peptides
APtPs	Anti-protist peptides
ATCC	American Type Culture Collection
AVPs	Antiviral peptides
BA	Blood agar
BF	Bright field
BHI	Brain-Heart Infusion
BSA	Bovine serum albumin
CDC	Centers for Disease Control and Prevention
CFU	Colony forming unit
CL	Cardiolipin
CLSI	Clinical and Laboratory Standard Institute
CO_2	Carbon dioxide
CRE	Carbapenem-resistant enterobacterioceae
CTAB	Cetyl trimethylammonium bromide

D	Aspartic acid
DF	Dark field
diSC3(5)	3,3′ -dipropylthiadicarbocyanine iodide
DMEM	Dulbecco's Modified Eagle's Medium
DMSO	Dimethyl sulfoxide
DNA	Deoxyribonucleic acid
DPBS	Dulbecco's phosphate-buffered saline
EDTA	Ethylenediaminetetraacetic acid
ELISA	Enzyme-linked immunosorbent assay
EMSA	Electrophoretic mobility shift assay
ESBL	Extended-spectrum beta lactamases
EtBr	Ethidium bromide
F	Phenylalanine
FBS	Fetal bovine serum
FITC	Fluorescein isothiocyanate
G	Glycine
g	Gravitational constant
GAS	Group A streptococcus
GP	General practitioner
H	Histidine
HBD-3	Human β-defensin-3
HCl	Hydrochloric acid
HDPs	Host defence peptides
HNPs	Human neutrophil peptides
H$_2$O$_2$	Hydrogen peroxide

hRBCs	human red blood cells
HRP	Horse-radish peroxidase
HTS	High-throughput screening
I	Isoleucine
ICUs	Intensive care units
IDRs	Innate defence regulators
IPTG	Isopropyl β-d-1-thiogalactopyranoside
K	Lysine
L	Leucine
LB	Luria-Bertani
LPS	Lipopolysaccharide
LTA	Lipoteichoic acid
M	Methionine
MBC	Minimum Bactericidal Concentration
MDR	Multidrug-resistant
MH	Mueller-Hinton
MIC	Minimum Inhibitory Concentration
MRSA	Methicillin-resistance *Staphylococcus aureus*
mRNA	messenger ribonucleic acid
MSA	Mennitol-salt agar
MTT	3-(4,5-dimethylthiazol-2-yl)-2,5-diphenyltetrazolium bromide
N	Asparagine
NaCl	Sodium chloride
NADH	Nicotinamide adenine dinucleotide + hydrogen
NaHCO₃	Sodium bicarbonate

NaI	Sodium iodide
NaN$_3$	Sodium azide
NEB	New England Biolabs
NMR	Nuclear magnetic resonance
OD	Optical density
OMPs	Outer membrane proteins
P	Proline
PBPs	Penicillin-binding proteins
PBS	Phosphate-buffered saline
PC	Phosphatidylcholine
PDR	Pandrug-resistant
PE	Phosphatidylethanolamine
PEG	Polyethylene glycol
PFU	Plaque forming unit
PG	Phosphatidylglycerol
PrAMPs	Proline-rich antimicrobial peptides
PS	Phosphatidylserine
R	Arginine
RBCs	Red blood cells
RFU	Relative fluorescence unit
RNA	Ribonucleic acid
RP-HPLC	Reverse-phase high-performance liquid chromatography
rpm	Rotation per minute
rRNA	Ribosomal ribonucleic acid
S	Serine

Sak	Staphylokinase
SD	Standard deviation
SDS	Sodium dodecyl sulfate
SEM	Scanning electron microscope/microscopy
SM	Sphingomyelin
T	Threonine
TA	Teichoic acid
TAE	Tris-acetate-EDTA
TBS	Tris-buffered saline
TBST	Tris-buffered saline supplemented with TWEEN-20
TE	Tris-EDTA
TNF	Tumor necrosis factor
TSA	Tryptic Soy agar
UV	Ultraviolet
V	Valine
v/v	Volume over volume
VRE	Vancomycin-resistant enterococci
VRSA	Vancomycin-resistant *Staphylococcus aureus*
W	Tryptophan
WHO	World Health Organization
w/v	Weight over volume
XDR	Extensively drug-resistant
Xgal	5-bromo-4-chloro-3-indolyl-β-D-galactopyranoside

CHAPTER 1

INTRODUCTION

The initial availability of antibiotics in the era of 1940s was unarguably one of the greatest achievements in modern medicine, which leads to the drastic reduction of mortality rate caused by bacterial infections (Spellberg and Gilbert, 2014). However, shortly thereafter, the spread of antibiotic-resistance had substantially become a clinical problem. Despite the efforts by many researchers, clinician and pharmaceutical industries to discover, develop and deploy new antibiotics in order to counterstrike the issue, new phenotypes of antibiotic-resistance and multidrug-resistance continued to emerge and spread globally due to unwarranted use of these compounds. Even though repeating cycles of the above-mentioned efforts were carried out to introduce more new antibiotics from the late 1960s until early 1980s, the threat of antibiotic-resistance has never ceased. Different types of multidrug-resistance such as methicillin-resistance *Staphylococcus aureus* (MRSA), vancomycin-resistant enterococci (VRE), extended-spectrum beta lactamases (ESBL)-producing bacteria and carbapenem-resistant enterobacterioceae (CRE) continue to emerge and responsible for causing unbearable clinical and financial burden to healthcare system, patients and their families (Centers for Disease Control and Prevention, 2013; Lushniak, 2014, Rossolini et al., 2014). The rapid dissemination of these resistant bacteria has raised the concern about sustainability of conventional antibiotics in combating bacterial infections, especially in recent years where new antibiotic development is no longer a major

investment by many pharmaceutical industries (Rossolini et al., 2014; Viswanathan, 2014). In consideration of the crisis that may possibly lead to a post-antibiotic era, alternative antibacterial agents that work in novel mechanisms are seriously needed to complement or even replace the conventional antibiotics that are easily compromised by bacterial resistance. Among the potential antibacterial agents that are understudied, antibacterial peptides (ABPs) are gaining considerable research attention in consideration of their strength and advantages over the others (Bahar and Ren, 2013; Mahlapuu et al., 2016; Rončević, Puizina and Tossi, 2019).

Since their first discovery in 1938, ABPs have been extensively studied by many research groups due to numerous breakthrough features which raise optimism on their potential use as alternative or complementary medicine to conventional antibiotics against bacterial infections. Initially recognized as the host defence peptides (HDPs), ABPs were found as part of the immune defence elements in many organisms encompassing bacteria, viruses, plant, mammals and humans (Zhang and Gallo, 2016; Sun et al., 2018). As the name implies, these compounds are peptides that possess antibacterial activity towards many bacteria. Accumulating findings on ABPs revealed that these peptides inhibit or kill their target bacteria by means which are distinct from the conventional antibiotics, thereby reducing the risk of inducible resistance from bacteria exposed to the peptide stress (Wang et al., 2016; Lei et al., 2019). More importantly, the actions of many ABPs are not limited to direct inhibitory or killing of the bacteria, but also include immunomodulatory properties that enhance host immune system to fight against the bacteria (Yeung, Gellatly and

Hancock, 2011; Fjell et al., 2012). These remarkable findings clearly suggested that ABPs are interesting compounds to be further studied and developed into novel antibacterial agents.

Pioneer studies on ABPs mainly focused on the isolation of these compounds from natural resources followed by screening for their antibacterial effects (Ayaad, Shaker and Almuhnaa, 2012; Rončević, Puizina and Tossi, 2019). A large repertoire of these natural ABPs were shown active against many pathogenic bacteria and many of them were documented in Antimicrobial Peptide Database (APD, http://aps.unmc.edu/AP/database/antiB.php). However, the number of these ABPs which successfully made it to preclinical or clinical trials is limited due to incomprehensive studies and potential toxicity to host or mammalian cells (Falagas and Kasiakou, 2006; Matsuzaki, 2009; Takahashi et al., 2010; Seo et al., 2012), which set a major drawback to these biological compounds. Therefore, it is crucial to produce an ABP with high therapeutic index, in which the agent not only must demonstrate potent antibacterial effects to the pathogens, but also possess minimal toxicity to host or mammalian cells.

In order to achieve this goal, alternative strategies can be considered to yield ABPs which are selectively against bacteria but not human or mammalian cells. Among these, phage-display selection of peptides with antibacterial activities has been employed by several research groups for drug discovery, including search for ABPs that act exclusively on bacteria (Tanaka, Kokuryu and

Matsunaga, 2008; Bishop-Hurley, Rea and McSweeney, 2010; Sainath Rao, Mohan and Atreya, 2013). Using this high throughput screening method, multiple peptide candidates that bind to a bacterial ligand can be affinity-selected from a phage-displayed peptide library of large peptide diversity through a process called biopanning. After ensuring their binding selectivity to the bacterium, genomic DNAs are extracted for sequencing to determine the oligonucleotide insert sequence that encodes the displayed peptide. Finally, linear free peptide can be synthesized chemically based on the sequence of the phage-displayed peptide for further antibacterial evaluation (New England Biolabs). This method offers the simplest high throughput screening for bacterial-binding peptides if the bacteria is used as the panning target, thereby precluding the risk of yielding peptides that interact with mammalian cells with high affinity. More importantly, by using computational tool such as online peptide prediction and calculation software, the affinity-selected peptides can be subjected to rational modification via amino acid substitution or length reduction/elongation in order to improve antibacterial potency and peptide stability as well as reducing toxicity/haemolytic effect to mammalian cells.

In consideration of the feasibility of this method, phage display selection was used to screen and select for peptide/s with potent antibacterial properties in this study. This method began with biopanning of random phage-displayed peptide library against *Pseudomonas aeruginosa* ATCC 27853, followed by rational modification of the selected peptides using online peptide calculation and prediction tool in order to improve their antibacterial features. The modified peptide was screened for its antibacterial potency towards the target bacterium

4

of biopanning, *P. aeruginosa* ATCC 27853, as well as a panel of pathogenic bacteria from reference and clinical strains, encompassing both Gram-negative and Gram-positive bacteria using microbroth dilution assay.

In order to access its stability in plasma, the peptide was screened for its potency towards a bacterium between *in vitro* and *ex vivo* conditions of microbroth dilution assays, and the minimal inhibitory concentration (MIC) and/or minimal bactericidal concentration (MBC) against the bacterium between these two conditions was/were compared.

Next, the killing kinetic of the peptide was estimated by determining the duration of time required by the peptide to kill its target bacteria completely via time kill assay. Besides, the killing kinetic of the peptide was also compared to selected antibiotics.

Understanding on the mechanism of action by the antibacterial peptide may provide crucial information for development of a novel alternative therapeutic agent that work in different ways than conventional antibiotics to inhibit or kill the bacteria. Therefore, after ensuring its antibacterial potency, the mechanistic action of the peptide was further evaluated by screening for its ability to cause outer membrane disruption. Using scanning electron microscopy, peptide-treated bacteria were examined for any morphological and structural changes as compared to the untreated bacteria. Next, SYTOX Green uptake assay was carried out to screen for its ability to cause inner membrane permeabilization.

In order to explore its additional intracellular mechanism on the target bacteria, gel retardation assay was conducted to study the ability of the peptide to bind bacterial nucleic acids.

Having a strong antibacterial potency may not conclusively justify its clinical application without sufficient information on its potential toxicity to mammalian cells. Therefore, the peptide was screened for its cytoxicity towards HeLa cells and Vero cells by PrestoBlue cell viability assay. Additionally, the peptide was also screened for its haemolytic effect towards human red blood cells via *in vitro* haemolytic assay. The preliminary findings of these toxicity studies may justify the therapeutic potential of this peptide before proceeding for further future pre-clinical and clinical studies.

In summary, the objectives of this study are:

1. Developing an ABP via phage display selection from a phage displayed-peptide library, followed by rational modification using online databadse prediction to enhance its antibacterial characteristics.

2. Screening for antibacterial effect by determining the minimal bacteriostatic concentration (MIC) and/or minimal bactericidal concentration (MBC) of the peptide against a panel of bacteria encompassing Gram-positive and Gram-negative bacteria of both reference and clinical isolates via *in vitro* microbroth dilution assay.

3. Determination of the peptide stability by comparing the minimum bactericidal concentration of the peptide against *P. aeruginosa* between *in vitro* and *ex vivo* antibacterial assay.

4. Determination of killing kinetic of the developed peptide against selected bacteria by using time kill assay. The killing kinetics between the peptide and selected antibiotics were compared.

5. Determining the mechanisms of action of the peptide towards selected bacteria, encompassing screening for outer membrane disruption by scanning electron microscopy, inner membrane permeabilization via SYTOX Green uptake assay and DNA-binding via gel retardation assay.

6. Screening for toxicity of the peptide towards HeLa cells and Vero cells via PrestoBlue cell viability assay, as well as hemolytic effect towards human erythrocytes using hemolytic assay.

CHAPTER 2

LITERATURE REVIEW

2.1 Antibiotic Resistance

2.1.1 Overview of Antibiotic Resistance

The discovery of penicillin by Sir Alexander Fleming in 1928 is regarded as one of the greatest contributions in modern medicine, which eventually opened the era of antibiotic chemotherapy against bacterial infections that saved millions of lives (Piddock, 2012; Sengupta, Chattopadhyay and Grossart, 2013). Since then, antibiotics were mass produced and used to treat, control and prevent dissemination of bacterial infections (Aminov, 2010). Many new classes of antibiotics were discovered from natural sources or chemically synthesized by pharmaceutical companies during the golden age of antibiotics, resulting in significant reduction of mortality rate of bacterial infections among human population (Fair and Tor, 2014).

Nevertheless, despite the early optimism on the potency of antibiotics in controlling bacterial infectious diseases, the occurrence of antibiotic-resistant bacteria had prompted scientists and clinicians to the fact that this antibacterial agent is not absolutely invincible. With the first case of penicillin-resistant *Staphylococcus* reported in 1940 (Centers for Disease Control and Prevention, 2013), resistance has later been observed against nearly all antibiotics available

in clinical setting. Despite the early efforts of introducing more novel or improved versions of antibiotics between 1960s and 1980s, the resistance problem could hardly be controlled or preventable (Spellberg and Gilbert, 2014).

2.1.2   Causes and Challenges of Antibiotic Resistance

Several factors are reported to account for the emerging and spread of antibiotic -resistant bacteria. Among these, inappropriate prescription of antibiotics by clinician for empiric treatment appears to be the most common factor for the rise of this medical issue. This was supported by studies reporting that 30% to 50% of bacterial infectious cases were mistreated due to incorrect treatment indication, choices of antibiotics and duration of therapy (Centers for Disease Control and Prevention, 2013; Luyt, 2014). A study by the Public Health England (PHE) reported that approximately 20% of all antibiotic prescription by general practitioner (GP) in primary care are inappropriate or unnecessary, where the infections are more commonly due to viruses (Kmietowicz, 2018).

Even though the antibiotics are correctly prescribed, poor patient compliance in consuming the antibiotics is another key driver for the spread of antibiotic resistance. A global multivariate analysis revealed that 22.3% of patients prescribed with antibiotics did not consume the compounds according to the correct dosage and duration (Pechere et al., 2007). These poor compliances may have serious negative impact on the clinical outcome of antibacterial therapy, such as delayed clearance of infectious agent and recovery, followed by prolonged treatment. Worse, the sub-therapeutic antibiotic concentration due to

irregular or discontinued dosing is the major risk that promotes stress-induced genetic alterations that confers antibiotic resistance to the surviving bacteria. As reported by Viswanathan (2014), insufficient or sub-inhibitory concentrations of certain antibiotics had been shown to induce broad proteomic changes and strain diversifications, which eventually confer resistance to certain bacteria such as *Pseudomonas aeruginosa* and *Bacteroides fragilis*.

Apart from that, overuse of antibiotics in agricultural livestock is another reason that further worsen the issue of antibiotic resistance. In both developed and developing countries, antibiotics are used as growth supplement primarily to promote growth and prevent infections in livestock (Gross, 2013; Spellberg and Gilbert, 2014). However, these practices may indeliberately promote and transmit resistant bacteria from the fed animal to human via food chain (Verraes et al., 2013). Antibiotics given to the animals may kill susceptible bacteria but not the resistant strains. Subsequently, these resistant bacteria are transmitted to human through meat consumption, which leads to infections that are difficult to be treated.

Besides, the diagnostic procedure applied in many clinical laboratories could be another factor for the rapid spread of antibiotic-resistance. Most laboratories of clinical microbiology have begun to replace the time-consuming and painstakingly manual method in bacterial identification and antibiotic susceptibility profiling with automated systems, for instance, VITEK® 2 System. Under these systems, the isolated bacteria from the clinical samples are tested

with graduated dilutions of drugs, which can produce result of antibiotic-susceptibility in hours (Pincus, 2014). However, these tests were criticized for yielding misleading results that cause physicians to prescribe doses or types of antibiotics that are not only failed to cure the infections but promote the occurrence of drug-resistant bacteria. According to a study conducted by Joyanes et al. (2001) on the evaluation of VITEX 2 system, one of the major limitations of the automated system was its inability to provide the reading of minimal inhibitory concentrations (MICs) for certain bacteria. Meanwhile, discrepancies in certain bacterial antibiotic susceptibility profiles derived from manual microbroth dilution assay and VITEX 2 system were also reported (Bobenchik et al., 2014). These shortcomings may impede the appropriate antibiotic prescription to patients suffering from certain bacterial infections. Consequently, resistant bacteria in the patients are not eliminated but continue to spread via nosocomial or/and community-acquired infections.

In worse scenario, the development of new antibiotics by pharmaceutical companies seems to come to a deadlock. Other than modifications or improvements to the pre-existing classes of antibiotics, there was no new class of antibiotics with novel antibacterial mechanism being introduced from pharmaceutical industry to address the drug-resistant infections since 2003 (Conly and Johnston, 2005; Ventola, 2015). This is because antibiotic development is no longer considered to be an investment with profitable return. Out of the 18 largest pharmaceutical companies in the world, only Merck, Roche, GlaxoSmithKline, and Pfizer continue to research on potential new antibiotics (Infectious Diseases Society of America, 2010). In fact, the

investment and efforts of developing a new antibiotic by pharmaceutical company does not seem to be comparably remunerative as compared to other drugs with higher and longer demand, such as cholesterol-lowering agents, drugs for hypertension, diabetes, psychiatric disorders and other metabolic illnesses of chronic conditions (Piddock, 2012; Gould and Bal, 2013; Wright, 2014). As compared to the latter, antibiotics are generally needed for short courses of treatment that last 5 to 7 days (Gould and Bal, 2013). Moreover, as a result of strict policy in antibiotic prescription, physicians are sparingly using the most powerful antibiotics to control the occurrence of drug-resistant bacteria (Özgenç, 2016). These factors resulted in slow demand for antibiotics that may have costed huge amount of investment for research and development of the drugs by pharmaceutical industries. More tragically, the race between antibiotic development and evolution of resistance is always dominated by the latter. The development of a new antibiotic may take several years or even longer from the stage of prototype development to clinical trials followed by regulatory approval by governing authority (Simpkin et al., 2017). Ironically, as documented in many literature and scientific reports, bacteria that survived an antibiotic pressure usually take only hours to days to mutate and acquire resistance to the antibiotic (Martinez and Baquero, 2000; Braine, 2011; Jorth et al., 2017; Sanz-García, Hernando-Amado, and Martínez, 2018). Therefore, the clinical efficacy of a new class of antibiotic with novel mechanism of action usually does not last long due to the rapid counter response from bacterial strains exposed to the antibiotic. Consequently, pharmaceutical industry that had put in significant investment in antibiotic development may not be rewarded with sustainable

return. From the business perspective, this low-returned, non-lucrative profit may not sustain commercial viability and does not worth for further investment.

2.1.3   Trends of Antibiotic Resistance

As described in the previous sections, antibiotic resistance is a multifactorial issue. In other words, overcoming this medical problem requires the compliances and coordinated efforts from various parties (e.g. general practitioners, patients, laboratories, farmers, etc.) under a regulated standardized protocol, which seems difficult to be achieved. Failure to control the usage of antibiotics, therefore, has driven the evolution of resistance, leading to the rise of bacteria with different degrees and phenotypes of resistance to the conventional antibiotics used today (Read and Woods, 2014). In fact, the threat of antibiotic-resistance is progressively alarming with the increasing prevalence and incidence of resistance under various categories, which include drug-resistant, multidrug-resistant (MDR), extensively drug-resistant (XDR) and pandrug-resistant (PDR) (Magiorakos et al., 2012; Basak, Singh and Rajurkar, 2016). Several bacteria are notorious for their high probability and frequencies of acquiring drug- or multidrug-resistance in clinical setting. These bacteria, which are known as ESKAPE pathogens, encompass *Enterococcus faecium* (*E. faecium*), *Staphylococcus aureus* (*S. aureus*), *Klebsiella pneumoniae* (*K. pneumoniae*), *Acinetobacter baumannii* (*A. baumannii*), *Pseudomonas aeruginosa* (*P. aeruginosa*), and *Enterobacter* species (Rice, 2010; Pendleton, Gorman and Gilmore, 2013; Santajit and Indrawattana, 2016). The common resistant profiles acquired by these bacteria include methicillin-resistant *S.*

aureus (MRSA), vancomycin-resistant *S. aureus* (VRSA), vancomycin-resistant Enterococci (VRE), extended-spectrum beta-lactamases (ESBL)-producing *K. pneumoniae* and *E. coli*, and carbapenem-resistant Enterobacteriaceae (CREs). In particular, CREs are commonly regarded as "superbug" due to their ability to compromise the most powerful class of antibiotics, namely carbapenems (Kelly, Mathema and Larson, 2017). With the resistance to this last resort of treatment, infections with these nasty pathogens are usually associated with inadequate and delayed antibacterial treatment, leading to poor prognosis and high mortality rate (Ibrahim et al., 2000; Anderson et al., 2006). According to a study, the mortality rate for infections with CREs had risen to 50% due to the lack of alternative treatment (van Duin et al., 2013). More recently, a systemic meta-analysis had demonstrated that patients with CREs are usually associated with two to three-fold higher mortality rate as compared to patients with carbapenem-susceptible Enterobacteriaceae (CSE) (Martin et al., 2018).

Apart from Enterobacteriaceae, carbapenem-resistance was also found in other bacteria. The genes encoding this resistant phenotype is transferable and was shown to be disseminated worldwide in other bacteria which include *P. aeruginosa* and *A. baumannii* (Sarı, Biçmen and Gülay. 2013; Potron, Poirel and Nordmann, 2015). Despite the warning from the World Health Organization (WHO) on the overuse of antibiotics, these superbugs are still spreading rapidly causing sporadic outbreaks in different regions in the world (Cullen, 2018, Gulland, 2018; Keogh, 2018; Payne, 2018).

According to Clinical Laboratory Standard Institute (CLSI), a bacterium with resistance to one class of antibiotics is also commonly associated with cross-resistance to other classes of antibiotics. This statement was derived from several studies on cross-resistance in several bacteria. In a study by Chen et al. (2009), *E. coli* treated with sub-lethal kanamycin was able to develop cross-resistance towards streptomycin, tetracycline and ampicillin. As the results of cross-resistance, the choices of effective antibiotics available to treat these bacterial infections are getting limited, leading to higher mortality rate. Even though strict policies on antibiotic prescription are implemented in healthcare system, the development of resistance among pathogenic bacteria is evolutionary inevitable. In 2014, WHO had warned the world about the possibility of "post-antibiotic era", in which death can be caused by common bacterial infections where no effective antibiotics are available against these infections. According to the Review of Antimicrobial Resistance (AMR) reported by Jim O'Neill in 2014, if there is no serious action to be taken against this medical issue, the global death toll caused by resistant bacteria could reach 10 million by 2050. As shown in **Figure 2.1**, of this projected figure, the highest death toll is estimated to occur in Asian countries, possibly due to the higher population in this region.
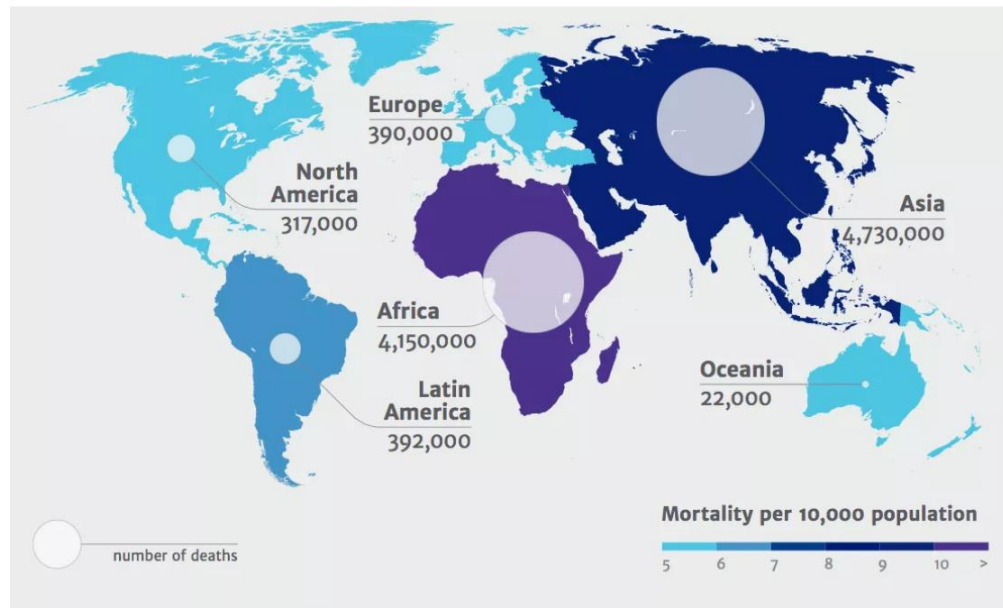
Figure 2.1: Estimated deaths attributable to AMR by 2050 (via the Review on Antimicrobial Resistance by Jim O'Neill, 2014).

2.1.4   Limitations of Classical Antibiotics

Although antibiotic-resistance is always associated with uncontrolled use of the compounds in healthcare setting and agriculture livestock, the intrinsic limitations of the drugs may also compromise their efficacy and potency towards their target bacteria. These limitations must be given considerations as they are of equal significant to the extrinsic factors as mentioned above in promoting resistant bacteria.

2.1.4.1 Use of Narrow Spectrum Antibiotics

Among all the classes of conventional antibiotics commonly used in the clinical settings, almost half of them are narrow spectrums, in which they are only active

against a specific group of bacteria. For instance, penicillin, first and second generations of cephalosporins and glycopeptides are usually only active against Gram-positive bacteria, while monobactams are only active against Gram-negative bacteria (Werth, 2018). Aminoglycosides, as exemplified by gentamicin, amikacin and neomycin, are only effective against aerobic bacteria due to the requirement of active transport of these antibiotics across the cell membrane before targeting the ribosomes (Mingeot-Leclercq, Glupczynski, and Tulkens, 1999). The ideal practice in prescription of these antibiotics requires prior identification of bacterial agents that cause the infections, which could only be carried out via culture and sensitivity procedures in big scale healthcare settings such as hospitals or medical centres. In smaller or community clinics where these procedures are uncommon, this spectrum limitation is always associated with difficulty in deciding the suitable antibacterial therapy. Common practice of antibiotic prescription is usually carried out empirically by doctors without identifying the pathogen and its corresponding antibiotic susceptibility profile (Leekha et al., 2011). Consequently, inappropriate antibiotic prescription is common in this scenario and this may promote the incidence of resistant bacteria (Centers for Disease Control and Prevention, 2013). Even though in well-equipped healthcare settings, empiric treatment is a common practice especially for patients of serious condition who may be prescribed with antibiotics before the diagnosis from culture and sensitivity is completed. This may occur in patients with primary immunodeficiency or chemotherapy-mediated immunodeficiency, where the patients are prone to opportunistic infections by more than one type of bacterium. In this situation, choosing a wrong antibiotic of limited spectrum may not ease the patient's condition, but

instead may increase the risk of selecting more drug-resistant bacteria. Although broad-spectrum antibiotics are available, but they are prescribed at the risk of promoting more powerful drug-resistant bacteria (e.g. multidrug-resistant, pan-resistant bacteria). According to a study, majority of broad spectrum antibiotics prescribed in intensive care units (ICUs) were either inappropriate, unnecessary, or suboptimal (Luyt et al., 2014), which explains the high prevalence and incidence of drug-resistant bacteria in hospital settings.

2.1.4.2 Slow Antibacterial Kinetics

Most of the classical antibiotics execute their bacteriostatic or bactericidal actions at slow kinetic manner. As documented in several time-kill kinetic studies, upon initiating antibiotic treatment, complete bacterial clearance only can be achieved after hours or even days. In a study by Mohamed et al. (2016), vancomycin required 24 hours to kill methicillin-resistant *S. aureus* (MRSA) completely, while ciprofloxacin and linezolid took even longer to achieve that. An earlier study by Johnson and Levin (2013) showed that ciprofloxacin, gentamicin, oxacillin and vancomycin took more than 22 hours to kill *S. aureus*. Meanwhile, Mahmoud and colleagues (2012) demonstrated that amikacin, levofloxacin and tetracycline failed to kill *P. aeruginosa* completely even though after 24 hours of treatment. Along with other reports, it is clearly evidenced that classical antibiotics require a long duration (from hours to days) to eliminate their target bacteria. On the other hand, the doubling time for majority of cultivable bacteria ranges from approximately 15 minutes to 1 hour (Todar, 2013). In each doubling time, the bacteria will reproduce and evolve

rapidly in response to the microenvironmental changes or stresses. Bacteria that survived the antibiotic treatment could possibly undergo gene mutation or acquire plasmid-mediated resistance from other bacteria to resist the actions from the antibiotics (Pray, 2008). Thus, the short generation time may allow the bacteria to acquire resistance before they are completely killed by the slow acting antibiotics.

2.1.4.3 Site Restriction of Antibiotic Action

Several classes of antibiotics inhibit or kill their target bacteria by disrupting the intracellular components or metabolic activities in the bacteria. This means the effectiveness of these antibiotics is depending on their ability to penetrate or translocate across the bacterial membrane which usually serves as the first barrier to the compounds. However, a number of bacteria possess natural or intrinsic resistance to these antibiotics by altering the membrane permeability to block the entry of the drugs. In Gram-negative bacteria, the outer membrane represents the most important barrier that blocks the entry of many foreign molecules, including antibiotics. One of the major components in the outer membrane is lipopolysaccharide (LPS), which is the intermediate target binding site for certain antibiotics before facilitating their uptake into the Gram-negative bacteria (Peterson, Hancock and McGroarty, 1985). Several bacteria were found able to alter this membrane constituent in order to reduce the binding affinity by antibiotics such as polymyxin and aminoglycosides, rendering them unable to be taken into the cell (Groisman, Kayser and Soncini, 1997; Macfarlane, et al., 1999; Macfarlane, Kwasnicka and Hancock, 2000). On the other hand,

quinolones, tetracycline and chloramphenicol that act intracellularly utilize certain membrane transporters such as porins to reach the bacterial cytoplasm before disrupting intracellular components (Chopra and Roberts, 2001; Delcour, 2008; Nikaido and Page`s, 2012). However, several bacteria are able to inactivate or reduce the expression of these transporters, thus reducing the entry and intracellular accumulation of these antibiotics (Mortimer and Piddock, 1993; Nikaido and Page`s, 2012). Furthermore, many Gram-negative bacteria, for instance, *P. aeruginosa*, *E. coli* and *Stenotrophomonas maltophilia* (*S. maltophilia*), are equipped with multidrug efflux pumps that are able to extrude various compounds or substrates out of the cell, including antibiotics. Consequently, the intracellular concentrations of these antibiotics are insufficient to execute the necessary antibacterial action (Blair and Piddock, 2009; Martinez, et al., 2009; Nikaido and Takatsuka, 2009).

Collectively, with the presence of these resistant mechanisms which reduce the membrane permeability to those intracellularly active antibiotics, the bacterial susceptibility to these antibiotics is reduced. Since more than half of the currently available antibiotics are targeting different intracellular components or activities such as ribosomes, DNA and RNA synthesis as well as mycolic or folic acid synthesis (Carryn et al., 2003), coupled with the fact that many Gram-positive and Gram-negative bacteria possess these resistant mechanisms (Bambeke, Balzi and Tulkens, 2000), the choices of effective antibiotics against the evolving nastier bacteria are getting limited.

2.1.4.4 Specific and Limited Target of Action

The most major drawback of classical antibiotics that limits their antibacterial efficacy is the specific drug-target interaction. The inhibitory or killing actions of many antibiotics are usually initiated by certain physical interaction between the drug molecules and their corresponding specific bacterial ligand, which could be either proteins which are essential for cell wall biosynthesis (Grundmann et al., 2006; Džidic, Šuškovic and Kos, 2008), enzyme for DNA replication (Higgins, Fluit and Schmitz, 2003, Drlica et al., 2008), DNA and RNA for transcription and translation (Floss and Yu, 2005) or ribosomal units that are involved in protein synthesis (Katz and Ashley, 2005; Mukhtar and Wright, 2005). Upon interacting with these ligands, the normal metabolic and enzymatic activities of the bacteria will be affected at biochemical, molecular or ultrastructural levels, followed by cell death. It is well characterized that most of the antibiotics only interact with single target site of the bacteria to exert their antibacterial action (Kohanski, Dwyer and Collins, 2010; Peach et al., 2013; Khan, 2018). In fact, the actions on these specific bacterial targets serve as the basis for the classification of antibiotics. However, this specific targeted action, conversely, might turn out to be a drawback of the antibiotics that limits their efficacy. As reported by many studies, bacteria which survive an antibiotic treatment may adapt to the pressure by altering the antibiotic-target sites or ligands via mutation or other complex series of regulation, rendering the drug incapable to bind to its specific target. Consequently, the pre-existing antibiotic is rendered ineffective against the mutated bacteria. For example, *S. aureus* acquired resistance towards vancomycin by synthesizing additional peptidoglycan with D-Ala-D-Ala residues that bind to vancomycin and prevent

it from reaching the target site of the bacteria (Lowy, 2003). On the other hand, macrolide becomes less effective against a bacterium that survives its inhibitory action when the bacterium undergoes methylation of the 23 rRNA of the 50S ribosomal subunit. This methylation impairs binding of the antibiotic to the ribosome (Munita and Arias, 2016). Similarly, many Gram-positive and Gram-negative bacteria may undergo mutation to change their penicillin-binding proteins (PBPs) so that beta-lactam antibiotics can no longer bind to them (Osaki et al., 2005; Rimbara et al., 2008; Yamachika et al., 2013; Sun, Selmer and Anderson, 2014). Resistance to fluoroquinolones was also reported by several studies which demonstrated that certain bacteria are able to mutate and alter DNA gyrase and topoisomerase IV which are targeted by these antibiotics, rendering them unable to bind to the enzymes (Oizumi et al., 2001; Weigel, Anderson and Tenover, 2002; Bansal and Tandon, 2011). Based on these findings, it is clearly indicated that antibiotics that possess single mechanism of action by targeting a specific ligand are usually at the higher risk of being compromised once the ligands are altered by fast-mutating bacteria, rendering them less effective against the mutated bacteria.

As described above, antibiotic-resistant bacteria represent one of the major public health issues that is hardly to be eradicated with the current available therapeutic agents. In view of the limitations by the pre-existing conventional antibiotics as described above, exacerbated by the decreasing in new antibiotic pipeline, it is crucial to explore or develop alternative antibacterial agents that are not only able to demonstrate novel antibacterial actions but also able to overcome the limitations of the former.

2.2 Overview of Antimicrobial Peptides (AMPs)

Among the potential alternative antibacterial agents that have been studied, antimicrobial peptides (AMPs) are the most promising candidate due to their biological entities that possess lesser risk of toxicity as compared to other chemical compounds. As the name implies, antimicrobial peptides (AMPs) are peptides that possess antimicrobial effects. These compounds were initially characterized as biologically active molecules which serve as part of the innate immune defence against invading microorganisms in a wide variety of organisms (Zhang and Gallo, 2016; Sun et al., 2018). In higher level organisms such as vertebrates, AMPs may also serve as immune modulators that regulate host immune responses against invading bacteria, virus and fungus (Diamond et al., 2009; Niyonsaba et al., 2009; Niyonsaba et al., 2010). As the element of innate immune system, these molecules are usually produced and secreted abundantly in bodily sites that are constantly exposed to environmental microorganism, for instance, skin and mucosa epithelia lining the respiratory, gastrointestinal, reproductive and urinary tract (Yang et al., 2004; Tecle, Tripathi and Hartshorn, 2010; de Sousa-Pereira et al., 2013; Wang, 2014). In human, the most important sources of AMPs are neutrophils, mast cells, dendritic cells and macrophages, in which these molecules are stored in granules of the leukocytes and released at the sites of infection to provide early defence against invading microbial pathogens before the adaptive immune response takes place (Nijnik and Hancock, 2009; Hancock, Haney and Gill, 2016).

Despite possessing significant antimicrobial effects, most of the AMPs are just short peptides of low molecular weight, in which the length is usually range from 8 to 50 amino acid residues and are 2 to 9 kDa in molecular weight (Watkins and Bonomo, 2016). Nevertheless, some AMPs which belong to host defence system (hence called host defence peptides, HDPs) may extend to 100 amino acids. These peptides are usually present in secondary configuration, such as β-sheets with helical structure (Hancock, 2001; Nguyen et al., 2011; Muthuirulan, Paramasamy and Jeyaprakash, 2013). As more studies are conducted to explore novel and elaborating the previously discovered AMPs, the detailed insights about the structures and configuration, microbial target and mechanisms of antimicrobial action for these compounds are accumulating, thus increasing their diversity from different perspective. Therefore, a systematic classification of these peptides is required in order to facilitate the understanding of the structure-function relationship and their biological actions which are important information for future research on drug design.

2.2.1 Classification of Antimicrobial Peptides

Following the discovery of the first AMP cecropin from the largest North American native moth named *Hyalaphora cecropia* (Steiner et al., 1981), the search for these antimicrobial compounds have been further expanded in different organisms ranging from microorganisms, insects, plants, amphibians to mammals (Xiao, Liu and Lai, 2011; Liu et al., 2012; Egan et al., 2016; Tang et al., 2018; Brand et al., 2019). To date, a total of 3039 AMPs have been documented in the Antimicrobial Peptide Database (APD)

(http://aps.unmc.edu/AP/main.php), where these peptides were naturally isolated or chemically synthesized. AMPs are diversified into many categories based on different criteria such as their targets, sizes, structures or configurations, origins, amino acid compositions and sequences, biological actions, mechanism of actions, etc. (Takahashi et al., 2010; Nguyen, Haney and Vogel, 2011; Pasupuleti, Schmidtchen and Malmsten, 2012). Considering the scope of research for this study, classification which are based on biological action, structural configuration, amino acid composition and mechanism of action will be further discussed.

2.2.1.1 Classification Based on Structural Configuration

Despite being short peptides, AMPs are generally present in different configurations or structures, which can be divided into three major classes as determined by nuclear magnetic resonance (NMR): alpha (α)-helical peptides, beta (β)-sheet peptides and extended peptides (Bhattacharjya and Ramamoorthy, 2009; Nguyen, Haney and Vogel, 2011). Representatives of these peptide structures and their corresponding examples are depicted in **Figure 2.2**.
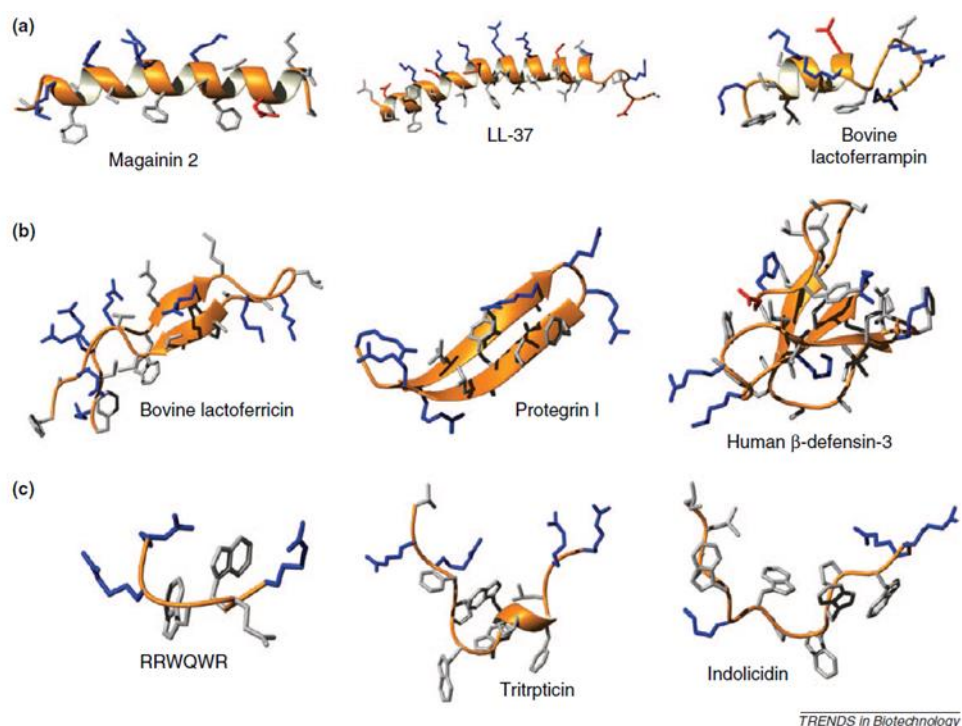
Figure 2.2: Representative structural classes of antimicrobial peptides (AMPs) as determined by solution state NMR. (a) α-helical peptides, (b) β-sheet peptides and (c) extended peptides (Nguyen, Haney and Vogel, 2011).

Among these classes, α-helical peptides represent the most common structural class of AMPs (Haney et al., 2009). As the name implies, these peptides are characterized by their spiral or helical conformation when they are present in secondary structure [**Figure 2.2(a)**]. A special feature for this class of peptides is their structural dynamicity. When the peptides are present in solution, they mainly exist as linear or unstructured conformers. However, upon interacting with phospholipid membranes, these conformers will turn into helical form (Yamaguchi et al., 2001; Salditt, Li and Spaar, 2006; Jeong et al., 2016). Exemplified by magainin, LL-37 (derivative of human defensins) and bovine lactoferrampin, these peptides always configure from their initial linear to

helical form upon interacting with bacterial membrane and utilize their lengthy helical structure to span the thickness of bacterial membrane bilayers, thus promoting membrane insertion which is essential for the antibacterial activity (Haney, 2009; Pasupuleti, Schmidtchen and Malmsten, 2012).

The second structural group is the beta (β)-sheet peptides, which are commonly exist as β-hairpin or β-sheet cyclical conformations [**Figure 2.3(b)**]. These peptides normally consist of cysteine residues, in which the disulfide bonds between these residues promote the stabilization of the hairpin or beta conformations (Conibear et al., 2013; Koehbach, 2017). Despite the common feature of β-sheet, different member of AMPs under this structural group may possess different mechanism of action. For instance, bovine lactoferricin kills its target bacteria via non-lytic mechanism by translocating into bacterial cytoplasm where it can disrupt DNA, RNA and protein synthesis (Gifford et al., 2005). Meanwhile, human β-defensin-3 (HBD-3) exerts its antibacterial activity via pore formation in anionic membranes (Sudheendra et al., 2015). Protegrin I, on the other hand, employs another bactericidal mechanism which targets a specific protein that leads to inhibition of outer membrane biosynthesis (Srinivas et al., 2010). Tachyplesin, a cyclical AMP with anti-parallel β-sheet structures, was shown to permeabilize bacterial lipid membrane followed by transient pore formation (Matsuzaki et al., 1997). As described in the above-mentioned studies, it is clearly indicated that the presence of β-sheet structure in different AMPs does not correlate to their mechanism of actions. In fact, instead of peptide structure, the peptide dynamics appear to be a more important factor that attribute for these functional differences (Nguyen et al., 2011). According to the

research groups headed by Gifford (2005) and Ramamoorthy (2006), AMPs with β-hairpin or β-sheet conformations may exist in the secondary structure when they are positioned at the membrane interphase or in linear form after translocating the membrane into the bacterial intracellular compartment. Depending on the types of the AMPs, the antimicrobial activity of the peptide is usually retained in either one of the structural conformations but become inactive when they change to another conformation.

Less commonly, the third structural group is represented by AMPs that appear in extended structure. Unlike the former two structural classes, these peptides do not regularly fold into secondary structure but may possess a loop within the peptide (hence they are also called loop peptides) [**Figure 2.3(c)**]. Another special characteristic of these peptides is the presence of one or two predominant amino acid/s that form/s the peptides, especially arginine (Arg), tryptophan (Trp), proline (Pro) or histidine (His) (Zasloff, 2002; Brogden et al., 2003; Marshall and Arenas, 2003). Most of these peptides are not membrane-active, a phenomenon which could be explained by their lack of secondary structure. However, the presence of the above-mentioned special amino acids renders these peptides with the ability to inhibit or kill their target bacteria by other means of mechanisms. For example, tritrpticin (VRRFPWWWPFLRR) and indolicidin (ILPWKWPWWPWRR-amide) are two extended AMPs which are rich in tryptophan (W), where this amino acid was found to promote partitioning of AMPs into bacterial membranes (Schibli et al., 2006; Rokitskaya et al., 2011; Arias et al., 2016). Proline-rich antimicrobial peptides (PrAMPs), a group of AMPs that are enriched in proline residues, mainly kill bacteria by inhibiting

their essential intracellular metabolic activities without disrupting the bacterial membrane integrity. Exemplified by apidaecin, oncocin and PR-39, these extended AMPs with high proportion of proline residues kill their bacteria by inhibiting protein synthesis via ribosome binding and interfering with certain chaperone proteins such as DnaK and Hsp70 (Veldhuizen et al., 2014; Lomakin, Gagnon, and Steitz, 2015; Roy et al., 2015; Graf et al., 2017). The significance of these predominant amino acids was further supported by several truncated studies whereby removal of these amino acids remarkably reduced their antibacterial efficacy and potency (Xie et al., 2011; Gagnon et al., 2016; Boto et al., 2018; Tan et al., 2018).

As described above, the difference in the structural classes of AMPs is associated with their corresponding mechanism of actions. This knowledge provides important fundamental information for designing an ideal AMP with high efficacy and good potency against pathogenic bacteria along with minimal risk of resistance.

2.2.1.2 Classification Based on Microbial Target

In terms of nomenclature, although these biological compounds are collectively named as "antimicrobial peptides" (AMPs) in many literatures, specific nomenclature is also given to a particular group of peptides based on their biological target. Hence, different categories of microbe-acting peptides were subdivided from AMPs, such as antibacterial peptides (ABPs), antifungal peptides (AFPs), antiviral peptides (AVPs), anti-parasitic peptides (APPs) and

anti-protist peptides (APtPs), in which their specific targets are bacteria, fungus, virus, parasite and protist, respectively. Despite the differences in the microbial targets, there is no clear-cut classification for many antimicrobial peptides as many of them were shown to demonstrate broad spectrum of microbial targets, where their target of inhibition or killing encompass different kingdoms of microorganisms. For instance, a member of the α-defensin family, HNP1, was shown to exert antimicrobial effect towards different species of bacteria (Wilmes et al., 2011; Varney et al., 2013; Furci et al., 2015), viruses (Hazrati et al., 2006; Salvatore et al., 2007; Smith et al., 2010; Demirkhanyan et al., 2012) and fungus (Edgerton et al., 2000; Vylkova et al., 2006). Similarly, a derivative from the cathelicidins family named LL-37 was shown to kill various species of bacteria, viruses and fungi (Sigurdardottir et al., 2006; Tripathi et al., 2013; Currie et al., 2016; Xhindoli et al., 2016). Interestingly, the corresponding derivatives and analogs of these peptides were also shown to demonstrate similar broad spectrum of antimicrobial activity, as documented in a review by Pachón-Ibáñez et al. (2017). This broad target reflects the non-specific nature of innate defence in vertebrates, where the AMPs are isolated from.

Among these categories of AMPs, antibacterial peptides (ABPs) appear to be the peptide category with the greatest number of discoveries, contributing to a number of 2671 peptides with various potencies of antibacterial activities up to February 2020 (The Antimicrobial Peptide Database). Nevertheless, as majority of the ABPs were shown to cross-react with microorganisms of other kingdoms, the terms "antibacterial peptides" and "antimicrobial peptides" are often used interchangeably in many documentations. As the main subject in this study, the

term "antibacterial peptides" (ABPs) will be used for the following description in all the chapters.

2.2.1.3 Classification Based on Mechanism of Action

The diversity of ABPs can be further reflected by their various mechanisms of action. In general, ABPs can be classified into two major classes based on their activity on bacterial membrane: membrane-active peptides and non-membrane-active peptides. The former depicts the bactericidal action of ABPs via disruption of membrane integrity, which may lead to transmembrane pore formation, leakage of intracellular components or lysis which ended with cell death (Li et al., 2017). On the other hand, ABPs that are non-membrane-active execute their action by translocating bacterial membrane into the intracellular compartment without damaging the membrane (Aisenbrey et al., 2019; Lei et al., 2019). The elaboration of these mechanisms will be further discussed in **Section 2.2.3**.

2.2.2   Important Features of Antibacterial Peptides

Despite the diversity of ABPs as described above, most of the ABPs share certain common characteristics which are essential to their antibacterial potency. Firstly, the vast majority of ABPs are cationic in nature, attributed to the presence of basic amino acids such as arginine (R), histidine (H) and/or lysine (K) (Jiang et al., 2008; Papanastasiou et al., 2009; Kumar, Kizhakkedathu and Straus, 2018). Due to the predominance of these basic amino acids over acidic amino acids, ABPs usually acquire net positive charges, which range from +2 to

+9 at physiological pH (Bahar and Ren, 2013). This cationic property plays a significant role to their antimicrobial action, which promotes the initial attraction and interaction with the anionic bacterial membrane before initiating their antibacterial action. Several studies have correlated the cationicity and antimicrobial activity of ABPs, where increment of peptide charge was associated with significant improved antibacterial activity against Gram-positive and Gram-negative bacteria (Dathe et al., 2001; Lyu et al., 2016; Gagnon et al., 2017). Conversely, decreasing the net positive charge of certain ABPs may reduce their antimicrobial activity (Jiang et al., 2009). The details of this initial interaction will be discussed in further detailed later in this chapter. Although the mainstream of ABPs are cationic, but a few anionic ABPs were discovered from vertebrates, invertebrates and plants (Harris, Dennison and Phoenix, 2009, Barbosa Pelegrini et al., 2011). However, these peptides are less common and will not be highlighted in this study.

Secondly, many ABPs possess an amphipathic nature, in which different ABPs have different relative composition of hydrophilic and hydrophobic regions within the peptides (Giangaspero, Sandri and Tossi, 2001; Chrom, Renn and Caputo, 2019). The hydrophilic region is attributed to the presence of polar amino acid residues. This feature contributes to their water solubility in aqueous solution, which explains their presence in the body fluid such as plasma or serum upon secretion from the cells. On the other hand, the hydrophobicity of ABPs is influenced by the number of hydrophobic or non-polar amino acids present within the peptide sequence, such as leucine, isoleucine, valine, methionine, alanine, phenylalanine, tyrosine and tryptophan. As reported in several studies,

the degree of peptide hydrophobicity is associated with their extent of partitioning into the membrane lipid bilayer (Chen et al., 2006; Yin et al., 2012; Hollmann et al., 2016). In other words, this feature is required to permeabilize bacterial membrane upon interacting with the bacteria, which explains the significance of peptide hydrophobicity as part of the criteria for ABPs. This amphipathic conformation is essential for the peptide actions on the bacterial membrane, which will be also discussed in the next section.

Although the above-mentioned properties are important for the antibacterial activity of an ABP, excessive levels of these features may conversely result in reduced or loss of antibacterial selectivity and increased toxicity. In a study by Dathe et al. (2001), an improvement of antimicrobial activity against Gram-positive and Gram-negative bacteria was observed for magainin 2 when the peptide cationicity was increased from +3 to +5. However, further increasing the peptide cationicity resulted in increased haemolytic effect and loss of antibacterial activity. Similarly, an optimal hydrophobicity is essential for an ABP to exert good antibacterial activity. Below or above this threshold hydrophobicity may render the peptide inactive against the bacteria, along with enhanced haemolysis to human RBCs (Yeaman and Yount, 2003; Chen et al., 2006; Yin et al., 2012). Therefore, one should take these optimal properties into consideration when designing an ABP with optimal therapeutic index, which is characterized by high antibacterial potency but low toxicity effect.

2.2.3 Mechanisms of Action of ABPs

Broadly described in the literature, the antibacterial activity of an ABP is closely related to its structure, amino acid composition, cationicity, hydrophobicity, amphipathicity and other physical chemical properties. Any slight changes or modifications to these properties would greatly affect its antibacterial activity (Smirnova et al., 2004; Chen et al., 2006; Jiang et al., 2009; Yin et al., 2012; Mihajlovic and Lazaridis, 2012). However, regardless of the differences in these properties, it is generally accepted that all ABPs exert their bacteriostatic or bactericidal effects via membrane-active and/or non-membrane active actions. Furthermore, apart from the direct antibacterial effects on the bacteria, certain ABPs were found to eradicate the bacteria indirectly via modulating host immune response against the pathogens (Hilchie, Wuerth and Hancock, 2013).

2.2.3.1 Membrane-Active Mechanism

Majority of the well-studied ABPs exert their action by targeting bacterial membrane which is characterized by a series of sequential events. These include (i) attraction of ABPs to bacterial membrane, (ii) attachment of ABPs onto bacterial membrane, (iii) insertion of ABPs into bacterial membrane, (iv) membrane permeabilization or pore formation followed by membrane disruption.

As mentioned earlier, most ABPs are cationic and amphipathic, the two important features that contribute to their selective binding to bacterial membranes which contain a high proportion of negatively charged constituents.

These anionic elements are mainly phosphate groups within the lipopolysaccharide (LPS) commonly found in the outer membranes of many Gram-negative bacteria, which include phosphotidylglycerol (PG), phosphotidylserine (PS) and cardiolipin (CL) (Epand, Savage and Epand, 2007; Sani, Whitwell and Separovic, 2012; Pöyry and Vattulainen, 2016; Hädicke and Blume, 2017). On the other hand, anionic teichoic and teichuronic acids are found in cell wall of Gram-positive bacteria at lesser extent (Malanovic and Lohner, 2016; Brown, Santa-Maria and Walker, 2013). As the results, the bacterial outer layers are rendered with net negative charge, which promotes the attraction and attachment of the cationic ABPs to the bacteria via electrostatic interaction between the two moieties of opposite changes (Glukhov et al., 2005; Meincken, Holroyd and Rautenbach., 2005; Jiang et al., 2008; Ebenhan et al., 2014). The successful attachment of these ABPs to bacterial surface represent the first essential step of antibacterial activity, which will initiate the subsequent mechanisms leading to bacteriostatic or bactericidal effects to the bacteria.

Upon attaching to bacterial outer membrane, the membrane-active ABPs will accumulate on the surface layer until a threshold concentration is achieved to initiate the subsequent steps (Melo, Ferre and Castanho., 2009; Kumar, Kizhakkedathu and Straus, 2018). At this concentration, certain amount of ABPs which are initially adsorbed parallel to the membrane lipid bilayer will begin to orientate themselves perpendicularly to their original orientation, followed by insertion into the lipid bilayer to form transmembrane pores (Chen et al., 2007; Bahar and Ren, 2013). Others may disrupt the membrane integrity without pore formation (Lee, Hall, and Aguilar, 2016).

Depending on the type of ABP and the membrane composition which varies from one bacterial species to another, the membrane disruption can be induced by ABPs via one of the following proposed models of membrane-active mechanisms, namely (i) the barrel-stave model, (ii) the toroidal model, (iii) the carpet model, and (iv) the detergent-like model (**Figure 2.3**) or combination of the models (Malmsten, 2016). The former two models are associated with pore formation in bacterial membrane, which are commonly mediated by ABPs with amphipathic structure but at relatively higher degree of hydrophobicity (Chen et al., 2007). The amphipathicity of these peptides is an important criterion for the pore formation, in which the hydrophobic regions of the peptides interact with the lipid residues of bacterial membrane, while the hydrophilic regions form pore lumen that spans the lipid bilayer (Brogden, 2005; Jean-François et al., 2008). Examples of ABPs that were found to carry out these mechanisms of actions include alamethicin, pardaxin, protegrins and zervamicin (Rapaport and Shai, 1991; Shenkarev, et al., 2002; Wimley, 2010). Since these peptides execute their antibacterial action by spanning across the membrane lipid bilayer, a minimum peptide length is required. For ABPs with α-helical structure, a minimum length of approximately 22 amino acids is required (Wimley, 2010; Kumar, Kizhakkedathu and Straus, 2018). However, for β-sheet peptides, the minimum length can be as short as 8 residues (Kumar, Kizhakkedathu and Straus, 2018). This information provides a crucial guideline for future research in designing and developing new ABP in order to optimize its antibacterial potency.
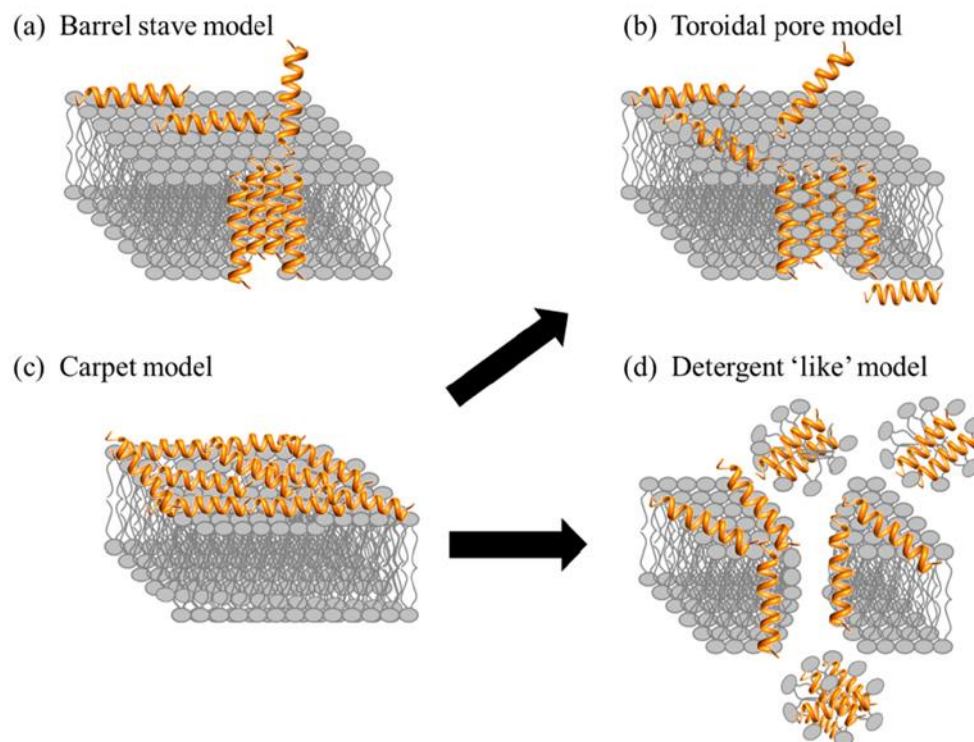
Figure 2.3: Proposed models of membrane-disruptive mechanisms by ABPs (Kumar, Kizhakkedathu and Straus, 2018).

On the other hand, certain ABPs may disrupt bacterial membrane without forming pores, as depicted in the carpet model and detergent-like model (Yeaman and Yount, 2003; Lee, Hall and Aguilar, 2016). Under the carpet model, ABPs act by spanning and covering the bilayer surface in a carpet-like manner. At certain threshold, the carpeted-bilayer begins to rupture as the accumulated ABPs sink into the inner leaflet from the outer leaflet of bacterial membrane due to peptide-mediated imbalance between the two leaflets. As the results, the membrane integrity is lost. Examples of ABPs that utilize this model to disrupt bacterial membrane including cecropin (Sitaram and Nagaraj, 1999), aurein (Fernandez et al., 2012), indolicidin (Rozek, Friedrich and Hancock, 2000) and LL-37 (Shai, 2002). Under detergent-like model, ABPs tend to

accumulate and cover the surface of the membrane, leading to membrane disintegration and ended by membranous collapse to form micelles (Yeaman and Yount, 2003). An example of ABP that acts by this manner is magainins (Papo and Shai, 2002).

Membrane-active ABPs are regarded as a structurally and mechanistically diverse group of antibacterial agent with distinct powerful killing action. Despite the differences in the above-mentioned mechanisms, the common ultimate outcomes to the bacterial membrane exposed to these ABPs include depolarization of outer membrane, increased permeability, leakage of ions and other metabolites and/or loss of cytoplasmic essential components, which ensure cell death (Yoneyama et al., 2009; Lam et al., 2012; Epand et al., 2016; Kumar, Kizhakkedathu and Straus, 2018). These membrane-active mechanisms represent a unique mode of action as compared to conventional antibiotics that target other specific bacterial systems, where resistance can be easily acquired by modifying these systems through mutations and render the antibiotics ineffective against the bacteria. Conversely, ABPs that target bacterial membrane in a non-receptor-mediated or non-specific manner (Shai, 2002; Yeaman and Yount, 2003) could overcome the limitation as mentioned above. Even though a particular ligand on/in the bacterial membrane which is bound by ABPs may undergo mutational-mediated alteration, but the bacterial susceptibility to these peptides may not be seriously impeded as the peptides are still able to interact with other membranous binding sites to initiate their action. It is unlikely for the bacteria to alter the entire membrane structure simultaneously due to the high structural complexity.

Moreover, regardless of bacterial species or strains, the biological structures or components that made up the bacterial membranes are relatively conserved, which allow ABPs to act on a broad spectrum of bacteria with less specificity (Schmitt, Rosa and Destoumieux-Garzón, 2016; Oppedijk, Martin and Breukink, 2016). As the actions of these peptides on bacterial membrane are not receptor-restricted, one can assume that the peptide can cause extensive damage to the membrane from all dimension of the bacteria, followed by cell death. Additionally, extensive membrane damage by many membrane-active ABPs is lethal enough to kill the bacteria without the need to traverse across the membrane for intracellular target that is time-consuming (Farkas et al., 2017). Thus, many membrane-disruptive ABPs are able to exhibit rapid killing activity before the bacteria achieve their doubling time (Zhang, Rozek and Hancock, 2001; Zhu et al., 2015; O'Brien-Simpson et al., 2016; Dias et al., 2017). Thus, these ABPs represent an ideal antibacterial agent that deprives the bacteria of opportunity of striking back with resistance.

2.2.3.2 Non-Membrane-Active Action

Although membrane disruption is regarded as a major key action for many ABPs, certain ABPs are able to inhibit or kill their target bacteria via mechanisms independent of membrane damage. In general, the actions of these non-membrane-active ABPs can be divided into two categories: (1) direct inhibitory or killing action by interfering with intracellular components, and (2) indirect action by modulating host immune response to fight against the bacterial pathogens. These peptides are able to penetrate, translocate the bacterial

membrane or taken up by the living bacteria followed by accumulation in the cytoplasm (Richard et al., 2005; Madani et al., 2011; Gomarasca et al., 2017). Once achieving certain concentration, these peptides are able to exert their cytotoxic effects via various mechanisms that disrupt the normal metabolic or enzymatic activities that are vital for bacterial survival. These cytotoxic activities include inhibition of enzymes that are required for DNA, RNA and protein synthesis (Heddle et al., 2001; Marchand et al., 2006; Ho et al., 2016); binding to ribosome units which leads to inhibition of protein synthesis (Patrzykat et al., 2002; Mardirossian et al., 2014); disruption of chaperone activity that leads to inhibition of proper protein folding (Kragol et al., 2001; Chesnokova, Slepenkov and Witt, 2004; Rahnamaeian et al., 2015); inhibition of cell-wall synthesis (Brötz et al., 1997; Hasper et al., 2006); binding to DNA followed by inhibition of DNA and RNA synthesis (Park, Kim and Kim, 1998; Marchand et al., 2006; Hao et al., 2013).

For instance, many ABPs are able to inhibit the biosynthesis and metabolism of nucleic acids. Once translocated the bacterial membrane, these peptides are able to interact with certain regions of nucleic acids resulting in inhibition of DNA replication and transcription (Ghosh et al., 2014; Shruti et al., 2016). In a study by Park et al. (1998), buforin II, a 21-amino acid ABP isolated from the stomach of the Asian toad, was shown able to penetrate bacterial membrane followed by inhibition of essential cellular functions via DNA/RNA-binding. The ability to bind DNA by these peptides is believed to be attributed to the electrostatic interaction between the positively charged ABPs and negatively charged phosphate groups of the nucleic acid (Mardirossian et al., 2014). As the results

of this DNA binding, bacterial viability and proliferation are seriously affected due to failure in normal DNA replication, gene expression and metabolism.

Besides, certain ABPs are able to inhibit protein biosynthesis and metabolism. Several sequential steps are involved in protein synthesis, beginning with transcription of DNA to mRNA, translation of mRNA to polypeptides via 70S ribosome and finally peptide folding and assembly into functional proteins as mediated by chaperone proteins. Inhibition of enzymatic activity or other effector molecules that are essential to these events could interfere with or even block the protein synthesis. A number of ABPs were found to kill their target bacteria by targeting these effector molecules. For example, a proline-rich ABP, Bac7, was shown to inhibit translation by binding to bacterial 70S ribosome and blocks the peptide exit tunnel (Gagnon et al., 2016). In a study by Florin et al. (2017), Api137, a derivative from an insect ABP named apidaecin, was shown able to inhibit protein synthesis by shutting down translation termination at the stop codon, thereby inhibiting the release of nascent polypeptide chain from the ribosome. As the consequence of these inhibitions, bacteria are not able to produce proteins which are important to their biochemical metabolism and cellular integrity, which eventually lead to cell death.

2.2.3.3 Immune Modulator

Extensive studies on certain ABPs have further revealed that the antibacterial activity of these bioactive compounds is not only restricted to direct bacteriostatic or bactericidal actions. In fact, many of the well-studied ABPs are

able to serve as important regulator of host immune response. This additional role of ABPs, termed as immune modulator, is characterized by their ability to regulate a wide range of elements in the immune systems to enhance host immune response towards pathogens and tissue healing. The best characterized ABPs with immunomodulation features are defensins (e.g., human neutrophil peptides, HNPs) and cathelicidin LL-37, which are classes of human defence peptides secreted by innate immune cells such as neutrophils, mast cells and macrophages (Ganz et al., 1985; Zanetti, 2004; Tomasinsig and Zanetti, 2005). Apart from their direct killing action on Gram-positive and Gram-negative bacteria, these ABPs have been shown to modulate or regulate various host immune responses in a fine-tuned manner. These modulations include chemoattraction of immune cells (Tjabringa et al., 2006; Grigat et al., 2007; Soruri et al., 2007), stimulating production of chemokine and cytokines (Reinholz, Ruzicka and Schauber, 2012; Chen et al., 2013), anti- or pro-apoptotic effects of innate immune cells (Nagaoka, Tamura and Hirata, 2006; Nagaoka et al., 2010; Nagaoka et al., 2012) and regulation of inflammatory response (Niyonsaba and Ogawa, 2005; Soehnlein et al., 2008; Miles et al., 2009; Méndez-Samperio, 2013). These regulations are important to control the type, degree and duration of immune responses towards the invading pathogens while minimizing the immune-mediated damages to the host caused by uncontrollable inflammatory response.

Besides natural ABPs, chemically synthesized ABPs were also shown to possess similar role in immunomodulation, and some of them were experimentally tested as adjuvant in vaccine formulation. For instance, a short synthetic ABP,

KLKL(5)KLK, was reported as a good adjuvant to a DNA vaccine aimed to enhance and prolong immune response against *Mycobacterium tuberculosis* infections (Li, Yu and Cai, 2008). Wieczorek and his colleagues (2010) reported that a 12-residue synthetic ABP possesses immunomodulatory action apart from direct killing of Gram-positive and Gram-negative bacteria. This peptide, namely 1018, was demonstrated for its ability to induce chemokine response and suppress tumor necrosis factor (TNF) response induced by lipopolysaccharide (LPS). Certain synthetic versions of natural ABPs from host innate defence system, which are given the name as innate defence regulators (IDRs), were shown to suppress pro-inflammatory cytokines in mouse models infected with Gram-positive and Gram-negative pathogens, thus preventing serious immune-mediated damage to the mouse due to the infections (Scott et al., 2007).

As compared to the single antibacterial action by many conventional antibiotics, the antimicrobial-immunomodulatory duality of ABPs may further enhance the battle against bacterial infections. While exerting direct antibacterial action against the bacteria, the peptides may strengthen the host immune system to response and attack the foreign invaders. This extra function renders ABPs with more promising features to be considered as potential candidate of alternative antibacterial agents

2.2.4 Advantages of ABPs

Accumulating data from the research on ABPs strongly suggested that these bioactive compounds can be further developed into novel alternative antibacterial agent that could complement or even replace conventional antibiotics to fight against multidrug-resistant bacteria. As highlighted in **Section 2.1.4**, the limitations of conventional antibiotics render them less effective against many emerging drug-resistant bacteria. Conversely, as will be described later, the powerful action as well as other special features of ABPs allow them to overcome the above-mentioned limitations of classical antibiotics, thus reducing the issue of drug-resistance.

2.2.4.1 Broad Spectrum of Target Bacteria

One of the prominent features that define an ideal antibacterial agent is the ability to act against a broad spectrum of target bacteria. Interestingly, most of the well-studied ABPs demonstrated broad spectrum of antibacterial effect towards different species of Gram-positive and Gram-negative bacteria (Rathinakumar, Walkenhorst and Wimley, 2009; He, Krauson and Wimley, 2014; Liu et al., 2015; Narayana and Chen, 2015). According to a study by Bharal and Sohpal (2013), bacteriocin, an ABP produced by *Lactobacillus acidophilus*, was shown to demonstrate bactericidal effect towards several Gram-negative bacteria such as *Salmonella* Typhi, *Micrococcus luteus*, *S. aureus*, *P. aeruginosa* and *E. coli*. In addition, it also exhibited bacteriostatic effect towards Gram-positive bacteria that encompassed *Enterococcus faecalis* and *Streptococcus pyogenes*. EC5, a synthetic 12-mer ABP derived from phage-

displayed selection with high binding affinity to *E. coli*, demonstrated bacteriostatic effects towards different strains of *E. coli* and *P. aeruginosa* (Sainath Rao et al., 2013). An arginine-rich ABP modified from Hepatitis B virus core protein, namely HBc147-183, was shown to display broad-spectrum of bactericidal activity towards Gram-negative bacteria encompassing *P. aeruginosa*, *K. pneumoniae* and *E. coli*, as well as *S. aureus* from the Gram-positive category (Chen et al., 2013). Similar findings were also found for Salusin-β, an endogenous parasympathomimetic peptide with broad spectrum of antibacterial activity against many species of Gram-positive bacteria (Kimura et al., 2014). Indeed, the list of ABPs with this special antibacterial property is constantly being updated with additional new peptide candidates from numerous study groups.

The broad spectrum of antibacterial activity might be attributed to two important features of ABPs. As mentioned earlier, ABPs are found in various secondary structures such as α-helices, β-strands, loop shape and extended form. This structural flexibility and diversity allow the peptides to interact with different bacteria in different binding configuration, thus allowing them to target on different bacteria species (Hancock, 2001; Salditt, Li and Spaar, 2006). Secondly, given the evidence that the interaction between ABPs and bacterial membranes is not strictly mediated by specific receptors or ligands on the membranes, and many common structural targets for peptide binding are conserved across different species of bacteria (e.g. lipid II, lipopolysaccharide and teichoic acids), ABPs with membrane-active mechanisms are able to bind to these structures across many species and strains of bacteria before executing

45

their bacteriostatic or bactericidal actions (Münch and Sahl, 2015; Schmitt, Rosa and Destoumieux-Garzón, 2016).

In contrast to the limited spectrum by many classical antibiotics, the broad spectrum of bacterial targets potentiates the use of ABPs in clinical setting, especially for empiric treatment against bacterial infection where the causative agent is yet to be identified.

2.2.4.2 Rapid Killing Kinetic by ABPs

In contrast to the slow killing or inhibitory effects by many classical antibiotics, most of the bactericidal ABPs are able to kill their target bacteria rapidly (Narayana and Chen, 2015). As mentioned earlier, the extensive membrane disruptions by ABPs characterized by outer membrane depolarization, inner membrane permeabilization and/or pore formation serve as the main lethal events that contribute to the bactericidal effect by these peptides. These mechanisms also explain the relatively rapid killing by ABPs as compared to many classical antibiotics that target intracellular components, in which the antibacterial actions of the latter require translocation of the compounds across the bacterial membrane to act on an intracellular target (Olson et al., 2006; Chopra and Reader, 2015; Vergalli et al., 2017). With reference to the study by Mohamed et al. (2016) as described in **Section 2.1.4.2**, while vancomycin, ciprofloxacin and linezolid took 24 hours or longer to achieve complete killing of MRSA, a novel synthetic ABP under their study, namely WR12, achieved the clearance only within 30 minutes. In a similar study, RN7-IN8, a novel synthetic

ABP which was hybridized from indolicidin and ranalexinin, was shown to eliminate *S. pneumoniae* within 30 minutes, while erythromycin and ceftriaxone took more than two hours to clear the bacteria (Jindal et al., 2015).

Apart from the Gram-positive bacteria as mentioned above, other ABPs were shown to exert rapid killing on Gram-negative bacteria as well. Tritrpticin, a 13-amino-acid ABP under the family of cathelicidin, was demonstrated to kill *P. aeruginosa* completely after 30 minutes of exposure, whereby the same clearance by amikacin only could be achieved after 240 minutes, and 480 minutes for imipenem, ceftazidime, ciprofloxacin and piperacillin-tazobactam (Cirioni et al., 2006). Similar finding was found by Zhu et al. (2015), in which a 16-amino-acid α-helical peptide named TW9 was shown to kill different strains of antibiotic-resistant *P. aeruginosa* completely within 30 minutes.

Collectively, the above-mentioned findings suggested that ABPs are better than the classical antibiotics in terms of their killing kinetics, where most of them are able to eradicate the bacteria within an hour. This feature is particularly important in the race between bacterial killing and bacterial proliferation. As mentioned earlier, the doubling times for many bacteria range approximately from 15 minutes to 1 hour. If the pathogens are killed before their doubling time, they are deprived of the time and ability to acquire inducible resistance to the peptides. Thus, in consideration of this better pharmacokinetic property, ABPs are regarded as a better antibacterial agent as compared to conventional antibiotics due to their low likelihood of raising resistant bacteria.

2.2.4.3 Multiple Mechanisms of Action

In contrast to the classical antibiotics which mostly act on a specific target, many ABPs execute their antibacterial effects via multiple cellular targets on/in the bacteria. As mentioned in **Section 2.2.3.1** and **2.2.3.2**, ABPs exhibit their antibacterial effects via membrane-active or non-membrane-active mechanisms. In fact, several studies have demonstrated that the membrane-active and non-membrane-active actions might not be mutually exclusive for certain ABPs. Conversely, these peptides are able to inhibit or kill their target bacteria by means of two or more inhibitory mechanisms that may occur simultaneously or sequentially. This multi-hit hypothesis was proposed by Zhang et al. (2000), who suggested that antibacterial action of certain ABPs may combine a few cooperative mechanisms which aim at different structures or ligands located at both extracellular or/and intracellular compartment of the target bacteria. In a study by Friedrich and colleagues (2001), a synthetic variant of indolicidin named CP10A was shown to exert strong killing effect towards its target bacteria via membrane lysis and inhibition of various intracellular element or function such as DNA, RNA and protein synthesis. Another synthetic derivative, NK-18, which was truncated from a powerful effector molecule of cytotoxic T cell and natural killer cell named NK-lysin, exhibited potent antibacterial activity against *E. coli* and *S. aureus* by damaging bacterial membrane and binding to bacterial DNA (Yan et al., 2013). Meanwhile, an ABP which was derived from phage-displayed peptide library, namely EC5, was shown highly active against *E. coli* and *P. aeruginosa* via outer membrane depolarization, inner membrane permeabilization and ATP inhibition (Sainath, Mohan and Atreya, 2013). Clearly indicated by these studies, ABPs are able to act differently as compared

to many conventional antibiotics, in which the efficacy of the latter is usually compromised by their limited and specific mechanism.

Apart from the direct effect to planktonic bacteria, some of the ABPs were reported for their ability to inhibit biofilm formation. For instance, NA-CATH:ATRA1-ATRA1 is a synthetic ABP which was shown to inhibit biofilm production by *S. aureus* (Dean, Bishop and van Hoek, 2011). LL-37, a natural ABP from the cathelicidin family, was shown to inhibit biofilm production by reducing the initial attachment of *S. epidermidis* and *P. aeruginosa* onto the surface of medical devices (Overhage et al., 2008; Hell et al., 2010). More importantly, even though the biofilm is formed, certain ABPs were found able to induce dissolution of the matrix (Dawgul et al., 2014; Maisetta et al., 2016). The significance of this finding is indicated by the clinical application of polymyxin E (colistin) as the last resort of treatment against biofilm-associated infections when there is no other effective conventional antibiotics (Poirel, Jayol and Nordmann, 2017).

Due to the multiple killing mechanisms, ABPs may encounter lesser issue of inducible resistance. As many ABPs could act on several targets on/in the same bacteria, it is unlikely for the bacteria to alter these targets simultaneously as such drastic alterations would be too metabolically costly. Hence, the likelihood for bacteria to develop resistance to ABPs with multiple killing mechanisms is relatively low (Guilhelmelli et al., 2013; Munita and Arias, 2016; Le et al., 2017).

2.2.4.4 Selective Toxicity to Bacteria

The fact that ABPs are given prior consideration to be developed into alternative therapeutic agent over other chemical compounds is attributed to their selective toxicity towards bacteria. As mentioned previously, the cationicity of many potent ABPs renders them with binding preference to bacterial membrane over mammalian cell membranes (Epand et al., 2016). This selective binding is attributed to the fundamental differences that exist between bacterial and mammalian cell membranes. Membranes of mammalian cells are mostly made up of neutral phospholipids such as phosphotidylcholine (PC), phosphotidylethanolamine (PE) and sphingomyelin (SM) (Coskun and Simons, 2011). Moreover, the presence of neutral sterols such as cholesterol and ergesterol also contributes to the zwitterionicity of the membrane (Dufourc, 2008; Verly et al., 2017). On the other hand, bacterial membranes are composed of phosphotidylglycerol (PG), phosphotidylserine (PS) and cardiolipin (CL) that are negatively charged (Yeaman and Yount, 2003). **Figure 2.4** illustrates the differences between mammalian and bacterial cell membrane that account for the selective action of many ABPs on the latter. In addition, the cell walls of Gram-negative bacteria contain anionic lipopolysaccharide while anionic teichoic acid and lipoteichoic acid are found in the cell walls of Gram-positive bacteria (Matsuzaki, 2009). All these components contribute to the net negative charge of bacterial cell surface, rendering it a target for many cationic ABPs. To a certain extent, this selective action of ABPs may reduce the risk of toxicity to mammalian or human cells, thus further suggesting them as alternative therapeutic agent against bacterial infections.
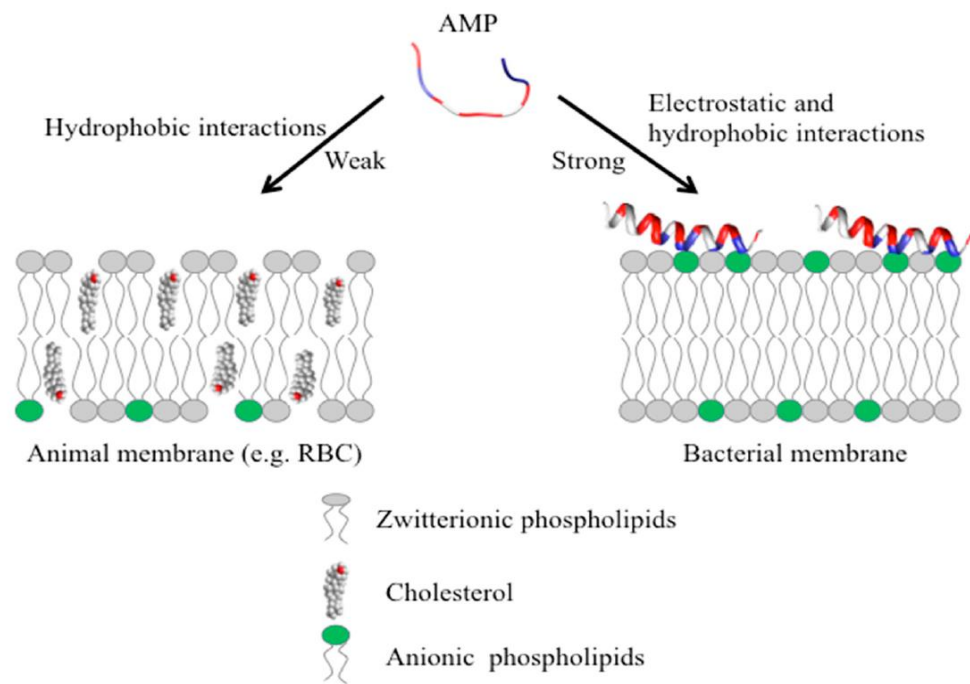
Figure 2.4: Structural and ionic differences between animal (mammalian) membrane and bacterial membrane that cause the difference in the binding strength by AMP/ABP (Kumar, Kizhakkedathu & Straus, 2018).

However, the toxicity of ABPs to eukaryotic cell is still a debatable issue when several studies reported considerable haemolytic effect on human erythrocytes by these compounds, particularly by natural ABPs (Laverty and Gilmore, 2014; Bacalum and Radu, 2015; Inui Kishi et al., 2018). These peptides, as will be further discussed in **Section 2.2.5**, are mostly derived from natural resources. Nevertheless, numerous efforts have been carried out to reduce the toxicity by modifying the peptides through various approaches, as will be further discussed in the following sections.

2.2.5 Current Status in Clinical Application of ABPs

As mentioned in **Section 2.1.2**, many pharmaceutical companies have given up on research and development of new antibiotics that work in classical mechanisms of actions. However, the significant findings on ABPs as described previously may have lightened up the hope of creating alternative novel antibacterial agents that work in different ways from the conventional antibiotics. In consideration of the ABP features that might be able to overcome the antibiotic shortcomings, the focus on novel antibacterial agent has been directed towards these peptide compounds. This can be reflected by the recent trend of antibiotic development which is almost dominated by ABPs. The newest class of antibiotics, termed lipoglycopeptides, is a group of peptide antibiotics that contain lipophilic sidechains linked to glycopeptides, where the latter is another group of peptide antibiotics which was approved for clinical use in 1956 (McCormick, 1955). More recently, Telavancin became the first lipoglycopeptide approved by U.S. Food and Drug Administration (FDA) for clinical use in 2009, followed by dalbavancin and oritavancin in 2014 (Kahne et al., 2005). In 2003, Daptomycin, a peptide antibiotic under the class lipopeptide, was introduced to the market (Tally and DeBruin, 2000; Baltz, 2009). Apart from these marketed ABPs, several ABPs for different indications are currently under different phases of clinical trials and development, in which some of them demonstrated promising findings. **Table 2.1** depicted some of the most potential ABPs that are currently under different levels of clinical trials. Clearly indicated from the table, the research interest on ABPs is indicated by the increasing number of pharmaceutical companies that have allocated significant investment in the research and development of these compounds.

Product	Description	Indication	Phase	Company (location)
Magainin peptide/pexiganan acetate	22-amino-acid linear antimicrobial peptide, isolated from the skin of the African clawed frog (*Xenopus laevis*)	Diabetic foot ulcers	3	Dipexium Pharma (White Plains, New York)/MacroChem/Genaera
Omiganan	Synthetic cationic peptide derived from indolicidin	Rosacea	2	BioWest Therapeutics/Maruho (Vancouver)
OP-145	Synthetic 24-mer peptide derived from LL-37 for binding to lipopolysaccharides or lipoteichoic acid	Chronic bacterial middle-ear infection	2	OctoPlus (Leiden, The Netherlands)
Novexatin	Cyclic cationic peptide, 1,093 daltons	Fungal infections of the toenail	1/2	NovaBiotics (Aberdeen, UK)
Lytixar (LTX-109)	Synthetic, membrane-degrading peptide	Nasally colonized MRSA	1/2	Lytix Biopharma (Oslo)
NVB302	Class B lantibiotic	*C. difficile*	1	Novacta (Welwyn Garden City, UK)
MU1140	Lantibiotic	Gram-positive bacteria (MRSA, *C. difficile*)	Preclinical	Oragenics (Tampa, Florida)
Arenicin	21 amino acids; rich in arginine and hydrophobic amino acids	Multiresistant Gram-positive bacteria	Preclinical	Adenium Biotech Copenhagen
Avidocin and purocin	Modified R-type bacteriocins from *Pseudomonas aeruginosa*	Narrow spectrum antibiotic for human health and food safety	Preclinical	AvidBiotics (S. San Francisco, California)
IMX924	Synthetic 5-amino-acid peptide innate defense regulator	Gram-negative and Gram-positive bacteria (improves survival and reduces tissue damage)	Preclinical	Iminex (Coquitlam, British Columbia, Canada)

Table 2.1: List of ABPs for different indications and under different stages of clinical trials or development (Zasloff, 2002; Gordon et al., 2005)

2.2.6 Limitations of the Previous Studies on ABPs

Despite the potential medical significance of ABPs, there are major drawbacks that impede the development of these bioactive compounds into clinical therapeutic agents. This is reflected by the huge discrepancy between the number of ABPs that were documented in the Antimicrobial Peptide Database and the actual number of ABPs approved by FDA for clinical use. One of the reasons for this lagging is the incomprehensive study of these peptides from various perspectives. A detailed review on the previous research articles on ABPs would show that many researchers or research groups were just focused on the isolation or design of novel ABPs followed by *in vitro* screening for their antibacterial potency. Others may extend further on the study of *in vitro* peptide toxicity and/or structure prediction. However, very limited data on the peptide stability *in vivo/ex-vivo*, structure-function relationship, mechanisms of action, surface interaction and *in vivo* toxicity were documented. It is also regrettable that the above-mentioned incomprehensive studies were not followed up or further studied in detailed, thus impeding them from progressing to clinical trial due to insufficient valuable data.

Next, the findings on the potency of ABPs as reported by many research groups were mainly based on *in vitro* testing, which may not reflect the true condition in the host body environment. One should take into consideration that the actions of ABPs are strongly influenced by different pH conditions (Kacprzyk et al., 2007; Wu et al., 2007; Schroeder et al., 2014) which might vary at different parts of the body. Moreover, the efficacy and potency of the compounds are also

affected by physiological concentrations of divalent cations in the plasma or serum (Lee, Cho and Lehrer, 1997; Wu et al., 2007; Clifton et al., 2014). As reported by Lee, Cho and Lehrer (1997), in the presence of increasing concentrations of sodium chloride (NaCl), the antibacterial activities of magainin and cecropin were greatly diminished, while changes of pH between 5.5. and 7.4 significantly affected the activity of clavanin A. It is believed that the changes in the concentrations of hydrogen ion and other divalent cations (e.g. Ca^{2+} and Mg^{2+}) may affect the binding between the ABPs and bacterial membrane as well as reduction of peptide-mediated depolarization of bacterial outer membrane. Therefore, the effects of these two physiological parameters should be taken into consideration in the future design and development of novel ABPs with optimised antibacterial potency.

Additionally, the overrating of many natural ABPs as promising candidates of therapeutic agents by many research groups may cause certain misconception to scientists who are desperately exploring new alternative antibacterial agent due to the antibiotic crisis. One of the major concerns on the application of ABPs in clinical field is the risk of toxicity to mammalian or human cells. Natural resources may offer some of the best ABP candidates with high antibacterial potency, for instance, polyphemusin I from horseshoe crab (Miyata et al., 1989; Powers, Rozek and Hancock, 2003), polymyxin B from *Bacillus polymyxa* (Shaheen et al., 2011), and protegrin from porcine (Zhao, Liu and Lehrer, 1994). These ABPs are able to inhibit or kill their target bacteria at concentrations which are much lower than conventional antibiotics (Bahar and Ren, 2013). Unfortunately, the potencies of these peptides are offset by the low therapeutic

index due to their potential toxicity to mammalian or human cells. For instance, polyphemusin was found to exhibit haemolytic effect at higher concentrations (Zhang, et al. 2000). Melittin, a naturally occurring ABP isolated from bee venom, possess powerful antibacterial effect towards many bacteria. Nevertheless, its use in human therapeutic is restricted due to its haemolytic and cytotoxic effects to mammalian cells (Sharon et al., 1999; Raghuraman and Chattopadhyay, 2007; Choi et al., 2015). Iseganan, a protegrin derivative, was hold for clinical application when it failed in Phase III clinical trial due to its cytotoxicity (Trotti, et al. 2004). Even though Polymyxin B and E (colistin) had successfully passed the clinical trial, their clinical application is restricted to the last resort of treatment against multidrug-resistant bacteria due to their potential renal and neural toxicity (Roberts et al., 2015). Consequently, these severe adverse complications raised controversial debates over the safety of these compounds in clinical application, which explains the reason on the limited numbers of approved ABPs for clinical use against bacterial infections.

Undeniably, the mother nature provided the first inspiration towards discovery and development of many ABPs. Ever since the discovery of gramicidins from the soil bacteria *Bacillus brevis* in 1939 (Van Epps, 2006), the search for novel ABPs has been continued on many living sources. As demonstrated in many pioneer studies, microorganisms have been the major source of many novel ABPs (Hassan et al., 2006; Boulanger, Bulet and Lowenberger, 2006, Cotter, Ross and Hill, 2013). In the earlier phase, the exploration for these biological active compounds was carried out in high-throughput screening (HTS) manner. Under this method, naturally occurring peptides were isolated and purified from

prokaryotic and eukaryotic cells, followed by screening for their antibacterial activity by *in vitro* methods (Parachin and Franco, 2014). Such method may generate large numbers of novel peptides that require high-throughput *in vitro* and *in vivo* screening and testing. However, the successful isolation and purification of these bioactive substances followed by antibacterial screening for each of the isolated peptide require tedious, laborious and time-consuming processes (Ming and Epperson, 2002; Li et al., 2008; Sousa et al., 2016). After the extraction procedures, the presence of other proteins may reduce the purity of the peptides, thus affecting the reliability of the assay data. Even though the peptides are successfully extracted and purified, the yield of the extract might not be sufficient to meet the requirement of downstream assays.

As mentioned in **Section 2.2.4**, although bacterial resistance to ABPs is relatively low, several findings on inducible resistance to the peptides were reported (Jin et al., 2004; Sieprawska-Lupa et al., 2004; Galvan, Lasaro and Schifferli, 2008; Frick et al., 2011; Shelton et al., 2011). These inducible resistances might set a major drawback to these remarkable antibacterial agents, particularly to those ABPs which are bacteriostatic to bacteria. With respect to the antibacterial action, ABPs can be categorized into two major classes: bacteriostatic and bactericidal ABPs. From the perspective of effectiveness, it is always a wise strategy to select an antibacterial agent which can completely eliminate the bacteria directly (bactericidal) instead of interfering with their growth (bacteriostatic). Therefore, bactericidal ABPs appear to be the better agent with lower risk of inducible resistance by the remaining bacteria once the treatment is discontinued.

Based on the above-mentioned limitations, there is a need to optimise and improve the efficiency of ABPs via alternative strategies instead of direct isolation. The selection of an ideal strategy should be based on considerations which enable the generation of ABPs that fulfil the following criteria: strong antibacterial potency, broad spectrum of bacterial targets, multiple mechanisms of actions, selective toxicity towards bacterial target, high peptide stability and minimal adverse effects towards host cells. In addition, prior considerations should be given to peptide candidates that are bactericidal instead of bacteriostatic.

2.3   Development of Novel Synthetic Antibacterial Peptides

Recent work on ABP development has seen some improved strategies from the previous conventional isolation method. In common, many research groups tend to search for novel ABPs through systemic mining from the peptide database, followed by rational modifications to yield peptides with optimised therapeutic index. These combined strategies can be divided into three categories as will be further elaborated in the following sections.

2.3.1   Template-based Design

Under this strategy, a known natural ABP is used as a template to yield other peptide derivative/s with greater antibacterial effect but minimal toxicity via random mutagenesis (Robinson, 2011). The existing natural ABP is modified using various approaches either through addition, deletion or amino acid substitution to produce chimeric peptides that will be screened individually for

their antibacterial property. Using this method, several peptide derivatives from cecropin, magainin, protegrin and lactoferrin were generated (Haukland et al., 2001; Dijkshoorn et al., 2004; Pag et al., 2008; Wiradharma et al., 2011). However, the limitation of this method is the unpredictable influence of the modification to the peptide variant without carrying out antibacterial assay. A peptide with a particular amino acid replacement may increase its antibacterial activity, but the opposite effect might occur to another peptide with the similar modification (Huang, Huang and Chen, 2010). Therefore, the unpredictability of the modified or truncated peptide variants sets a major drawback to this method.

2.3.2   Rational Design of ABP Using Computational Tool

Unlike the template-based method which creates peptide variants from the naturally occurring ABPs via peptide modification, rational design of ABP usually utilizes a limited set of amino acid residues with special characteristics to create a new peptide with the desired antibacterial properties. As this method allows researchers to create conceptual model of bioactive peptides based on the correlation between biological activity and molecular properties, knowledge about the characteristics and nature of certain amino acids is required. By using certain basic (arginine and lysine) and hydrophobic amino acids (tryptophan, leucine, alanine or phenylalanine) along with computational design and calculation, a new ABP with optimum antibacterial potency and minimum toxicity can be rationally designed followed by chemical synthesis before

subjecting them to a series of experiments to determine their antibacterial properties.

Several research groups had used this method to produced novel cationic peptides that fulfil the criteria of an ideal ABP. For example, using the Antimicrobial Peptide Database (APD), Liu et al. (2015) had designed and created a 13-amino acid peptide named KW-13 (KWKYPKLLKKLLK) which was shown to demonstrate bacteriostatic effect towards *S. aureus* and *S. epidermidis*. In another study by Deslouches et al. (2015), a rationally designed 12-mer cationic ABP, namely WR12, was created with only arginine (R), tryptophan (W) and valine (V). Despite the simplicity of the amino acid composition, the peptide demonstrated strong antibacterial effect towards a number of bacteria due to the presence of these cationic and hydrophobic residues.

However, the design of new ABP using this method could be an infinite task. As mentioned earlier, an ABP is commonly consists of 8 to 50 amino acids (N). With the total 20 types of amino acids, the number of possible combinations for an ABP of N residues is 20^N. Considering the testing of this huge number of ABPs from the stage of chemical synthesis to downstream screening assays and analysis, the cost and time that are required are simply beyond the capability and capacity of any laboratory.

Therefore, it is more practical and feasible if the starting point for developing an effective ABP begins with determination of a peptide motif which can interact or bind selectively to a bacterium, followed by some rational modifications to optimize it based on the common criteria of an ABP.

2.3.3 Combinatorial Phage Displayed-Peptide Library Screening

Since its introduction in 1985, phage display selection has been applied in various areas of research, including study of protein-protein/peptide interactions, epitope mapping, drug discovery, ligand identification, antibody-antigen binding and cancer research (Hetian et al., 2002; Su et al., 2005; Wu et al., 2016). This method encompasses the usage of a phage displayed-peptide library to select specific peptide/s that bind to a target ligand through a process called biopanning or affinity selection (**Figure 2.5**). The target ligand can be any surface structures or molecules on a cell, bacteria, virus, fungus or other biological entities. In brief, the phage displayed-peptide library with huge diversity of displayed-peptides is panned against a target ligand which is immobilised on a surface (e.g., wells of microtiter plate or petri dish). Specific or strong peptide binders will interact strongly with the ligand while non-specific or weak binders will be removed through extensive washing. The bound phages are subsequently eluted chemically and subjected to repeat panning in order to enrich the specific binding clones. Upon the last round of biopanning, individual clones of phage displayed-peptides are randomly selected and propagated. The genomic DNAs from these phage clones are extracted and sequenced in order to identify the oligonucleotide sequence/s that encode/s the displayed peptide/s.

Finally, the sequence/s of the displayed peptide which bind specifically to the ligand can be deduced from the oligonucleotide sequence/s.
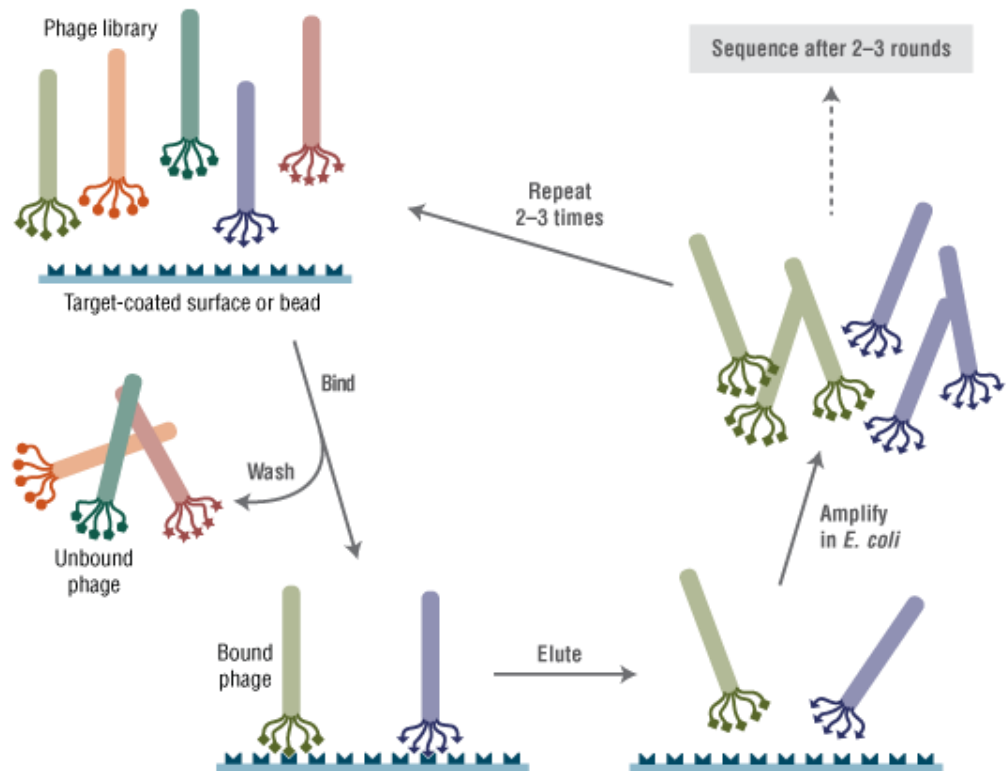
Figure 2.5: Application of phage displayed-peptide library in biopanning to select peptides that bind specifically to a ligand (New England Biolabs).

The availability of several commercial phage displayed-peptide libraries in the market has made the screening for ABPs even easier without the hassle of constructing the phage library, as was practised in the earlier years when this technology was first introduced (Creative Biolabs, 2007; New England Biolabs, 2020). These libraries allow the selection of peptides with high binding affinity

to a bacterium from a population of peptide clones of large diversity. Using a commercially available phage displayed-peptide library, Sainath Rao and colleagues (2013) were able to select a 12-mer ABP named EC5 (RLLFRKIRRLKR) via biopanning against *E. coli*. Downstream studies revealed that this peptide was strongly potent against several Gram-negative bacteria but without significant haemolytic and cytotoxicity effects to mammalian cells. In a similar study, Pini et al. (2004) successfully developed several dendrimeric peptides (10-mer peptide) with potent antibacterial effects towards several Gram-positive and Gram-negative bacteria. However, these peptides were subjected to post-selection modification to enhance their stability.

Phage display selection offers several advantages for ABP development as compared to other conventional methods. As the biopanning process will only select phage clones displaying peptides with high binding affinity to bacterial surface ligands, it is believed that these peptides may contain certain motif/s that is/are involved in the interaction with the bacterial structure/s. Through sequencing of the oligonucleotide insert that encode for the peptide, the motif can be determined if it is consistently present in different peptides isolated from independent rounds of biopanning against the same bacterial target. Subsequently, further development of the peptide to an ABP can consider to include this motif.

Secondly, phage display selection may simultaneously select multiple peptides with potent antibacterial activity towards a target bacterium from a single set of biopanning. As diverse clones of phage displayed-peptides from the library are panned against the whole bacteria, it may allow selection of various peptides that bind to different surface structures or ligands from different angle of the bacteria simultaneously. Upon confirming their binding affinity and/or specificity to the bacteria (e.g. via enzyme-linked immunosorbent assay, ELISA), only peptide candidates that demonstrate strongest bacterial interaction and antibacterial features are chosen for downstream screening. This strategy allows the selection of the best peptide candidates to be developed into potent ABPs.

While the template-based design or computational-assisted rational design may generate ABPs with desirable antibacterial features, the risk of toxicity of these peptides to mammalian cells is sometimes unpredictable (Giuliani, Pirri and Nicoletto, 2007; Fjell et al., 2012). In contrast, phage display selection of ABPs might reduce the probability of generating cytotoxic or haemolytic peptides. As the affinity selection (or biopanning) is performed against a bacterium target, in which the conserve surface structures of the bacterium are commonly different from the mammalian cells, the selected peptides might contain motifs that are exclusively binding to the former but not the latter. Thus, this approach may generate peptides with high selectivity to the bacteria instead of mammalian cells. In a study conducted by Zhang et al. (2014), a number of hypothetical ABPs were selected from a phage displayed peptide library via biopanning against several outer membrane proteins (OMPs) of a human pathogenic Gram-

negative bacterium *Brucella abortus*. Apart from exhibiting significant anti-infective activity *in vitro* and *in vivo*, these peptides did not affect the growth and survival of host macrophages, indicating the selection of peptides that bind exclusively to the membrane of the bacteria.

However, phage display selection may not be the perfect strategy for ABP discovery if it stands alone. Though the peptides displayed by the phage particles may possess characteristics of ABPs, they may not be able to exert antibacterial action directly to the target bacteria due to the effect of steric hindrance from the phage particles. In many studies, these attached peptides only served as the template for the synthesis of free peptides through solid-phase synthesis method (Pini et al., 2005; Tanaka, Kokuryu and Matsunaga, 2008; Sainath Rao, Mohan and Atreya, 2013, Flachbartova et al., 2016). Even though the free peptide is exactly similar to the phage displayed counterpart, it may not possess sufficient criteria to be directly used as an ABP. As the affinity selection is a random process, it may select those peptides with certain motifs that are involved in the bacterial binding but lack of the cationicity and/or amphipathicity required for antibacterial action. Moreover, as the biopaninng is performed against the whole bacteria using a random phage display library, it may allow the selection of phage-displayed peptides that bind to any site or surface structures of the target bacteria, which may include elements that are not crucial for the biological function or survival of the bacteria (Christensen et al., 2001). Due to these limitations, to date, there are only very few studies on potent ABP discovery by using phage display strategy solely. Apart from the studies by Bishop-Hurley et al. (2010) and Sainath Rao et al. (2013), so far there is no other studies which

successfully isolated a peptide which can be directly applied as ABP without any modification.

2.3.4 Combination of Phage Display Selection and Computational-Assisted Optimisation for Development of Novel ABP

In consideration of the limitations by the single strategy as described above, one can consider combining these strategies to develop ABPs with optimised antibacterial potency and minimal toxicity. Starting from a peptide that contains motif/s that interact with certain bacterial ligand/s, one can improve the antibacterial potency and reduce the haemolytic activity of the peptide by systematic alteration of residue/s that led to appropriate cationicity and hydrophobicity. On this aspect, phage-display selection can be considered to achieve the first goal, followed by peptide modification using computational tool or online software to attain the second goal. As demonstrated from a study by Tanaka, Kokuryu and Matsunaga (2008), unmodified peptides selected from a phage display selection only exhibited limited spectrum of antibacterial activity towards *Bacillus subtilis*. However, the peptide potency against the bacterium was greatly enhanced while the antibacterial spectrum further encompassed *E. coli* and *S. cerevisiae* when proline, glutamine and asparagine in the original peptide were substituted with phenylalanine, valine, and tryptophan, respectively. These findings suggested that rational modification to peptides that are selected from random phage display selection may serve as a better strategy to optimise the antibacterial efficiency of the peptides.

In this study, phage displayed-peptide library was used to select peptides with high binding affinity to a target bacterium via a process called biopanning. The affinity-selected peptides were used as templates for synthesis of free linear peptides. In consideration to the cationicity and hydrophobicity that contribute to optimum antibacterial potency and minimum toxicity of a peptide, the peptide was modified by substituting certain amino acids with residues which can enhance the peptide cationicity that falls within +5 to +9, as well as attaining moderate hydrophobicity within the range of 45% to 50%. All these modifications were carried out using the online database for antimicrobial peptide (APD II).

CHAPTER 3

MATERIALS AND METHODS

3.1   General Outlines of Experiment

The entire experiment was begun with a series of affinity selection of phage-displayed peptides with high binding affinity to *Pseudomonas aeruginosa* (*P. aeruginosa*). In order to achieve this, a 12-mer phage-displayed peptide library was used to biopann against the whole bacterium of *P. aeruginosa*. After four rounds of repeated biopanning, individual clones of phage displaying peptides that bound to the bacterium were randomly selected. The binding affinities of the selected phage displayed-peptides were screened by direct phage-bacteria ELISA. High affinity phage binders to the bacterium were selected and amplified for DNA extraction and sequencing. The DNA sequences were deduced into peptide sequences and aligned and analysed using bioinformatics tools to search for consensus sequence or peptide motif/s that was/were present among the peptides. Phage-displayed peptide with the highest frequency of selection from the biopanning was chosen as the template for rational modification and design for a free linear peptide with improved features of antibacterial peptides. The designated antibacterial peptide, namely PAM-5, was synthesized via multipin peptide synthesis technique by an outsourced company.

The synthesized peptide was tested for its antibacterial potency against a list of Gram-positive and Gram-negative bacteria from the reference and clinically isolated strains. By using a modified microbroth dilution assay as recommended by Clinical Laboratory Standard Institute (CLSI), the minimal bacteriostatic concentrations (MICs) or/and minimal bactericidal concentrations (MBCs) of PAM-5 towards these bacteria were determined. In order to study the kinetic killing of PAM-5, selected bacteria were treated with the peptide and incubated for a range of different time intervals before inoculating them on media agar for the evaluation of bacterial viability. The killing kinetics between PAM-5 and selected bactericidal antibiotics were also compared. Subsequently, the stability of PAM-5 in *ex vivo* condition was assessed by determining the antibacterial potency of the peptide using a simulated *in vivo* condition, in which the bacteria were incubated with the peptide in human plasma before inoculation on culture media. The resulting MICs and/or MBCs by this *ex vivo* assay were compared to the value obtained from the *in vitro* assay as determined previously.

Next, the mechanisms of antibacterial activity of PAM-5 were studied. Firstly, the effect of PAM-5 on bacterial outer membrane was observed via scanning electron microscopy to screen for any morphological difference between peptide-treated and untreated bacteria. Secondly, the ability of the peptide to permeabilize bacterial inner membrane was studied by SYTOX Green uptake assay, in which the degree of bacterial uptake of the membrane-impermeable, fluorescent probe corresponds to the degree of inner membrane permeabilization by the peptide. Then, the ability of PAM-5 to bind bacterial nucleic acid was screened by gel retardation assay. In this assay, genomic DNAs were extracted

from several target bacteria by conventional phenol-chloroform extraction method. The extracted DNAs were treated with PAM-5 before subjecting them to DNA electrophoresis. The relative migration rate between the treated and untreated DNAs may justify the DNA-binding ability of the peptide.

The toxicity of PAM-5 was screened on two mammalian cell lines and human red blood cells (hRBCs). Using PrestoBlue cell viability assays, the cytotoxic effects of the peptide to HeLa cell and Vero cell at various peptide concentrations were evaluated. On the other hand, the peptide of the same range of concentrations was also tested for its haemolytic effect on hRBCs using *in vitro* haemolytic assay. Finally, the cytotoxic effect of PAM-5 was further analysed based on its ability to cause membrane permeabilization to Vero cells at all the tested concentrations. Using fluorescent microscopy, the amount of PAM-5-treated Vero cells which exhibited fluorescent green was compared to the positive and negative control for toxicity. The degree of fluorescent green, which corresponds to the degree of peptide toxicity, was also measured by fluorescent spectrophotometry.

All the above-mentioned assays were carried out in triplicate to ensure reproducibility of the data.

3.2 Materials

3.2.1 Labware, Consumables and Equipment

Refer to **APPENDIX A**.

3.2.2 Preparation of Solutions, Buffers and Media

Refer to **APPENDIX B**.

3.2.3 Bacterial Strains

A total of 17 strains of bacteria from twelve species were used for different experiments in this study. For affinity selection of phage displayed-peptides, the target bacterium of biopanning was a reference strain of *P. aeruginosa* ATCC 27853, which was kindly provided by Dr Sit Nam Weng from the Department of Biomedical Science, Faculty of Science, Universiti Tunku Abdul Rahman. Upon selection and rational modification of the phage-displayed peptides, the newly designed and synthesized free linear peptide was screened for its antibacterial potency against the *Pseudomonas* and other bacterial strains of both ATCC reference and clinically isolated strains. The reference strains of bacteria were supplied by the Department of Biomedical Science, Faculty of Science, Universiti Tunku Abdul Rahman, which included *Klebsiella pneumoniae* (*K. pneumoniae*) ATCC 13883, *Escherichia coli* (*E. coli*) ATCC 25922, *Acinetobacter baumannii* (*A. baumannii*) ATCC 19606, *Staphylococcus aureus* (*S. aureus*) ATCC 25923, *Enterococcus faecalis* (*E. faecalis*) ATCC 19433 and *Streptococcus pyogenes* (*S. pyogenes*) ATCC 19615. On the other hand, the

71

clinical isolates were acquired from the microbiology division of Pathology Laboratory, Gleneagles Medical Centre, Penang. These included *Salmonella enterica serovar* Typhi (*S.* Typhi) with the laboratory number 1238912, *Shigella flexneri* (*S. flexneri*) 1109563, *Acinetobacter junii* (*A. junii*) 1191828, *P. aeruginosa* 1320026 and 12594264, *E. coli* 1160702, *K. pneumoniae* 1139142 and 1208398, *Serratia marcescens* (*S. marcescens*) 1191741 and *Streptococcus anginosus* (*S. anginosus*) 1360589. The identity of these clinical isolates and their corresponding antibiotic susceptibility profiles were determined by VITEX 2 system. According to the analysis, these bacteria possessed different profiles of drug or multidrug resistance. The list of these clinically isolates and their corresponding antibiotic susceptibility profiles are listed in **APPENDIX C**.

In order to propagate phage clones selected from the biopanning processes, *E. coli* ER2738 [*F′ proA+ B+ lacIq Δ(lacZ)M15 zzf::Tn10(TetR)/fhuA2 glnV Δ(lac-proAB) thi-1 Δ(hsdS-mcrB)5*] was used. This genetically modified bacterium is a robust F$^+$ strain with rapid growth capability. It is well suited for propagation of M13 phage, which is the phage vector used in the peptide display system for this study. The bacterial stock was supplied together with the phage-displayed peptide library kit which was purchased from New England Biolabs.

3.2.4   Preparation of Bacterial Glycerol Stock and Master Culture

The bacterial strains as mentioned previously were grown on enrichment and/or selective media catered for each bacterium. The types of media used for these cultures are described in **Appendix B**. Briefly, the bacteria were inoculated on their selective agar media and incubated overnight at 37°C. After ensuring the purity of the bacteria on the next day, each bacterium was grown in its enrichment broth. After reaching its growth at log phase, the bacterial culture was centrifuged at $6,000 \times g$ for 6 minutes to pellet down the bacteria. Upon removing the supernatant, the bacterial pellet was washed with phosphate buffered saline (PBS, pH 7.4) and re-centrifuged to discard the supernatant. After $2 \times$ washing with PBS, the bacterial pellet was re-suspended thoroughly in 1 mL of PBS (pH 7.4) followed by addition of equal volume of 50% (v/v) glycerol to produce a bacterial stock at the final concentration of glycerol of 25% (v/v). Finally, 500 μL of the bacterial glycerol stock was aliquoted into each microcentrifuge tube, followed by storing them in cryogenic box at -80°C.

For every downstream assay when these bacteria were to be used, the bacteria were retrieved from the glycerol stock and inoculated on their selective agar. These cultures served as the master culture for all the assays utilizing the bacteria. The master culture plates were stored at 4°C for a maximum of seven days to ensure freshness of the bacteria.

3.2.5   Phage-Displayed Peptide Library

The phage-displayed peptide library utilized in the affinity selection in this study was purchased from New England Biolabs (Ipswich, Massachusetts, United States). The display system is based on a M13 phage vector in which its genome was modified for pentavalent display of 12-mer peptides on its surface. These displayed peptides are encoded by an oligonucleotide insert fused to its minor coat protein gene (*pIII*), where the displayed peptide is linked to the pIII protein via a short linker sequence Gly-Gly-Gly that will be further described in **Section 4.1.3**. The library is constructed with a phage titer of 1×10^{13} plaque forming units per millilitre (PFU/mL) displaying a diversity of 1.28×10^9 peptide clones. The library was aliquoted into several cryotubes and stored at -20°C for long term storage. Before use, the tube was thawed on ice to avoid heat shock stress that may affect the phage clones.

3.3   Affinity Selection of Phage Displayed-Peptides Binding to *Pseudomonas aeruginosa* via Biopanning

3.3.1   Whole Bacteria Biopanning

A total of four rounds of biopanning were performed to select phage displayed-peptides which bind to whole cell of *P. aeruginosa*. During the first round of biopanning, a hundred-fold dilution of the 12-mer phage displayed-peptide library was made by adding 10 µL of the library into 990 µL of Tris-buffered saline (TBS) [50 mM Tris-HCl (pH 7.5), 150 mM NaCl]. Then, the entire diluted phage was poured into a 60 mm-diameter petri dish containing 2 ml of *P. aeruginosa* ATCC 27853 at the titer of 10^9 colony forming unit per millilitre

(CFU/mL). The phage-bacteria mixture was incubated at room temperature for 60 minutes with gentle agitation on a rotary shaker. Upon the incubation, the mixture was precipitated by centrifugation at $5,000 \times g$ for 5 minutes at 4°C (Velocity 14R Centrifuge, Dynamica). The supernatant was discarded and the pellet was washed with TBS supplemented with 0.1% of TWEEN-20 (0.1% TBST). In the washing steps, the pellet was re-suspended with 2 ml of the TBST and vortexed briefly till it completely dissolved. The suspension was centrifuged again at $5000 \times g$ for 5 minutes at 4°C. These washing steps were repeated for another nine rounds to wash away unbound or weakly bound phages. After the final round of washing, the bound phages were separated from the bacteria with 200 µL of elution buffer [0.2 M Glycine-HCl (pH 2.2), 1 mg/mL bovine serum albumin (BSA)] with gentle agitation on an orbital shaker at room temperature for 10 minutes. Immediately upon the elution, the content was neutralized with 30 µL of neutralization buffer [1 M Tris-HCl (pH 9.1)]. The neutralized suspension was centrifuged at $5,000 \times g$ for 5 minutes at room temperature. Eighty percent of the supernatant was transferred into a fresh microcentrifuge tube. Ten microliters of the phage eluate were used for phage titer determination, while the rest of the eluate was amplified to enrich the phage clones for the subsequent rounds of biopanning. The procedure for phage titer determination will be described in **Section 3.3.2**.

The biopanning procedures were repeated for another three rounds using the amplified phage eluate from the preceding round. Except for the washing buffer, all the steps for these subsequent biopanning were similar to the first biopanning. In order to increase the washing stringency, the final concentrations of Tween-

20 in the TBST used for washing steps in the second, third and fourth round of biopanning were 0.2%, 0.3% and 0.5%, respectively. After the final round of biopanning, the unamplified eluted phages were plated on the titer agar (LB/IPTG/Xgal agar). On the next day, individual phage clones which appeared as blue plaques on the titer plate were randomly selected and propagated for subsequent analysis as will be described below. The procedures for the individual phage propagation was similar to the phage eluate amplification, which will be described in **Section 3.3.4**.

In order to avoid bias in the affinity selection, another set of biopanning for phage-displayed peptides binding to *P. aeruginosa* was carried out independently. The biopanning was also carried out for four subsequent rounds.

3.3.2   Phage Titering

The titer of the eluted phages from each round of biopanning was examined in order to determine the percentage of selection in every cycle of the affinity selection. An overnight culture of *E coli* ER2738 was diluted in 20 mL of fresh Luria-Bertani (LB) broth according to the ratio 1:100. The freshly inoculated liquid culture was incubated at 37°C in a shaker incubator until the mid-log growth phase of the bacterium was achieved (OD$_{600}$ ~ 0.5), which was ready for phage infection. Meanwhile, the phage eluate derived from every round of biopanning was serially diluted in TBS to the desire dilution (pre-amplified phage eluate was serially diluted until 10^{-4}; while post-amplified phage eluate was diluted till 10^{-10}). Ten microliters of each diluted phage were added into 200

µL of *E. coli* ER2738 at mid log phase growth and the mixture was incubated for 5 minutes in room temperature. After that, the phage-infected *E. coli* was transferred to 3 mL of molten top agar (45°C). The top agar was briefly mixed and layered onto LB agar supplemented with IPTG/Xgal (0.05 g/mL IPTG, 0.04 g/mL Xgal). Upon solidification of the top agar, the inoculated agar plate was incubated overnight at 37°C. On the next day, the number of blue plaques on the agar was counted and the phage titer (in PFU/mL) can be calculated.

3.3.3. Phage Eluate Amplification and Purification

Phage eluate yielded from the biopanning was amplified according to the protocols as described by the manufacturer (New England Biolabs). Briefly, culture of *E. coli* ER2738 for phage amplification was set up as described in **Section 3.3.2**. When the optical density of the host bacterium has reached its early-log phase (OD_{600} between 0.01 and 0.05), the remaining phage eluate after the tittering was added into the bacterial culture followed by incubation in a 37°C shaking incubator at agitation rate of 200 rpm. After 4 ½ hours of amplification, the culture was centrifuged at $12,000 \times$ g for 10 minutes at 4°C. The supernatant containing the phages was transferred into a fresh tube and re-spun. After centrifugation, the upper 80% of the supernatant (approximately 16 mL) was carefully transferred into another fresh tube which was pre-filled with 1/6 volume (~3 mL) of 20% (v/v) PEG/NaCl [20% (w/v) polyethylene glycol-8000, 2.5 M NaCl]. The supernatant-PEG/NaCl mixture was mixed well and incubated overnight at 4°C in standing position to precipitate the phages.

On the next day, the PEG precipitation was centrifuged at 12,000 × g at 4°C for 15 minutes. The supernatant was discarded completely. The whitish pellet at the bottom edge of the tube was re-suspended with 1 mL of TBS (pH 7.5) and transferred to a fresh microcentrifuge tube, followed by centrifugation at 14,000 rpm at 4°C for 5 minutes. The upper 80% of the supernatant was transferred to a fresh microcentrifuge tube and precipitated again with PEG/NaCl for 1 hour on ice. Then, the content was spun at 14,000 rpm for 5 minutes at 4°C and the supernatant was removed completely. Finally, the whitish pellet at the bottom of the tube was re-suspended with 200 µL of TBS, and this is the amplified phage eluate. Before proceeding to the next round of biopanning using this amplified phage eluate, the titer of the eluate was determined by the protocol as described in **Section 3.3.2.** This titer represented the input phage titer for the subsequent round of biopanning.

3.3.4 Individual Phage Clone Amplification

Following the random selection of individual phage clones (blue plaques) from the LB/Xgal/IPTG plate inoculated with phage eluate of the final round of biopanning as described in **Section 3.3.1**, the phages were amplified individually in a small-scale manner in order to prepare the phage clone stock for downstream analysis which will be described later. The bacterial host used to amplify these phage clones (*E. coli* ER2738) was grown in culture broth for overnight at 37°C. The next day, the overnight culture was diluted according to the dilution factor 1:100 in fresh LB broth. One millilitre of the diluted culture was dispensed into 1.5 mL-sized microcentrifuge tubes, each one for one phage clone to be

amplified. Well separated individual phage clones which appeared as blue plaques on the titer agar inoculated with the pre-amplified phage eluate were carefully picked up by sterilized cut tips. Each of the plaques was then transferred to the diluted bacterial culture in the microcentrifuge tube, followed by incubation for 4 ½ hours at 37°C with agitation of 200 rpm. After incubation, the microcentrifuge tubes were centrifuged at 12,000 rpm for 30 seconds. The supernatant was carefully transferred into a fresh microcentriguge tube without disturbing the bacterial pellet. After re-centrifugation, the upper 600 µL of the supernatant was then mixed with 600 µL of 50% (v/v) glycerol in a fresh tube. These glycerol stocks of phage clones were then stored at -80°C.

For the downstream assays and analysis, higher amounts of the phage clones were needed. Therefore, the individual phage clone was amplified in larger scale by growing the phage clone in 20 mL of host bacterial culture. The amplification steps were similar as described in **Section 3.3.3**. However, instead of phage plaques from the titer plate, 100 µL of the phage glycerol stock as described in this section was added into 20 mL of the diluted bacterial culture for the phage amplification.

3.3.5   Screening for Binding Affinity of the Selected Phage Displayed-Peptides to *Pseudomonas aeruginosa* by Phage-ELISA

Each of the randomly selected phage-displayed-peptide clone was tested for its binding selectivity to *P. aeruginosa* by using phage-bacteria ELISA as recommended by the manufacturer protocols (New England Biolabs). Prior to

the immunoassay, individual phage clones were freshly amplified according to the protocols as described in **Section 3.3.3** by adding 20 µL of phage glycerol stock into 20 mL of *E. coli* ER2738. After amplification and separation from the host bacterium via centrifugation, the pellets of the amplified phages were re-suspended in 200 µL of TBS. Next, the wells of a 96-well microtiter plate were coated with 150 µL of bacterial suspension (1.2 x 10^8 CFU/mL). A separate set of wells were filled with 150 µL of bovine serum albumin (BSA, 30 µg/mL) in coating buffer [0.1 M $NaHCO_3$ (pH 8.6)], which served as the negative control. The plate was incubated overnight at 4°C in an air-tight humidified box. On the next day, the content in the wells was discarded and replaced with 200 µL of blocking buffer [0.1 M $NaHCO_3$ (pH 8.6), 5 mg/mL BSA, 0.02% NaN_3], followed by incubation at 4°C for one hour. After that, the wells were washed for six times with 0.5% TBST. The amplified individual phage clones were subjected to four-fold serial dilutions using TBS. Each of the diluted phage clones (10^{11} PFU/mL; 150 µL) was added into the bacterial-coated wells and negative control, and the microtiter plate was placed on a rotary shaker with gentle agitation at room temperature. After one hour of incubation, the wells were washed for six times with 0.5% TBST. Upon washing, the wells were filled with 200 µL of horse-radish peroxidase (HRP)-linked anti-M13 monoclonal antibody that had been diluted according to 1:1000 in blocking buffer. After one hour of incubation at room temperature with gentle agitation, the wells were washed for six times again with 0.5% TBST. Finally, the wells were added with 200 µL of 2,2'-azino-bis (3-ethylbenzothiazoline-6-sulfonic acid) diammonium salt (ABTS) in 50 mM of sodium citrate (pH 4.0) with 30% H_2O_2. The microtiter plate was incubated at room temperature with gentle agitation. After 20 minutes

of incubation, the absorbance in the wells was read at the wavelength 405 nm (OD$_{405}$) using a microplate reader (FLUOstar Omega, BMG LabTech).

3.3.6 Phage Genomic DNA Extraction

A 10 mL of *E. coli* ER2738 was grown overnight at 37°C in a rotating incubator (200 rpm). On the next day, the overnight culture was diluted into fresh LB medium according to the dilution 1:100. The diluted bacterial culture was dispensed into microcentrifuge tubes, one millilitre in a tube for each phage clone to be amplified. Then, the bacterial culture was infected with 100 μL of phage glycerol stock as prepared in **Section 3.3.4**. The phage-bacteria mixture was incubated in a rotating incubator (200 rpm, 37°C) for 4 ½ hours. After that, the tubes containing the amplified phages were centrifuged at 12,000 × g for 1 minute at 4°C to pellet down the bacterial host. The supernatant was carefully transferred into another fresh microcentrifuge tube before another round of centrifugation. Next, 800 μL of the upper supernatant was carefully transferred into a new tube, followed by addition of 200 μL of 20% (v/v) PEG/2.5 M NaCl. The mixture was mixed well and allowed to stand in ice for approximate one hour to precipitate the phages. Subsequently, the content in the tube was centrifuged for 10 minutes at 14,000 rpm at 4°C. After removing the supernatant completely, the pellet was re-suspended thoroughly with 100 μL of iodide buffer [10 mM Tris-HCl (pH 8.0), 1 mM EDTA, 4 M sodium iodide (NaI)]. Then the suspension was added with 250 μL of absolute ethanol and incubated at room temperature for 20 minutes. After centrifuging the tubes at 14,000 rpm for 10 minutes at 4°C, the supernatant was discarded, and the pellet was washed with

iced-cool 70% ethanol. Upon another centrifugation, the supernatant containing the 70% ethanol was removed, and the pellet was dried completely in vacuum at 37°C. Finally, the dried pellet was re-suspended with 30 μL of TE buffer. The DNA samples were kept in -20°C before analysis.

The concentration of the extracted phage DNAs was determined using NanoDrop 2000 spectrophotometer. Meanwhile, the purity of the DNA was analysed by 1.5% agarose gel electrophoresis which was conducted at 60 V for one hour in $1 \times$ TAE running buffer. The agarose gel was then stained with 0.5 μg/mL of ethidium bromide solution for five minutes, followed by de-staining with distilled water for ten minutes. Phage DNA bands in the gel were viewed on an UV illuminator. DNA samples that unanimously demonstrated similar bands at approximately 6400 nucleotides were selected for sequencing. The DNA samples were sequenced by 1st Base Sequencing Company using 96 gIII sequencing primer (5'- HOCCCTCATAGTTAGCGTAACG-3') provided by the manufacturer of the phage-displayed peptide library.

3.3.7 Analysis of Phage-Displayed Peptide from DNA Sequencing

The electropherogram of the DNA sequence was viewed using Sequence Scanner v2.0 to identify the oligonucleotide sequence that encodes the displayed-peptide. According to the manufacturer, the oligonucleotide insert is located after a conserved 39-nucleotide linker sequence within the phage genome   (ATGGGATTTTGCTAAACAACTTTCAACAGTTTCGGCCGA). Then, the complementary sequence of the oligonucleotide insert was determined

and deduced into peptide sequence by using ExPASy DNA translate tool (available at http://web.expasy.org/translate/). The physiochemical properties of the peptide were analysed using an online software named Antimicrobial Peptide Calculator and Predictor (http://aps.unmc.edu/AP/main.php). The peptides were aligned using GeneDoc to examine the frequency of selection for a particular peptide as well as to identify any consensus motif/s between all the selected peptides.

3.4   Screening for Antibacterial Effect of Pa1 and Pa4

3.4.1   Synthesis of Free Linear Peptide Pa1 and Pa4

Two phage-displayed peptides with the highest frequency of selection from the two independent biopanning, namely Pa1 and Pa4, were chosen for synthesis of free linear peptides to be screened for their antibacterial potencies. Free linear form of Pa1 and Pa4 with the peptide sequences of GPVNKSSTILRM and KWHWKDKNALRM, respectively, were synthesized by Bio Basic Inc. (Canada) using N-9-fluorenylmethyloxycarbonyl (Fmoc) chemistry. The synthesized peptides were purified by analytical reverse-phase high-performance liquid chromatography (R P-HPLC) to the purity level of > 95%. The peptide molecular weights were determined by mass spectrophotometry. The lyophilised form of the peptide was packaged in a tightly sealed tube and stored at -20°C.

Before use, the peptides were equilibrated to room temperature for about 30 minutes. Degassed water and phosphate-buffered saline (PBS, pH 7.4) were used to dissolve and dilute the peptides since the peptides contain methionine residue, in which its side chain is susceptible to oxidation. The peptide solutions were prepared in which their concentrations were determined from the weighed samples. Upon weighing, the peptides were dissolved in 100 μL of degassed sterile distilled water. The completely dissolved peptide was subsequently added with 900 μL of sterile PBS (pH 7.4) followed by two-fold serial dilution using the buffer to yield a set of peptide solutions with concentrations ranging from 2 μg/mL to 512 μg/mL, as illustrated in **Figure 3.1**. The diluted peptide solutions were stored in silica bottles at 4°C for a maximum of seven days to ensure the peptide efficiency.

Polymyxin B (Merck Millipore), which was used as comparative antibacterial agents for antibacterial assay, was prepared as described above.
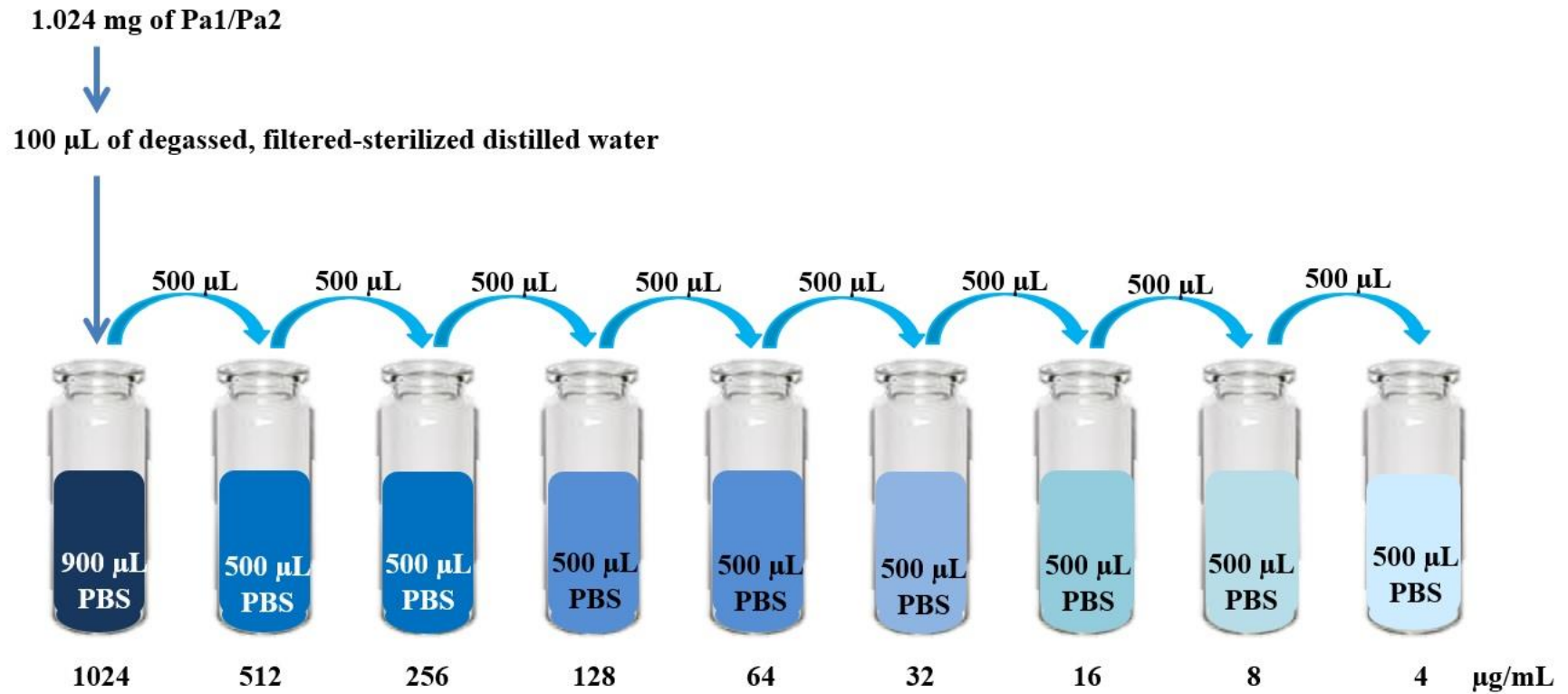
Figure 3.1: Illustration on peptide dissolving and serial dilutions into concentrations that range from 1024 µg/mL to 4 µg/mL.

3.4.2 Screening for Antibacterial Effect of Pa1 and Pa4 on *Pseudomonas aeruginosa* by Microbroth Dilution Assay

The antibacterial potencies of Pa1 and Pa4 against *P. aeruginosa* ATCC 27853 were screened by using microbroth dilution assay as recommended by Clinical Laboratory Standard Institute (CLSI) with slight modification (CLSI, 2012). Briefly, an overnight culture of the reference strain of *P. aeruginosa* was prepared by inoculating one to two single colonies of the bacterium from the master culture plate (as described in **Section 3.2.4**) into 10 mL of Mueller Hinton (MH) broth, followed by overnight incubation (16-18 hours) at 37°C in a shaking incubator (200 rpm). On the next day, a hundred-fold dilution of the overnight culture was performed by adding 200 µL of the bacterial culture into 19.8 mL of fresh MH broth. The diluted culture was then incubated at 37°C with agitation at 200 rpm until the bacterium grew to its mid-log phase ($OD_{600} \sim 0.5$). Then, the bacteria were pelleted by centrifugation at $6,000 \times g$ for 6 minutes at 4°C. The supernatant was discarded, and the pellet was washed twice by re-suspending with PBS (pH 7.4) followed by re-centrifugation at the same centrifugal force and duration. After the last washing, the bacterial pellet was re-suspended in 1 mL of PBS, which served as the concentrated bacterial stock. The titer of the bacterial stock was determined by a series of ten-fold dilutions followed by inoculation of the diluted bacteria on MH agar media. After overnight incubation, the number of colonies on the media was counted for titer determination.

Then, the bacterial stock was serially diluted with PBS (pH 7.4) to the dilution which corresponded to the titre of 10^5 CFU/mL. One hundred microliter of the diluted bacteria was then loaded into wells of 96-well microtiter plate. The bacteria were treated with 100 µL of Pa1/Pa4 at the final concentrations ranging from 2 µg/mL to 256 µg/mL. Positive control of antibacterial effect was set up by treating the bacteria with polymyxin B at the same range of concentrations. On the other hand, untreated bacteria suspended in equal volume of PBS was set up as the negative control. **Table 3.1** depicts the above-described contents in the wells of the microtiter plate. After setting up the assay, the microtiter plate was pre-incubated for 1 hour at 37°C, followed by addition of 50 µL of MH broth into each well. The microtiter plate was then further incubated overnight for 16-18 hours at 37°C.

Table 3.1: Contents filled into the wells of samples, positive control and negative control during the microbroth dilution assay

Contents	Sample Well	Positive Control Well	Negative Control Well
Bacterial suspension	100 µL	100 µL	100 µL
Pa1/Pa4	100 µL	-	-
Polymyxin B	-	100 µL	-
PBS (pH 7.4)	-	-	100 µL
MH broth	50 µL	50 µL	50 µL

* The hyphen (-) in the table indicates the absence of the particular variable.

On the next day, the contents in the wells were visually inspected for turbidity which indicated bacterial growth. Then, 10 µL of the content in every well was spread onto MH agar to examine the presence of viable bacteria after the treatment. Cultures in the wells with observable turbidity were serially diluted up to 10^{-6} with PBS, followed by inoculation on MH agar for bacterial titering. All the inoculated media were incubated overnight at 37°C.

On the next day, the growth pattern of the peptide-treated bacteria, positive and negative control on the media was examined and compared to estimate the minimal inhibitory concentration (MIC) and/or minimal bactericidal concentration (MBC) of the peptide towards the bacteria. The number of bacterial colonies growing on the media plates with countable colonies was counted to determine any growth reduction from the peptide-treated bacteria as compared to the non-treated bacteria. According to CLSI, MIC for an antibacterial agent tested in microbroth dilution assay is the lowest concentration of the agent that is able to inhibit visible bacterial growth in the growing medium (Cockerill, 2012). On the other hand, MBC is the lowest concentration of the agent that is required to kill at least 99.99% of the bacteria (Wikler et al., 2009). **Figure 3.2** depicts the determination of MIC and MBC of an antibacterial agent in a microbroth dilution assay. The determination of the peptide potency in this study was carried out thrice to ensure reproducibility.
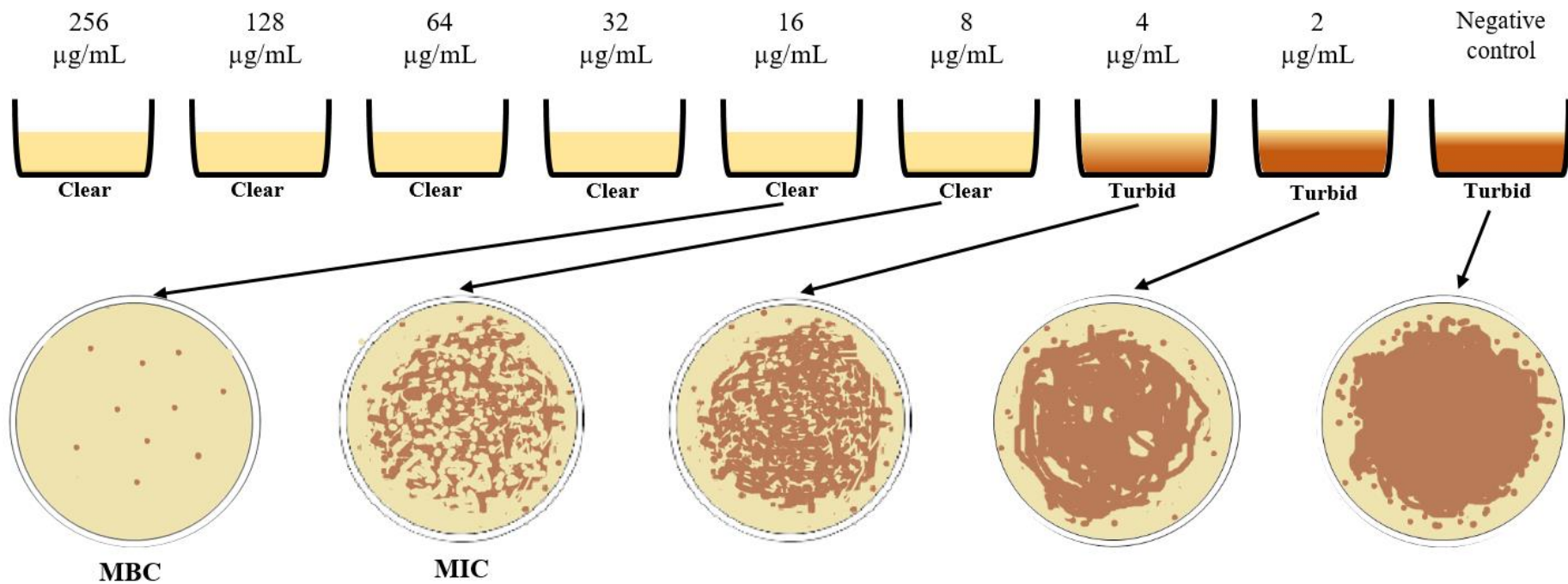
Figure 3.2: MIC and MBC determination in microbroth dilution assay. In this scenario, bacteria in the wells were treated with an antibacterial agent at concentrations ranging from 2 μg/mL to 256 μg/mL. Wells containing bacteria treated with the agent at 2 μg/mL and 4 μg/mL are turbid similar to the negative control. MBC in this figure is 16 μg/mL.

3.5   Evaluation of Antibacterial Effect of PAM-5

3.5.1   Modification of Pa4 to PAM-5

Pa4, the 12-mer peptide with the highest selection frequency from the biopanning, was modified to enhance the peptide length, cationicity and hydrophobicity. These modifications were performed by using two online softwares, namely Antimicrobial Peptide Calculator and Predictor (http://aps.unmc.edu/AP/prediction/prediction_maim.php) and Antimicrobial Peptide Designer (http://aps.unmc.edu/AP/design/design_improve.php). Firstly, the original 12-mer peptide Pa4 with the sequence of K-W-H-W-K-D-K-N-A-L-R-M was elongated to 15-mer by adding three amino acids consisted of arginine (R), proline (P) and leucine (L) into the position between the fourth (tryptophan, W) and the fifth (lysine, K) amino acid of Pa4. In addition, the less cationic histidine (H) and negatively charged aspartic acid (D) in Pa4 were replaced with cationic lysine (K) and arginine (R), respectively. In order to increase the peptide hydrophobicity, the less or non-hydrophobic residues such as asparagine (N) and alanine (A) were substituted with leucine (L) and valine (V) of higher hydropathy index. The newly modified peptide, namely PAM-5, possessed the sequence K-W-K-W-R-P-L-K-R-K-L-V-L-R-M.

Similarly, PAM-5 was synthesized and purchased from Bio Basic Inc. (Canada) using the same method as for Pa4. The peptide, synthesized at the purity level of > 95%, arrived as lyophilized form and was packaged in a tightly sealed tube and stored at -20°C. Preparation of the peptide solution was carried out according to the protocols as described in **Section 3.4.1**.

3.5.2 Screening for Antibacterial Effect of PAM-5 on *Pseudomonas aeruginosa* by Microbroth Dilution Assay

The newly synthesized PAM-5 was tested for its potency against *P. aeruginosa* ATCC 27853 by the same protocols as described in **Section 3.4.2**. Similarly, the potency of the peptide towards the bacterium was expressed as MIC and/or MBC obtained from the microbroth dilution assay, which was performed thrice to ensure data reproducibility.

3.5.3 Screening for Antibacterial Spectrum of PAM-5 Towards Selected Panel of Gram-Positive and Gram-Negative Pathogenic Bacteria

Using the same assay, the spectrum of bacterial species or strains targeted by PAM-5 was also determined on selected bacteria that are commonly associated with infections. These bacteria are listed in **Appendix C**.

In consideration to the requirement for optimal growth of certain bacteria, several modifications to the microbroth dilution assay were made when it was carried out for *S. pyogenes* ATCC 19615 and *E. faecalis* ATCC 19433. Instead of MH broth, these bacteria were grown in brain heart infusion (BHI) medium without agitation as they are facultative anaerobes. Besides, ampicillin was used as the positive control as polymyxin B is not effective against both the bacteria. After treatment, the bacteria were inoculated onto tryptic soy agar (TSA) for titre enumeration. Untreated bacteria were also set up as the negative controls.

3.6 Assessment of PAM-5 Stability in Human Plasma

To address the question whether PAM-5 is able to retain its antibacterial potency in human plasma, the antibacterial assay was carried out in a simulated *in vivo* condition and the MBC obtained from this assay was compared to the MBC derived from the *in vitro* assay as described previously. Briefly, the microbroth dilution assay as described in **Section 3.4.2** was set up with slight modification. All the parameters and conditions for the assay were resumed except for the buffer that was used to prepare the bacterial suspension. Instead of PBS, the bacteria were re-suspended and serially diluted using fresh human plasma separated from blood sample freshly taken from a healthy individual with ethical approval from the university.

3.7 Study of Kinetic Killing of PAM-5

The kinetic killing of PAM-5 on selected bacteria was determined by using time-kill assay according to the guidelines as recommended by CLSI with slight modification. Similarly, the procedures for bacterial preparation which included overnight culture, dilution of overnight culture, harvesting and serial dilutions of the bacteria were performed as described in **Section 3.4.2**. Subsequently, 100 µL of the diluted bacteria (~10^3 CFU/mL) was dispensed into each of the six wells of a 96-well-microtiter plate. The bacteria in all the six wells were then simultaneously treated with 100 µL of PAM-5 at its $2 \times$ MBC as determined in **Section 3.5**.**2** and **3.5.3**. On the other hand, six wells of bacteria added with 100 µL of PBS (pH 7.4) were set up as the negative controls. In order to compare the kinetic killing between PAM-5 and antibiotics, bacteria treated with gentamicin

and polymyxin B at their $2 \times$ MBCs were also set up. The contents for each well are summarised in **Table 3.2**.

Upon treatment, each of the bacterial categories (PAM-5-treated bacteria, gentamicin-treated bacteria, polymyxin B-treated bacteria and negative control) was inoculated onto MH agar at every 10 minutes for a total duration of 60 minutes. The media plate was divided into four quadrants, each to be inoculated with one of the bacterial categories as mentioned above. During the inoculation at each 10-minute interval, the bacterial suspension in the wells was mixed well before inoculating three suspensions (60 μL each) onto each quadrant on the MH agar as shown in **Figure 3.3**. The inoculated media were incubated overnight at 37°C, and the number of colonies from each inoculation was counted on the following day.

Table 3.2: Contents and volume loaded into the wells of 96-well microtiter plate in the time-kill assay

Contents	Sample Well	Antibiotic Well	Antibiotic Well	Negative Control Well
Bacterial suspension	100 μL	100 μL	100 μL	100 μL
PAM-5	100 μL	-	-	-
Gentamicin	-	100 μL	-	-
Polymyxin B	-	-	100 μL	-
PBS (pH 7.4)	-	-	-	100 μL

* The hyphen (-) in the table indicates the absence of the particular variable.

Figure 3.3: Schematic representation of quadrant setting on the inoculating media for the time-kill assay. At each 10-minute interval, the treated- and non-treated bacteria were inoculated on respective quadrant

3.8 Screening for Bacterial Outer Membrane Disruption by PAM-5 via Scanning Electron Microscopic (SEM)

Structural or morphological changes to the surface of PAM-5-treated bacteria were examined by scanning electron microscopy (SEM). Briefly, *P. aeruginosa* ATCC 27853 was treated according to the protocols as described for the antibacterial microbroth dilution assay. However, the bacteria titer was adjusted to 10^7 CFU/mL as it was the minimum required titer for SEM analysis. In a microcentrifuge tube, 100 µL of the bacterium was treated with PAM-5 at the final concentration of 128 µg/mL. Bacteria treated with 128 µg/mL of polymyxin B and untreated bacteria in PBS were used as the positive and negative control, respectively. Following incubation for one hour at 37°C, the treated and untreated bacteria were centrifuged at $6000 \times$ g for 5 minutes. The supernatant was discarded, and the bacterial pellet was washed twice with PBS (pH 7.4). Then, the bacteria were fixed with 500 µL of 3% (v/v) glutaraldehyde in 0.1 M PBS for 18 hours at 4°C. Next, the glutaraldehyde was removed by centrifugation at $4000 \times$ g for 5 minutes, followed by two-times washing the bacterial pellet with PBS (pH 7.4). Then, the bacteria were subjected to sequential dehydration by a series of ethanol at ascending concentrations as follows:

i. 25% (v/v) ethanol, 5 minutes

ii. 50% (v/v) ethanol, 10 minutes

iii. 75% (v/v) ethanol, 10 minutes

iv. 95% (v/v) ethanol, 10 minutes

v. 100% (v/v) absolute ethanol, 10 minutes (3 changes)

The ethanol-dehydrated bacterial specimens were subjected to freeze drying for 18 hours. After that, the bacterial specimen was transferred to a carbon tape adhered to a copper stub. Following sample coating with platinum for 90 seconds, the copper stub was placed onto a specimen holder of a scanning electron microscope (JSM-7610F), where the specimen was observed under magnification power of 18,000 $\times$, 30,000 $\times$ and 40,000 $\times$.

3.9 Screening for Ability of PAM-5 to Permeabilize Bacterial Inner Membrane via SYTOX® Green Uptake Assay

The integrity of bacterial inner membrane after treatment with PAM-5 was accessed by the membrane impermeable SYTOX® Green dye. The antibacterial microbroth dilution assay was set up as described in **Section 3.4.2** with slight modification. Instead of 10^5 CFU/mL, the wells of 96-well microtiter plate were loaded with 100 µL of *P. aeruginosa* at the titre of 10^6 CFU/mL. Then, the bacteria were treated with equal volume of PAM-5 at the final concentrations ranging from 2 µg/mL to 256 µg/mL. Concurrently, both polymyxin B-treated and non-treated bacteria were set up as the positive and negative controls, respectively. After one hour of incubation at 37°C, 100 µL of the treated bacterial suspension was transferred to a flat bottom, white opaque 96-well microtiter plate. Each of the wells was added with 50 µL of 1 µM of SYTOX® Green dye. After 15 minutes of incubation in the dark, the fluorescent signal generated from each well was measured by Tecan Infinite M200 microplate reader, in which the excitation and emission wavelength were set at 485 nm and 520 nm, respectively. The assay was triplicated to ensure data reproducibility.

3.10 Screening for Nucleic Acid Binding by PAM-5

3.10.1 Bacterial Genomic DNA Extraction

Genomic DNAs were extracted from selected four reference strains of bacteria, which were *E. coli* ATCC 35218, *P. aeruginosa* ATCC 27853, *A. baumannii* ATCC 19606 and *K. pneumoniae* ATCC 13883. An overnight bacterial culture was set up as described in **Section 3.4.2**. Next, 5 mL of the overnight culture was transferred into a sterile 15 mL-centrifuge tube, and the tube was centrifuged at $6000 \times g$ for 5 minutes at room temperature to pellet down the bacteria. Upon centrifugation, the supernatant was discarded, and the pellet was re-suspended in 1.5 mL of PBS. Next, the bacterial suspension was transferred into a sterile 2.0 mL-microcentrifuge tube and centrifuged at 14,000 rpm for 5 minutes at room temperature. After discarding the supernatant, the bacterial pellet was re-suspended in 570 µL of Tris-EDTA (TE) buffer (pH 8.0), followed by addition of 30 µL of 10% (w/v) sodium dodecyl sulfate (SDS) buffer and 8 µL of proteinase K (18 µg/mL). The mixture was incubated at 37°C for 1 hour 30 minutes. Then, 100 µL of 5 M NaCl and 80 µL of 10% CTAB/0.7 M NaCl solution were added and the mixture was further incubated at 65°C for 20 minutes. Next, 780 µL of chloroform/isoamyl alcohol at the ratio of 24:1 was added to the mixture followed by centrifugation at 14,000 rpm for 5 minutes at room temperature. After centrifugation, the aqueous supernatant was aspirated carefully and transferred into a new microcentrifuge tube. An equal volume of phenol/chloroform/isoamyl alcohol at the ratio 25:24:1 was added to the supernatant and the mixture was centrifuged at 14,000 rpm for 5 minutes at room temperature. This step was repeated for three times to minimize protein contamination and increase the purity of the extracted DNA. After that, the

supernatant was aspirated to a new microcentrifuge tube, followed by addition of 2.5 volumes of ice-cooled absolute ethanol. The tube was gently inverted for a few times before being incubated at -20°C for 40 minutes to precipitate the DNA. After the precipitation, the tube was centrifuged at 14,000 rpm for 5 minutes at room temperature. The supernatant was discarded, and 1 mL of 70% ethanol was added to the pellet. The tube was then centrifuged at 14,000 rpm for 5 minutes at room temperature. These washing steps were repeated twice to reduce the salt contamination as much as possible. After washing, the supernatant was removed, and the pellet DNA was dried at 70°C for about 15 minutes. Finally, the DNA pellet was dissolved in 100 µL of TE buffer and stored overnight at 4°C. On the next day, the concentration and purity of the extracted DNA were determined using nanophotometer (Implen, Germany).

3.10.2 Gel Retardation Assay

In order to screen for the DNA-binding ability of PAM-5, gel retardation assay or electrophoretic mobility shift assay (EMSA) was conducted using the genomic DNA extracted from the four bacteria as described in **Section 3.10.1**. In addition, the peptide was also screened for its ability to bind to a plasmid DNA, pBR322, which was purchased from Thermo Fisher Scientific.

Before the assay, the extracted DNAs which were stored at 4°C were equilibrated to room temperature. Based on the concentration of the extracted DNA as determined in **Section 3.10.1**, the DNA was diluted accordingly to 100 ng/µL by TE buffer. Five microliters of the diluted DNA were aliquoted into

every microcentrifuge tube, each treated with 5 µL of PAM-5 at the final concentrations which ranged from 4 µg/mL to 256 µg/mL. In terms of negative control, the DNA was added with 5 µL of TE buffer (pH 8.0). The contents in these microcentrifuge tubes are illustrated in **Figure 3.4**. All the treated and untreated DNAs were incubated at room temperature for 1 hour 30 minutes. After that, 10 µL of the DNA-peptide mixture was mixed with 2 µL of 6× loading buffer (Norgen Biotek) before loading the mixture into wells of 1.5% agarose gel for electrophoresis. The electrophoresis was then carried out at 100 V for 30 minutes.

Upon electrophoresis, the agarose gel was stained with freshly prepared 0.5 µg/mL ethidium bromide (EtBr) for three minutes followed by destaining in distilled water for ten minutes. After that, the gel was viewed under an UV illuminator to compare the relative band migration pattern between PAM-5-treated- and non-treated DNAs. This gel assay was conducted in triplicates to ensure data reproducibility.

On the other hand, EMSA was also conducted for DNAs treated with polymyxin B of the same range of concentrations in order to compare the relative migration between PAM-5-treated and polymyxin B-treated DNAs. In addition, the similar procedures were carried out to study the binding ability of PAM-5 and polymyxin B to plasmid DNA pBR322.
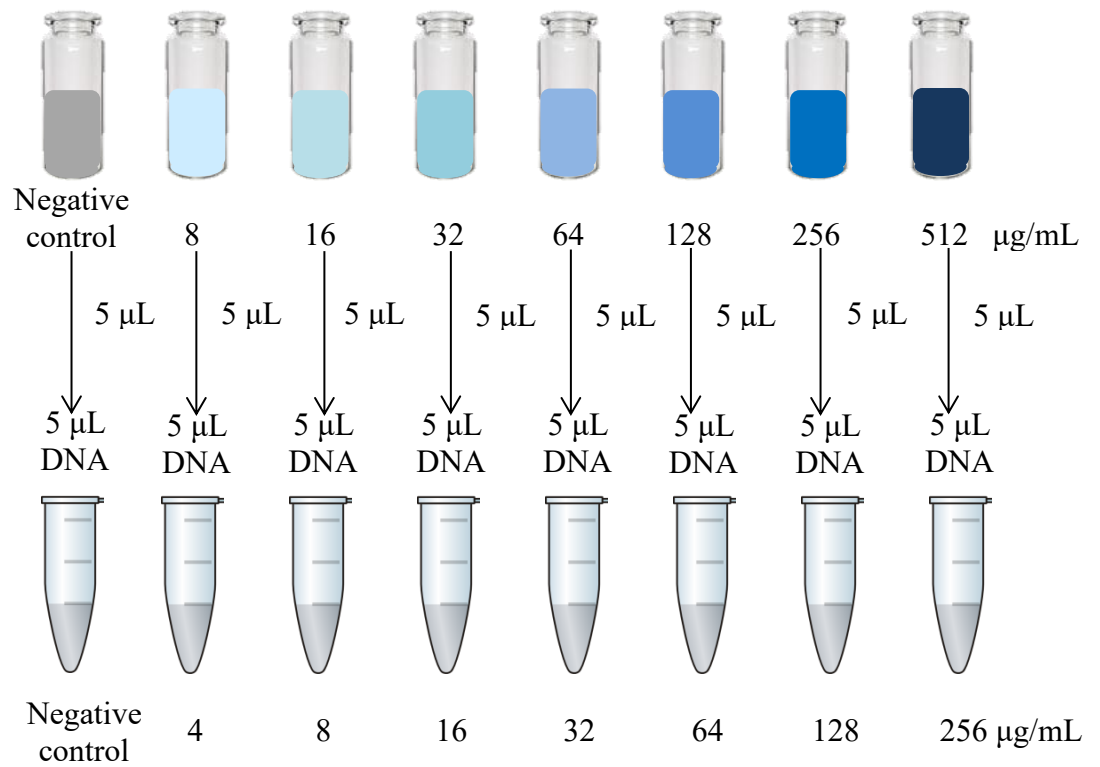
Figure 3.4: Illustration on the treatment of bacterial DNA with PAM-5 or polymyxin B prior to gel retardation assay. Five µL of peptide with the concentrations ranging from 8 µg/mL to 512 µg/mL was added to 5 µL of bacterial DNA to achieve the final peptide concentrations ranging from 4 µg/mL to 256 µg/mL. For negative control, the DNA was added with 5 µL of TE buffer.

3.11 Screening for Toxicity of PAM-5 on Mammalian Cells

3.11.1 Cell Lines

Vero cell and HeLa cell lines were provided by Dr Sit Nam Weng and Ms Sangeetha, respectively, from the Department of Biomedical Science, Universiti Tunku Abdul Rahman. These cells were used as the mammalian cells for toxicity study of PAM-5. Both cell lines were cultured in T75 flask containing Dulbecco's Modified Eagle's Medium (DMEM) supplemented with 10% fetal bovine serum (FBS) that supplied the cells with growth factors. The cells were incubated at 37°C in CO_2 incubator with 5% CO_2, where the cells were continuously monitored for their confluence in the flask. Once the cell line reached 80% confluence, they were sub-cultured into new flasks. The media was changed every three to four days to ensure continuous supply of nutrient to the cells. When the cells were needed for cytotoxicity assay, they were grown to 70% or 80% confluence and harvested. A titre of 10^4 cells/well was prepared by serial dilutions of the harvested cells using DMEM before setting up the assay. On the other hand, when the cells were not used instantly, they were maintained in cryopreservation medium containing 10% dimethyl sulfoxide (DMSO) and 20% FBS and stored in liquid nitrogen for prolonged storage.

3.11.2 Human Red Blood Cells (hRBCs)

Human red blood cell (hRBC) was kindly provided by a healthy donor from the Department of Biomedical Science, Faculty of Science, Universiti Tunku Abdul Rahman under ethical approval. Upon obtaining the blood through phlebotomy, it was maintained in Alsever's solution (2.0% dextrose, 0.8% sodium citrate,

0.5% citric acid and 0.42% sodium chloride), followed by centrifugation to remove the plasma. The packed cells were washed twice with PBS (pH 7.4) through resuspension and centrifugation. After removing the supernatant, the blood cell pellet was re-suspended in 1 mL of PBS. Then, 10% (v/v) of red blood cell suspension was prepared by diluting one portion of the concentrated RBCs with 9 portions of PBS. The RBC suspension was maintained at 4°C. The degree of RBC haemolysis in the suspension was monitored from time to time before the haemolytic assay. RBC suspension that showed signs of haemolysis prior to the assay will not be used.

3.11.3 PrestoBlue^{TM} Cell Viability Assay

The toxicity of PAM-5 towards the above-mentioned two cell lines was screened by PrestoBlue^{TM} cell viability assay. Both the cell lines were prepared as described in **Section 3.11.1**, followed by seeding 100 µL of the cells in the wells of a white-opaque, flat-bottom 96 well-microtiter plate. Then, the cells were treated with PAM-5 (2 µg/mL to 256 µg/mL), polymyxin B (2 µg/mL to 256 µg/mL), 50% (v/v) DMSO (positive control) and DPBS (negative control). The setting for the PrestoBlue^{TM} assay is shown in **Figure 3.5**.

After overnight incubation at 37°C in 5% CO_2, the contents in the wells were mixed with 20 µL of PrestoBlue^{TM} Cell Viability reagent (Invitrogen^{TM} Life Technologies). The plate was protected from light and further incubated for another 24 hours at 37°C in 5% CO_2. On the next day, the fluorescent intensities of the well content were measured by microplate reader (BMG LABTECH) with excitation and emission wavelength set at 544 nm and 620 nm, respectively. The fluorescence for each well was recorded in relative fluorescence unit (RFU). The assay was performed thrice independently to ensure data reproducibility.
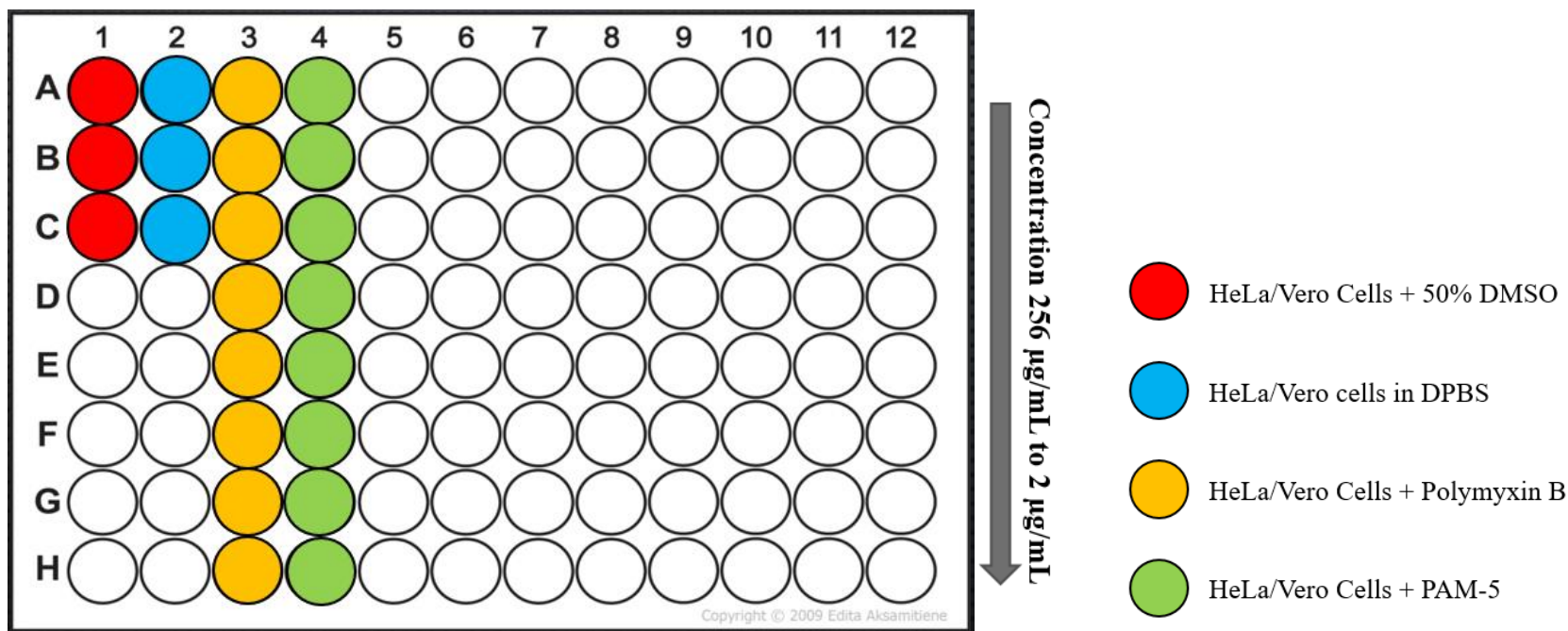
Figure 3.5: Microtiter plate setup for PrestoBlue cell viability assay to screen for PAM-5 toxicity on HeLa/Vero cells. Well 1A to 1C: cells treated with 50% DMSO which served as the positive control for toxicity; well 2A to 2C: cells in DPBS which served as the negative control for toxicity; well 3A to 3H: cells treated with polymyxin B at concentrations ranging from 256 µg/mL to 2 µg/mL; well 4A to 4H: cells treated with PAM-5 at concentrations ranging from 256 µg/mL to 2 µg/mL. After overnight treatment, the wells were added with 20 µL of PrestoBlue reagent.

3.11.4 Screening for Permeabilization Effect of PAM-5 on Mammalian Cells Membranes by SYTOX® Green Uptake Assay

The toxicity of PAM-5 on mammalian cells via membrane-permeabilization was studied by SYTOX® Green uptake assay. Vero cells were grown and harvested according to the protocols as described in **Section 3.11.1**. The concentrated cell suspension was serially diluted to the desired cell titre for this assay (10^5 cells/mL) with DMEM. Then, 100 µL of the diluted cell suspension was seeded into a black opaque, clear-flat bottom 96 well-microtiter plate. The microtiter plate containing the seeded cells was then incubated overnight at 37°C in a 5% CO_2 incubator.

On the next day, the DMEM and any unattached cells were removed from the wells, followed by washing the adhered cells in the wells for three times with 100 µL of DPBS. Next, the cells in different wells were treated with 100 µL of PAM-5 at each concentration ranging from 2 µg/mL to 256 µg/mL. Positive and negative controls for cell permeabilization were set up by adding 100 µL of melittin and DPBS to the cells in separate wells, respectively. In addition, a blank was set up by adding only 100 µL of DPBS into an empty well. After 15 minutes of incubation at 37°C in 5% CO_2, 50 µL of 1 µM SYTOX® Green reagent was added into each well simultaneously by using multichannel pipette. **Figure 3.6** shows the setup of this assay.
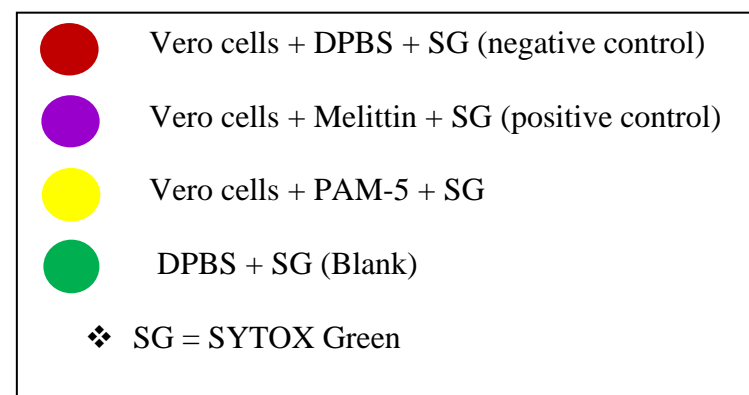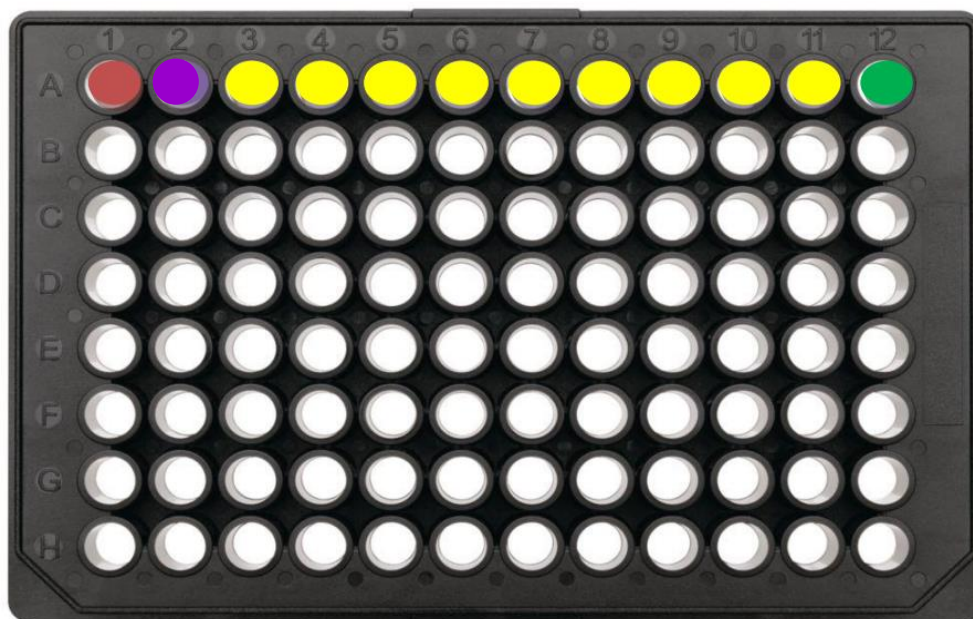
Figure 3.6: Microtiter plate setup for SYTOX Green uptake assay for treated and non-treated Vero cells. Well A1 was filled with untreated Vero cells which served as the negative control. Well A2 was filled with Vero cells treated with melittin which served as the positive control. Well A3 to A11 were filled with Vero cells treated with PAM-5 at concentrations ranging from 256 µg/ml to 2 µg/ml. Well 12 served as the blank which was filled with only DPBS. All the wells were added with 50 µL of SYTOX Green after the treatment.

The cells were cultured for 15 minutes. After that, the fluorescent intensities generated from the treated and untreated cells were measured by using TECAN Infinite M200 spectrophotometer with the excitation and emission wavelength set at 485 nm and 520 nm, respectively. The images of the cells were observed and captured with Nikon Eclipse Ti inverted fluorescent microscope. To ensure the reproducibility of the data, this assay was repeated for another two times.

3.11.5 Screening for Haemolytic Effect of PAM-5 on Human Red Blood Cells via *in vitro* Haemolysis Assay

Apart from its toxicity towards the above-mentioned mammalian cells, PAM-5 was further screened for its haemolytic effect on human red blood cells (hRBCs). The cells were prepared as described in **Section 3.11.2**. One hundred microliter of 10% (v/v) hRBCs in PBS was filled into a series of microcentrifuge tubes, each to be tested for a concentration of PAM-5 that ranged from 2 µg/mL to 256 µg/mL. Then, the cells were added with 100 µL of PAM-5. In terms of comparative study, another set of hRBCs was set up in a series of microcentrifuge tubes in which they were treated with polymyxin B at the same range of concentrations. For positive control of haemolysis, 100 µL of the RBC suspension was treated with 100 µL of 0.1% Triton-X. In contrast, untreated hRBCs added with the same volume of PBS was used as the negative control.

The microcentrifuge tubes containing the treated and untreated hRBCs were incubated for one hour at room temperature. After that, the tubes were subjected to centrifugation at 4000 $\times$ g for 2 minutes at room temperature. Upon

centrifugation, 150 µL of the supernatant from each tube was carefully transferred into wells of a flat-bottom 96 well-microtiter plate. The absorbance of these supernatant in the microtiter plate was measured at 540 nm using a microplate reader (BMG LABTECH). This assay was performed in triplicate to ensure data reproducibility. Finally, the average percentage of haemolysis was calculated using the equation as follow:

$$\text{Percentage of hemolysis} = \frac{A_{supernatant} - A_{negative\ control}}{A_{positive\ control} - A_{negative\ control}} \times 100\%$$

Where,

$A_{supernatant}$ = absorbance of supernatant obtained from hRBC suspension treated with PAM-5/polymyxin B

$A_{negative\ control}$ = absorbance of supernatant obtained from hRBC suspension in PBS

$A_{positive\ control}$ = absorbance of supernatant obtained from hRBC suspension treated with 0.1% Triton-X

3.11.6 Statistical analysis

The data derived from the above-mentioned toxicity assays were statistically analysed by Student T-Test. For each of the toxicity assay, a total of three independent experiments were carried out, and the outcome data were expressed as mean $\pm$ standard deviation (SD). T-test for paired samples was used to assess whether there was any difference in terms of viability between PAM-5-treated cells and untreated cells (negative control), PAM-5-treated cells and DMSO/Triton-X-treated cells (positive control) as well as viability between cells treated with PAM-5 and polymyxin B, with $P < 0.05$ considered statistically significant at a 95% confidence level.

CHAPTER 4

RESULTS

4.1 Selection of Phage-Displayed Peptides Binding to *Pseudomonas aeruginosa*

In order to select for phage-displayed peptides that bind to *P. aeruginosa* with high affinity, a 12-mer random phage-displayed peptide library was used to biopann against the whole cell of *P. aeruginosa* ATCC 27853. This biopanning was performed in two independent sets, and a total of four rounds of these selection procedures were carried out for each set. In each round of biopanning, the eluted phages that bound to the target bacterium were titered, and the degree of enrichment for the affinity-selected phage-displayed peptides from each round of biopanning can be calculated from the input and output phage titers as described in **Section 3.3.2** and **3.3.3**. The input phage titer was the amount of phages initially used to biopann against the target bacteria, while the output phage titer was the amount of phages eluted from a particular round of biopanning after the affinity selection. Both titers can be determined by calculating the number of blue plaques that represent the selected phage clones on the titering plates. **Figure 4.1(a)** and **(b)** demonstrate the titering plates of one of the biopanning sets that were inoculated with the phage eluate after serial dilutions. The blue plagues represented the desired phages selected from the biopanning.

110
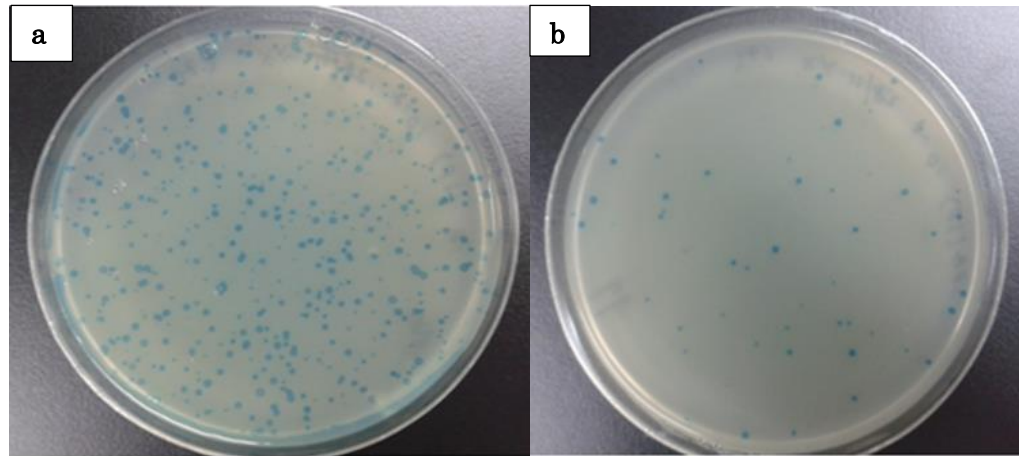
Figure 4.1: Affinity selected phages from biopanning as represented by the blue plaques on IPTG/Xgal plate. **Figure (a)** shows the IPTG/Xgal titer plate inoculated with phage eluate after subjecting to 10^{-1} dilution, while **Figure (b)** shows the titer plate inoculated with phage eluate after 10^{-2} dilution.

Clearly demonstrated from the figures, all the blue plaques appeared on the titering media plates represented clones of phages which were affinity-selected from the phage displayed-peptide library during the biopanning. This was indicated by the presence of only blue plaques on the titering media plates, where the blue plaques represent the common cloning vector M13mp19 used for the construction of the phage displayed-peptide library. This phage carries the lacZα gene, which contributes to its blue appearance when it is cultured on media containing Xgal and IPTG. In contrast, contaminant phages from the environment that do not harbour the gene will produce colourless plaques on the media plates. As shown in the figure, no colourless plaque was seen on the titering media, indicating the biopanning procedures had selectively isolated phage clones from the library without contamination by environmental wild type phages.

In the effort of selecting clones of phage-displayed peptides with strong binding to *P. aeruginosa*, enrichment of affinity-selected phages that bound to the bacterium was seen throughout the consecutive four rounds of biopanning. This was indicated by the increase in recovery rate of phages bound to the bacterium after every round of biopanning from the two independent sets. As tabulated in **Table 4.1**, trends of affinity selection were clearly seen as the output titers from the phage eluate after the biopanning were consistently lower than the input titer before the biopanning. For example, from the initial titer of 1.0×10^{12} PFU/mL in the phage-displayed peptide library, approximately 1.2×10^5 PFU/mL of phages were recovered from the eluate at the end of the first round of biopanning against the bacterium. This indicated that a proportion of phages from the library that may bound to certain surface structures of *P. aeruginosa* were selected while the non-binding phages were excluded from the biopanning. The selected phages were amplified to 4.9×10^{11} PFU/mL to enrich the specific binding clones for the subsequent rounds of biopanning. As occurred for the first round of biopanning, the titer of the selected phages after the second round of biopanning was reduced to 4.6×10^5 PFU/mL, indicating further exclusion of non-specific or weak binders to the bacterium from the input phages. Nevertheless, the percentage of yield for the phage eluate from the second round of biopanning (9.4×10^{-7} %) was slightly higher than the one in the first biopanning (1.2×10^{-7} %). Similarly, the increment in the percentage of yield was also observed for the subsequent rounds of biopanning (**Table 4.1**), indicating selection of higher amount of phages that bound to the bacterium from the input phage of lesser diversity. Similar findings were also observed for the second set of affinity selection. Throughout the four rounds of biopanning,

phages displaying peptides that selectively bound to *P. aeruginosa* were

recovered, as indicated by the increased phage recovery rate and percentage of

selection yields (Set b, **Table 4.1**).

Table 4.1: Percentage of yield for the affinity-selected phages from the four
rounds of two independent sets (a and b) of biopanning.

Rounds of biopanning	Input titer (pfu/ml)	Output titer (pfu/ml)	Percentage of yield (%)
1a	1.0×10^{12}	1.2×10^5	1.2×10^{-7}
1b	1.0×10^{12}	9.1×10^5	9.1×10^{-7}
2a	4.9×10^{11}	4.6×10^5	9.4×10^{-7}
2b	2.9×10^{12}	3.7×10^6	1.3×10^{-6}
3a	8.6×10^{11}	1.6×10^6	1.9×10^{-6}
3b	2.4×10^{12}	2.7×10^7	1.1×10^{-5}
4a	8.3×10^{12}	3.5×10^7	4.2×10^{-6}
4b	5.2×10^{12}	2.1×10^7	4.0×10^{-6}

The percentage of yield was calculated by the formula: [(Output titer / Input
titer) x 100%].

At the final round of biopanning, a total of 30 individual phage plaques were randomly selected from the titering plate and propagated individually. Among these, phage 4A1 to 4A15 were selected from set (a) biopanning, while 4A16 to 4A30 were chosen from set (b) biopanning. These amplified phage clones were subjected to subsequent downstream analysis, which encompassed ELISA screening for their binding affinity to *P. aeruginosa* as well as DNA sequencing in order to determine the sequences of the displayed peptide.

4.1.1 ELISA Screening on Binding Selectivity of Selected Phage-Displayed Peptides towards *P. aeruginosa* ATCC 27853

Phage-ELISA was performed to determine the binding affinity of the selected phage-displayed peptides towards *P. aeruginosa* ATCC 27853, the target bacterium used in the biopanning to select these phages. As described in **Section 3.3.5**, the individually amplified phage clones were incubated with the whole cell of *P. aeruginosa* coated in the wells. The strength of binding between the bacterium and the phage clones via their displayed peptides was indicated by the absorbance from the ABTS colour development generated by the bound phages to the bacteria.

Figure 4.2 demonstrates the ELISA reactivity yielded by the interaction between some of the selected phage clones and the coated bacterium. Clearly demonstrated from the figure, the colour intensities of ABTS generated from the bacterial coated wells filled with the selected phages (row **B**, **Well B1 to B10**) were obviously high. Comparatively, the same clones of phages produced

almost colourless reaction when they were added into wells coated with bovine serum albumin (BSA) (row **A**, **Well A1 to A10**), which served as the negative control. This indicated that the phages bound selectively to the target bacterium instead of other non-related protein.

With reference to the comparative OD_{405} between the sample and negative control (**Figure 4.3**), it was found that all the OD_{405} produced by the phage-bacteria binding (samples) were relatively much higher than the negative control. The ratio of binding selectivity of the sample to the negative control was then calculated by dividing the OD_{405} reading of the former by the latter. In overall, all the selected phage clones demonstrated relatively high binding affinity to the target bacterium with the ratio that ranged from 10 to 20. In particular, phage clones 4PA1, 4PA2, 4PA3, 4PA4, 4PA5, 4PA6, 4PA7, 4PA8, 4PA9, 4PA10, 4PA12, 4PA14, 4PA15, 4PA16, 4PA17, 4PA18, 4PA19, 4PA20, 4PA21, 4PA24, 4PA27 and 4PA29 demonstrated relatively higher binding ratio as compared to other clones, in which the absorbance readings produced by these phage clones were higher than 1.0.
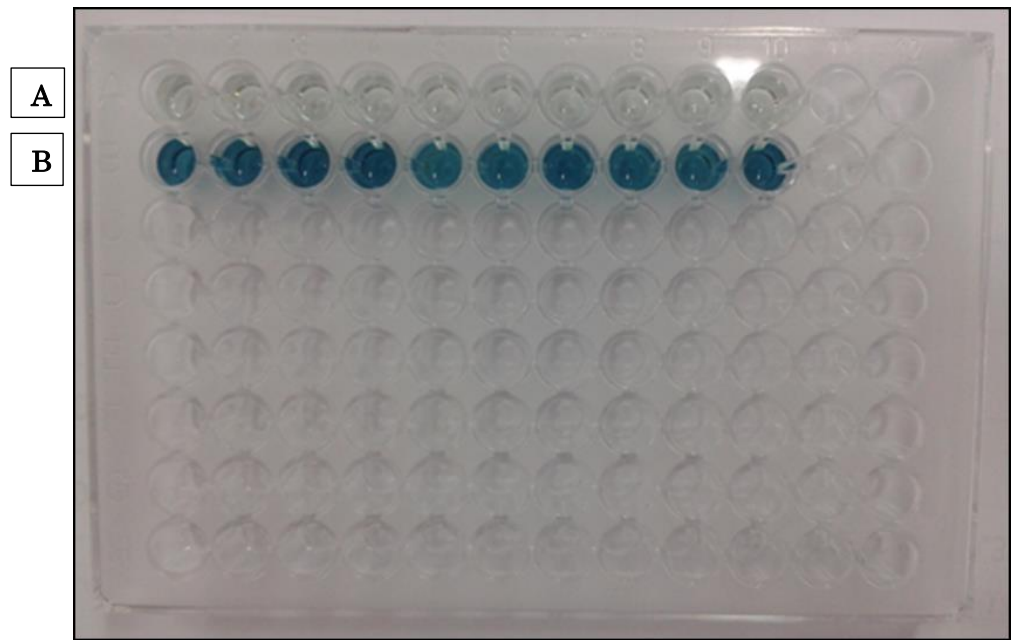
Figure 4.2: Reactivity of Phage-ELISA on selected clones of phage-displayed peptides. Row **A**: Selected phage clones added to wells coated with BSA (negative control); Row **B**: the same phage clones added to wells coated with *P. aeruginosa* ATCC 27853 (samples).
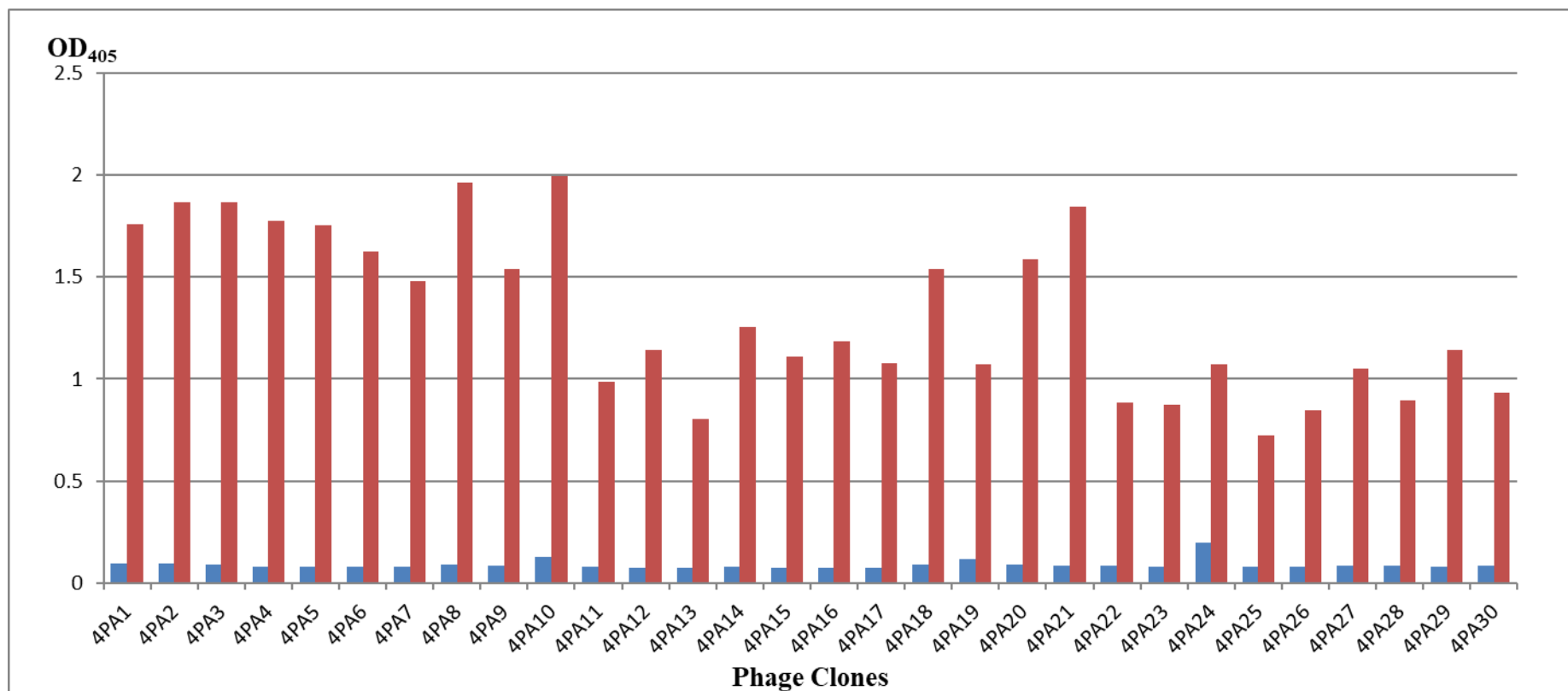
Figure 4.3: Absorbance of Phage-ELISA as measured in optical density at the wavelength 405 nm (OD_{405}). Thirty clones of phage-displayed peptides were tested for their binding affinity to *P. aeruginosa*. The absorbance from the reactivity between these phages and the bacteria (red bar) was compared to the negative control which consisted of phage and bovine serum albumin (blue bar)

4.1.2   Purity of Extracted Phage Genomic DNA

As reported in **Section 4.1.1**, 22 phage clones which produced absorbance readings that were higher than 1.0 were selected for DNA extraction. Genomic DNAs from all the phage clones were successfully extracted. However, the amount of the extracted genomic DNAs from different phage clones were inconsistent as shown in **Table 4.2**, which ranged from the lowest concentration of 18.9 ng/µL to the highest of 305.2 ng/µL. The purities of these DNAs were examined by 1.5% agarose gel electrophoresis, in which a 10 kb DNA ladder was used as the marker to estimate the size of the sample DNAs. As indicated in **Figure 4.4** which depicts the electrophoretic migration of five of the extracted DNA samples, only single band was observed in every lane of the agarose gel in which the phage genomic DNA was loaded (**Lane 3** to **Lane 7**). All the DNA bands were positioned at approximately 6,000 bp, which is the estimated size of genomic DNA from M13 phage, the phage vector that displays the peptides. These findings indicated that the phage genomic DNAs were successfully extracted without contamination from other DNAs.

After ensuring their purity and amount sufficiency, the extracted phage genomic DNAs were sequenced in order to determine the oligonucleotide sequences that encoded the displayed peptides.

Table 4.2: Concentrations of extracted ssDNAs from selected phage clones.

Phage Clone	DNA Concentration (ng/µL)
4PA1	120.9
4PA2	223.2
4PA3	133.0
4PA4	56.1
4PA5	218.2
4PA6	132.4
4PA7	83.2
4PA8	284.2
4PA9	229.1
4PA10	18.9
4PA12	47.9
4PA14	92.5
4PA15	182.4
4PA16	159.5
4PA17	90.2
4PA18	305.2
4PA19	56.2
4PA20	121.6
4PA21	82.3
4PA24	62.8
4PA27	88.2
4PA29	72.5
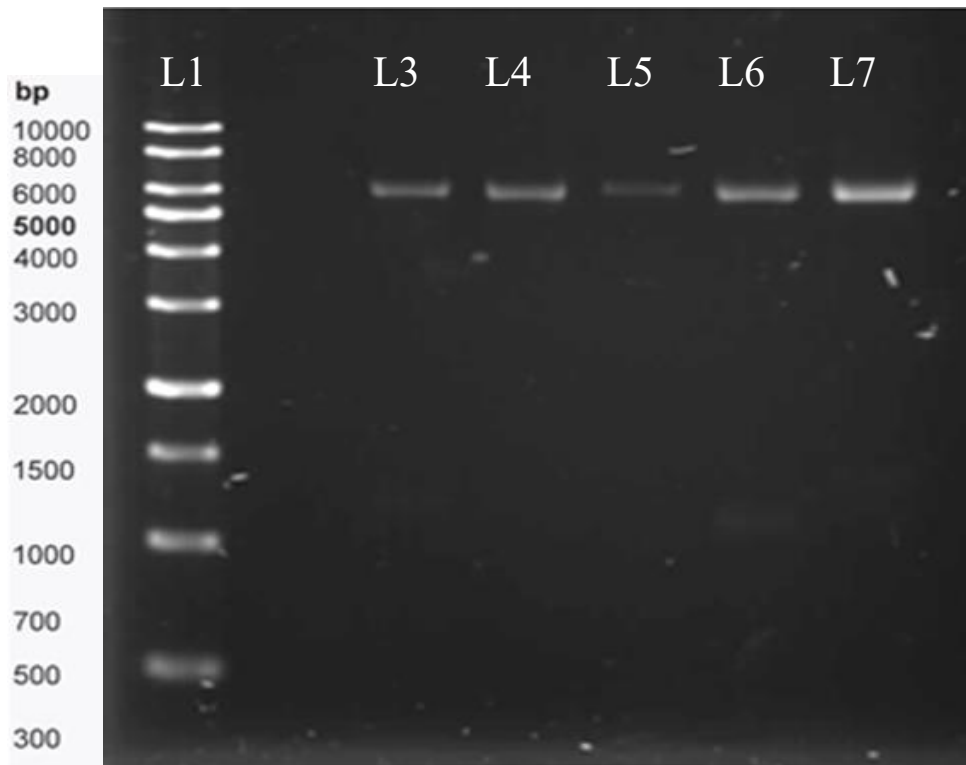
Figure 4.4: Agarose gel electrophoresis analysis of phage genomic DNAs. Lane L1 was loaded with the 10 kb DNA ladder. Lanes L3 to L7 were loaded with the extracted phage genomic DNAs. The bands in L3, L4, L5, L6 and L7 represent the migrated DNA extracted from phage clone 4PA1, 4PA2, 4PA4, 4PA5 and 4PA8, respectively.

4.1.3 Analysis of Phage-Displayed Peptide Sequences

As described by the manufacturer of phage-displayed peptide library used in this study (New England Biolabs), the sequence of the phage genomic DNA is being read in such a way that corresponds to its antisense strand of the template as the sequencing primer hybridizes downstream of the insert. The oligonucleotide insert (or library insert sequence, **Figure 4.5**) is located after a conserved leader sequence (ATGGGATTTTGCTAAACAACTTTCAACAGTTTCGGCCGA, green-boxed sequence in **Figure 4.5**) interspaced by an additional 9-nucleotide extension of the leader sequence (ACCTCCACC, red-boxed sequence in **Figure 4.5**) prior to the oligonucleotide insert sequence. Once the 36-nucleotide insert is identified, the 12-mer displayed peptide can be deduced.
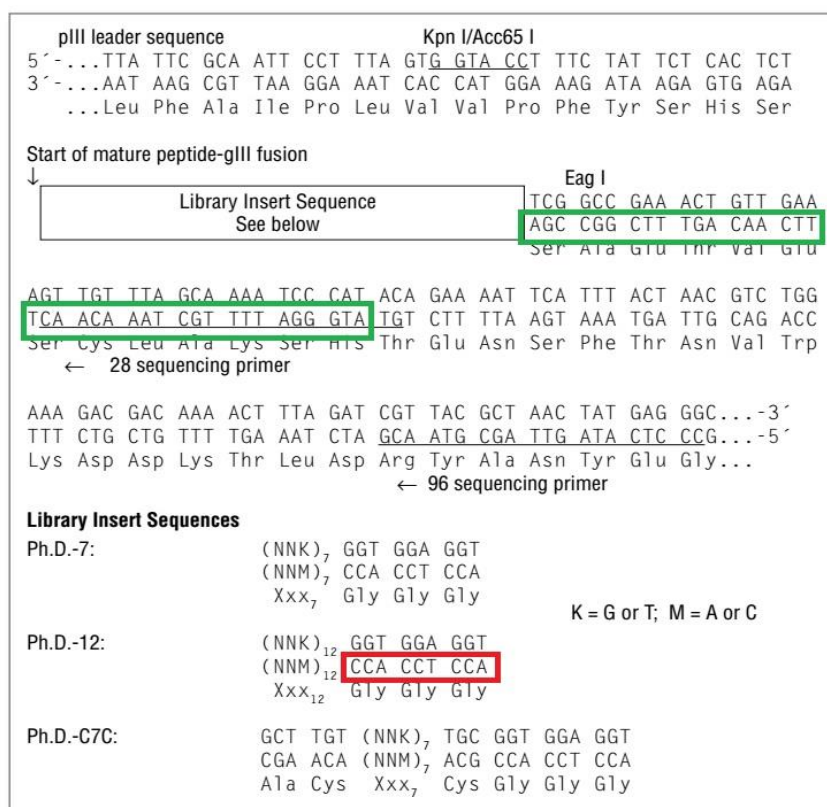
Figure 4.5: Sequence of the random peptide library-gIII fusion. The sequence is being read in antisense strand as indicated by the direction of the sequencing primers (Adopted from Ph.D.™ Phage Display Libraries Instruction Manual).

Out of the 22 phage DNA samples, only 15 of them in which the oligonucleotide inserts were successfully sequenced, while the remainder were either suffered from deletion of the oligonucleotide insert or came along with multiple noisy peaks. **Figure 4.6(a)** to **(c)** are three electropherograms of the six successful sequencing samples selected from set (a) biopanning. The yellow highlighted area is the 36-nucleotide sequence which represents the oligonucleotide insert that encodes for the displayed peptide. It is located right after the conserved leader sequence which is partially represented by "ACC" on the left of each figure. On the other hand, the remaining nine successful sequencing were belonged to DNAs extracted from phage clones isolated from the set (b) biopanning. Three of the electropherograms of these oligonucleotides (highlighted in green) are shown in **Figure 4.7** (a to c).

After locating these oligonucleotide sequences, the reverse complementary sequences of the oligonucleotide inserts were determined by a reverse complement tool from an online software named ExPASy DNA translate tool (http://web.expasy.org/translate/). Using the same software, the reverse complement sequences of the 36-nucleotide inserts were then deduced into peptides. As shown in **Table 4.3**, some of the 15 successfully sequenced phage-displayed peptides were sharing identical peptide sequences, and thus they were categorized into seven groups of peptides with distinct sequences. The sequences and features of these phage-displayed peptides are summarized in **Table 4.4**. The clones for the deduced peptides were renamed in consideration to the consensus peptides displayed by some of the phage clones.

(a)
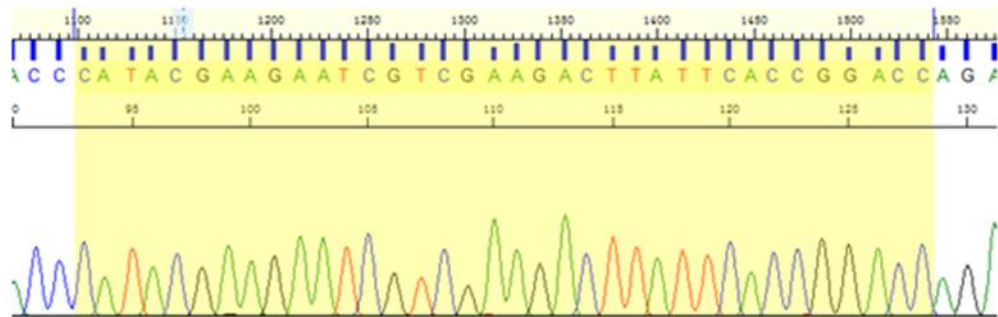
(b)
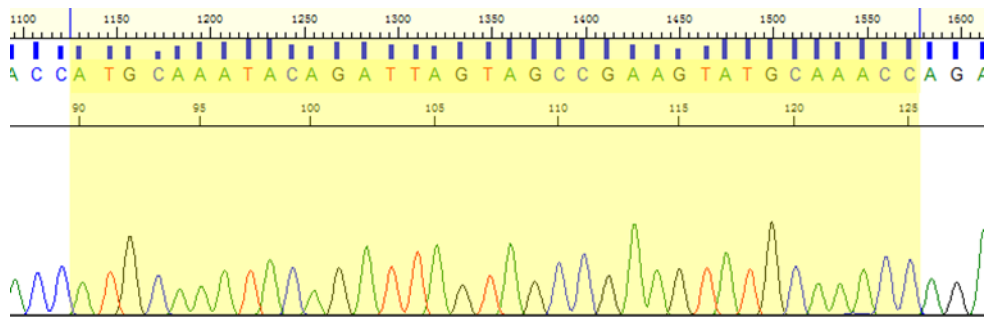
(c)
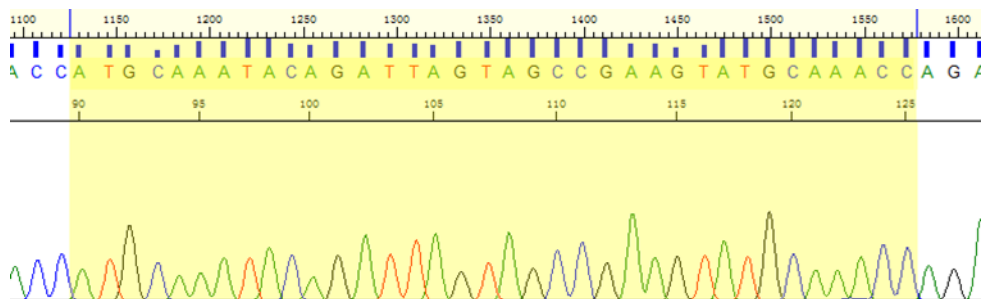
Figure 4.6 (a-c): Electropherograms of three representative oligonucleotide inserts of selected phage clones isolated from the final round of set (a) biopanning. The sequences of the oligonucleotide inserts are highlighted in yellow, which consist of 36 nucleotides.

(a)
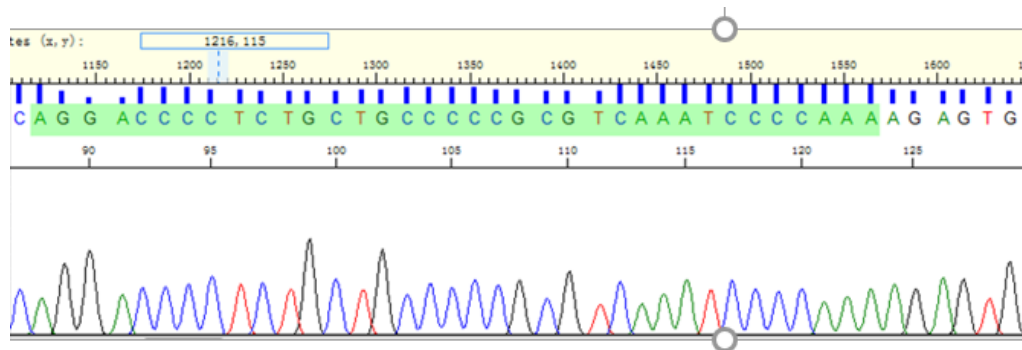
(b)
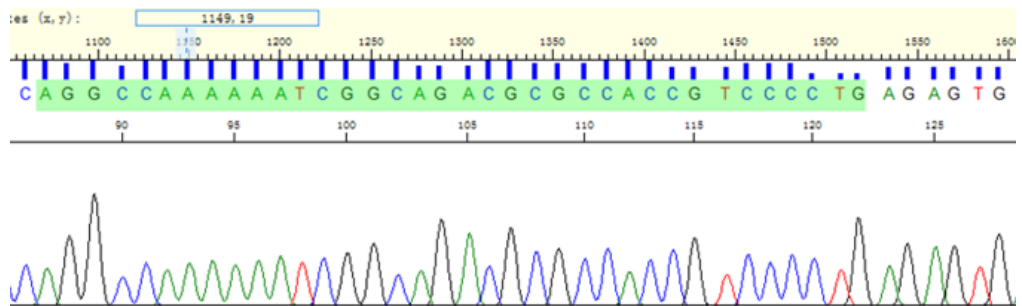
(c)
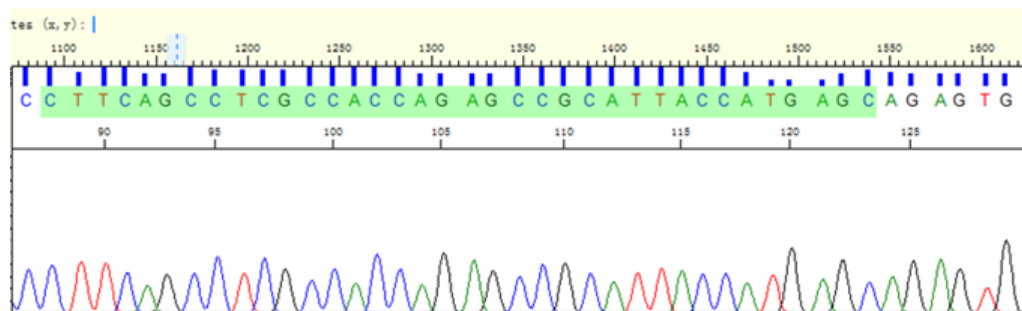
Figure 4.7 (a-c): Electropherograms of three representative oligonucleotide inserts of selected phage clones isolated from the final round of set (b) biopanning. The sequences of the oligonucleotide inserts are highlighted in green, which consist of 36 nucleotides.

Table 4.3: Successfully sequenced phage-displayed peptides in which some of them were identical peptides selected in multiple copies. These peptides were segregated into seven groups of peptides with different peptide sequences.

Successful Sequenced Phage-Displayed Peptides	Segregated Peptides
4PA14, 4PA18, 4PA20	Pa1
4PA4	Pa2
4PA2, 4PA9	Pa3
4PA5, 4PA8, 4PA10, 4PA20, 4 PA21	Pa4
4PA1, 4PA3	Pa5
4PA18	Pa6
4PA7	Pa7

Table 4.4: Affinity-selected phage-displayed peptides from the biopanning against *P. aeruginosa* and their corresponding frequency of selection, net charge and hydrophobicity. Yellow-highlighted residues or motif are consensus found in different peptides.

Biopanning Set A				
Peptide	**Sequence**	**Frequency**	**Net Charge**	**Hydrophobicity**
Pa1	GPVNKSSTILRM	3/6	+2	33%
Pa2	AHGNAALVARLK	1/6	+2	58%
Pa3	GLHTSATNLYLH	2/6	0	33%
Biopanning Set B				
Clone	**Sequence**	**Frequency**	**Net Charge**	**Hydrophobicity**
Pa4	KWHWKDKNALRM	5/9	+3	41%
Pa5	GSLRPGTTNALV	2/9	+1	33%
Pa6	FGDLTRGQQRGP	1/9	+1	16%
Pa7	QGTVARLPIFWP	1/9	+1	50%

A : Alanine	G : Glycine	T : Threonine
R : Arginine	H : Histidine	W : Tryptophan
N : Asparagine	K : Lysine	Y : Tyrosine
D : Aspartic acid	M : Methionine	V : Valine
C : Cysteine	F : Phenylalanine	I : Isoleucine
Q : Glutamine	P : Proline	L : Leucine
E : Glutamic acid	S : Serine	

Clearly demonstrated from **Table 4.4**, out of the six peptide sequences which were selected from set (a) biopanning, three of them shared the same sequence of GPVNKSSTILRM, hereafter referred as Pa1. Interestingly, a motif consists of three consecutive amino acids Leu-Arg-Met (LRM) in Pa1 was also found at the same terminal position of another phage-displayed peptide which was isolated from set (b) biopanning. Designated as Pa4 with the sequence of KWHWKDKNALRM, this peptide represented the most frequent clone of peptide selected from this set of biopanning (5/9). Besides, a lysine (K) residue was found as the fifth amino acid in the sequence of both peptides. In overall, out of the total 15 peptides selected from the two independent sets of biopanning, eight of them shared these two consensuses.

On the other hand, Pa3 and Pa5 with the sequence GLHTSATNLYLH and GSLRPGTTNALV, respectively, were peptides with the second highest recovery rate from the biopanning (2/15 each). Consensus was also found in these two peptides, where the amino acid glycine (G), threonine (T) and leucine (L) were found at the first, seventh and eleventh position of the peptides, respectively. The remaining clones encoded unique peptide sequences with no obvious consensus except for Pa6 and Pa7, where both the peptides harbour a proline (P) residue at the carboxyl terminal of the peptide sequence.

Analysis on the physiochemical properties of the peptides using the Antimicrobial Peptide Calculator and Predictor (http://aps.unmc.edu/AP/main.php) revealed that peptide Pa1, Pa2, Pa3 and Pa4

may fulfil the criteria of an antibacterial peptide. According to the database, these peptides may form alpha helices and may have at least 3 residues on the same hydrophobic surface. As tabulated in **Table 4.4**, the hydrophobicity of these peptides was contributed by the presence of different hydrophobic amino acids such as isoleucine (I), valine (V), leucine (L) and methionine (M) in these peptides. These characteristics may allow the peptides to interact with bacterial membranes, which is the initial step of antibacterial mechanisms. With the exception for Pa3, these peptides also possessed another common feature of antibacterial peptides, namely cationicity. Due to the presence of positively charged amino acid such as lysine (K) and arginine (R), these selected peptides acquired a net positive charge that ranged from +1 to +3, depending on the number of the cationic residues. When these peptides were aligned to the well-studied peptides in the database, no obvious similarity to other antibacterial peptides was found.

In contrast, no evidence of antibacterial feature was found for the other three peptides (Pa5, Pa6 and Pa7). According to the software prediction, these peptides may not be able to form helical structure that is long enough to exert its antibacterial action. In addition, their total hydrophobic residues on the same surface is zero, rendering them with difficulty to interact with the hydrophobic bacterial membrane. Therefore, these peptides were excluded from the subsequent downstream evaluation for their antibacterial effect.

4.1.4 Screening for Antibacterial Effect of Pa1 and Pa4

In consideration of the possible steric hindrance effect caused by the phage particles, the linear form of Pa1 and Pa4 were synthesized for the evaluation of antibacterial effect on their target bacteria. The relative degrees of bacterial growth upon treatment with Pa1 and Pa4 were compared to polymyxin B-treated bacteria and untreated bacteria, which served as the positive and negative controls, respectively.

As demonstrated in **Figure 4.8**, Pa1 failed to eliminate *P. aeruginosa* ATCC 27853 at concentrations that ranged from 2 µg/mL to 128 µg/mL. However, despite the failure to kill the bacteria completely at these concentrations, Pa1 was able to inhibit the bacterial growth by a slight titer reduction of approximately one $\log_{10}$ CFU/mL as compared to the untreated bacterium. Complete bactericidal effect was only achieved at 256 µg/mL.

Similarly, Pa4 was only able to kill the target bacterium completely at the highest tested concentration (256 µg/mL). At concentrations that ranged from 2 µg/mL to 128 µg/mL, instead of eliminating the bacterium, Pa4 only exerted low bacteriostatic effect by causing approximately one $\log_{10}$ CFU/mL titer reduction as compared to the untreated bacterium (**Figure 4.9**).
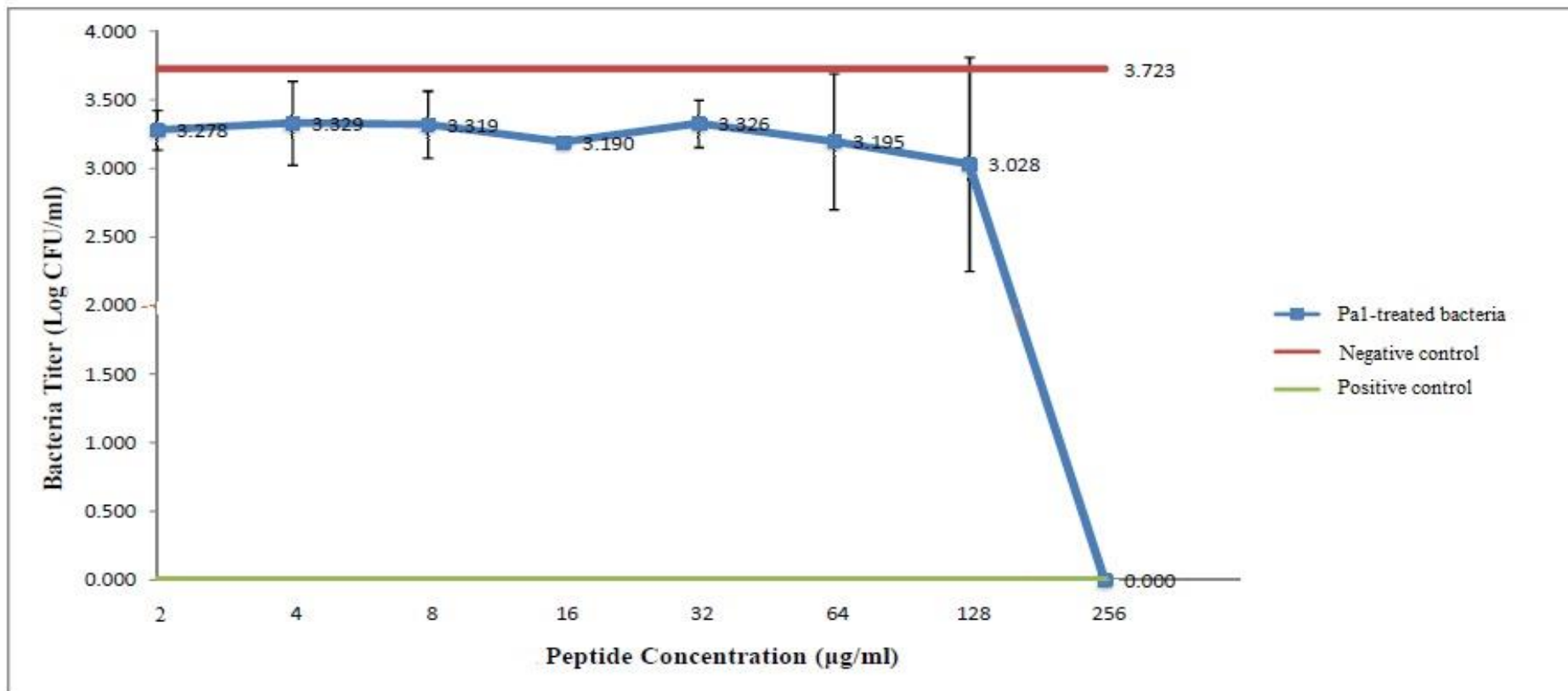
Figure 4.8: Assessment of antibacterial effect of Pa1 on *P. aeruginosa* ATCC 27853. Bacteria were treated with Pa1 of different concentrations ranging from 2 μg/mL to 256 μg/mL. Complete killing of bacteria could only be achieved at the highest peptide concentration, 256 μg/mL. Polymyxin B-treated bacteria, which served as the positive control, were unable to grow. Untreated bacterium consistently grew heavily.
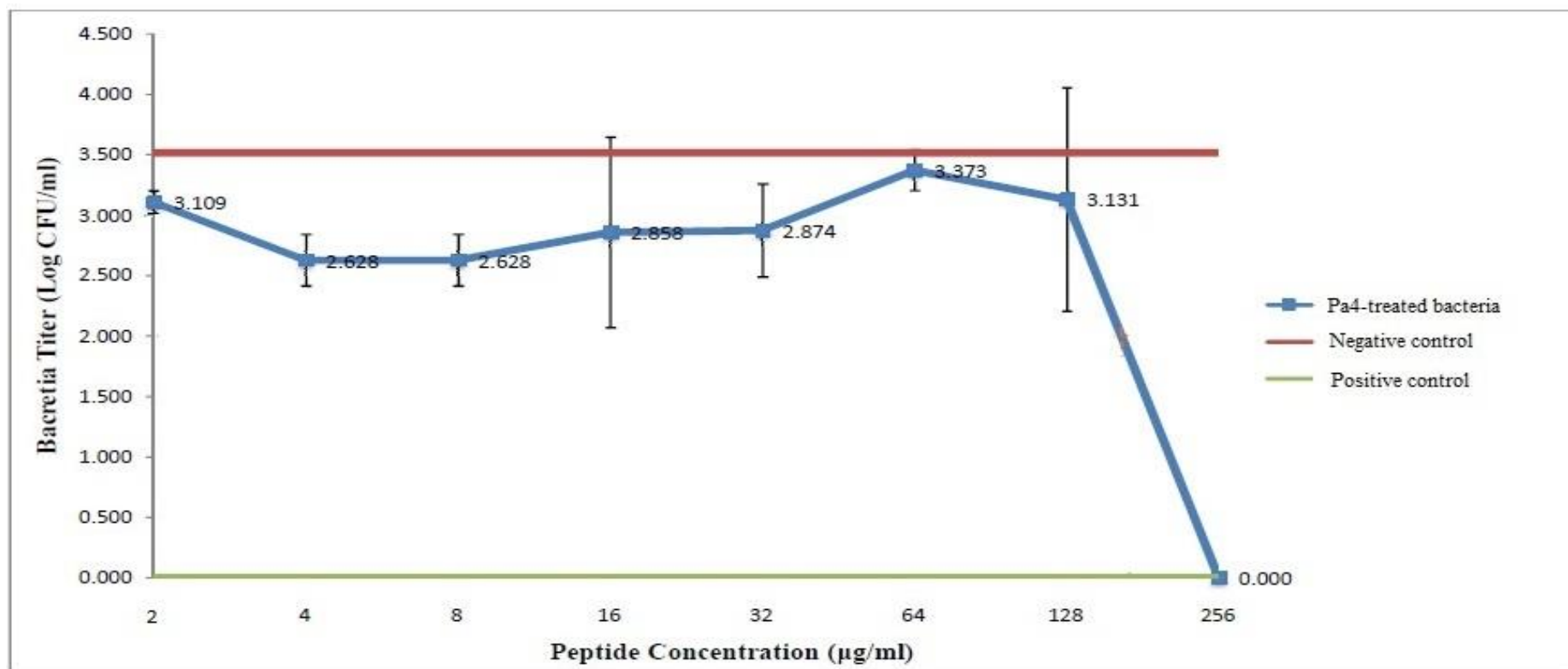
Figure 4.9: Assessment of antibacterial effect of Pa4 on *P. aeruginosa* ATCC 27853. Bacteria were treated with Pa4 of different concentrations ranging from 2 μg/mL to 256 μg/mL. Complete killing of bacteria could only be achieved at the highest peptide concentration, 256 μg/mL. Polymyxin B-treated bacteria, which served as the positive control, were unable to grow. Untreated bacterium consistently grew heavily.

4.1.5   Modification of Pa4 to PAM-5

Due to the poor antibacterial potency displayed by both Pa1 and Pa4, several modifications were made to Pa4 as described in **Section 3.5.1** in order to render the peptide with more features of an ideal ABP. Several factors were considered in order to design a new ABP based on the selected phage-displayed peptide. Firstly, the peptide with the highest frequency of selection from the biopanning, Pa4, was given prior consideration as the template for modification. Secondly, Pa4 carried the motif L-R-M and a K residue, which were also present in Pa1, in which the latter was the predominant phage-displayed peptide isolated from another independent set of biopanning. This indicated that these amino acids might play certain crucial role/s in the interaction with surface molecule/s of *P. aeruginosa*, thereby explaining the predominant selection of peptides harbouring these consensuses during the biopanning. Therefore, these amino acids were retained in the remodified antibacterial peptide. Thirdly, the biopanning-selected phage-displayed peptides may not possess sufficient strength of cationicity and length which are required for ideal antibacterial effect. In order to overcome these limitations, the modification of the selected phage-displayed peptide was done by means of increasing their net positive charge and number of amino acid residues. As shown in **Figure 4.10**, the improvement in cationicity was carried out by replacing some of the less cationic or anionic amino acids in the Pa4 with more cationic residues. For instance, the less cationic histidine (H) and negatively charged aspartic acid (D) in Pa4 were replaced with a cationic lysine (K) and arginine (R), respectively. Meanwhile, the hydrophobicity of Pa4 was also increased by replacing the less or non-hydrophobic residues such as asparagine (N) and alanine (A) with leucine (L)

and valine (V) of higher hydropathy index. In order to increase the length of the peptide, a motif which is consist of arginine (R), proline (P) and leucine (L) was added to the peptide as shown in the **Figure 4.10**.

KWHW - - -KDKNALRM   (Pa4)

KWKWRPLKRKLVLRM   (PAM-5)

Figure 4.10: Modification of peptide Pa4 to PAM-5. Anionic/less cationic residues in Pa4 (grey) were replaced by more cationic residues (green). An additional motif (light blue) was incorporated into the new peptide to increase the peptide length.

As the results of the above-mentioned modifications, the newly generated peptide, namely PAM-5, consists of 15 amino acids with the sequence lysine-tryptophan-lysine-tryptophan-arginine-proline-leucine-lysine-arginine-lysine-leucine-valine-leucine-arginine-methionine   (KWKWRPLKRKLVLRM). Peptide analysis using Antimicrobial Peptide Calculator and Predictor revealed that this newly designed peptide possesses enhanced physiochemical properties of an ABP with a net positive charge of +7 and a total hydrophobicity of 46% (http://aps.unmc.edu/AP/prediction/actionInput.php). Additionally, this peptide may form alpha helices and possesses at least 5 residues on the same hydrophobic surface.

4.2 Screening for Antibacterial Effect of PAM-5

In order to testify the speculated enhanced antibacterial features, PAM-5 was screened for its antibacterial effect against *P. aeruginosa* ATCC 27853. Besides, the antibacterial spectrum of PAM-5 was also screened for a list of bacteria as listed in **Appendix C**. Each of the treated bacteria (by PAM-5 and polymyxin B) as well as the untreated bacteria (negative control) was inoculated on MH media, followed by observation on their growth the next day. The gross views of the bacterial growth are presented in the next section; in which they are used to determine the minimal bactericidal concentrations (MBCs) of the peptide according to a modified version of microbroth dilution assay recommended by the Clinical Laboratory Standard Institute (CLSI).

The gross view analysis as mentioned above may provide visual information on the bactericidal effect of PAM-5. However, it may not reflect the quantitative inhibitory or bactericidal effect of the peptide on the bacteria. Titer determination on each of the treated bacteria with observable growth in the well of the microtiter plate was essential to disclose the degree of inhibition of the treated bacteria by the peptides at a particular concentration. Therefore, after three independent assays, the average titers of the bacteria treated with different concentrations of peptides (PAM-5 and polymyxin B) were determined and compared to the titers of untreated bacteria.

4.2.1 Antibacterial Effect of PAM-5 on *P. aeruginosa* ATCC 27853

In contrast to the low potency of Pa1 and Pa4, PAM-5 was found demonstrating enhanced antibacterial effect towards *P. aeruginosa* ATCC 27853 after the rational modification. As shown in **Figure 4.11 (a),** at concentrations ranging from 8 µg/mL to 256 µg/mL, PAM-5 was able to execute complete killing to the bacterium as indicated by the absence of bacterial growth on the inoculating media (Plate I to Plate N). However, the peptide was unable to kill the bacterium at lower concentrations (2 µg/mL and 4 µg/mL) as indicated by the bacterial lawn on the media plates O and P, in which the degree of bacterial growth was similar to the negative control (Plates Q and R). Polymyxin B, which served as the positive control, managed to kill the bacterium completely at all tested concentrations parallel to PAM-5 as no bacterial colony was seen on the inoculating media (Plates A to H).

Analysis on the degree of inhibition of *P. aeruginosa* by PAM-5 further confirmed that the peptide was not effective against the bacterium at 2 µg/mL and 4 µg/mL. Under the treatment by these low concentrations, *P. aeruginosa* was able to grow up to the titre that was almost similar to the negative control [**Figure 4.11(b**)]. However, the peptide was able to kill the bacterium completely at 8 µg/mL and other higher concentrations where a titre reduction of approximately 8 $\log_{10}$ CFU/mL was achieved. Thus, the MBC of PAM-5 against the reference strain of *P. aeruginosa* was determined as 8 µg/mL.
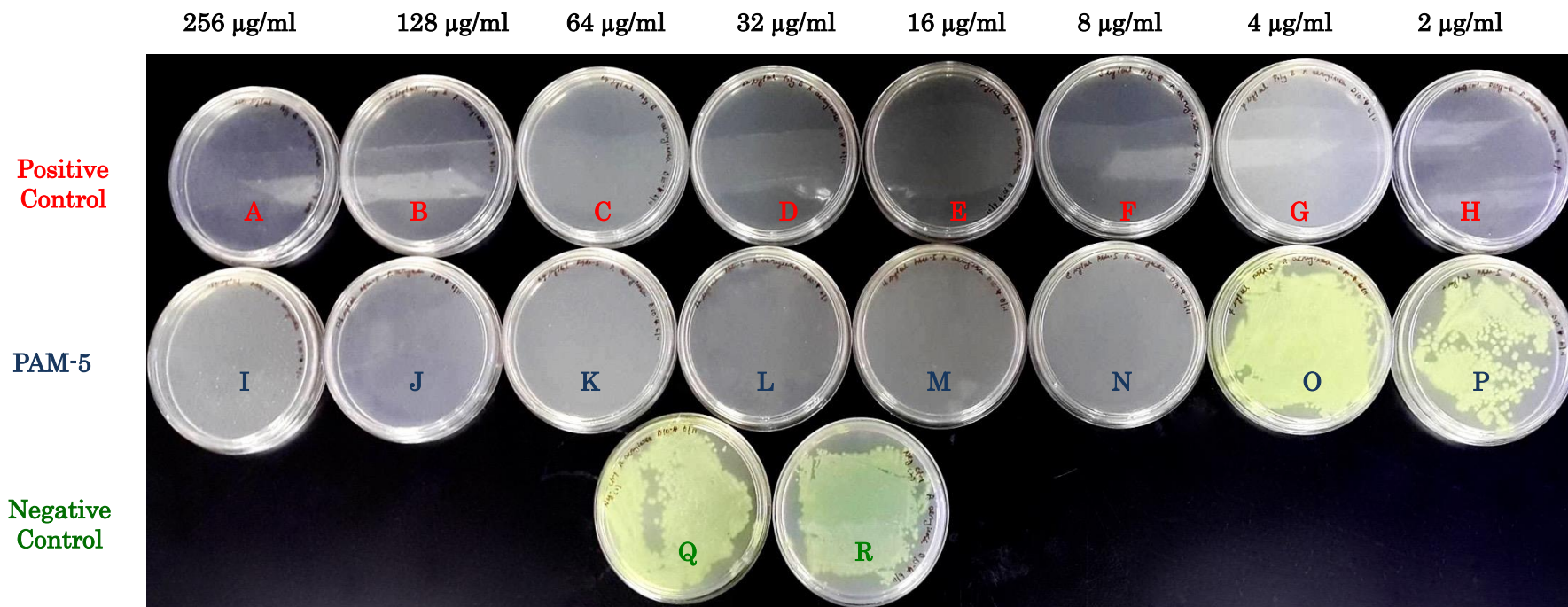
Figure 4.11 (a): Gross view of *P. aeruginosa* ATCC 27853 after peptide treatment. Plate A to Plate H which were inoculated with bacterial cultures treated with polymyxin B at concentrations from 256 μg/mL to 2 μg/mL served as the positive control. Plate I to Plate P were cultures of bacteria treated with PAM-5 at the same range of concentrations, while Plate Q and Plate R were untreated bacteria that served as the negative control. All plates were incubated overnight for 16 to 18 hours at 37ºC. The MBC of PAM-5 against *P. aeruginosa* ATCC 27853 was determined as 8 μg/ml (Plate N)
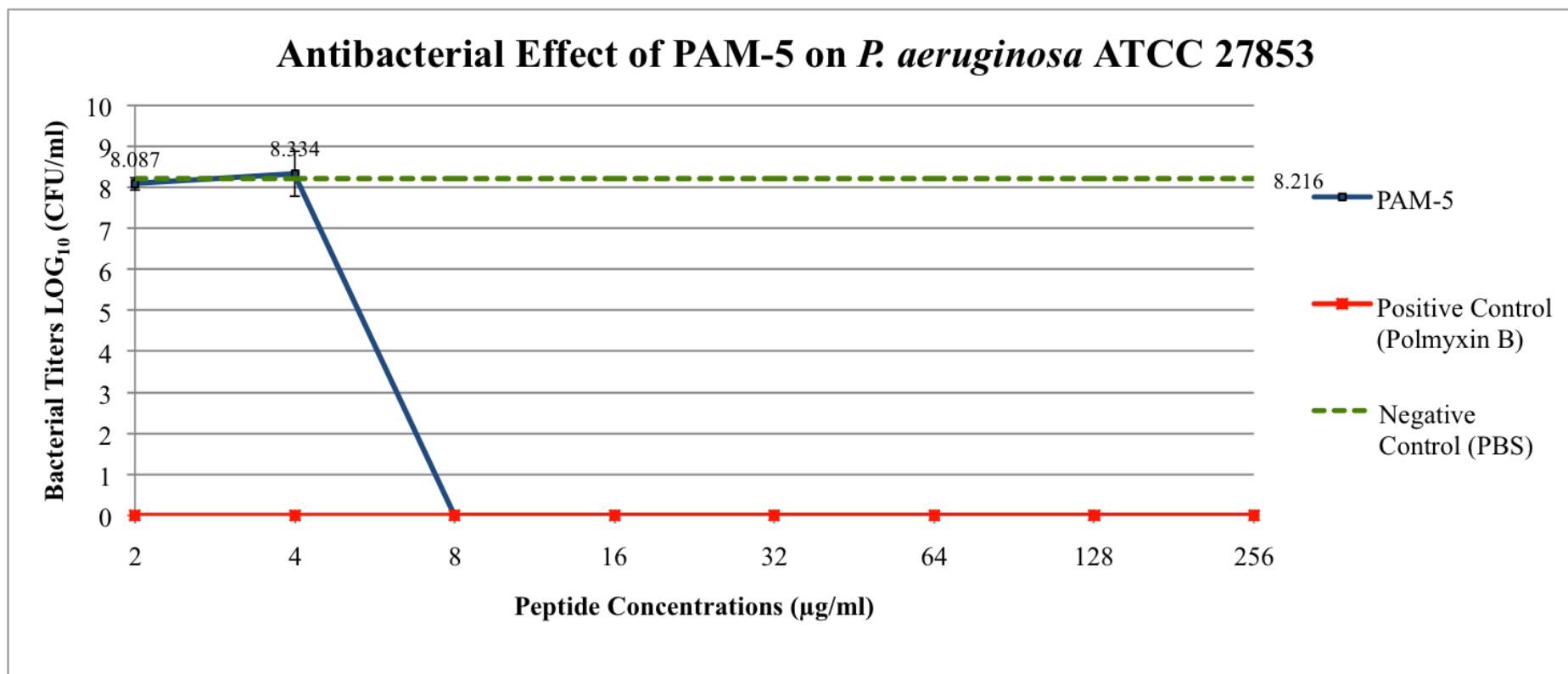
Figure 4.11 (b): Changes in titres of *P. aeruginosa* ATCC 27853 after treatment with different peptide concentrations. Bacteria were treated with different concentrations of PAM-5 and polymyxin B. Complete killing of bacteria was achieved by PAM-5 at concentrations of 8 µg/ml and above, while polymyxin B killed the bacterium at all tested concentrations. Untreated bacterium consistently grew heavily.

4.2.2   Screening for the Spectrum of Bacterial Targets by PAM-5

The antibacterial effect of PAM-5 was further screened for a list of Gram-negative and Gram-positive bacteria which encompassed ATCC reference strains as well as clinically isolated strains with different profiles of antibiotic resistance. The potencies of the peptide against these bacteria were determined by the values of MIC or MBC, which are tabulated in **Table 4.5**, while the gross view on the bacterial growth after peptide treatment and the degree of inhibition for each of these bacteria are presented in **Appendix D**.

As shown in **Table 4.5**, PAM-5 exhibited better potency against Gram-negative bacteria as compared to Gram-positive bacteria. This selective potency was reflected by the overall lower MBCs of the peptide against the former than the latter.   Triplicated assays confirmed the good activity of PAM-5 against *P. aeruginosa*, *E. coli*, *K. pneumoniae*, *Acinetobacter spp*. (*A. baumannii* and *A. junii*), *S.* Typhi and *S. flexneri* at different MBCs that ranged from 4 µg/mL to 32 µg/mL. Apart from its good antibacterial effect against the reference strains of some of the Gram-negative bacteria, PAM-5 was also active against the same species counterpart from clinical isolates with drug- or multidrug resistance. As reported above, PAM-5 was able to eliminate a reference strain of *P. aeruginosa* (ATCC 27853) at MBC of 8 µg/mL. Interestingly, this peptide remained active against another two clinical isolates of *P. aeruginosa* with cefazolin-resistance and multidrug-resistance at a slightly higher MBC (16 µg/mL). Similarly, PAM-5 also showed good antibacterial effect towards *K. pneumoniae*, where the peptide was able to kill the bacteria of both reference strain and clinical multidrug-resistant strains at MBCs that ranged from 8 to 32 µg/mL. This

included a carbapenem-resistant Enterobacteriaceae (CRE) strain of *K. pneumoniae*, which is considered as a superbug that is hardly to be treated with all available antibiotics. The two major human pathogens that cause serious gastrointestinal infections, *S.* Typhi and *S. flexneri*, were also susceptible to the bactericidal effect of PAM-5, where the bacteria were completely eliminated by the peptide at 32 µg/mL. Nevertheless, PAM-5 was inactive against a clinical strain of *S. marcescens* even though at the highest tested concentration (256 µg/mL).

Despite the overall good antibacterial effect against the tested Gram-negative bacteria, PAM-5 exhibited relatively poorer potencies towards most of the Gram-positive bacteria screened in this study, except for *Streptococcus anginosus* (*S. anginosus*). As tabulated in **Table 4.5**, PAM-5 was only able to achieve complete killing to reference strains of *S. aureus* and *S. pyogenes* at 128 µg/mL and 64 µg/mL, respectively. However, no sign of bacteriostatic or bactericidal effect was seen for PAM-5 against a reference strain of *E. faecalis*, where the bacterium was able to grow heavily despite treatment with the highest concentration of PAM-5 (256 µg/mL). In contrast to its low potency towards the above-mentioned *Streptococcus* spp., PAM-5, however, was found very potent against another species of Streptococcus, namely *S. anginosus*. The clinical isolate was completely eradicated by PAM-5 at concentration as low as 4 µg/mL.

Observation of the bacterial growth on the growing media after peptide treatment revealed that PAM-5 was mostly bactericidal towards the bacteria screened in this study. Except for the clinical isolates of ESBL-producing *E. coli* 1160702 and *K. pneumoniae* 1139142, all the other bacteria were directly killed by PAM-5 at its corresponding MBCs towards the bacteria without signs of growth inhibition.

Table 4.5: MICs and/or MBCs of PAM-5 towards selected Gram-positive and Gram-negative bacteria screened in this study.

Bacterial species and strains	Relevant features	Minimal bacteriostatic concentrations (MIC) (μg/mL)	Minimal bactericidal concentration (MBC) (μg/mL)
Pseudomonas aeruginosa ATCC 27853	Reference strain	ND	8
Pseudomonas aeruginosa 1320026	C.I. CFZ^R	ND	16
Pseudomonas aeruginosa 12594264	C.I. LVX^R MXF^R DOR^R ETP^R MEM^R CAZ^R CRO^R FEP^R (MDR)	ND	16
Escherichia coli ATCC 25922	Reference strain	ND	8
Escherichia coli 1160702	C.I. AMC^I CFZ^R CXM^R CTX^R CRO^R GEN^R CIP^R (ESBL)	8	16
Acinetobacter baumannii ATCC 19606	Reference strain	ND	8
Acinetobacter junii 1191828	C.I. CFZ^R CRO^R CAZ^R	ND	4
Klebsiella pneumoniae ATCC 138833	Reference strain	ND	32
Klebsiella pneumoniae 1139142	C.I. AMP^R CFZ^R CXM^R CTX^R CAZ^R CRO^R ATM^R GEN^R CIP^R NIT^I SAM^I (ESBL)	16	32

Table 4.5 (<u>Continued</u>):

Klebsiella pneumoniae 1208398	C.I. AMP^R AMC^R SAM^R TZP^R CFZ^R CXM^R FOX^R CTX^R CAZ^R CRO^R FEP^R ATM^R MEM^R AMK^R GEN^R CIP^R NIT^R (CRE)	ND	8
Salmonella Typhi 1238912	C.I. CAZ^R CTX^R GEN^R	ND	32
Shigella flexneri 1109563	C.I. CFX^R CFZ^R CXM^R AMK^R CIP^R	ND	32
Serratia marcescens 1191741	C.I. AMX^R CFZ^R CXM^R FOX^R	ND	>256
Staphylococcus aureus ATCC 25923	Reference strain	ND	128
Enterococcus faecalis ATCC 19433	Reference strain	ND	>256
Streptococcus pyogenes ATCC 19615	Reference strain	ND	64
Streptococcus anginosus 1360589	C.I.	ND	4

C.I.: Clinical isolate; CFZ^R: resistance to cefazolin; LVX^R: resistance to levofloxacin; MXF^R: resistance to moxifloxacin; DOR^R: resistance to doripenem; PB^R: resistance to polymyxin B; ETP^R: resistance to ertapenem, MEM^R: resistance to meropenem; CAZ^R: resistance to ceftazidime; CRO^R: resistance to ceftriaxone; FEP^R: resistance to cefepime; MDR: multi-drug resistance; AMC^I: reduced susceptibility to amoxicillin/clavulanic acid; CXM^R: resistance to cefuroxime; CTX^R: resistance to cefotaxime; GEN^R: resistance to gentamicin; CIP^R: resistance to ciprofloxacin; ATM^R: resistance to aztreonam; NIT^I: reduced susceptibility to nitrofurantoin; AMX^R: resistance to amoxicillin; AMP^R: resistance to ampicillin; SAM^I: reduced susceptibility to ampicillin/Sulbactam; TZP^R: resistance to piperacillin/Tazobactam; FOX^R: resistance to cefoxitin; AMK^R: resistance to amikacin; ESBL: extended spectrum beta-lactamases, CRE: Carbapenem-resistant Enterobacteriaceae

4.3   Assessment of PAM-5 Stability in Human Plasma

The stability of PAM-5 in human plasma was assessed by *ex-vivo* microbroth dilution assay as described in **Section 3.6**. By comparing the MBCs of PAM-5 on *P. aeruginosa* ATCC 27853 derived from the *in vitro* and *ex vivo* assays, the stability of PAM-5 in the latter could be estimated.

With reference to **Figure 4.12**, PAM-5 was unable to kill the bacterium completely at the tested concentrations ranging from 2 µg/mL to 8 µg/mL. The bacterium treated with PAM-5 at these concentrations was able to grow to the titer relatively similar to the untreated bacteria (negative control). Upon 16 µg/mL, the bacterium was completely eliminated by the peptide despite the presence of human plasma in the assay. This complete elimination corresponded to the titer reduction of approximately 8.5 $\log_{10}$ CFU/mL as compared to the untreated bacteria. As compared to the MBC of PAM-5 towards the same strain of bacterium in the *in vitro* condition (8 µg/mL), PAM-5 was slightly less effective in the *ex vivo* condition.
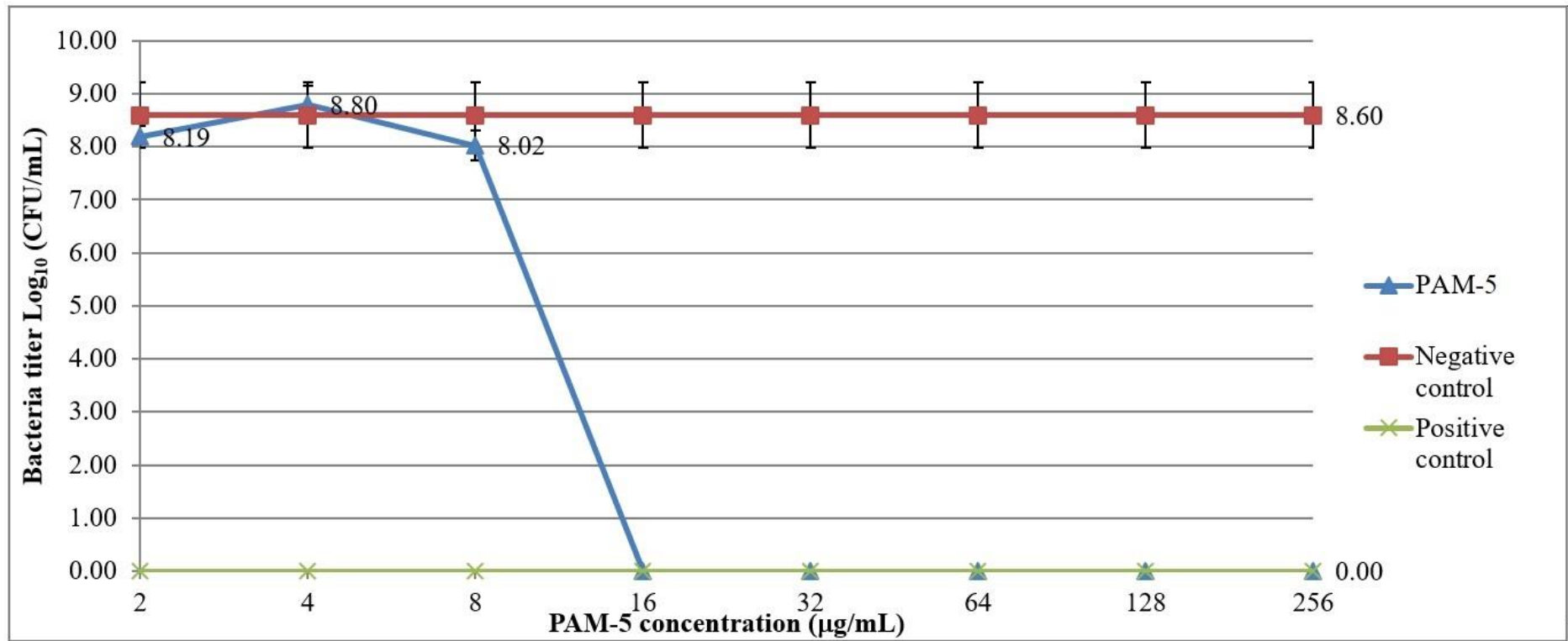
Figure 4.12: Antibacterial effect of PAM-5 on *P. aeruginosa* ATCC 27853 in the presence of human plasma. High bacterial viability was observed when the bacterium was treated with PAM-5 at concentrations lower than 16 µg/mL. The peptide demonstrated complete bactericidal effect to the bacterium at 16 µg/mL and other higher concentrations. Triplicate assay consistently showed this concentration was the MBC of this peptide to the bacterium.

4.4 Time-Kill Kinetic Assay for PAM-5, Gentamicin and Polymyxin B Towards *P. aeruginosa* ATCC 27853 and *E. coli* ATCC 35218

The kinetic killing of PAM-5 on *P. aeruginosa* and *E. coli* was studied via time-kill assay as described in **Section 3.7**. As mentioned, the treated and untreated (negative control) bacteria were inoculated on MH media according to the designated quadrant at every 10-minute interval upon treatment. The growth of the inoculated bacteria was observed after overnight incubation and the corresponding colonies of the PAM-5-treated bacteria were compared to the gentamicin-treated and polymyxin B-treated bacteria as well as the untreated bacteria.

As demonstrated from the top left quadrant of Plate A in **Figure 4.13**, *P. aeruginosa* was completely eradicated by PAM-5 at its $2 \times$ MBC within 10 minutes of treatment, indicated by the absence of bacterial colony in the quadrant. Throughout the triplicated assays, this rapid killing kinetic by PAM-5 was consistently observed, in which the peptide was able to reduce the bacterial titer by approximately 3 logs the initial inoculum within the first 10 minutes (**Figure 4.14**). Upon this time point, the complete killing was maintained throughout the entire 60 minutes.

On the other hand, the similar extent of rapid killing was not achieved by gentamicin and polymyxin B at their $2 \times$ MBCs. Even though after 60 minutes treated by these two antibacterial agents, colonies of *P. aeruginosa* were still present at the quadrants inoculated with the treated bacteria (**Figure 4.13**; **Plate**

144

A to **Plate F**). With reference to **Figure 4.14**, both gentamicin and polymyxin B did not kill *P. aeruginosa* at the similar rate as compared to PAM-5, even though a slight titer reduction was observed from the initial inoculum throughout the entire duration of treatment.

The similar rapid killing was also observed for PAM-5 on *E. coli*, in which the peptide was also able to kill the bacterium completely within the first 10 minute upon treatment. Clearly demonstrated from **Figure 4.15**, no bacterial colony was seen on the top left quadrants of **Plate A** which was inoculated with *E. coli* treated with PAM-5 at its $2 \times MBC$ for 10 minutes, indicating complete killing of the bacterium within the short duration of treatment. After this, no bacterial colony was seen at the same quadrants from **Plate B** to **Plate F** which were inoculated with PAM-5-treated bacteria at the time intervals from 20 to 60 minutes, respectively. This killing rate by PAM-5 was even faster than gentamicin and polymyxin B, in which the complete killing of the bacterium by the latter two can only be achieved after 40 minutes of treatment (**Figure 4.15**; **Plate D**; upper right quadrant and lower right quadrant). While PAM-5 achieved a 3 log titer reduction in 10 minutes, both the antibacterial agents were only able to reduce the bacterial titer by less than 0.5 log from the initial inoculation titer, before eliminating the bacterium completely after another 30 minutes of treatment (**Figure 4.16**).
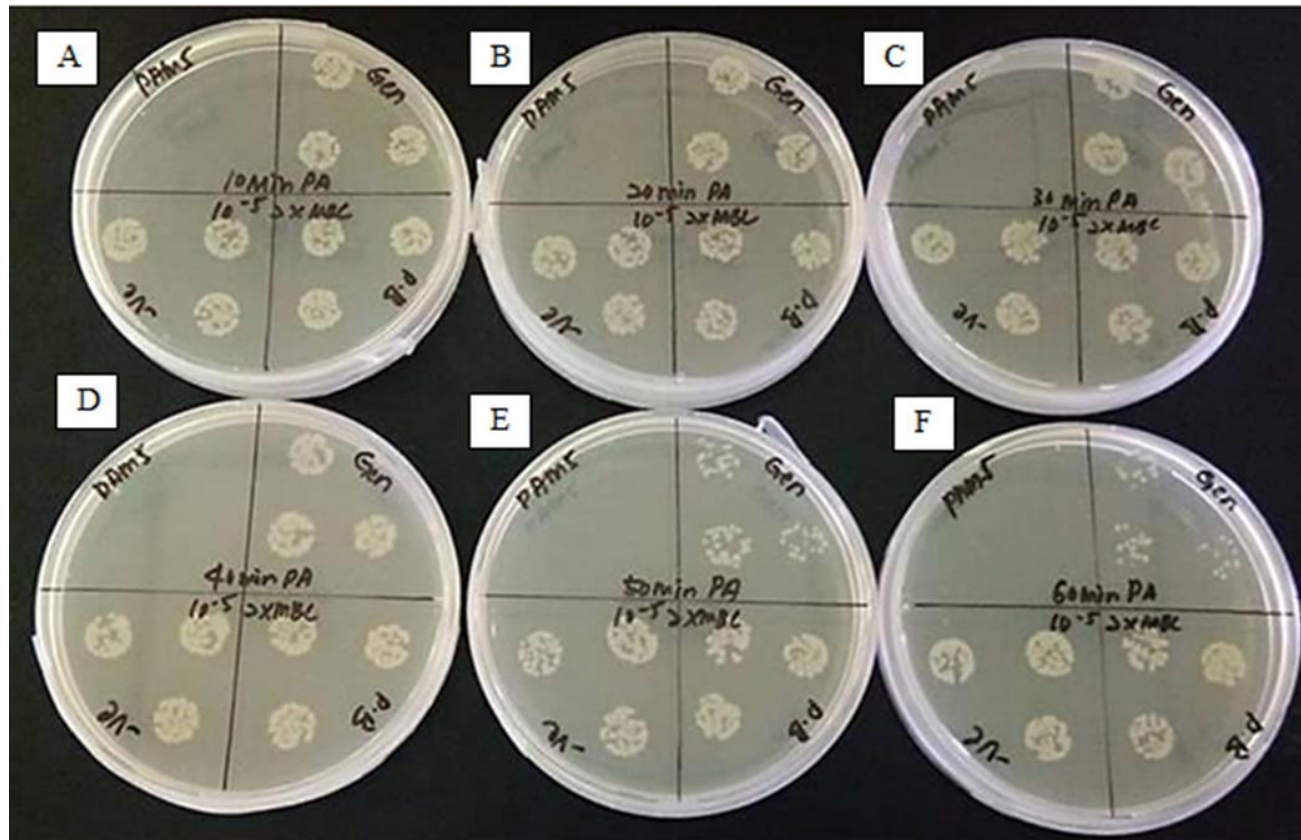
Figure 4.13: Gross view on the time-kill assay of PAM-5-, gentamicin- and polymyxin B-treated *P. aeruginosa* ATCC 27853. Inoculation of bacteria treated with PAM-5 (top left quadrant), gentamicin (top right quadrant), polymyxin B (bottom right quadrant) and untreated bacteria which served as the negative control (bottom left quadrant) from 10 minutes to 60 minutes (**Plates A** to **F**).
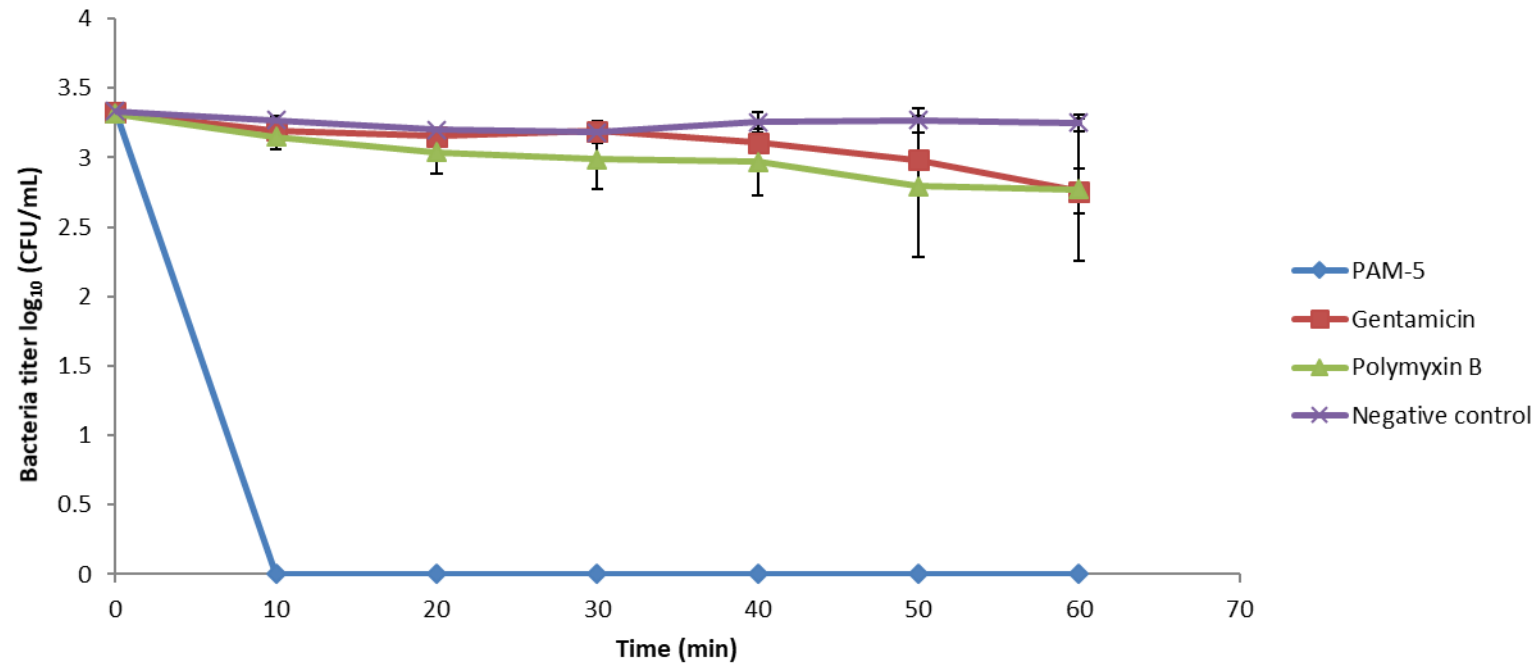
Figure 4.14: Titre changes of *P. aeruginosa* ATCC 27853 treated by PAM-5, gentamicin and polymyxin B in the time-kill assay for the duration of 60 minutes. The untreated bacterium suspended in PBS served as the negative control.
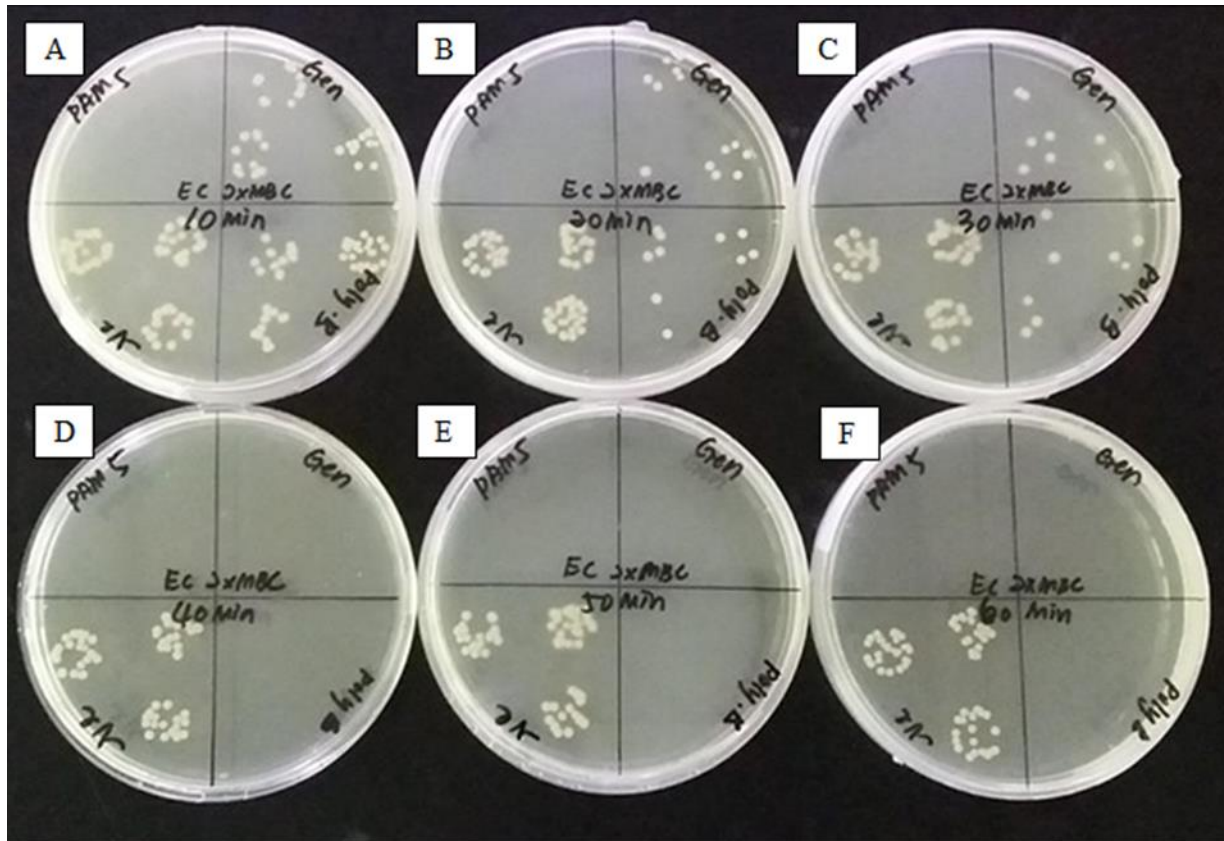
Figure 4.15: Gross view on the time-kill assay of PAM-5-, gentamicin- and polymyxin B-treated *E. coli* ATCC 35218. Inoculation of bacteria treated with PAM-5 (top left quadrant), gentamicin (top right quadrant), polymyxin B (bottom right quadrant) and untreated bacteria which served as the negative control (bottom left quadrant) from 10 minutes to 60 minutes (**Plates A** to **F**).
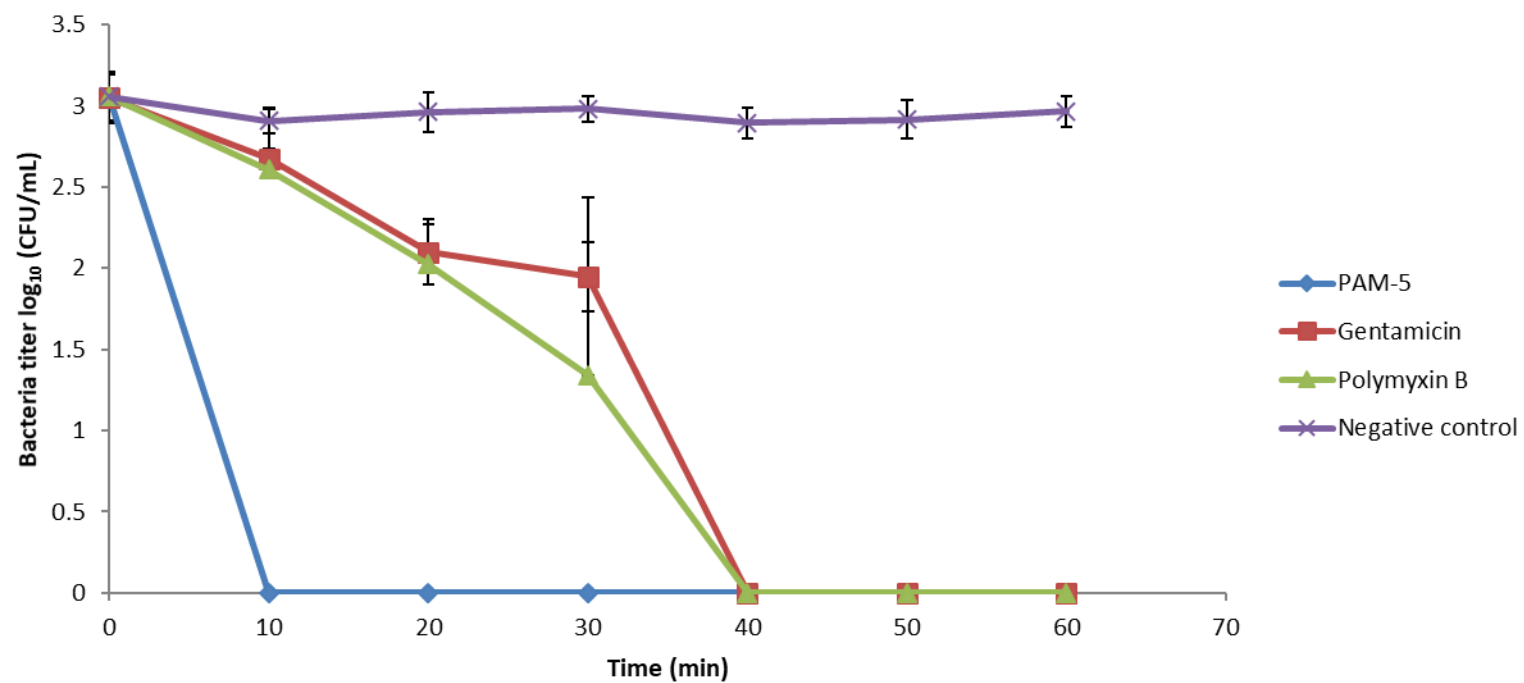
Figure 4.16: Titre changes for *E. coli* ATCC 35218 treated by PAM-5, gentamicin and polymyxin B in the time-kill assay for the duration of 60 minutes. The untreated bacteria suspended in PBS served as the negative control.

4.5   Screening for Membrane-Active Actions of PAM-5

As demonstrated in the microbroth dilution assay, PAM-5 exhibited bactericidal effect towards a number of bacteria especially Gram-negative bacteria. Therefore, it is noteworthy to investigate the type of mechanism/s of action in which PAM-5 employed to kill the bacteria. In consideration of the cationicity of this peptide, along with its moderate hydrophobicity, it is anticipated that PAM-5 may possess the classical mode of actions on the anionic bacterial membranes like other membrane-active ABPs. In order to obtain a direct insight into the action of PAM-5 on the bacterial membrane, the peptide-treated bacteria were observed and analysed under scanning electron microscope (SEM) which provides visualization of any structural or morphological changes to the bacterial surface. Apart from that, SYTOX® Green uptake assay was utilized to determine the ability of PAM-5 to permeabilize the bacterial inner membrane.

4.5.1   Scanning Electron Microscope (SEM) Analysis

As shown by the micrograph in **Figure 4.17 (a)**, untreated cells of *P. aeruginosa* which served as the negative control were morphologically and structurally intact with smooth surface when they were viewed under lower magnification power of $18,000 \times$. In contrast, polymyxin B-treated *P. aeruginosa* which served as the positive control displayed higher degree of surface corrugation [**Figure 4.17 (b)**]. Interestingly, *P. aeruginosa* treated with PAM-5 for 1 hour also demonstrated similar morphological changes as the positive control, in which the surface corrugation and roughening were clearly seen [**Figure 4.17 (c)**].

Under higher magnification power (30,000 ×), the characteristics of the membrane disruption were even more apparent. Apart from surface corrugation, the membranes of both Polymyxin B- and PAM-5-treated bacteria displayed small protuberant structures or blebbings that were present extensively throughout the entire bacterial outer surface [**Figure 4.18 (b) and (c)**]. However, these features were absent in the untreated bacteria as depicted in **Figure 4.18 (a)**.

On closer examination under the magnification of 40,000 ×, further contrastable surface morphology between the untreated and PAM-5-treated bacteria can be observed. With reference to **Figure 4.19 (c)**, the degree of membrane disruption caused by PAM-5 to a bacterium was so severe to a critical point that part of the membrane was ruptured (indicated by arrow). In contrast, these blister-like structures were not seen on the surface of untreated bacteria [**Figure 4.19 (a)**]. These observations provided direct morphological evidence on the membrane-active mechanism of PAM-5.

(a) **(b)** **(c)**
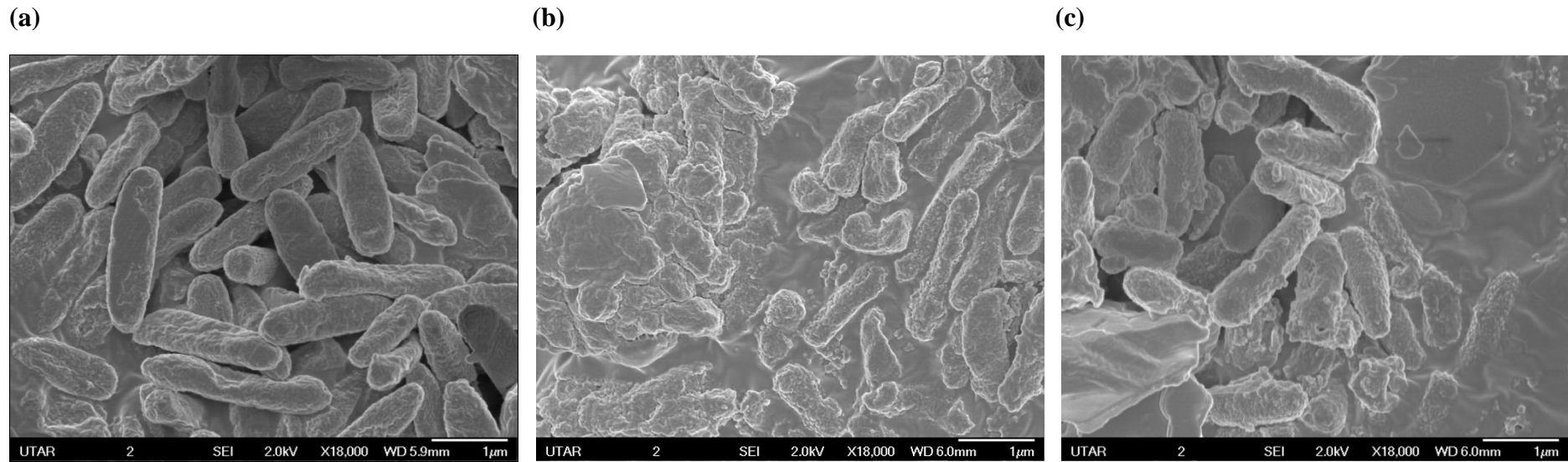
Figure 4.17: SEM micrographs of peptide-treated and untreated *P. aeruginosa* ATCC 27853 viewed under 18, 000 × magnification. (a) Untreated bacteria that served as the negative control; (b) bacteria treated with 128 μg/mL of polymyxin B which served as the positive control; (c) bacteria treated with 128 μg/mL of PAM-5.

(a)

(b)

(c)
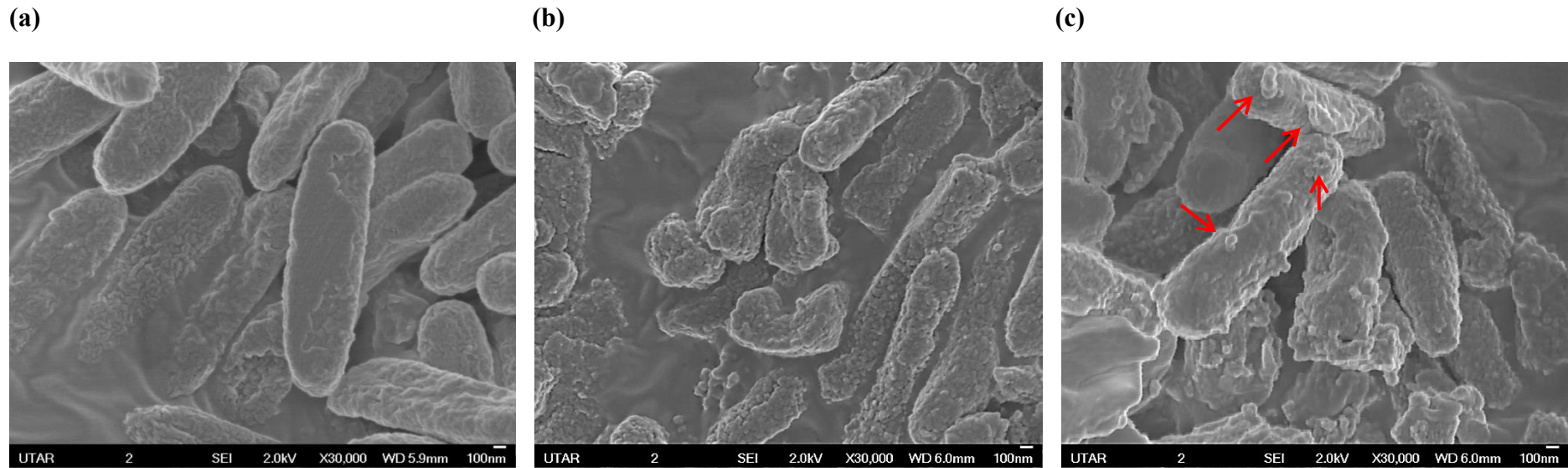
Figure 4.18: SEM micrographs of peptide-treated and untreated *P. aeruginosa* ATCC 27853 observed under 30,000 × magnification. Smoother surfaces are apparent for untreated bacteria (a). In contrast, surface roughening and corrugation are clearly seen from the polymyxin B-treated bacteria (b) and PAM-5-treated bacteria (c). Small protuberant structures can be seen on the surface of PAM-5-treated bacteria (indicated by red arrows).
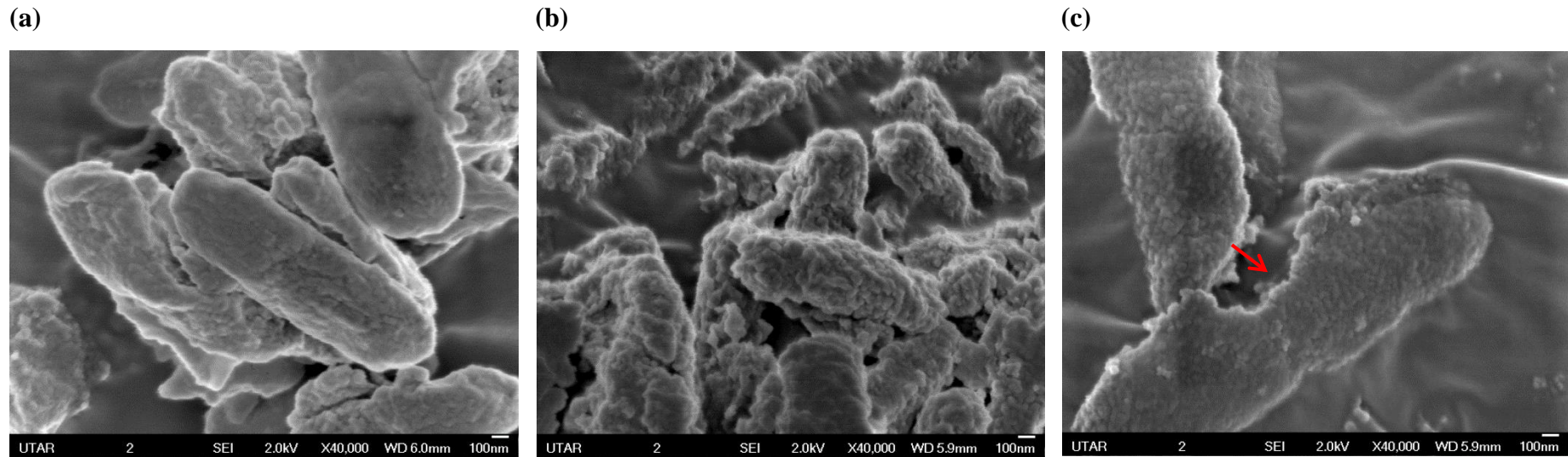
Figure 4.19: SEM micrographs of peptide-treated and untreated *P. aeruginosa* ATCC 27853 observed under magnification of 40,000 × magnification. (a) Untreated bacteria presented with smoother surface; (b) extensive surface corrugation which is characterized by blebbings or micellar-like structures can be seen on polymyxin B-treated bacteria; (c) severe damage characterized by membrane rupture (indicated by arrow) can be seen in one of the PAM-5-treated bacteria.

4.5.2 SYTOX® Green Uptake Assay

The findings on the membrane disruption by PAM-5 as observed in SEM gave rise to a speculation that the peptide may cause permeabilization to the bacterial plasma membrane. Therefore, SYTOX® Green uptake assay was conducted to verify this. As mentioned earlier, SYTOX® Green dye is a membrane-impermeable dye which is not able to translocate across an intact membrane. The dye is only able to enter a cell with disrupted or permeabilized inner membrane, which subsequently allow it to bind to intracellular nucleic acids followed by fluorescence emission (Thakur et al. 2015). Therefore, it is generally accepted that the fluorescent intensity emitted by the peptide-treated bacteria is proportional to the amount of SYTOX Green dye entering and binding to bacterial nucleic acids, which in turn reflecting the degree of membrane permeabilization by a membrane-active agent.

Figure 4.20 presents the data of average green fluorescent intensity generated by the PAM-5- and polymyxin B-treated *P. aeruginosa* from three independent assays. As demonstrated in the figure, extremely low fluorescence was consistently observed from the two untreated bacteria (negative control), in which the bacteria were suspended in PBS. Conversely, all the positive controls (polymyxin B-treated bacteria) generated 5- to 6-times higher fluorescent signals as compared to the negative control. In terms of PAM-5-treated bacteria, although the overall fluorescent signals emitted by these bacteria were lower than the positive control, but they were generally higher than the negative control. When the bacteria were treated with PAM-5 at concentrations that

ranged from 2 µg/mL to 64 µg/mL, the mean SYTOX Green fluorescent signals increased in a concentration-dependent manner. The fluorescent signals were slightly higher than the negative control at the first two PAM-5 concentrations (2 µg/ml and 4 µg/ml), and gradually increased along with the increasing treatment concentrations to a peak signal which was generated by bacteria treated with 64 µg/mL of PAM-5. However, instead of further increasing, the fluorescent intensity was seen declining from the bacteria treated with 128 µg/ml and 256 µg/mL of PAM-5. This unexpected pattern of fluorescent emission was consistent throughout the three independent assays.
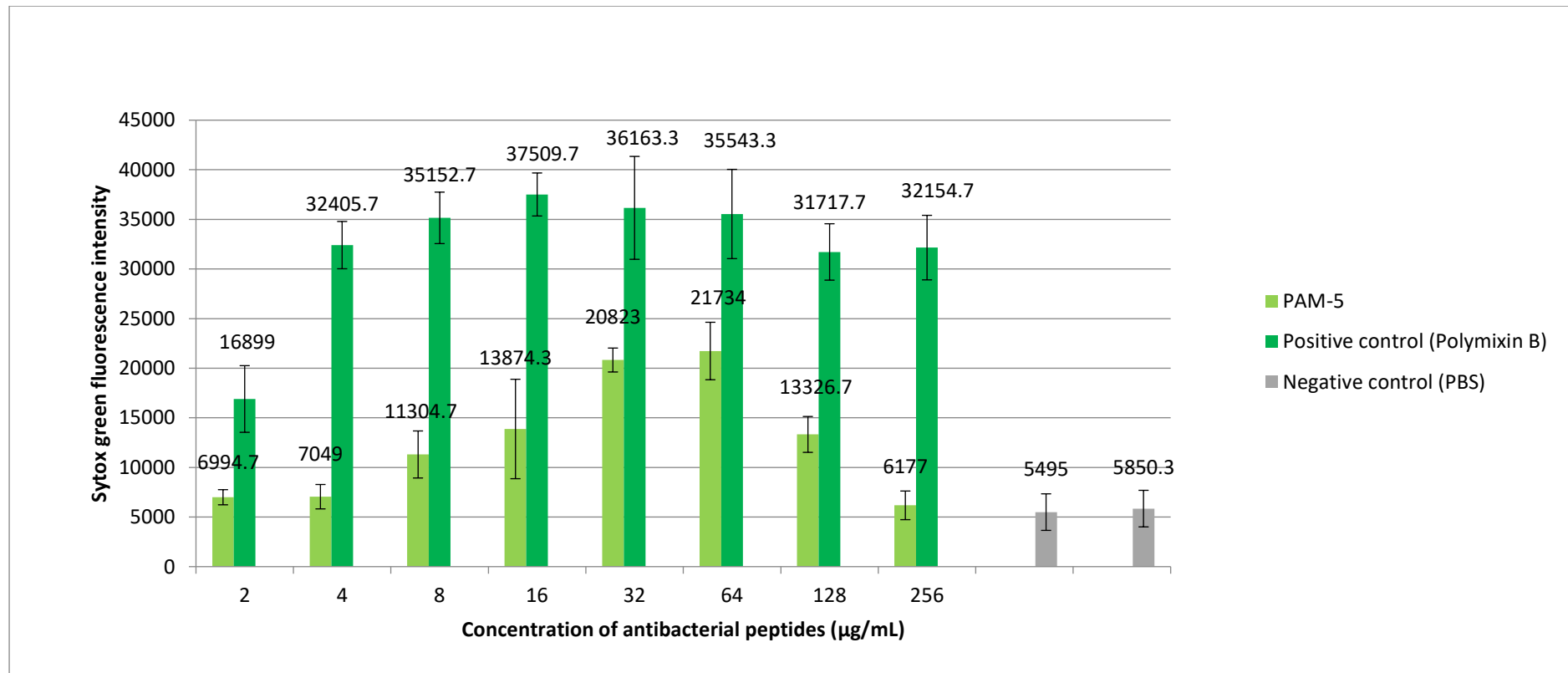
Figure 4.20: Bacterial cytoplasmic membrane permeabilization by different peptide concentrations as determined by SYTOX® Green uptake assay. *P. aeruginosa* with the titer of 10^6 CFU/ml were treated with two-fold serially diluted PAM-5 with the final concentrations ranging from 2 µg/ml to 256 µg/ml. Bacteria treated with polymyxin B of the same range of concentrations served as the positive control, while untreated bacteria served as the negative control. The data were presented as means ($\pm$ SD) of three independent assays.

4.6 Screening for PAM-5 Binding to Genomic DNA and Plasmid DNA from Selected Bacteria

Using gel retardation assay, the DNA-binding ability of PAM-5 was evaluated. This assay was conducted on genomic DNAs extracted from several bacteria as described in **Section 3.10.1** to probe any difference in DNA binding by the peptide across bacterial species. Apart from that, the peptide was also screened for its binding to a commercially available plasmid DNA isolated from *E. coli*, pBR322. Positive finding on DNA binding was indicated by the hindered or slower migration of PAM-5-treated DNA across the gel as compared to the untreated DNA (negative control) after the gel electrophoresis.

4.6.1 Binding Ability of PAM-5 to Genomic DNA from *E. coli* ATCC 35218

As demonstrated in **Figure 4.21**, PAM-5 could interact with genomic DNA from *E. coli* and retarded its migration in the agarose gel at high concentrations. At concentrations from 4 µg/mL to 32 µg/mL (Lane 2 to Lane 5), DNA migration was not hindered by PAM-5 as the peptide-treated DNAs were able to migrate out from the wells at the similar rate and band intensity in relative to the untreated DNA (Lane 1). However, beginning from 64 µg/mL to 256 µg/mL, PAM-5 caused complete retardation to the DNA migration as no DNA fragment was seen migrating out from the wells into the agarose gel. In contrast, the amount of DNA retained in the wells loaded with these DNA (Wells 6, 7 and 8) was higher as indicated by the higher fluorescence intensity from the ethidium

bromide (EtBr) in those wells. This showed that PAM-5 was able to bind to the

DNA from *E. coli* at high concentrations (64 µg/mL and 256 µg/mL).
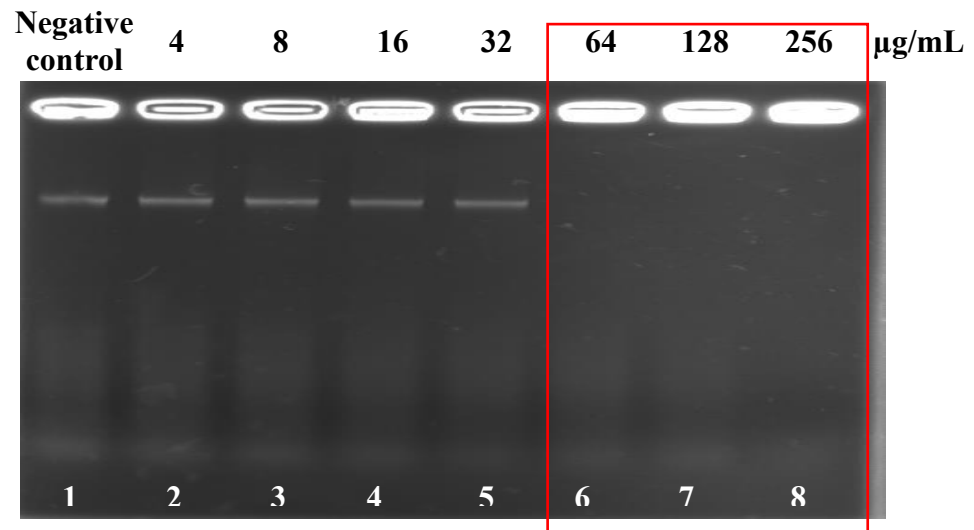
Figure 4.21: Gel retardation assay on the binding of PAM-5 to genomic DNA from *E. coli*. Lane 1: untreated DNA; lanes 2 to 8: DNA treated with increasing amount of PAM-5 ranging from 4 µg/mL to 256 µg/mL.

4.6.2 Binding Ability of PAM-5 to Genomic DNA from *P. aeruginosa* ATCC 27853

Apart from binding to the DNA from *E. coli*, PAM-5 was also able to bind to genomic DNA from other bacteria. As demonstrated in **Figure 4.22**, PAM-5 was able to bind to DNA isolated from *P. aeruginosa* in a concentration-dependent manner. Similar to the findings in **Section 4.6.1**, complete retardation to migration of the bacterial DNA only can be seen at high peptide concentrations. However, as compared to the DNA from *E. coli*, PAM-5 only showed complete retardation to the DNA migration at 128 µg/mL and 256 µg/mL (Lanes 7 and 8). Although no complete retardation was caused by PAM-5 at 64 µg/mL (Lane 6), the amount of DNA migrated out from the well was slightly lesser as compared to the untreated DNA (Lane 1) and DNAs treated with PAM-5 of concentrations from 4 µg/mL to 32 µg/mL (Lanes 2 to 5). This was indicated by the lower intensity of migrating DNA band in Lane 6 as compared to the band intensities in Lane 1 to Lane 5.
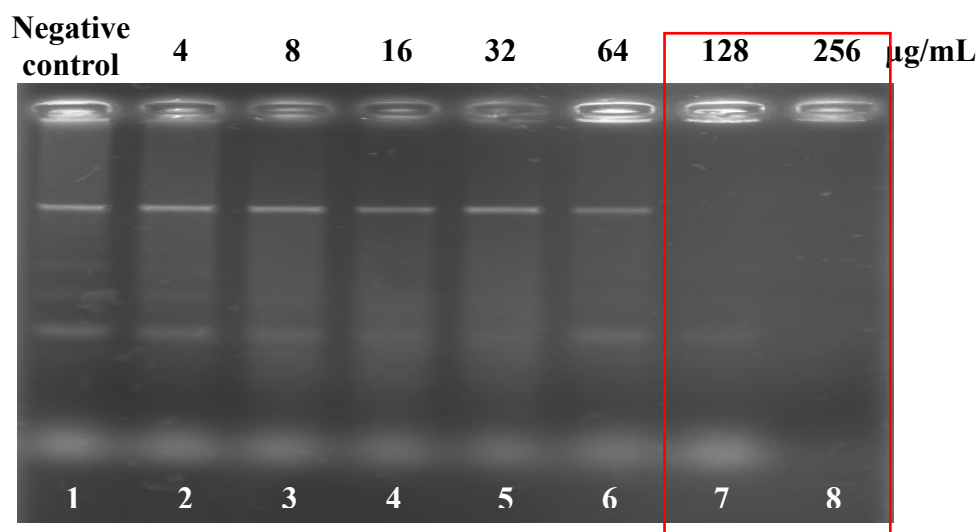
Figure 4.22: Gel retardation assay on the binding of PAM-5 to genomic DNA of *P. aeruginosa*. Lane 1: untreated DNA; lanes 2 to 8: DNAs treated with increasing amount of PAM-5 ranging from 4 µg/mL to 256 µg/mL.

4.6.3 Binding Ability of PAM-5 to Genomic DNA from *A. baumannii* ATCC 19606

Similar findings were also found on the binding ability of PAM-5 to genomic DNA from *A. baumannii*. As shown in **Figure 4.23**, the extent of retardation by PAM-5 to the migration of this bacterial nucleic acid was almost similar to the one from *P. aeruginosa*, in which complete retardation also occurred at the concentrations of 128 µg/mL and 256 µg/mL (Lanes 7 and 8). Again, this peptide was not able to retard the DNA migration at lower concentrations ranging from 4 µg/mL to 32 µg/mL (Lane 2 to Lane 5), where both the migration rates and band intensities of these treated-DNA were similar to the negative control. Although no complete retardation to the DNA migration by PAM-5 at 64 µg/mL, partial retardation was seen as indicated by the lower band intensity in lane 6.
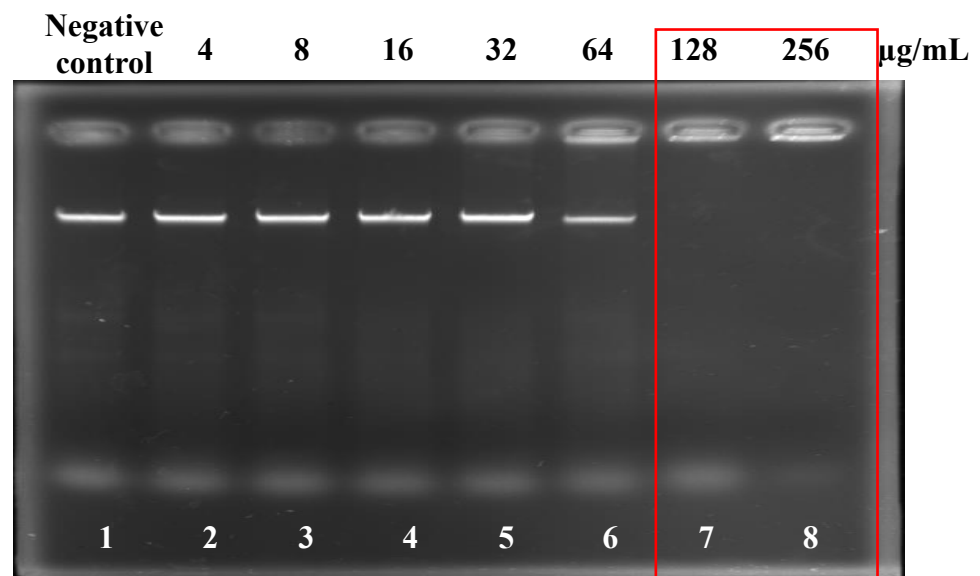
Figure 4.23: Gel retardation assay on the binding of PAM-5 to genomic DNA of *A. baumannii.* Lane 1: untreated DNA; lanes 2 to 8: DNAs treated with increasing amount of PAM-5 ranging from 4 µg/mL to 256 µg/mL.

4.6.4 Binding Ability of PAM-5 to Genomic DNA from *K. pneumoniae* ATCC 13883

Once again, similar pattern of retardation was seen for PAM-5 on genomic DNA isolated from *K. pneumoniae*. As depicted in **Figure 4.24**, after treatment with PAM-5 at concentrations from 4 µg/mL to 32 µg/mL, bands of DNA migration after the electrophoresis can be seen from Lane 2 to Lane 6, in which the band intensities and rates of migration were relatively similar to the negative control (Lane 1). Slight DNA retardation was observed in Lane 6, which was loaded with DNA treated with 64 µg/mL of PAM-5, as indicated by the slightly lower band intensity in the lane. Complete retardation of DNA migration was seen in Lane 7 and Lane 8, in which the DNAs were treated with PAM-5 at concentrations of 128 µg/mL and 256 µg/mL, respectively.
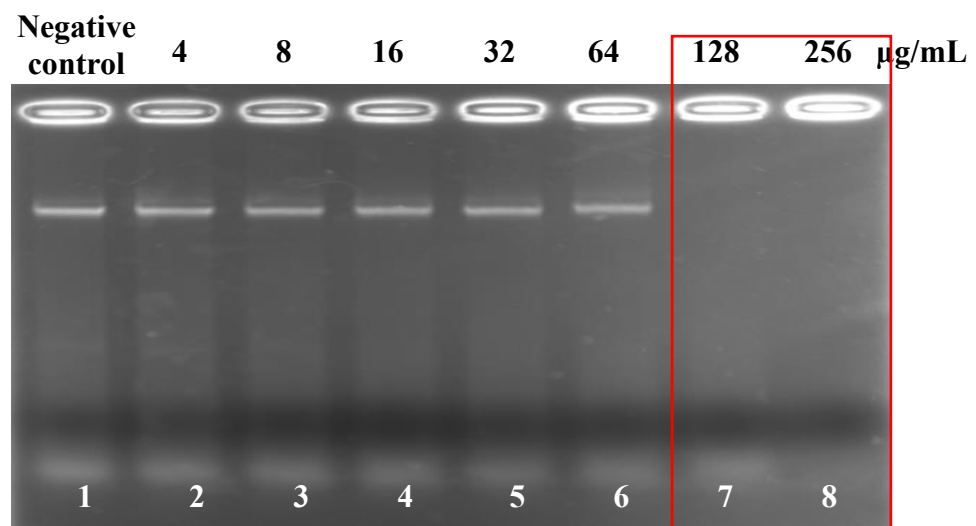
Figure 4.24: Gel retardation assay on the binding of PAM-5 to genomic DNA of *K. pneumoniae.* Lane 1: untreated DNA; lanes 2 to 8: DNAs treated with increasing amount of PAM-5 ranging from 4 µg/mL to 256 µg/mL.

4.6.5 Binding Ability of PAM-5 to Plasmid DNA pBR322

As seen in **Figure 4.25**, two visible bands can be seen in each lane when the plasmid was subjected to agarose gel electrophoresis. The upper bands with slower migration rate from Lane 1 to lane 5 represent the relaxed form of the plasmid, while the lower bands with faster migration rate represent the supercoiled form. Clearly demonstrated from the figure, at lower concentrations of PAM-5 (4 µg/mL to 32 µg/mL), retardation to the plasmid migration by PAM-5 was not evident, as indicated by the relatively similar band intensities and migration rate between the PAM-5-treated plasmid and the untreated plasmid. However, at the concentrations of 64 µg/mL and 128 µg/mL, the amount of plasmid that was able to migrate through the agarose gel was greatly reduced. This was indicated by the reduced intensity of the bands that represent the supercoiled and relaxed forms of the plasmid. At 256 µg/mL (Lane 8), the migration of the plasmid was totally retarded.
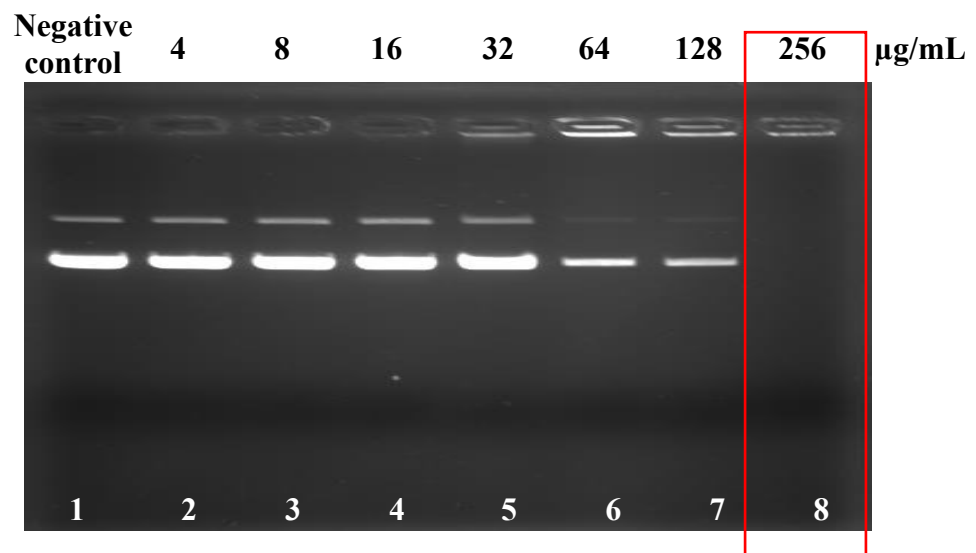
Figure 4.25: Gel retardation assay on the binding of PAM-5 to pBR322 *E. coli* plasmid DNA. Lane 1: untreated DNA; lanes 2 to 8: DNAs treated with increasing amount of PAM-5 ranging from 4 µg/mL to 256 µg/mL.

4.6.6 Binding Ability of Polymyxin B to Genomic DNA from *E. coli* ATCC 35218

The capacity of DNA-binding by PAM-5 was compared to polymyxin B, a powerful ABP which was approved for clinical application. However, instead of DNAs from the four bacteria as mentioned earlier, only DNA extracted from *E. coli* was chosen for this comparison. With reference to **Figure 4.21** and **4.26**, the capacity of DNA-retardation for polymyxin was relatively lower than PAM-5. This is because complete retardation of the DNA migration only can be achieved at the highest concentration of this peptide (256 µg/mL). At concentrations from 4 µg/mL to 64 µg/mL, no sign of DNA retardation could be seen as the polymyxin B-treated DNAs were still able to migrate out from the wells during the electrophoresis. Additionally, the rate and amount of these migrated DNAs were relatively similar to the untreated DNA. Partial retardation was observed for DNA treated with 128 µg/mL of polymyxin B, as indicated by the reduced band intensity of the migrated DNA.
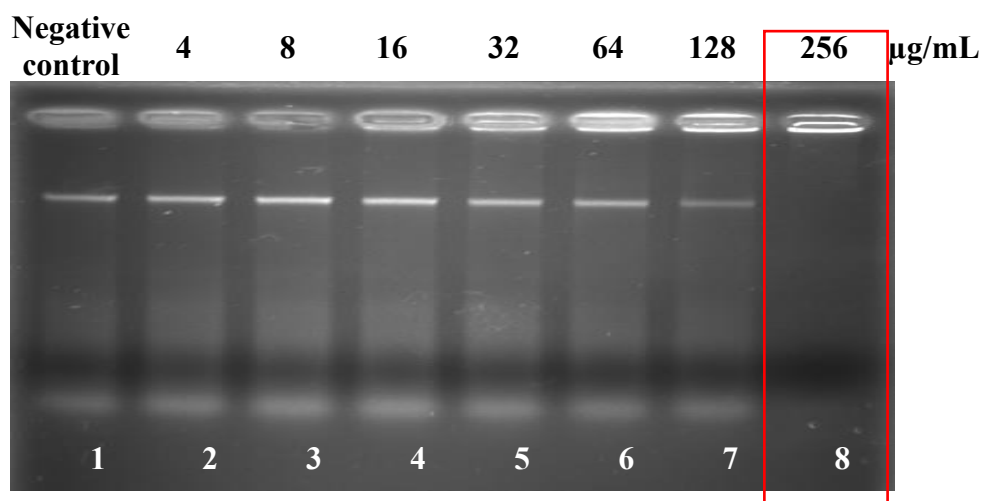
Figure 4.26: Gel retardation assay on the binding of polymyxin B to genomic DNA from *E. coli.* Lane 1: untreated DNA; lanes 2 to 8: DNAs treated with increasing amount of polymyxin B ranging from 4 µg/mL to 256 µg/mL.

4.6.7 Binding Ability of Polymyxin B to Plasmid DNA pBR322

Moreover, the strength of retardation by polymyxin B was even weaker when it comes to plasmid DNA. As shown in **Figure 4.27**, no complete retardation on the migration of plasmid DNA pBR322 was seen across all the tested concentrations of polymyxin B (lane 2 to lane 8, 4 µg/mL to 256 µg/mL). Only partial retardation can be seen at 256 µg/mL (lane 8), in which the relaxed form of the plasmid was retarded, while no obvious retardation to the supercoiled form of the plasmid DNA.
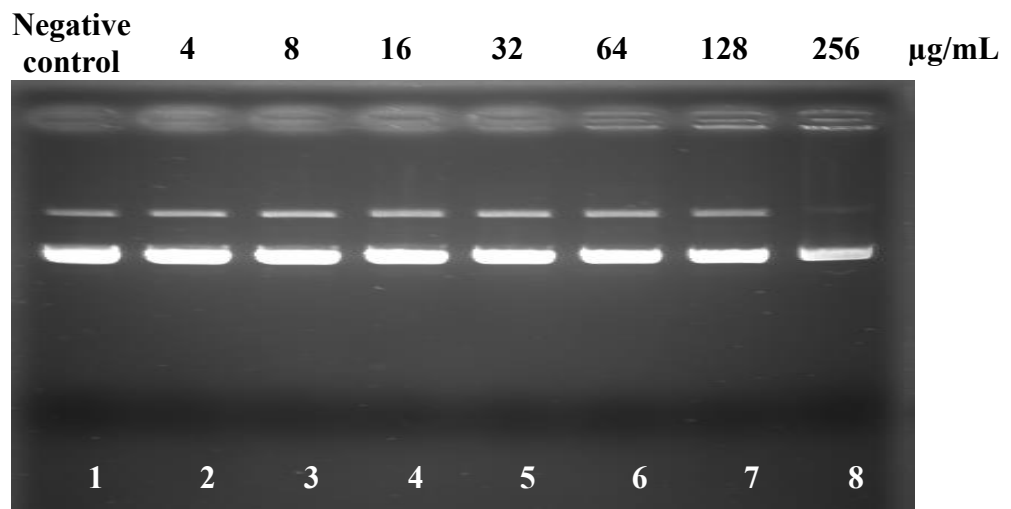
Figure 4.27: Gel retardation assay on the binding of polymyxin B to pBR322 *E. coli* plasmid DNA. Lane 1: untreated DNA; lanes 2 to 8: pBR322 treated with increasing amount of polymyxin B ranging from 4 µg/mL to 256 µg/mL.

4.7 Toxicity and Haemolytic Effects of PAM-5 on Mammalian Cells

To assess the toxicity of PAM-5 on mammalian cells, two types of cell lines were used, which were Vero cells and HeLa cells. The toxicity assays employed in this study was Presto Blue cell viability assay, in which the colorimetric signals generated by the treated cells represent the degree of cell viability after treatment with the peptide. Human red blood cell (hRBC), on the other hand, was used to study the haemolytic effect of the peptide. The degree of haemolysis caused by the peptide to the RBCs is proportional to the absorbance of the supernatant separated from the peptide-treated blood suspension. Finally, the detailed insight of the peptide toxicity to the mammalian cell was further studied by screening for its ability to permeabilize the inner membrane of the cells via fluorescent microscopy and SYTOX Green uptake assay.

4.7.1 PrestoBlueTM Cell Viability Assay

PrestoBlueTM cell viability assay, which is a highly sensitive assay for assessment of cell viability, is a resazurin-based reagent that is originally blue in colour. Viable cells that possess the reducing ability will change the bluish resazurin into fluorescent red resorufin, which is measured as relative fluorescence units (RFUs). Since only metabolically active viable cells possess this ability, thus the amount of red resorufin produced by the treated cells is proportionate to the number of viable cells, which in turn inversely proportional to the toxicity of PAM-5 in this study. In contrast, cells that were killed by 50% (v/v) dimethyl sulfoxide (DMSO), which served as the positive control for toxicity, were unable to produce the red fluorescent product and remained bluish

after adding with the reagent. On the other hand, untreated cells suspended in Dulbecco's phosphate buffered saline (DPBS) were used as the negative control for toxicity. Polymyxin B, which was previously reported for its association with neurotoxicity and nephrotoxicity, was used as a comparative peptide for the relative toxicity to PAM-5 in this study. The toxicities of both PAM-5 and polymyxin B were screened at concentrations ranging from 2 µg/mL to 256 µg/mL, which was the same range of concentrations used for the study of antibacterial effects of the agents towards the bacteria as described in **Section 4.2**.

As shown in **Figure 4.28**, HeLa cells treated with PAM-5 at concentrations ranging from 2 µg/mL to 256 µg/mL were able to change the blue resazurin of PrestoBlue reagent into red resorufin. This indicated that the viability of the peptide-treated cells was not affected by this range of peptide concentrations. Based on visual comparison, the intensities of the red colour product in wells which were filled with PAM-5-treated cells were almost similar to the negative control containing the untreated cells. As for HeLa cells treated with polymyxin B, the cells remained viable as indicated by the similar intensity of resorufin to that of the negative control. On the other hand, dark blue colour can be observed from the wells containing HeLa cells treated with 50% (v/v) DMSO (positive control for toxicity), indicating the absence or extremely low number of viable cells after treatment with the cytotoxic agent.
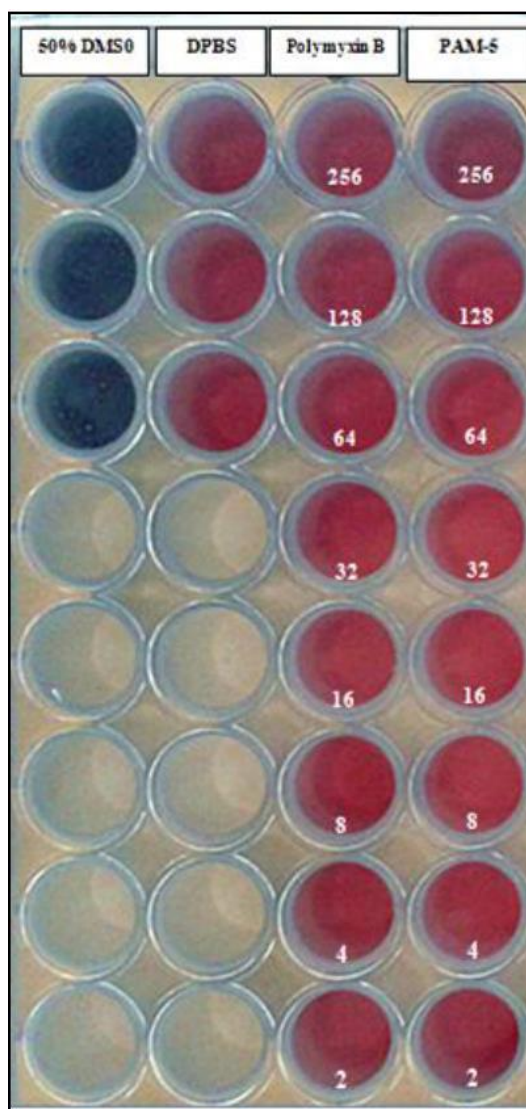
Figure 4.28: Visual inspection on the viability of PAM-5-treated, polymyxin B-treated and untreated HeLa cells based on PrestoBlueTM assay. Presence of viable cells is indicated by changing of blue colour of the PrestoBlue reagent into red colour. HeLa cells (initial titre of 10^4 cells/well) treated with PAM-5 and polymyxin B at concentrations from 2 µg/mL to 256 µg/mL were able to survive to the extent similar to the negative control (HeLa cells in DPBS), as indicated by the similar intensities of red resorufin. Low or absence of viability was seen for cells treated with 50% (v/v) DMSO that remained in blue colour, which served as the positive control for toxicity.

Visual observation on the colour development by the cells may not quantitatively reflect the cell viability. Therefore, the RFUs generated by the peptide-treated and non-treated cells were measured in order to compare the quantitative differences in viability between the two categories of cells. After triplicating the assays, the average RFUs produced by the cells were calculated and the data was plotted into graphs of RFUs against concentrations of peptides (PAM-5 and polymyxin B), as shown in **Figure 4.29**.

Based on the figure, the validity of the assay was verified by the distinct contrast between the positive and negative control for toxicity, which were represented by HeLa cells treated with DMSO and untreated HeLa cells, respectively. In the presence of 50% (v/v) DMSO, the treated HeLa cells could hardly maintain their viability as indicated by the extremely low RFU value. In contrast, untreated HeLa cells in DPBS produced high value of RFU, indicating the presence of high number of viable cells that were able to reduce the bluish resazurin into fluorescent red resorufin. In concordance to the visual observation as described earlier, HeLa cells treated with PAM-5 at all tested concentrations (2 µg/mL to 256 µg/mL) yielded relatively similar RFU values (RFU values ranged from 5179 to 6126) as compared to the untreated cells (RFU value: 5748). Moreover, no trend of decreasing RFU value was observed from the cells due to increasing concentration of PAM-5 from 2 µg/mL to 128 µg/mL, suggesting the viability of the cells was not affected by the peptide in dose-dependent manner at these concentrations. Nevertheless, cells treated with 256 µg/mL of PAM-5 recorded the lowest RFU (5179) as compared to other concentrations. However, the RFU values given by the cells treated at this concentration were not consistently

similar throughout the triplicate assays, thus producing a highly deviated error bar as shown in the graph. Statistical analysis showed no significant differences on the viability between PAM-5-treated cells and the negative control ($P > 0.05$), confirming that PAM-5 at these concentrations was not toxic toward HeLa cells.

As a comparative peptide, polymyxin B also did not affect the viability of HeLa cells at all the tested concentrations. Triplicated assays consistently showed that the RFU values generated by polymyxin B-treated HeLa cells maintained at the similar level as the negative control and PAM-5-treated cells. Similar to PAM-5, despite the increasing concentrations of polymyxin B, no trend of decreasing RFU value was observed for the treated cells, suggesting that the viability of HeLa cells was not affected by polymyxin B in dose-dependent manner. Similarly, no significant difference on the viability between cells treated with polymyxin B and the negative control ($P > 0.05$).

On the other hand, when both PAM-5 and polymyxin B were compared for their relative toxicity towards HeLa cells, no significant difference was found between the two ABPs ($P > 0.05$).
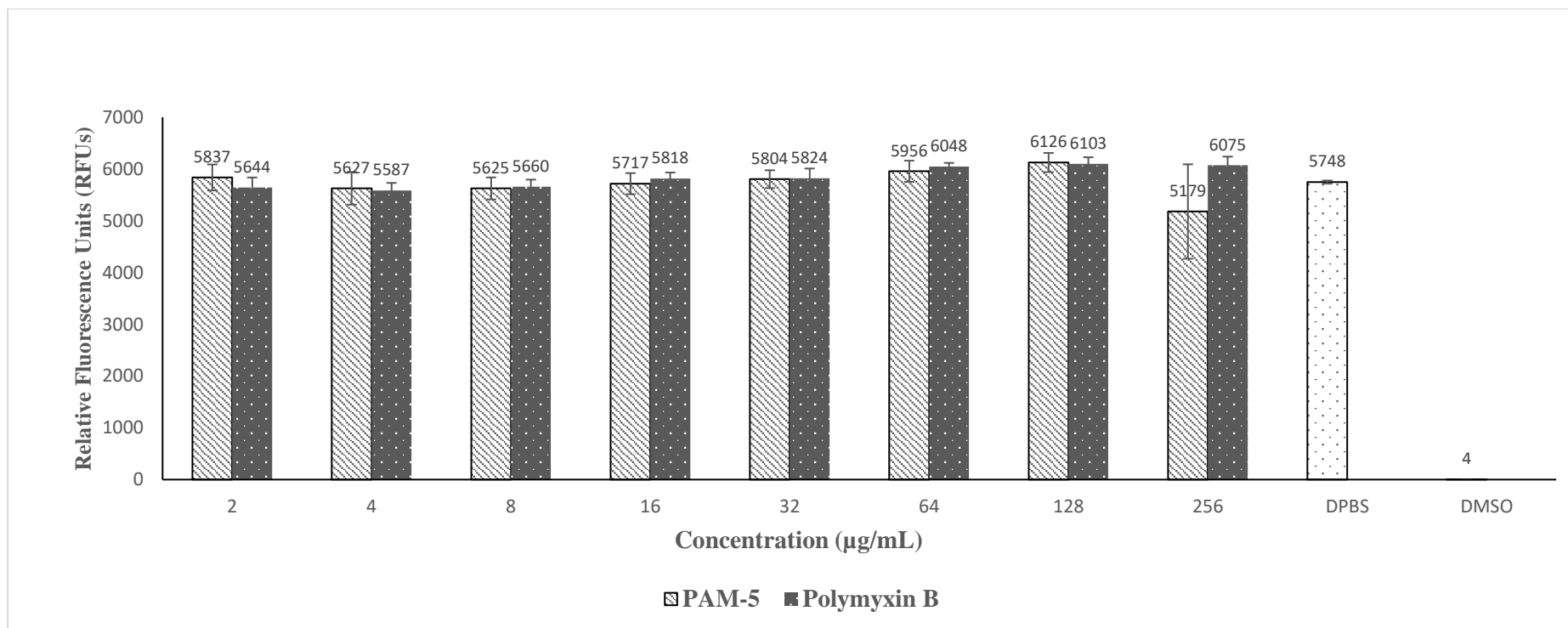
Figure 4.29: Relative fluorescence units (RFUs) produced by HeLa cells after different treatment based on PrestoBlue[TM] assay. The level of RFUs corresponds to the degree of cell viability. RFUs produced by cells treated with PAM-5 and polymyxin B were relatively similar to cells in DPBS, which served as the negative control for toxicity. Cells treated with 50% DMSO, which served as the positive control for toxicity, generated extremely low RFU.

For the toxicity screening on Vero cells, similar findings were also obtained. Based on the visual inspection on the assay as shown in **Figure 4.30**, Vero cells treated with PAM-5 at all tested concentrations (2 µg/mL to 256 µg/mL) were able to convert the blue resazurin into red resorufin, indicating high viability of these cells despite the peptide treatment. The intensities of red resorufin in the wells filled with these treated cells were visually similar to the content in the negative control (untreated cells). Meanwhile, polymyxin B-treated Vero cells also survived the treatment at all tested concentrations with the similar extend of red resorufin to the negative control. Conversely, the deep blue colour content in the wells of positive control indicated the low or absence of viable cells after treatment with 50% (v/v) DMSO.

The visual observation as described above was supported by the RFU data as presented in **Figure 4.31**. Throughout the triplicate assays, the RFU values generated by PAM-5-treated Vero cells were almost consistently similar despite treatment with increasing concentrations of the peptide. Based on the statistical analysis, PAM-5 was not toxic to Vero cells as there was no significant difference in the RFUs between the peptide-treated and untreated cells ($P > 0.05$). However, in contrast to the findings in visual observation, PAM-5 was less toxic than polymyxin B to Vero cells as reflected by the significantly higher RFUs from the former than the latter ($P < 0.05$).
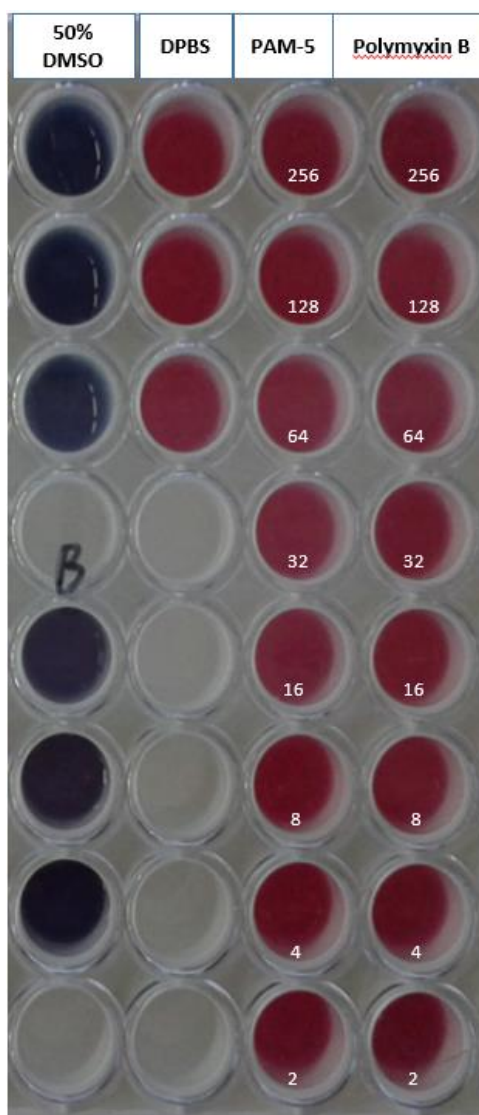
Figure 4.30: Visual inspection on the viability of PAM-5-treated, polymyxin B-treated and non-treated Vero cells based on PrestoBlue[TM] assay. Presence of viable cells is indicated by changing of blue colour of the PrestoBlue reagent into red colour. Vero cells (10^4 cells/well) treated with PAM-5 and polymyxin B at concentrations from 2 μg/mL to 256 μg/mL were able to survive to the extent similar to the negative control (Vero cells in DPBS), as indicated by the similar colour appearance. Low or absence of viability was seen for cells treated with 50% (v/v) DMSO, which served as the positive control for toxicity.
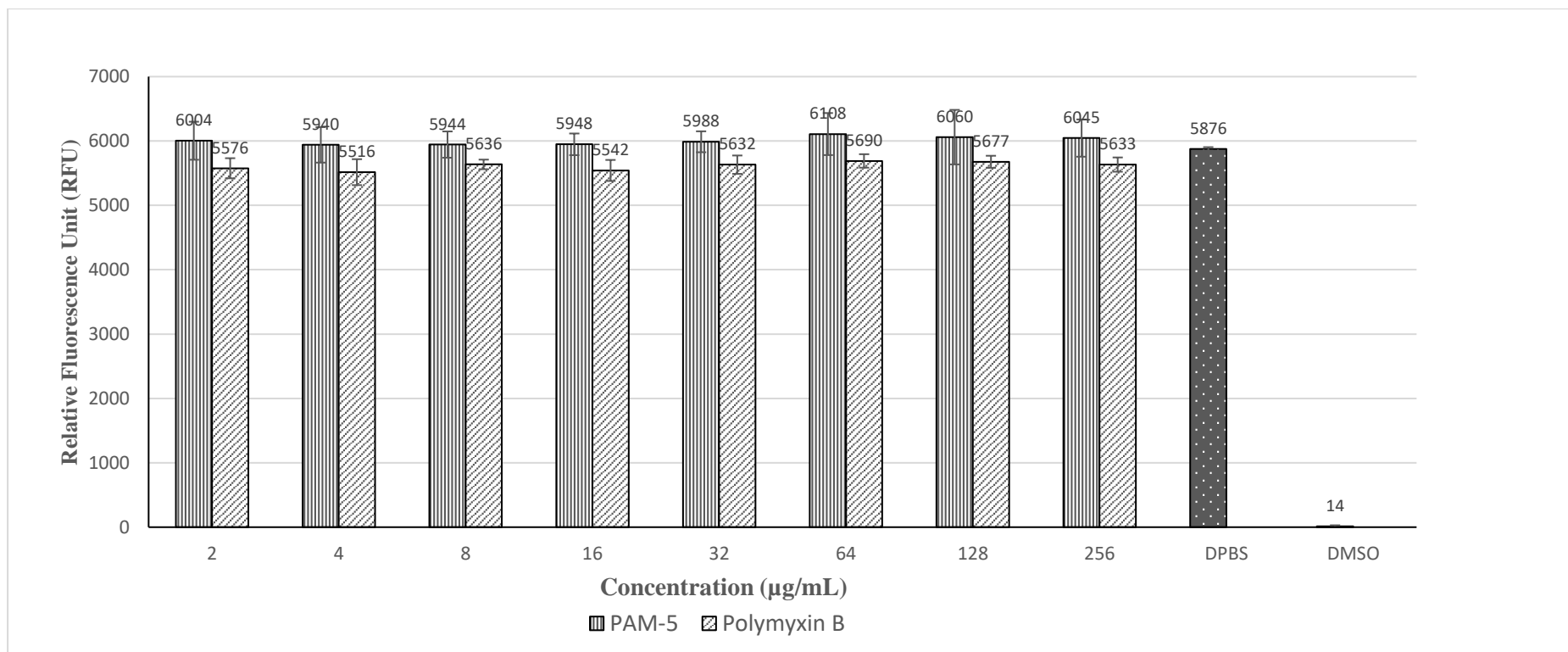
Figure 4.31: Relative fluorescence units (RFUs) produced by Vero cells after different treatments based on PrestoBlue[TM] assay. RFUs produced by cells treated with PAM-5 and polymyxin B were relatively similar to cells in DPBS, which served as the negative control for toxicity. Cells treated with 50% DMSO, which served as the positive control for toxicity, generated extremely low RFU.

4.7.2 *In vitro* Haemolytic Assay

The toxicity of PAM-5 was further evaluated by testing its haemolytic effect on human red blood cells (hRBCs) using *in vitro* haemolytic assay as described in **Section 3.11.5**. Similarly, a total of three independent assays were carried out in order to obtain reproducible data.

As demonstrated in **Figure 4.32**, the presence of haemolysis of the treated RBCs can be visually detected by the appearance of supernatant separated from the peptide-treated blood suspension. Serving as the agent for positive control of haemolysis, 0.1 % Triton X-100 was able to lyse the hRBCs as indicated by the red coloured-supernatant separated from the RBC suspension treated with the compound. On the other hand, hRBCs suspended in PBS which served as the negative control showed no sign of haemolysis. These two observations provided the validity to the haemolytic assay on PAM-5.

After treating the hRBCs with PAM-5 at concentrations from 2 µg/mL to 256 µg/mL, it was found that the supernatants separated from the treated hRBCs suspension were colourless, in which the appearance was relatively similar to the negative control. Despite the treatment with increasing concentrations of PAM-5 from 2 µg/mL to 256 µg/mL, the increasing gradient of reddish colour was not observed from all the supernatants separated from the hRBC suspension. This implies that PAM-5 was not haemolytic to hRBCs.

Similarly, hRBCs treated with polymyxin B at all the tested concentrations (2 µg/mL to 256 µg/mL) also produced colourless supernatants as observed by naked eyes. This indicates that the ABP had low or no haemolytic effect towards hRBCs.

In order to quantitate the degree of haemolysis on the hRBCs, the absorbance of each well containing the supernatant separated from the treated and non-treated blood suspension was measured at 540 nm. The data was recorded and further analysed into percentage of haemolysis according to the formula as stated in **Section 3.11.5**. The data were tabulated in a graph of percentage of haemolysis against peptide concentrations (**Figure 4.33**). In contrast to 0.1% Triton-X, PAM-5 did not produce measurable haemolytic effect to the RBCs as indicated by the significant differences in percentage of haemolysis between the peptide treatment and positive control ($P < 0.05$). Similarly, no significant difference in terms of percentage of haemolysis between PAM-5-treated and untreated hRBCs ($P > 0.05$), suggesting the extremely low absorbance readings generated from the peptide-treated hRBCs could be negligible. Furthermore, in all the tested concentrations, PAM-5 also recorded a significant lower percentage of haemolysis than polymyxin B ($P < 0.05$). This indicated that PAM-5 is less haemolytic than polymyxin B. All these data were consistently reproducible throughout the triplicate studies.
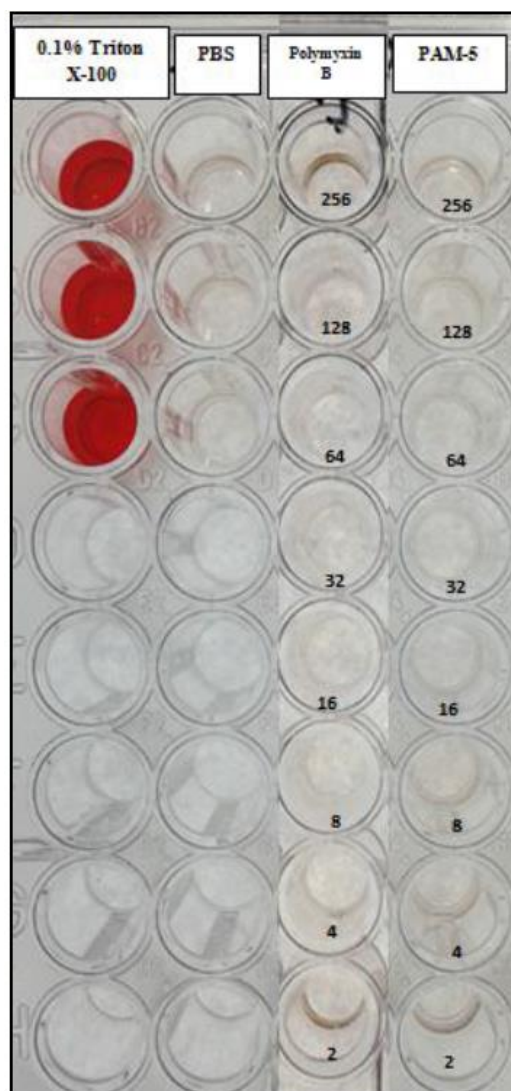
Figure 4.32: Visual observation on the haemolytic effect of peptide treatment on human red blood cells (hRBCs) by *in vitro* haemolytic assay. The presence of red-coloured supernatant in the wells indicates haemolysis of hRBCs. No obvious haemolytic effect was seen for hRBCs treated with PAM-5 and polymyxin B at all tested concentrations, as indicated by the absence of red coloured supernatant separated from the blood suspension treated with these peptides. Red colour was seen in the wells filled with supernatant separated from the blood suspension treated with 0.1% Triton X-100, which served as the positive control for haemolysis, while no haemolysis was seen for hRBCs suspended in PBS, which served as the negative control.
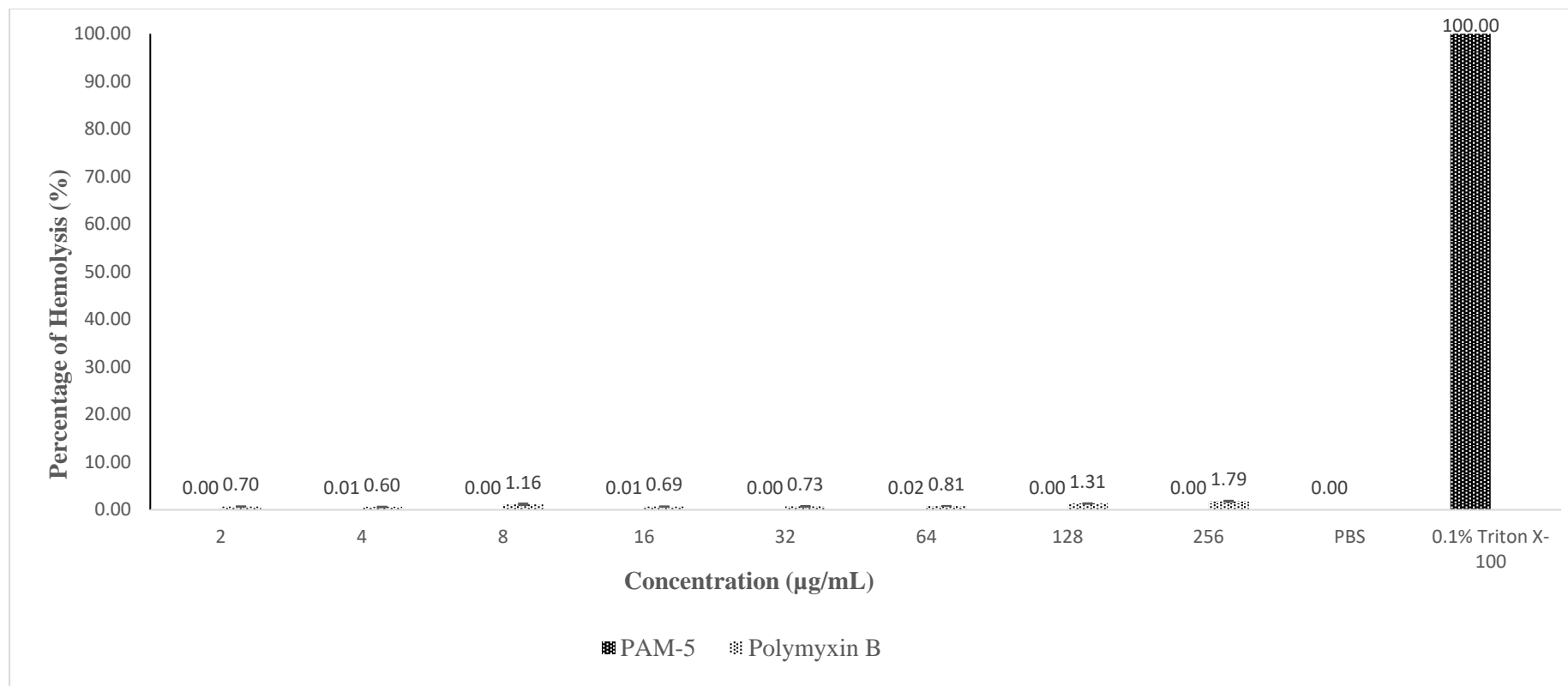
Figure 4.33: Percentage of haemolysis caused by peptide treatment to human red blood cells (hRBCs) based on haemolytic assay. hRBCs treated with PAM-5 at concentrations ranging from 2 µg/mL to 256 µg/mL showed almost undetectable haemolysis, and the degree of haemolysis was even lower than RBCs treated with polymyxin B. hRBCs treated with 0.1% Triton X-100 and suspended in PBS served as the positive and negative control for haemolysis, respectively.

4.8 Screening for Membrane-Permeabilization of Vero Cells by PAM-5

In order to assess the membrane permeabilization effect of PAM-5 on mammalian cell, SYTOX® Green uptake assay was performed on Vero cells treated with the peptide. As described previously, SYTOX Green is a membrane-impermeable probe that possess high binding affinity for nucleic acid. Once the cell inner membrane is permeabilized, the nucleic acid binding probe will easily penetrate into the cell and binds to the nucleic acid followed by fluorescence emission. Conversely, if a cell membrane is intact, the nucleic acid-binding probe is not able to translocate into the cell, thus unable to bind the nucleic acid. Consequently, no fluorescence is emitted. Thus, the presence of green fluorescence in the nucleus or cytoplasm of the cells indicates membrane disruption by an agent, while cells with intact membrane are left unstained.

Fluorescent microscopy was employed in this study to assess the membrane-permeabilization effect of PAM-5 on Vero cells. This was estimated by screening for the number of cells stained with the membrane impermeable SYTOX Green probe. The observation was presented in dark filed (DF) by using fluorescein isothiocyanate (FITC), as well as combination of bright field (BF) and DF under $100 \times$ magnification as shown from **Figure 4.34** to **Figure 4.36**.

Figure 4.34 (A) (i) and **(ii)** depict the fluorescent microscopy on the untreated Vero cells in DPBS in dark field and combination of dark and bright filed, respectively. Clearly demonstrated from the figures, the number of cells stained with SYTOX Green was remarkably lower as compared to the cells treated with

melittin [**Figure 4.34 (B) (i)** and **(ii)**], which served as the positive control for cell permeabilization. Under the observation by combination of BF and DF, only a small proportion of cell nuclei was fluorescent, which was far more insignificant as compared to the positive control. As these cells represented the untreated category, it was believed that the small proportion of stained cells appeared to be the dead cells during the process of cell culture and harvest, which were unrelated to the toxicity of the peptide.

Comparatively, PAM-5 was not seen to cause obvious permeabilization to Vero cells at each tested concentration from 2 µg/mL to 256 µg/mL. As compared to the abundant number of cell nuclei that were stained with SYTOX Green in the positive control, the scanty number of fluorescent nuclei present in the PAM-5-treated Vero cells may be the similar scenario as found for the negative control, where the stained cells might represent the dead cells before the peptide treatment. **Figures 4.35** to **4.36** demonstrate the images of fluorescent microscopy of Vero cells which were treated with PAM-5 at concentrations from 2 µg/mL to 256 µg/mL. Clearly seen from the DF and DF+BF of these fluorescent images, majority of the PAM-5-treated Vero cells were not stained with SYTOX Green in their nuclei, except for a few fluorescence nuclei which were believed to be the dead cells before peptide treatment. As compared to the abundantly stained nuclei in the positive control, these low number or negligible stained cells were consistently present in all the cell culture treated with increasing concentrations of PAM-5, which clearly indicated that the number of dead cells was not increased in a dose-dependent manner under the peptide

treatment. Therefore, it is believed that the presence of this scanty number of dead cells had no correlation to the peptide toxicity.
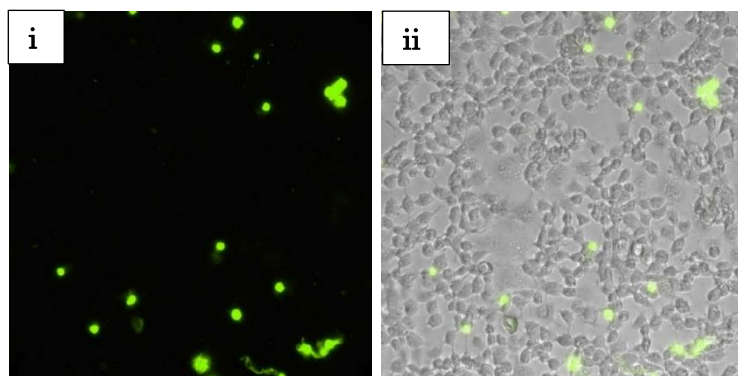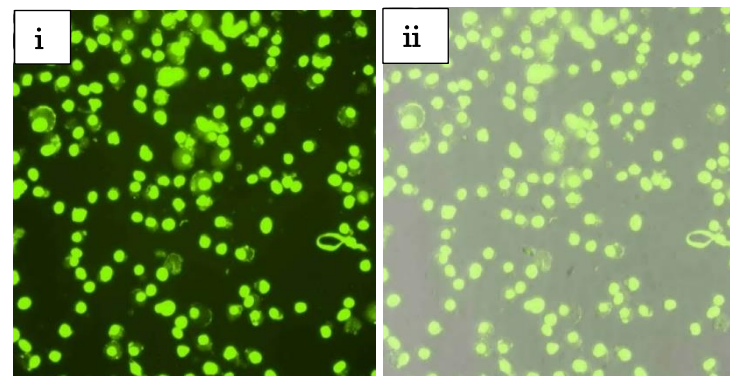
Figure 4.34: Fluorescent images of untreated and melittin-treated Vero cells in SYTOX Green cell viability assay. **(A)** untreated Vero cells which served as the negative control for membrane permeabilization, and **(B)** melittin-treated Vero cells which served as the positive control. The cell images are presented in (i) dark filed (DF), and (ii) combination of DF and bright field (BF) under 100 × magnification.
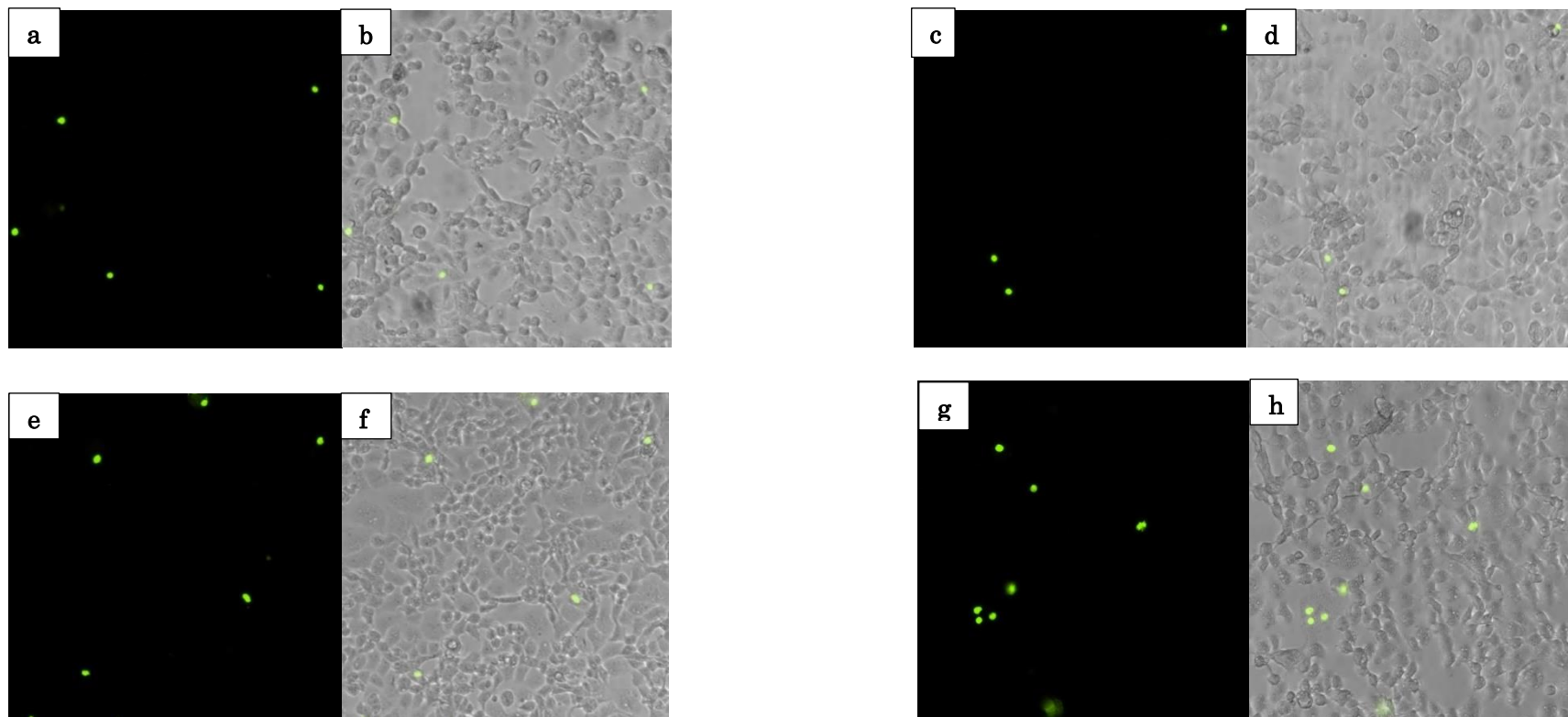
Figure 4.35: Fluorescent images of Vero cells treated with PAM-5 at concentrations from 2 µg/mL to 16 µg/mL in SYTOX Green cell viability assay. (Top left) Vero cells treated with 2 µg/mL of PAM-5 in (a) DF, and (b) combination of DF and BF; (Top right) Vero cells treated with 4 µg/mL of PAM-5 in (c) DF, and (d) combination of DF and BF; (Bottom left) Vero cells treated with 8 µg/mL of PAM-5 under (e) DF, and (f) combination of DF and BF; (Bottom right) Vero cells treated with 16 µg/mL of PAM-5 under (g) DF, and (h) combination of DF and BF. All images were viewed under 100 × magnification.
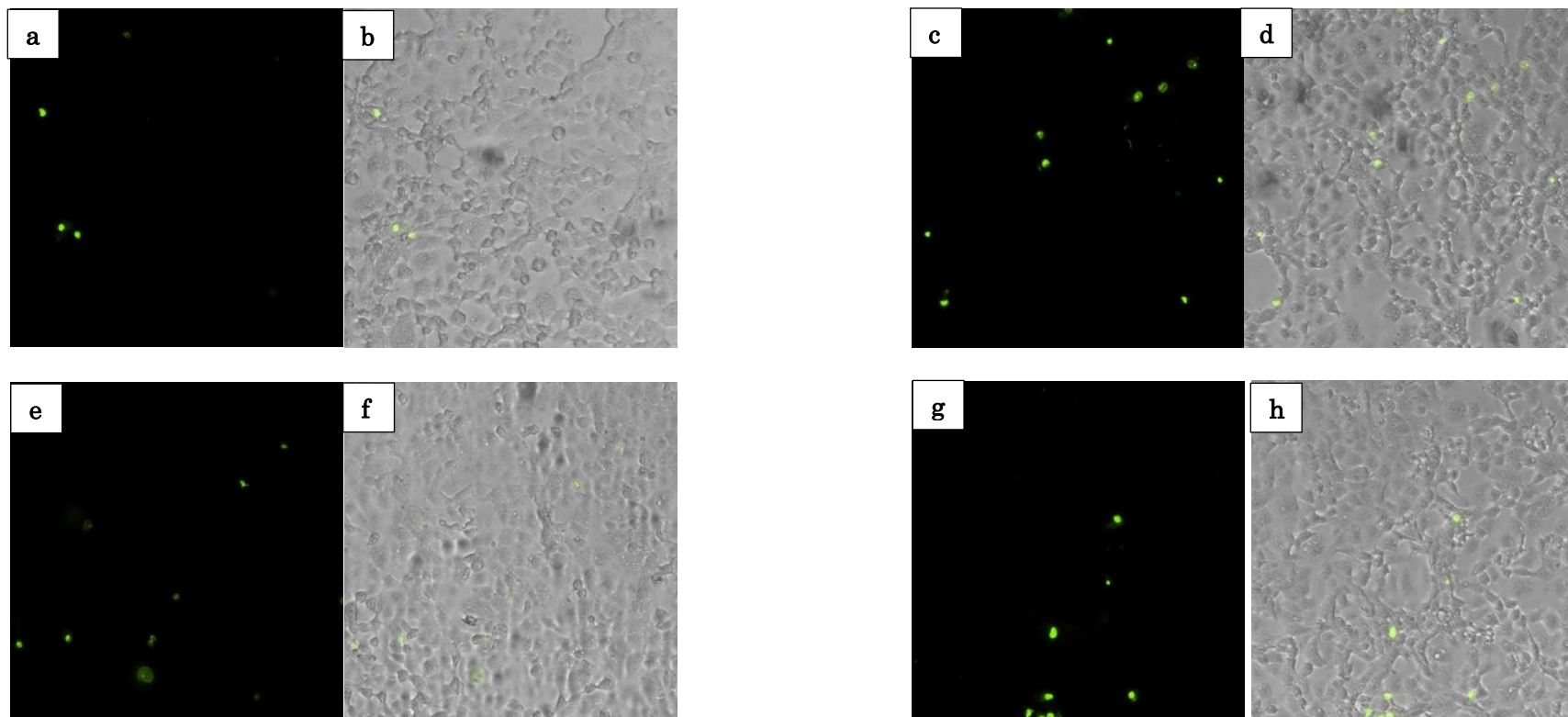
Figure 4.36: Fluorescent images of Vero cells treated with PAM-5 at concentrations from 32 µg/mL to 256 µg/mL in SYTOX Green cell viability assay. (Top left) Vero cells treated with 32 µg/mL of PAM-5 under (a) DF, and (b) combination of DF and BF; (Top right) Vero cells treated with 64 µg/mL of PAM-5 under (c) DF, and (d) combination of DF and BF; (Bottom left) Vero cells treated with 128 µg/mL of PAM-5 under (e) DF; and (f) combination of DF and BF; (Bottom right) Vero cells treated with 256 µg/mL of PAM-5 under (g) DF, and (h) combination of DF and BF. Images were viewed under 100 × magnification.

Under spectrophotometric measurement, the amount of SYTOX Green fluorescence is expected to be directly proportional to the number of membrane-permeabilized cells present in the peptide-treated cell culture, thus reflecting the relative toxicity of the peptide. The data for this fluorescent uptake was presented by the means of three independent assays, and the fluorescent intensity generated by the cells at each concentration of the peptide was subtracted from the background fluorescence of SYTOX Green.

Based on **Figure 4.37**, trace amount of fluorescence was recorded from the negative control, which was the untreated cells in DPBS. This finding corresponded to the microscopic observation as described above, where a trace number of fluorescent nuclei was seen in the untreated cells. However, the fluorescent intensity from these untreated cells was about ten times lower than the positive control. As for the cells treated with PAM-5 of all the tested concentrations, the fluorescence generated by these treated cells were approximately 13 to 28 times lower than the fluorescence produced by the positive control and even lower than the negative control. The low fluorescence recorded by these PAM-5-treated cells might be due to the trace number of dead cells present in the cell culture used for this assay, which were also similarly present in the untreated cells. Overall, the above findings indicate that the range of PAM-5 concentrations tested in this assay did not cause remarkable permeabilization to the membranes of Vero cells. Most importantly, this range of concentrations also spanned the peptide MBCs against the panel of bacteria as described earlier in this chapter.
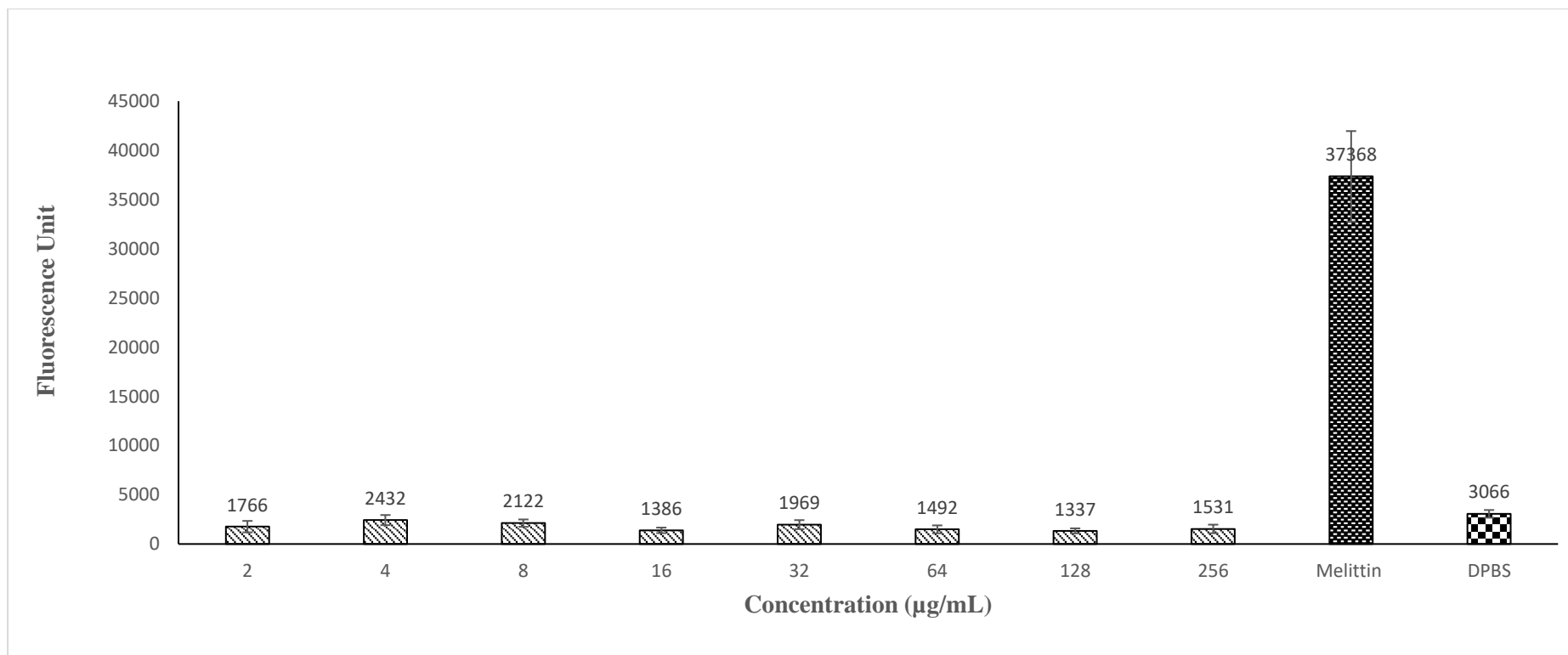
Figure 4.37: Fluorescent intensities generated by PAM-5-treated, melittin-treated and untreated Vero cells as assayed by SYTOX® Green cell viability assay. Vero cells treated with PAM-5 at concentrations ranged from 2 µg/mL to 256 µg/mL emitted relatively much lower fluorescent signals as compared to the melittin-treated Vero cells which served as the positive control, but close to the degree of fluorescence produced by untreated cells in DPBS. The data presented were the mean of three independent assay.

CHAPTER 5

DISCUSSION

The alarming state of global antibiotic resistance has drastically raised the mortality and morbidity rate of bacterial infections due to impaired efficacy of antibacterial chemotherapy (Friedman, Temkin and Carmeli, 2016; Aslam et al., 2018). Several approaches are currently undertaken in order to reduce or control the dissemination of antibiotic resistant bacteria. These include implementation of stricter policies associating with infection control in healthcare setting, prudent use of antibiotics in patients suffering from bacterial infections and reduction of antibiotic consumption in livestock (Phillips, 2001; Lee et al., 2013). However, these passive preventive measures may not successfully control the transmission of bacterial resistance as strict compliance from all the parties is required, which is usually difficult to be achieved. The most effective countermeasure is still depending on development of antibacterial agents with novel or unique mechanism of actions against those pathogens (Bassetti and Righi, 2015).

Antibacterial peptides (ABPs) are attracting considerable research interests since the last two decades in view of numerous promising findings which lead to the proposal that these peptides could potentially complement or even replacing conventional antibiotics in future treatment against bacterial

infections. ABPs were initially discovered as components of innate immune defence produced by organisms of broad diversity (Ganz, 2003; Pasupuleti, Schmidtchen and Malmsten, 2012). Subsequent studies revealed that these powerful compounds are not limited to direct antibacterial actions but also involved in regulation of immune responses against pathogenic invasion (Rehaume and Hancock, 2008; Wieczorek et al., 2010). Most importantly, many ABPs were found to inhibit or kill bacteria via distinct mechanisms from the conventional antibiotics, thus reducing the likelihood of bacterial resistance to these compounds (Lei, 2019). These promising findings have driven the research focus on alternative antibacterial agent towards ABPs, which is reflected by the increasing number of publications on these compounds (Sinha and Shukla, 2019; Wibowo and Zhao, 2019).

Originally, many of the well studies ABPs were isolated from natural resources (Jenssen, Hamill and Hancock, 2006; Liu et al., 2015; Nawrot et al., 2014; Salas et al., 2015; de Barros et al., 2019). However, the processes of isolating these peptides are usually tedious and laborious (Etchegaray and Machini, 2013), and the yield of the natural isolation is usually low (Bommarius et al., 2010; Zhang et al., 2015). Most importantly, many of the naturally extracted ABPs were found toxic or haemolytic to mammalian cells and human RBCs, respectively (Laverty and Gilmore, 2014; Roberts et al., 2015; Inui Kishi et al., 2018). These major drawbacks have prompted scientists to explore alternative approaches in ABP development that are able to overcome the above-mentioned limitations. One of these approaches is random phage display selection, which has been widely used to produce ABPs with high therapeutic index as this method could

be used to select peptides that are exclusively act on bacteria but yield minimal or no toxicity towards mammalian cells. In consideration of its feasibility in ABP development, phage display selection was used as the principal method in this study to screen and design an ABP with potent antibacterial effect but low toxicity towards mammalian cell.

5.1 Selection of Phage-Displayed Peptides Binding to *Pseudomonas aeruginosa*

5.1.1 *Pseudomonas aeruginosa* as the target bacteria for biopanning

In this study, *P. aeruginosa* was chosen as the target bacterium for the biopanning procedure due to several considerations. Being one of the most common opportunistic pathogens, *P. aeruginosa* is always associated with serious nosocomial infections with high morbidity and mortality rate (Hirsch et al., 2012; Kim et al., 2014). The difficulty of treating this bacterial infection is highly attributed to the multiple resistant mechanisms commonly found in this pathogen, which include modifications of bacterial structures targeted by antibiotics, production of enzymes that inactivate antibiotic active compound, reduction in membrane permeability to restrict entry of antibiotics which act intracellularly, and expression of efflux pump systems that prevent intracellular accumulation of antibiotics (Lambert, 2002; Breidenstein et al., 2011; El-Zowalaty et al., 2015; Stefani et al., 2017). Consequently, in the presence of antibiotic pressure, *P. aeruginosa* is usually rendered insusceptible to many classes of antibiotics such as cephalosporins, carbapenems, aminoglycosides and fluoroquinolones (Pachori, Gothalwal and Gandhi, 2019). Therefore,

searching for novel antibacterial agents that are able to overcome these resistant mechanisms is indeed needed.

Of all the above-mentioned resistant mechanisms, efflux systems and low membrane permeability have been identified as the main causes of resistance to multiple classes of antibiotics (Bassetti et al., 2018). As these two resistant mechanisms occur in bacterial membrane, compound or substance that is able to disrupt the integrity of bacterial membrane followed by disintegrating these efflux systems is definitely a prior consideration in the development of novel antibacterial agent against this bacterium. This is supported by findings that demonstrated high susceptibility of *P. aeruginosa* to polymyxin B (Tam et al., 2005; Poole et al., 2015; Gupta et al., 2015), which is a peptide antibiotic that exerts its bactericidal action via membrane disruption (Trimble et al., 2016). This is an important clue for this study which aims to search for membrane-active peptide/s that may overcome the issue of resistance due to efflux systems or low membrane permeability.

5.1.2 Whole cell solution biopanning

In this study, whole cell biopanning was employed where a phage-displayed peptide library was engaged with the whole bacterium of *P. aeruginosa*. According to Wu et al. (2016), this biopanning strategy may increase the probability of selecting multiple phage-displayed peptides that potentially bind to various surface molecules on the bacterial membrane, thus increasing the likelihood of obtaining peptides that possess antibacterial effect at multiple

membranous targets of the bacterium. Additionally, solution biopanning approach was chosen for this affinity selection so that the entire membrane surface of the bacterium was exposed to the phage-displayed peptides in all dimensions during the biopanning. Similarly, this approach might maximize the probability of isolating phage-displayed peptides which bound to various surface molecules of the bacterium.

Whole cell biopanning using phage-displayed peptide library has been used by many research groups to identify and design diagnostic ligands and antibacterial peptides against many pathogenic bacteria, including *S. aureus* (Yacoby et al., 2006; Yacoby, Bar and Benhar, 2007), *Listeria monocytogenes* (Carnazza et al., 2007; Gasanov et al., 2006), *P. aeruginosa* (Pini et al., 2005; Carnazza et al., 2008), *Campylobacter jejuni* (Bishop-Hurley et al., 2010) and *Haemophilus influenzae* (Bishop-Hurley et al., 2005). As demonstrated by these studies, one of the advantages of using whole cell biopanning is the selection of multiple peptide candidates that bound to different surface molecules of the target bacteria, which could provide researchers with the flexibility of identifying peptide/s with the most potent antibacterial activity for further development. For instance, in a study by Sainath Rao et al (2013), a total of six peptides were selected from a phage-displayed peptide library in a biopanning against whole bacterium of *E. coli*. This allowed the research group to choose the peptide candidate with the most potent antibacterial features to be further studied and developed into novel antibacterial agents. On the other hand, a total of 11 phage-displayed peptides with almost similar inhibitory effects towards *Campylobacter jejuni* were isolated from a biopanning process against the

bacterial whole cell (Bishop-Hurley et al., 2010). Among these peptide candidates, a species-specific peptide was finally chosen for further testing and development into an antibacterial peptide against *C. jejuni*.

5.1.3 Characteristics of affinity-selected phage-displayed peptides from biopanning

Correspondingly, using the whole bacterium of *P. aeruginosa* as the target of biopanning, the affinity selection in this study had selectively isolated multiple clones of phage-displayed peptides with high binding affinity to the bacterium. As reported in **Section 4.1.3**, these peptides possess different degree of cationicity and hydrophobicity. However, not all of them fulfil the criteria of an ideal bactericidal ABP with membrane-active mechanism, in which the cationicity usually range from +2 to +8 (centering around +6) while the hydrophobicity should range between 50% and 60% (Giangaspero, Sandri and Tossi, 2001; Yin et al., 2012; Rončević, Puizina and Tossi, 2019). Among the seven clones of phage-displayed peptides isolated from the two independent sets of biopanning, only three of them (Pa1, Pa2 and Pa4) possessed the cationicity within this range. Nevertheless, only Pa1 and Pa4 were selected for further evaluation of their antibacterial potency due to several factors that will be described below.

Firstly, both Pa1 and Pa4 were predominantly selected from the two independent sets of biopanning as compared to Pa2. This could be attributed to certain similarities in both the peptides that were essential for the selection during the

biopanning. Out of the total 15 peptides that were affinity-selected and successfully sequenced, five of them were belonged to Pa4 which possesses the sequence K-W-H-W-K-D-K-N-A-L-R-M. Interestingly, Pa1 (G-P-V-N-K-S-S-T-I-L-R-M), the peptide with the second highest selection frequency, also carried an identical 3-amino acid motif as occurred in Pa4. Constituted by leucine, arginine and methionine (L-R-M), this short motif was found at the same terminal position of both Pa1 and Pa4 but not in Pa2. The presence of this consensus motif in both the phage-displayed peptides indicated that it may play a crucial role in interaction with certain dominant binding ligand present on the surface membrane of *P. aeruginosa*, resulting in the predominant selection of two different phage-displayed peptides harbouring the same motif from the two independent sets of biopanning. Additionally, findings from the Phage-ELISA that demonstrated overall higher binding affinity by Pa1 and Pa4 also further strengthened the notion that this motif may played a significant role in the binding to the target bacterium. Apart from that, another consensus was also noticed in both Pa1 and Pa4, where a lysine (K) residue was found as the fifth amino acid of both the peptides. Along with the motif L-R-M, the binding of Pa1 and Pa4 to the bacterial surface ligand might be inferably occurred in certain peptide configuration that involved both the motif and the lysine residue together.

Based on the biochemical characteristics of amino acids, the consensus short motif contains two hydrophobic (leucine and methionine) and a positively charged amino acid (arginine). The combination of hydrophobicity and cationicity in this motif may promote its anchoring to multiple anionic and non-

polarized ligands that are commonly present on the surface of many Gram-negative bacterial membranes. With its hydrophobic nature, both leucine (L) and methionine (M) may promote partitioning of the peptide into the hydrophobic membrane lipid bilayer, while the cationic arginine (R) may further strengthen the binding between the motif and a possible anionic entity present within the vicinity of the bacterial ligand via electrostatic interaction. The role of arginine in ABP-membrane interaction had been demonstrated in several studies, where the strong atomic charge distribution and greater number of hydrogen bonds by this residue were reported as the two major factors contributing to its stronger and longer interaction time with the membrane bilayer (El-Sayed, Futaki and Harashima, 2009; Rice and Wereszczynski, 2017; Castelletto et al., 2018; Mishra et al., 2018). Other studies also revealed that arginine renders ABPs with cationicity which is required for electrostatic bonding to several anionic residues found in the lipid head group of bacterial membrane bilayer such as phosphatidylglycerol (PG), cardiolipin (CL) and phosphatidylserine (PS) (Giulio and Zhao, 2006; Ebenhan et al., 2014). As these anionic lipid molecules are also present abundantly in *P. aeruginosa* (Klein et al., 2004; Sohlenkamp and Geiger, 2016), the dominant selection of Pa1 and Pa4 during the biopanning could be explained. Based on these considerations, Pa1 and Pa4 were chosen for further evaluation of their antibacterial potency and other characteristics.

5.1.4 Synthesis of Free Linear Peptide Pa1 and Pa4

The strategy of phage display selection has been used by many research groups to isolate and search for antibacterial peptides from combinatorial phage

libraries. However, the affinity-selected phage-displayed peptides from these studies were commonly unable to accomplish desirable antibacterial activity towards the bacteria which were used as the target ligand for the peptide selection (Pini et al., 2005). As long as the peptide is fused to the pIII protein on the phage particles, it could hardly achieve strong antibacterial effect due to steric hindrance by the phage particles that might interfere with the peptide carpeting on bacterial membrane (Smith and Petrenko, 1997; Hoess, 2001; Pini et al., 2005; Larimer et al., 2015). Additionally, the number of peptides interacting with bacterial membrane may not be sufficient to initiate antibacterial effect to the bacteria due to the limited copy number of displayed peptides by the phage (Pini et al., 2005). In many studies, the phage vector used as the peptide display system is M13KE, which could only display five copies of cloned peptides fused to the pIII proteins (New England Biolabs). Added to the nature that all the cloned peptides are only expressed at one tip of the phage particle, the steric hindrance effect by the phage may prevent sufficient accumulation of peptides to the threshold required to initiate promising antibacterial effect. In this study, phage-display selection from the combinatorial library may have successfully selected peptides that possessed a motif and an amino acid that were believed to enhance binding of the peptides to the target bacteria, but these attached peptides may not be able to execute strong antibacterial action due to the above-mentioned limitations.

In order to overcome this obstacle, chemically synthesized linear free peptide analogous to the phage-displayed peptide is commonly applied by many research groups to produce ABPs with potent antibacterial potency (Pini et al.,

2005; Tanaka, Kokuryu and Matsunaga, 2008; Sainath Rao et al., 2013; Flachbartova et al., 2016). As the peptides are present in free or unbound form, the amount of the peptides could be adjusted accordingly to achieve the threshold concentration which is required to initiate antibacterial action on the bacterial membranes. Driven by the promising findings by the above-cited research groups, Pa1 and Pa4 were synthesized as free linear peptides by a peptide synthesis core facility (BioBasic, Canada) via automated solid-phase peptide synthesis method before testing for their antibacterial effects.

5.1.5 Antibacterial Potencies of Pa1 and Pa4

Nevertheless, despite the synthetic unbound form, both Pa1 and Pa4 were still not strongly active against *P. aeruginosa* as demonstrated from the microbroth dilution assays. As reported in **Section 4.1.4**, complete eradication of the bacterium only can be achieved at the highest testing peptide concentration (256 µg/mL), way too high from the MBC to be characterized as an ideal ABP. According to Hancock and Chapple (1999), an ideal ABP is able to kill bacteria *in vitro* with MICs that range from 1 µg/mL to 8 µg/mL. Based on these defining criteria, both Pa1 and Pa4 were regarded as weak ABPs.

The weak bactericidal effect of both Pa1 and Pa4 might be attributed to their relatively lower cationicity as compared to other more powerful ABPs such as polymyxin B (net positive charge +5) and melittin (+6) (Velkov et al., 2010; Li et al., 2017). It is well documented that peptide cationicity serves as an important factor to many ABPs that mainly exert their antibacterial action via membrane-

disruptive or permeabilizing mechanisms, as it promotes the initial interaction of the peptide to the anionic lipid head groups within bacterial membrane (Bi et al., 2014; Hollmann et al., 2018). For most of the membrane-active ABPs, certain minimal positive net charge is essential to regulate their antibacterial action. According to the findings by Vega-Chaparro et al. (2018), the degree of antibacterial effect of an ABP is directly proportional to its net positive charge. Furthermore, a study by Jiang et al. (2008) had demonstrated that decrement in net positive charge below +4 may impair the antibacterial activity of an ABP. As mentioned earlier, most of the strong bactericidal ABPs carry positive charges centering around +6, which is far more cationic that Pa1 and Pa4 with the cationicity of only +2 and +3, respectively. This lower strength of cationicity might be insufficient to establish strong electrostatic interaction between the peptide and the anionic molecules on bacterial membrane. Moreover, the presence of anionic amino acid/s in a peptide might further reduce its cationicity. For example, with the sequence of K-W-H-W-K-D-K-N-A-L-R-M, Pa4 carries several positively charged amino acid such as lysine (K), arginine (R) and histidine (H) that rendered the peptide with total cationicity of +4. However, due to the presence of a negatively charged aspartic acid (D), the total net positive charge was reduced to +3. Consequently, this might reduce the strength of electrostatic interaction between Pa4 and the anionic entities in the bacterial membrane, thus reducing its antibacterial potency.

As mentioned earlier, peptide amphipathicity was identified as one of the determining factors that contribute to the potency of an ABP. This feature is particularly important to those ABPs that mediate their bactericidal effect via

membrane-active mechanisms. An amphipathic ABP utilizes its hydrophobic and hydrophilic regions to form transmembrane pores in bacterial membrane, in which the hydrophobic region of the peptide engages with the lipid core of the membrane, while the hydrophilic region faces the water-filled lumen (Sato and Feix, 2006; Verly et al., 2017; Avci, Akbulut and Ozkirimli, 2018). These transmembrane pores result in the leakage of bacterial intracellular contents along with influx of water and other membrane-impermeable substances into the intracellular compartment that kill the bacteria. Structural and functional association studies on many natural ABPs revealed that almost half of the amino acids in the primary sequence of these peptides belonged to hydrophobic residues (Jenssen, Hamill and Hancock, 2006; Bahar and Ren, 2013; Mirski et al., 2017). This indicates that the hydrophobicity of a potent ABP is approximately at 50%, which might be another reason for the failure of Pa1 and Pa4 to exert potent antibacterial effect due to their relatively lower hydrophobicity.

Therefore, the biopanning-selected peptides were subjected to rational modifications in order to enhance their antibacterial features. Among the two peptides, Pa4 was chosen for these modifications as it was selected at a higher frequency from the biopanning. As compared to Pa1, Pa4 possessed better features of an antibacterial peptide due to its higher cationicity and hydrophobicity, which may promote stronger electrostatic interaction with the negatively charged ligand from the bacterial membrane. This notion was supported by the overall higher binding affinity of Pa4 to the bacterium as demonstrated by the phage-ELISA assay as compared to Pa1(**Figure 4.3** and

Table 4.3), which might explain the predominant selection of Pa4 from the combinatorial phage library during the biopanning.

5.2   Enhancement of Antibacterial Features of ABP via Rational Modification

5.2.1   Previous Studies on ABP Enhancement via Peptide Modification

Accumulating evidence have shown that the type and number of certain amino acids do play crucial roles that determine the efficacy of an ABP. Firstly, a study by Wang (2010) reported that glycine (G), leucine (L) and lysine (K) are the three most common residues in ABPs derived from animals, which render these peptides with alpha-helical structures for membrane-perturbation in bacterial membrane. Next, many potent ABPs also harbour tryptophan (W) and arginine (R) at high proportions, and the roles of these residues to the effect of ABPs have been well described (Shepherd, Vogel and Tieleman, 2003; Jing, Demcoe and Vogel, 2003; Bagheri, Amininasab and Dathe, 2018; Mishra et al., 2018). For examples, tryptophan and arginine in an ABP were shown to complement each other in several aspects of antibacterial action for the peptide, where the cationicity of arginine promotes the initial electrostatic interaction between the peptide and bacterial membrane, while the hydrophobic tryptophan enables prolonged interfacial engagement between the two entities (Bagheri, Amininasab and Dathe, 2018). Subsequently, both the residues allow the peptide to penetrate deeper into the membrane which eventually result in membrane disruption. These findings clearly deduced that glycine, leucine, lysine, arginine and tryptophan serve as important elements in an ABP with membrane-active

mechanism. Therefore, modification of a pre-existing ABP should consider to include these residues.

Modifications of natural ABPs have been carried out in several research groups in order to enhance the antibacterial effect of the peptides along with improved stability. The types of modifications that are commonly practiced include acetylation or amidation of peptide terminal for stability improvement, as well as amino acid substitution for adjustment of peptide cationicity and hydrophobicity in order to improve antibacterial effects along with reduction of peptide toxicity. For example, using amino acid substitution strategy where tyrosine (Y) and lysine (K) were replaced with arginine (R) and tryptophan (W), respectively, two peptide derivatives named RW-BP100 and R-BP100 which were active against both Gram-positive and Gram-negative bacteria were produced from their parental peptide named BP100 which was only active against Gram-negative bacteria (Torcato et al., 2013). Similarly, CP10A, a 13-mer peptide derivative from a natural ABP named indolicidin, was shown to exert better antibacterial activity than its parental peptide after replacing three proline (P) residues from the latter with alanine (A) (Friedrich et al., 2001).

More related to this study, modifications of pathogen-targeted phage-displayed peptides to yield potent ABPs were also employed by many research groups to optimise the antibacterial effect of the peptides. In their studies, amino acid substitution of the biopanning-selected phage-displayed peptides had successfully enhanced the antibacterial activity of peptides against *S. aureus*

(Yacoby et al., 2006; Yacoby, Bar and Benhar, 2007), *Listeria monocytogenes* (Gasanov et al., 2006; Carnazza et al., 2007), *P. aeruginosa* (Pini et al., 2005), *Campylobacter jejuni* (Bishop-Hurley et al., 2010) and *Haemophilus influenzae* (Bishop-Hurley et al., 2005). The feasibility of this method in generating novel ABPs provided some informative inspiration towards the development of a potent ABP from the biopanning-selected phage-displayed peptide in this study.

5.2.2 Modification of Pa4 to PAM-5

As reported in **Section 4.1.5**, the aims of modifying Pa4 were to increase the peptide cationicity and hydrophobicity so that it would fulfil the basic requirement of an ABP. The former was achieved by replacing some of the zwitterionic or anionic amino acids in the Pa4 with positively charged residues, while the latter was improved by replacing the less or non-hydrophobic residues such as asparagine (N) and alanine (A) in Pa4 with leucine (L) and valine (V) of higher hydropathy index. Moreover, three additional amino acids were added into the peptide in order to increase the peptide length. As the results of these modification, the newly modified peptide, namely PAM-5, possessed a total hydrophobicity rate of 46% and total net charge of +7. Based on the peptide calculation and prediction from Antimicrobial Peptide Database (http://aps.unmc.edu/AP/prediction/actionInput.php), this peptide may form alpha helices and contains at least five residues on the same hydrophobic surface, which are essential for membrane-active action. The higher cationicity of the new peptide may promote its selective binding to the anionic bacterial membrane instead of zwitterionic membranes from mammalian cells, while the

moderate hydrophobicity may contribute to its hydrophobic interaction with the lipid head groups on the bacterial membrane. By improving these peptide features, it is believed that PAM-5 could exert a better antibacterial potency with minimal toxicity to mammalian cells as compared to its parental peptide, Pa4.

5.3 Antibacterial Effect of PAM-5

5.3.1 Antibacterial Effect of PAM-5 Towards *P. aeruginosa* ATCC27853

PAM-5, a derivative from Pa4 after rational modification via amino acid substitution and peptide elongation, was shown to possess enhanced antibacterial effect towards the reference strain of *P. aeruginosa* ATCC 27853 which was used as the target bacterium for affinity selection of Pa4. As reported in **Section 4.2.1**, at the concentration of 8 µg/mL, the peptide was able to eliminate the bacterium completely. This MBC was five-fold lower than the MBC required by Pa4 to achieve the same bactericidal effect. Recalling the criteria that define a potent ABP by Hancock (1997), in which the MICs of an ideal ABP should range between 1 µg/mL and 8 µg/mL, it is generally accepted that the value of MBC for an ABP is rationally higher than its MIC. Since PAM-5 was able to eliminate the target bacterium at the MBC of 8 µg/mL, it is proposed that this peptide is a potent ABP towards this bacterium.

The striking difference in the antibacterial effect between PAM-5 and Pa4 towards *P. aeruginosa* had significantly justified the roles of rational modification to the phage-displayed peptide Pa4. As mentioned earlier,

substitution of some of the anionic and zwitterionic residues in Pa4 with cationic and hydrophobic residues renderred the peptide with higher cationicity and hydrophobicity, which could enhance its interaction to the anionic bacterial membrane via stronger electrostatic and hydrophobic interactions. On the other hand, the extension of peptide length from 12 to 15 amino acids might serve as another contributing factor to the enhanced antibacterial activity for PAM-5. Although there was no direct evidence for this correlation in this study, longer-chain linear peptides were found more effective in their bactericidal effects towards many bacteria in some other studies. A study by Liu et al. (2006) had provided clear evidence that the length of an ABP is correlated to its antibacterial activity. It was found that the killing strength of an ABP named RW was greater when the peptide chain is longer. Generally, increased peptide length means increase in peptide molecular weight, and this was speculated to produce higher lateral pressure to the bacterial membrane interface upon intecalation by the peptide, leading to local disruption to the bacterial membrane lipid. According to Bahar and Ren (2013), peptide length is essential for the amphipathicity and helical structure of an ABP, where the latter two factors are required by a membrane-active ABP to traverse the lipid bilayer of bacterial membrane. Correspondingly, based on the peptide structural prediction from the Antimicrobial Peptide Database, the elongation of Pa4 with 12 amino acids to PAM-5 with 15 amino acids resulted in increase helical structure and number of hydrophobic interfaces to the peptide, and these may have contributed to the enhanced disruptive action of the ABP to the bacterial membrane.

The promising antibacterial effect of PAM-5 against *P. aeruginosa* signifies its potential clinical application against this pathogenic bacterium over many conventional antibiotics. *P. aeruginosa* is notorious for its regular resistance towards many classes of conventional antibiotics such as penicillin, ampicillin, tetracycline, chloramphenicol, sulphonamides and certain aminoglycosides, primarily due to the presence of membranous porins that limit the entry of these compounds to the periplasmic space of the bacterium (Poole, 2000; Poole, 2011; Chevalier et al., 2017). Additionally, the active efflux pumps could further reduce intracellular accumulation of these antibiotics by excluding them out from the bacterial cytoplasmic compartment (Blair, Richmond and Piddock, 2014; Sun, Deng and Yan, 2014; Housseini et al., 2018). Worse, the expression of inducible resistance such as beta-lactamase serves as another obstacle impeding the potency of many effective antibiotics currently used to fight against this bacterium (Berrazeg et al., 2015; Mp and Bv, 2019). Therefore, the bioactivity of PAM-5 against *P. aeruginosa* as demonstrated in this study may light up the hope for an alternative antipseudomonal agent that might overcome the complication in treating patients with serious burn injuries, cystic fibrosis and immunosuppression.

5.3.2 Antibacterial Spectrum of PAM-5

The potency of PAM-5 was not just limited to the reference strain of *P. aeruginosa*, but also encompassed other reference strains such as *E. coli* ATCC 25922, *A. baumannii* ATCC 19606 and *K. pneumoniae* ATCC 13883. Clearly demonstrated from these findings, PAM-5 is not only specifically active against

the bacterium which served as the bacterial ligand for the biopanning, but also targets other Gram-negative bacteria that might be morphological and structurally dissimilar from the former. The non-bacterial-specific action may render this peptide with the ability to inhibit or kill a broad spectrum of bacterial targets, where a single agent is able to kill bacteria from different families such as Pseudomonadaceae (*P. aeruginosa*), Enterobacteriaceae (*E. coli* and *K. pneumoniae*) and Moraxellaceae (*A. baumannii*). This might imply that PAM-5 could serve as a potential candidate for empiric treatment against bacterial infection where the etiological agent of infection is yet to be determined.

Interestingly, the spectrum of bacterial target also included several clinically isolated pathogenic bacteria with different profiles of antibiotic-resistance. Apart from its good potency against the reference strain of *P. aeruginosa* as described previously, PAM-5 was also active against two clinically isolated *P. aeruginosa* with drug and multidrug-resistance, respectively. This finding highlights the potential therapeutic significance of PAM-5 that it is not only able to overcome the bacterial intrinsic resistance mediated by low permeable porins and efflux pumps, but also able to surpass inducible resistances that are commonly found in clinical isolates of this bacterium which rendered it with reduced susceptibility to some of the commonly used anti-pseudopodal antibiotics.

Similarly, PAM-5 was shown active against *S*. Typhi and *S. flexneri*, which are the agents for typhoid fever and shigellosis, respectively. At 32 μg/mL, PAM-5

was able to eliminate the two antibiotic-resistant Enterobacteriaceae which were isolated from patients suffering from the infections. However, as compared to its potency against *P. aeruginosa*, PAM-5 was moderately active against these two human pathogens as reflected by the higher MBC values towards the bacteria. The slightly lower potency of PAM-5 towards these two bacteria could be attributed to certain peptide resistance mechanisms which were reported from these bacteria. A study by Peschel and Sahl (2006) revealed that an outer membrane protease produced by *S*. Typhi, namely PgtE, was able to cause proteolytic degradation to a human antimicrobial peptide LL-37. On the other hand, *S. flexneri* was found to produce two major extracellular serine proteases that might be associated with ABP resistance. According to several studies, these proteases, namely SepA and Pic, were able to hydrolyse various proteins and peptides (Benjelloun-Touimi et al., 1995; Dutta et al., 2002; Dautin, 2010). It is assumed that the proteases produced by these two bacteria may cross-react with PAM-5 in this study, thus reducing the peptide potency towards these pathogens. Nevertheless, according to Yoshino and Murakami (2015), many proteases are subjected to substrate inhibition, whereby the enzyme activities are inhibited by their substrates when the latter is present in excess. This could explain the higher MBC of PAM-5 towards the two bacteria despite the presence of the above-mentioned peptide resistant mechanisms, which could be possibly due to the peptide-mediated inhibition of the proteases, thus enabling the peptide to kill the bacteria when it is present at higher concentration.

More importantly, the bactericidal potency of PAM-5 was not even compromised by some of the most common resistant mechanisms found in

Gram-negative bacteria such as extended spectrum beta-lactamases (ESBL) and carbapenem-resistant Enterobacteriaceae (CRE). ESBL-producing bacteria and CRE are bacteria with resistance that are able to compromise the efficacy of wide range of antibiotics, thus limiting the treatment option against the bacteria. In particular, CRE is always considered as superbug due to its ability to compromise carbapenems which are commonly used as the last resort of antibiotic treatment (Papp-Wallace et al., 2011; Nordmann, Dortet and Poirel, 2012). Moreover, CRE also exhibit cross-resistance to many classes of antibiotics of structurally unrelated such as fluoroquinolones and aminoglycosides (Deshpande et al., 2006), which was also exhibited by the CRE-*K. pneumoniae* as one of the screening bacteria in this study. However, PAM-5 was able to kill the resistant bacterium at the MBC as low as 8 μg/mL. This indicate that the efficacy of PAM-5 was not affected by these bacterial resistant mechanisms that are able to knock off many conventional antibiotics. These data are indeed prominent findings that indicate PAM-5 is a more powerful antibacterial agent than many conventional antibiotics against these nasty pathogens.

However, PAM-5 failed to inhibit or kill a Gram-negative bacterium in the screening list. Despite treatment with 256 μg/mL of PAM-5, *S. marcescens* was able to survive the antibacterial effect of the peptide. The insusceptibility of this opportunistic pathogen to PAM-5 could be attributed to its intrinsic resistance which is mediated by extracellular proteases such as serine proteases, metalloproteases and serratiopeptidase (Di Cera, 2009; Salarizadeh et al, 2014;

Gupte and Luthra, 2017; Vélez-Gómez et al., 2019). Studies had demonstrated that some of these enzymes are able to hydrolyse amide bonds present in certain positively charged amino acids such as arginine (R) and lysine (K), while others are able to cleave polypeptides by targeting hydrophobic residues such as phenylalanine (F), tyrosine (Y) and tryptophan (W) (Di Cera, 2009). Since PAM-5 harbours considerable numbers of these amino acids (**K**-**W**-**K**-**W**-**R**-P-L-**K**-**R**-**K**-L-V-L-**R**-M), it is speculated that the peptide was highly susceptible to different degrees of cleavage or degradation by these enzymes, which might render the peptide losing its cationicity and hydrophobicity that are essential properties for antibacterial activity. Hence, this could explain the low potency of PAM-5 towards *S. marcescens* in this study.

Except for *S. marcescens*, PAM-5 overall exhibited moderate to good antibacterial potencies towards the list of Gram-negative bacteria selected for antibacterial screening in this study. As described in **Section 4.2.2**, the antibacterial effect of PAM-5 seemed to be bactericidal rather than bacteriostatic. Thus, it is speculated that PAM-5 exerts its killing effect by targeting bacterial structure/s or element/s that is/are essential to bacterial survival. Like many other ABPs, PAM-5 is a cationic peptide with moderate hydrophobicity, which are features of ABPs that mediate their bactericidal effects via membrane-active mechanism. With a positive charge of +7 and hydrophobicity of 46%, it is believed that PAM-5 could initiate a strong electrostatic interaction with the bacterial outer membranes which are generally anionic (Melo et al., 2009). Indeed, PAM-5 was found as a membrane-active

ABP in this study, and the detailed mechanisms will be further discussed in **Section 5.5**.

In terms of Gram-positive bacteria, PAM-5, however, demonstrated heterogeneous potencies towards different Gram-positive bacteria selected for antibacterial screening in this study. As compared to its efficacy towards Gram-negative bacteria, PAM-5 was generally less active against Gram-positive bacteria. As reported in **Section 4.2.2**, PAM-5 was not active against *Enterococcus faecalis* ATCC 19433 despite treatment with the highest concentration of the peptide (256 μg/mL). Similarly, PAM-5 was less active against *Staphylococcus aureus* ATCC 25923 as reflected by the high MBC (128 μg/mL) required to kill the bacterium completely. The low potencies of PAM-5 on these two bacteria corresponded to several other ABPs with the similar ineffectiveness towards Gram-positive bacteria. These ABPs include EC5 (Sainath et al., 2015), M6 (Pini et al., 2005) and PAMP-36 (Lv et al., 2014), which are strong cationic ABPs against many Gram-negative bacteria but failed to kill or suppress the growth of Gram-positive bacteria.

The reduced potency of PAM-5 on these Gram-positive bacteria might be due to several factors. Firstly, the structural and compositional differences in the outer layer between Gram-positive and Gram-negative bacteria may be one of the key factors that lead to this distinct bioactivity. As will be described later, PAM-5 executes its antibacterial actions through membrane-active mechanism which is attributed to direct electrostatic interaction between the cationic peptide

and the anionic membrane of Gram-negative bacteria. However, the presence of a thick peptidoglycan layer in Gram-positive bacteria could serve as a physical barrier that need to be traversed by ABPs to reach the bacterial outer membrane (**Figure 5.1**). Additionally, the cell walls of Gram-positive bacteria commonly contain a high proportion of anionic lipoteichoic acid (LTA), which may sequester certain amount of the cationic ABPs via electrostatic binding before reaching the outer membrane (Rosenfeld and Shai, 2006). These surface structures may reduce or even block the accumulation of ABPs on the plasma membrane, thus preventing the peptide achievement to its threshold concentration required to initiate membrane-active actions. Consequently, the membrane-disruptive effects as occurred to Gram-negative bacteria may not be achieved at the same peptide concentration in Gram-positive bacteria, and higher amounts of ABPs are required to overcome the barrier effect before initiating the bactericidal mechanisms. This barrier effect by Gram-positive bacteria was reported by Torcato et al. (2013), in which an ABP named BP100 was only able to kill Gram-positive bacteria at much higher concentrations as compared to the amount which was required to kill Gram-negative bacteria.
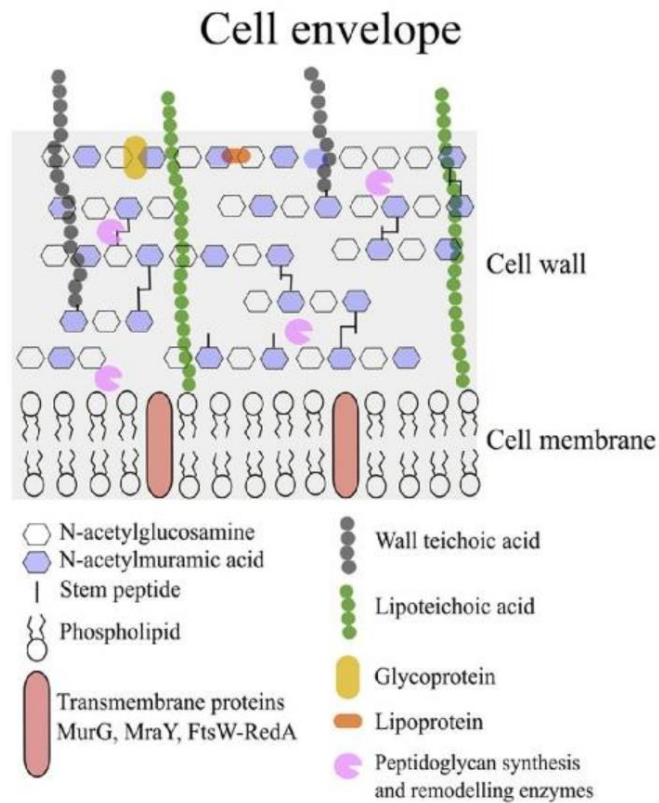
Figure 5.1: Cell envelop of Gram-positive bacteria. The presence of a layer of thick cell wall on top of cell membrane of Gram-positive bacteria may serve as a barrier to direct access of membrane-active ABPs to bacterial membrane (Silhavy et al., 2010).

Secondly, even though some of the cationic ABPs are able to exert antibacterial effect towards Gram-positive bacteria by binding to anionic LTA before traversing the bacterial cell wall and membrane, many bacteria are able to modify the cell wall constituents that would reduce the peptide binding to the bacterial outer layer. Several studies have demonstrated that Gram-positive bacteria under the genus of *Staphylococcus*, *Bacillus*, *Enterococcus*, *Streptococcus* and *Lactobacillus* are able to reduce the anionicity of teichoic acids (TAs) and lipoteichoic acids (LTAs) via D-alanylation, where positively-charged D-alanine residues are introduced to these negatively-charged glycopolymers (Perego et al., 1995; Peschel et al., 1999; Poyart et al., 2003;

Walter et al., 2007; Abi Khattar et al., 2009; Cox et al., 2009; Le-Jeune et al., 2010). As the results of this alteration, the negative charges of bacterial cell wall are masked, thereby reducing the electrostatic interaction between cationic ABPs with this outer layer (Neuhaus and Baddiley, 2003). Apart from that, modification of membrane anionicity via aminoacylation by some Gram-positive bacteria such as *S. aureus*, *E. faecalis*, *E. faecium. B. subtilis*, and *B. anthracis* also reduces the susceptibility of these bacteria to many cationic ABPs (Peschel et al., 2001; Kristian et al., 2003; Hachmann, Angert and Helmann, 2009; Samant et al., 2009; Bao et al., 2012; Cox et al., 2014). These bacteria express an enzyme named multipeptide resistance factor protein (MprF) which catalyses incorporation of a positively charged lysine (Lys) into the negatively charged phosphatidylglycerol (PG) found in bacterial membrane. Similar to D-alanylation, the aminoacylated phosphatidylglycerol also decreases the net negative charge on the membrane of these Gram-positive bacteria, thus reducing the binding tendency or even causes repulsion to many cationic ABPs if the modified membrane become more cationic. These membrane-modifications may occur in *S. aureus* and *E. faecalis* that were screened in this study, thus explaining their low susceptibility and resistance to PAM-5, respectively.

Furthermore, *S. aureus* was found to secrete an extracellular protein named Staphylokinase (Sak), which is able to sequester many cationic ABPs extracellularly, thereby preventing engagement of the peptides to bacterial surface. This protein was found able to complex with α-defensin 1 and 2 (Jin et al., 2004) and LL-37 (Braff et al., 2007), thus reducing their effective bactericidal concentration on the core bacteria. Although it was not clearly

defined in this study, the similar sequestration effect may also occur in the *S. aureus* treated by PAM-5 and thus reduced the peptide effect to this bacterium.

As compared to *S. aureus*, which was still susceptible to high concentration of PAM-5 (128 µg/mL), *E. faecalis* was completely resistant to the peptide at all tested concentrations (2 µg/mL to 256 µg/mL). As mentioned earlier, *E. faecalis* may possess the similar evasive mechanisms as described for *S. aureus*, but it may also exert more aggressive strategies that confront the antibacterial agent. This assumption is supported by studies that discovered ABP-degrading proteases produced by *E. faecalis* which protects the bacterium from the inhibitory or bactericidal effects of several ABPs that included α-defensins (Schmidtchen et al., 2002) and HYL-20 derived from bee venom (Nesuta et al., 2017). These proteases mediate proteolytic cleavage by targeting peptide bonds between two specific amino acids (Makinen and Makinen, 1994). One of the most studied proteases from *E. faecalis*, gelatinase, was demonstrated to confer resistance to short α-helical ABP by cleaving them at certain peptide region/s. According to a study by Nesuta et al. (2017), this protease targets peptide bonds between amino acids lysine and isoleucine (K-I) as well as lysine and leucine (K-L) within ABPs, thus breaking them into shorter fragments which are insufficient to exert antibacterial effect. As the motif K-L also present in PAM-5 (K-W-K-W-R-P-L-K-R-**K-L**-V-L-R-M), it is assumed that the ineffectiveness of PAM-5 towards *E. faecalis* was due to peptide degradation by this bacterial protease.

In contrast to the low potency towards *S. aureus* and *E. faecalis*, PAM-5 was more potent against Streptococcus species that included *Streptococcus pyogenes* (*S. pyogenes*) and *Streptococcus anginosus* (*S. anginosus*). However, as compared to its bioactivity towards the Gram-negative bacteria as described earlier, the concentration of PAM-5 required to eliminate *S. pyogenes* completely was still far away from the range of MBCs characterized for an ideal ABP (Hancock and Chapple, 1999). Like other Gram-positive bacteria, *S. pyogenes* possesses additional layers of cell surface structures that need to be traversed by ABPs before reaching the plasma membrane. Additionally, a distinct feature of *S. pyogenes*, which is classified under Group A streptococcus (GAS), is the presence of hyaluronic acid capsule and surface M protein that contribute to the bacterial resistance to host immune elements such as antibody opsonisation, complement-mediated lysis as well as antibacterial peptides secreted by neutrophils (Lauth et al., 2009; Ghosh, 2011, LaRock and Nizet, 2015). This exopolysaccharide layer shields the underlying anionic cell layers from cationic ABPs, which was supported by a study that mutations altering the expression of these capsules can sensitize GAS to killing by ABPs (Buchanan et al., 2005; Llobet, Thomas and Bengoechea, 2008). Correspondingly, as PAM-5 is a cationic ABPs which exerts its bactericidal effects through membrane-active mechanism, the presence of this capsular layer may serve as additional barrier to the cationic peptide besides cell wall. Consequently, higher amount of PAM-5 was required to saturate or overcome the barrier effect in order to kill the bacterium, which might explain the relatively higher MBC (64 µg/mL) of this peptide against *S. pyogenes* in this study.

Nevertheless, among the four Gram-positive bacteria screened in this study, *S. anginosus* was the only bacterium that was highly susceptible to PAM-5. This was indicated by the much lower peptide MBC (4 µg/mL) required to eliminate the bacterium as compared to the other three Gram-positive bacteria. Even though under the same genus, *S. anginosus* was much more susceptible to PAM-5 as compared to *S. pyogenes*. The difference in susceptibility to PAM-5 between these two streptococci might be attributed to their structural discrepancy. Unlike the more virulent streptococcal species such as *S. pneumoniae* and *S. pyogenes*, *S. anginosus* possesses lesser virulent factors. One of these virulent factors, exopolysaccharide capsule, is highly expressed in *S. pyogenes* but rarely expressed in *S. anginosus*. In fact, serotypes of non-encapsulated *S. anginosus* were isolated from clinical specimens from patients suffering from non-invasive infections (Kanamori et al., 2004), where these categories of streptococcus were found with impaired pathogenicity and highly susceptible to phagocytosis by neutrophils and other host antibacterial compounds (Mitchell, 2011). Similarly, without this barrier, it is believed that the non-encapsulated bacterium is vulnerable to attack by cationic ABPs which are able to reach the bacterial cell wall or even plasma membrane at concentration which is sufficient to kill the bacterium. This might explain the difference in susceptibility to PAM-5 between *S. pyogenes* and *S. anginosus* in this study.

Additionally, it is also believed that the slow bacterial doubling time for *S. anginosus* might be another factor leading to its high susceptibility to PAM-5. As compared to the doubling time for *S. aureus*, *E. faecalis* and *S. pyogenes*,

which were averagely determined as 30 minutes (Domingue et al., 1996), 40 minutes (Vebo et al., 2010) and 48 minutes (Gera and McIver, 2014), respectively, the duration required by *S. anginosus* to double its number was estimated between 150 to 195 minutes (Stinson et al., 2003). This longer doubling time might render the bacterium susceptible to antibacterial agents with fast killing kinetics. As PAM-5 was reported to exert rapid killing kinetic in **Section 4.4** (will be further discussed later), it is assumed that the slow growing *S. anginosus* was completely killed by the peptide before achieving its doubling time, thereby explaining the relatively low peptide MBC towards this bacterium.

5.4   Stability of PAM-5 in Human Plasma

The stability of ABPs in *in vivo* condition remains as a major challenge to clinical microbiologists who intent to develop these compounds into alternative antibacterial agents for clinical application. As reported in many other studies, many ABPs were shown effective *in vitro* against different bacteria, but whether they could retain the similar potency in human body is still debatable. This could explain the phenomenon that despite the increasing numbers of ABPs being documented in the Antimicrobial Peptide Database (http://aps.unmc.edu/AP/database/antiB.php), only a minority of them have made it to preclinical and clinical trials (Butler and Cooper, 2011; Fjell et al., 2012; Koo and Seo, 2019). Once being administered into host body, ABPs might be subjected to different degrees of impairment due to proteolytic degradation by proteases found in serum, plasma, blood and in other tissues (Goodwin,

Simerska and Toth, 2012; Starr and Wimley, 2017; Chen et al., 2018), leading to their diminished antibacterial activity. Despite possessing good antibacterial potency towards several bacteria in this study, the stability of PAM-5 *in vivo* is of equally important in order to substantiate further studies on its potential clinical application.

In this study, an *in vivo* condition was simulated by using human plasma freshly prepared before setting up the *ex-vivo* antibacterial assay. The bacteria were treated with PAM-5 in human plasma. The stability of PAM-5 was determined by comparing the peptide MBC towards the target bacterium in the *ex vivo* microbroth dilution assay to the MBC of *in vitro* assay as reported previously. This approach of simulating *in vivo* condition via *ex vivo* assay using plasma or serum was utilised by several research groups in order to access the stability of ABPs in human host conditions (Sainath Rao et al., 2013; Dong et al., 2018), justifying the feasibility and reliability of the assay in providing finding that could reflect the true *in vivo* condition in host body. As reported in **Section 4.3**, PAM-5 was slightly less potent against *P. aeruginosa* in the *ex vivo* condition as reflected by its two-fold higher MBC against the bacterium as compared to the *in vitro* condition. However, this MBC value was still in the range of MBCs which is characterized as an ideal ABP. The most possible explanation to these observations is the presence of certain inhibitory factors in human plasma that might reduce the peptide bioactivity but yet to cause complete inactivation or degradation to the peptide. One of the possible inhibitory factors is the plasma cations such as ionized calcium, sodium or magnesium which might serve as competitors to PAM-5 for binding to the ligands on bacterial surface. As the

result of this possible competition, higher amount of PAM-5 might be required to bind and displace the bound cations on the membrane in order to achieve the bactericidal effect. The slightly higher MBC indicated that the peptide was relatively stable and able to retain its antibacterial potency despite the presence of these inhibitory factors in the plasma. It is speculated that the presence of certain amino acids within the peptide sequence rendered the peptide with the stability. According to Nguyen et al. (2010), the number of tryptophan (W) and arginine (R) in a peptide is directly proportionate to the peptide stability due to the ability of these residues to reduce interaction between the peptide and proteolytic enzymes. Since these amino acids are also present in PAM-5 in considerable proportions (two tryptophan and three arginine), it is believed that PAM-5 is rendered with certain degree of resistance towards the proteolytic enzymes in the plasma, thus explaining its similar potency despite the presence of plasma.

5.5   Antibacterial Mechanisms of PAM-5

It is well established that cationic and amphipathic ABPs often exert their antibacterial effects via membrane-active mechanisms. In particular, cationic ABPs with α-helical structures were shown to have strong bactericidal effect by causing destruction to bacterial membrane (Chen et al., 2007; Huang, Huang and Chen, 2010). In view of the relatively high cationicity, moderate hydrophobicity and presence of α-helical structures in PAM-5, it is speculated that this peptide exerts its antibacterial effect via membrane-active mechanisms too. To address this speculation, scanning electron microscopy and SYTOX Green uptake assay

were carried out to screen for its ability to cause outer membrane disruption and cytoplasmic plasma permeabilization.

Clearly demonstrated from the scanning electron microscopy, extensive morphological changes characterized by membrane disruption were seen on the PAM-5-treated *P. aeruginosa*. As compared to the untreated bacteria which possessed smoother surfaces, signs of outer membrane disruption characterized by surface roughening and corrugation, formation of blebbings and micelles were only seen on the surface of PAM-5-treated bacteria. The similar appearance of membrane disruption was also demonstrated by bacteria treated by polymyxin B, a well-studied ABP with strong membrane-active mechanisms that served as the positive control in this study. Apart from this comparison, the morphological changes to the membrane induced by PAM-5 also resemble the appearance of disrupted membranes that were caused by several membrane-active ABPs from other studies such as a cathelicidin derivative named SMAP29 (Saiman et al., 2001), human epididymis 2 (Yenugu et al., 2004), gramicidin S and PGLa (Hartmann et al., 2010), HAHp2-3-1 (Song et al., 2012) and short designated peptides named PP, PQ and Qa (Dong et al., 2018). The comparable findings between PAM-5 and these ABPs suggested that disruption of bacterial membrane integrity is one of the antibacterial actions for PAM-5.

The actions of membrane-active ABPs have been well documented in many structure-function association studies. As described in **Chapter 2**, several models on how these peptides induce membrane destructions have been

proposed, which include 'barrel-stave', 'toroidal pore' and 'carpet' models. The former two models depict how the peptides induce pore or lumen formation on the bacterial membrane by inserting themselves into and spanning across the phospholipid bilayer, which lead to leakage of cellular contents and bacterial death (Brogden, 2005; Melo, Ferro and Castanho, 2009). However, these two models require a minimum peptide length of 20 amino acids to be long enough to span the lipid bilayer (Song et al., 2012; Shahmiri, Enciso and Mechler, 2015). Therefore, the membrane-active mechanism of the 15-amino acid PAM-5 may not be mediated by these two models.

With reference to the SEM micrograph, it is assumed that PAM-5 may cause membrane disruption via the combination of 'carpet' and 'detergent-like' models. In the 'carpet' model, ABPs form a layer of carpet that is parallel to the surface of bacterial membrane. The peptide carpeting was shown to weaken the bacterial membrane by gradually causing curvature to the phospholipid bilayer, which leads to collapse of the membrane into micellar structures by detergent-like action as could be seen in the SEM micrograph in this study [**Figure 5.2 (b)**]. It is postulated that the blebbings found on the surface of treated *P. aeruginosa* might be resulted from PAM-5-induced membrane collapse which highly resemble the micelles depicted by the arrows in **Figure 5.2 (a)**.

(A)

Carpet model

Detergent 'like' model

(B)

UTAR   2   SEI   2.0kV   X30,000   WD 6.0mm   100
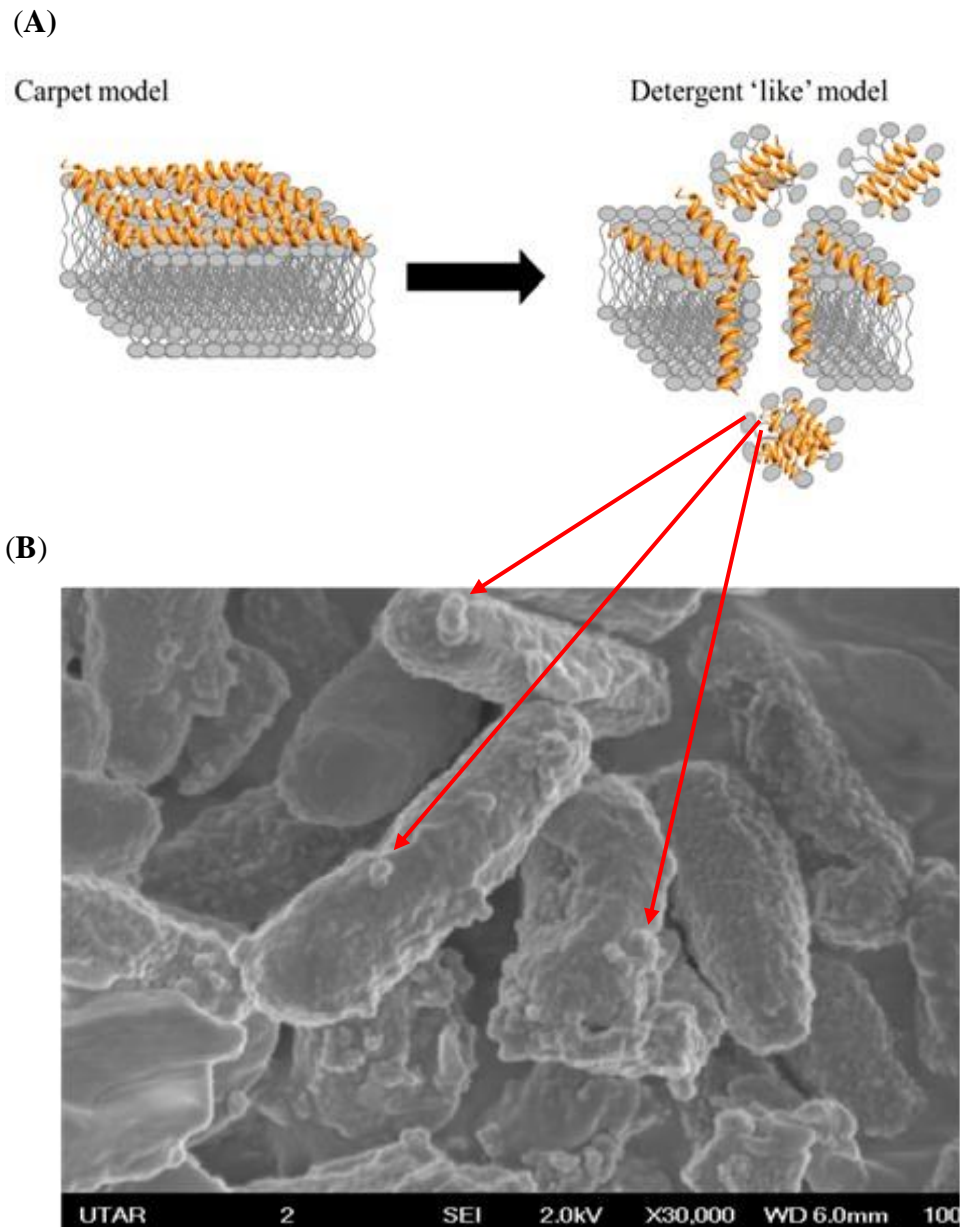
Figure 5.2: Resemblance of micelle to the blebbings on the surface of PAM-5-treated bacteria (as indicated by red arrow). (**A**) Illustration of a micelle structure resulted from the action of ABPs on cell membrane via detergent-like model (Adopted from Brogden, 2005); (**B**) SEM micrograph of PAM-5-treated *P. aeruginosa* (magnification × 30,000)

According to Shai (2002), there is no requirement for minimum peptide length for ABPs that disrupt bacterial membrane via 'carpet' and 'detergent-like' models as these peptides usually do not insert and span across the phospholipid bilayer. Besides, the peptides that are classified under these models of actions possess high proportions of cationic arginine (R) and lysine (K) distributed along

the peptide chain, which promote strong contact with the anionic lipid head groups for membrane permeation. As these features are also present in PAM-5, and coupled with the above-mentioned findings from the SEM, it is assumed that the actions of PAM-5 on the bacterial membrane were mediated through both 'carpet' and 'detergent-like' models.

Following the outer surface disruption, it is believed that PAM-5 could further permeabilize bacterial cytoplasmic membrane if the peptide concentration is sufficient to reach the inner membrane. In order to verify this assumption, SYTOX Green uptake assay was carried out. SYTOX Green is a membrane-impermeable, high affinity nucleic acid stain which is unable to enter the intracellular compartment of a membrane-intact cell or bacterium. However, when the cytoplasmic membrane is compromised or permeabilized by a membrane-active agent, the nucleic acid-binding probe can readily penetrate the layer into the intracellular compartment of the bacteria followed by binding to nucleic acids. The nucleic acid-bound SYTOX Green can emit green fluorescence once the complex is excited by a light source of 450 nm – 490 nm (Invitrogen). The amount of fluorescence emitted is directly proportionate to the extent of cytoplasmic membrane permeabilization. This method was commonly used to relate cell viability associated with membrane-permeabilization caused by many compounds, including ABPs (Rathinakumar, Walkenhorst and Wimley, 2009; Dias et al., 2017; Omardien et al., 2018; Yasir, Dutta and Willcox, 2019).

Based on this principle, it was found that PAM-5 at concentrations ranging from 2 µg/mL to 64 µg/mL was able to induce membrane permeabilization to the treated bacteria in a concentration-dependent manner. This finding indicated that the increasing amount of PAM-5 could extensively cause more permeabilization to the bacterial cytoplasmic membrane, which allowed entry of more SYTOX Green into the bacteria to bind with more nucleic acids. Logically, as the concentration of PAM-5 increased further, one would expect that the amount of emitted SYTOX green fluorescence was to be proportionally higher. Unexpectedly, after 64 µg/mL, the trend of fluorescence was inversely proportionate to the increasing peptide concentration from 128 µg/mL to 256 µg/mL. Despite repeated assays on this, the fluorescent signals consistently decreased even though the bacteria were treated with the two highest concentrations of PAM-5. As the fluorescent reduction occurred at the concentration-dependent manner, it is speculated that the ABP also might exert a direct effect towards the fluorescent probe or even the bacterial nucleic acids.

Nevertheless, this unexpected observation might optimistically provide a clue that PAM-5 may possess another antibacterial characteristic. One of the possible abilities is direct nucleic acid binding by the peptide upon permeabilizing and penetrating the bacterial membrane. In fact, the similar findings were also demonstrated by another study which was conducted by Taute et al. (2015). According to the report, a novel ABP which was derived from defensin, namely Os, was discovered for its DNA-binding ability after demonstrating the similar trend of fluorescent emission as seen for PAM-5. It was later found that the

peptide possessed the ability to bind to bacterial DNA and thus able to displace SYTOX Green probe from the DNA when it was present at high concentrations. Similarly, at high concentrations, PAM-5 is speculated to compete with the SYTOX Green to bind to the bacterial nucleic acids, thus reducing the amount of SYTOX Green that bind to the nucleic acids followed by reduction in the emitted fluorescence. This could explain the decrement of the fluorescent emission from the bacteria treated with PAM-5 at concentration from 128 μg/mL to 256 μg/mL.

Interestingly, this speculation was eventually confirmed by DNA gel retardation assay which is also known as electrophoretic mobility shift assay (EMSA). Using a modified protocol as described by Scott et al. (1994), PAM-5 was initially revealed for its ability to bind to genomic DNA extracted from *P. aeruginosa* at high peptide concentrations. Subsequently, the similar bindings were also seen for genomic DNAs isolated from *E. coli*, *A. baumannii* and *K. pneumoniae*, suggesting the non-specific and universal binding strength of this peptide to bacterial DNAs regardless of bacterial species. Besides genomic DNAs, the peptide was also able to bind plasmid DNA, suggesting its ability to bind with different forms of nucleic acids present in bacteria. Interestingly, the peptide-DNA binding as indicated by retardation of DNA migration in the EMSA were generally occurred at high concentrations of PAM-5 (64 μg/mL to 256 μg/mL), which corresponded to the peptide concentrations that resulted in fluorescent reduction in the SYTOX Green uptake assay as described above.

The ability of PAM-5 to bind bacterial nucleic acids might be attributed to its peptide cationicity. According to Yan et al. (2013), alkalescent and positively charged amino acids such as lysine (K) and arginine (R) in an ABP might promote electrostatic interaction between the peptide and the negatively charged phosphate fragments on the DNA backbone. Correspondingly, as PAM-5 also carries considerable numbers of these amino acids (**K**-W-**K**-W-**R**-P-L-**K**-**R**-**K**-L-V-L-**R**-M), strong electrostatic bonding is presumably to be formed between the peptide and bacterial DNA. The higher molecular weight of the peptide-bound DNA complex as well as the reduced net negative charge of the nucleic acid due to partial neutralization by cationic PAM-5 may resulted the slower or retarded migration of the bound DNA as compared to untreated DNA during EMSA. This notion was supported by a few studies on ABP-DNA binding with similar findings (Sugiarto and Yu, 2007; Tang et al., 2008; Yan et al., 2013; Sousa et al., 2016; Diaz-Roa et al., 2019), where the ABPs under these studies were able to complex with bacterial DNA in concentration-dependent manner.

From the macroscopic view on the antibacterial actions of PAM-5, the findings generated from the scanning electron microscopy, SYTOX Green uptake assay and DNA gel retardation assay indicated that this peptide possesses more than one mechanism of action by targeting different bacterial targets. The sequel antibacterial actions of PAM-5 may begin with initial contact with certain anionic constituents on the surface of bacterial outer membrane. Upon weakening the outer membrane architecture by the proposed models as described earlier, the phospholipid bilayer started to collapse, thus allowing more peptides to reach the cytoplasmic membrane which may become the

second target of the peptide. Even though the detailed mechanism is yet to be determined, PAM-5 may disrupt the integrity of bacterial cytoplasmic membrane which resulted in increased permeability of the layer to foreign substance. This would allow the translocating and accumulation of PAM-5 in the inner compartment of the bacteria, which may end up with spontaneous interaction with the nucleic acids that was indicated as the third target of the peptide in this study. Following the peptide binding, the nucleic acids, particularly DNA, may not be able to undergo certain normal molecular and physiological activities. These include DNA replication, DNA repair as well as gene expression for proteins needed for cellular processes. According to van Eijk et al. (2017), a replisome complex which consists of primase, helicase, DNA polymerase and single-stranded DNA-binding proteins is required to bind to the DNA before initiating DNA replication. Any other substance that interferes with the formation of this complex would inhibit DNA replication which subsequently results in bacterial death. In this scenario, it is believed that the binding of PAM-5 to bacterial DNA might disrupt the formation of replisome complex, thus inhibiting DNA replication. This could explain the bactericidal effect of many DNA-binding ABPs, including PAM-5 in this study.

The multiple targets hit by PAM-5 during the antibacterial action is indeed an advantage to this ABP as compared to many conventional antibiotics which commonly act on a single target. Most antibiotics possess very limited or specific mechanism to their target bacteria. For instance, antibiotics classified under β-lactams and glycopeptides inhibit cell wall synthesis by binding to penicillin-binding proteins (PBPs), while aminoglycosides inhibit protein

synthesis by binding to bacterial ribosomes (Rice, 2012; Krause et al., 2016; Zeng et al., 2016). However, alterations to these antibiotic targeted structures via amino acid substitution or other forms of mutations can easily compromise the efficacy of these compounds by reducing their binding affinity to these specific bacterial targets, thus leading to resistance to the antibiotics. This limitation indeed highlights the significance of ABPs, where many of them could overcome this shortcoming by targeting more than one bacterial cellular components. In addition to bacterial membrane, accumulating evidence have shown that a number of ABPs could simultaneously act on certain intracellular targets or bioactivities that are essential to bacterial survival or proliferation. In a review by Le et al. (2017), these targets include mitochondria, nucleic acids, protein synthesis and folding as well as enzymatic activities. In a study by Ho et al. (2016), a total of 30 proteins and a range of 47 to 231 other intracellular components in *E. coli* were shown to be common targets by lactoferricin B, bactenecin 7, a hybrid of pleurocidin and dermaseptin and a proline-arginine-rich peptide. The ability of these ABPs to interact with multiple targets may limit the chances for the bacteria to develop resistance via target alterations, as it is unlikely for a bacterium to change all the targets simultaneously.

Concordantly, for certain reasons, the multiple bacterial structural targets hit by PAM-5 as revealed in this study may decrease the likelihood of inducible resistance towards this peptide. Firstly, as the membrane-active mechanisms by PAM-5 are mediated through non-specific ligand binding, simultaneous alterations to all the possible binding ligands in/on the entire membrane via mutations are biological costly to the bacteria (Cho and Kim, 2010; Jang et al.,

2012). Next, even though the bacteria might structurally modify the membranous targets, PAM-5 may still be able to permeabilize and translocate the plasma membrane followed by binding to nucleic acids as the alternative target. Even though the inner membrane permeabilization and DNA binding may not occur simultaneously, but the events may take place sequentially in a rapid manner. Similarly, it is unlikely for the bacteria to modify both the membrane and other intracellular targets concurrently upon exposure to the antibacterial agent.

Additionally, apart from genomic DNAs, PAM-5 was also found to bind plasmid DNA. The role of plasmid in disseminating antibiotic resistance among bacterial community has been well studied and documented (Lopatkin et al., 2017; San Millan, 2018; Dolejska and Papagianitsis, 2018). Some plasmids may harbour more than one antibiotic-resistant gene, rendering the host or recipient bacteria of these plasmids with multidrug-resistance (Bennett, 2008). An antibacterial agent that is able to bind and interfere with the normal physiological function or replication of the plasmid may interrupt the carriage or expression of resistance gene within the plasmids. Therefore, the ability of PAM-5 to bind to plasmid DNA may significantly reduce the dissemination of resistant genes among bacteria.

5.6   Rapid Kinetic Killing of PAM-5

As described earlier in Chapter 2, slow antibacterial kinetics by many conventional antibiotics may be one of the reasons for antibiotic resistance. Fast

228

replicating bacteria that outpace the slow-acting antibiotics may provide the interval sufficiently to acquire resistance via mutation (Pray, 2008; Beatriz et al., 2015). Therefore, a compound or substance with rapid killing kinetic is indeed a prior consideration in the development of an effective novel antibacterial agent. Based on the findings of time-kill assay in this study, PAM-5 is considered to fulfil this criterion in view of its ability to kill the tested bacteria rapidly. In just ten minutes, PAM-5 was able to eliminate both *E. coli* and *P. aeruginosa* completely. Conversely, the doubling time for both the bacteria were estimated to be 20 minutes and 30 minutes, respectively (Gibson et al., 2018). This implied that both the bacteria could be totally eradicated by PAM-5 before achieving their complete replication, in which mutational-mediated resistance and dissemination of resistant plasmids may occur at any point. Thus, it is assumed that the likelihood for the bacteria to acquire resistance towards PAM-5 is relatively low.

Interestingly, the duration required by PAM-5 to kill these two bacteria completely was even shorter than the duration by gentamicin, which killed the *E. coli* and *P. aeruginosa* completely after 30 minutes and > 60 minutes, respectively. From the perspective of antibacterial mechanism, the rapid killing kinetic of PAM-5 might be attributed to the multiple targets hit by PAM-5 as compared to the single specific mode of action by gentamycin. Due to the fact that PAM-5 could compromise the integrity of bacterial membrane as well as interfering with intracellular events due to DNA-binding, the bacteria could be killed in a rapid manner. Even though if PAM-5 utilizes membrane-disruptive action as its sole antibacterial mechanism, the extensive damage to the bacterial

membrane is fast enough to kill the bacteria as compared to gentamycin that mainly act intracellularly by inhibiting protein synthesis. The disrupted membrane may lead to leakage of intracellular content which are essential to many bacterial biological activities, including protein synthesis which is targeted by gentamycin. Thus, in terms of killing kinetics, PAM-5 is given an advantage over the slow-acting aminoglycoside in which the latter is usually confronted with bacterial resistance via ribosome modification. This indicated that PAM-5 is a more potent antibacterial agent as compared to gentamicin in fighting against pathogenic bacteria.

5.7   *In vitro* Cytotoxic Effect of PAM-5 to Mammalian Cells

In order to develop an ABP into a pharmaceutical agent which is safe to be used in clinical setting, it is important that the peptide possess good antibacterial activity along with high safety feature. The former characteristic was demonstrated by PAM-5 in view of its potent bactericidal effect towards a spectrum of Gram-negative and certain Gram-positive bacteria. To address the latter, PrestoBlue cell viability assay and haemolytic assay were conducted to screen for the potential toxicity and haemolytic effect caused by PAM-5 to Vero cells, HeLa cells and human erythrocytes. Both HeLa and Vero cells are immortal mammalian cell lines that are commonly used in many toxicity studies on ABPs (Vaucher et al., 2010; Paiva et al., 2012; Artun et al., 2016; Reinhardt and Neundorf, 2016) as they are easily cultivated and well characterized (Ammerman et al., 2008). The toxicity of PAM-5, if any, to these two cell lines may reflect the potential harmful effect of the peptide to mammalian or even

human epithelial and kidney cells. On the other hand, screening for the haemolytic effect of PAM-5 on human erythrocytes could provide a clue for its possible application intravenously.

In contrast to many other studies which utilized MTT [3-(4,5-dimethylthiazol-2-yl)-2,5-diphenyltetrazolium bromide] assay as screening test for peptide cytotoxicity (Vaucher et al., 2010; Hilchie et al., 2011; Laverty and Gilmore, 2014; Soundrarajan et al., 2019), PrestoBlue assay was chosen for this study due to several reasons. Firstly, it was found that PrestoBlue reagent is far more sensitive than MTT reagent by its ability to detect viable cells at the titre as low as 12 cells per well, as compared to the minimum cell number of 1000 cells per well required by MTT assay (Boncler et al., 2013; Xu, McCanna and Sivak, 2015). In addition, it was found that MTT could exhibit possible light toxicity to cells. The process of reducing tetrazolium dye in MTT to formazan product that occurs in the cell cytosol as well as exocytosis of the formazan product from the cell were found to cause certain cell injury (Lu et al., 2012; Riss, 2013). Moreover, the metabolism of MTT requires NADH which is a critical co-enzyme for redox reactions in a normal cell (Riss, 2014). Diversion of NADH away from the critical cellular functions for MTT metabolism may affect the normal metabolic activity of the cell which may ended up with cell death. Consequently, these shortcomings of MTT assay might provide false positive data for the toxicity studies.

Comparatively, PrestoBlue cell viability assay has gradually becoming a preferred choice for many research groups to study cell viability and compound toxicity. Developed by Invitrogen, Life Science®, PrestoBlue is a resazurin-based reagent which can be used to evaluate cell viability and proliferation for a wide range of cell types. Viable cells which are metabolically active are able to reduce the initially blue resazurin into red-coloured resorufin product which can be quantified as relative fluorescent unit (RFU). In contrast, dead cells which are deprived of this reducing ability failed to produce the red resorufin. Thus, the amount of RFU is directly proportionate to the degree of metabolic activity as well as the number of viable cells, which in turn reflecting the degree of toxicity of the tested substance. Apart from having higher sensitivity to viable cells as mentioned previously, PrestoBlue reagent is generally non-toxic to cells, which could allow extended incubation period for certain assays without causing harmful effect to the cells (Promega). This distinct feature makes PrestoBlue cell viability assay a preferred choice for many studies to screen for compound toxicity, which can be estimated by determining viability of treated cells in a qualitative and quantitative manner (Emter and Natsch, 2015; Inui Kishi et al., 2018).

With reference to the findings in **Section 4.7.1**, it was shown that PAM-5 has a remarkable safety profile where no significant *in vitro* toxicity was shown by the peptide to both HeLa and Vero cells. This was reflected by the generally high RFUs produced by the cells treated with this peptide at all tested concentrations from 2 µg/mL to 256 µg/mL. Moreover, the RFUs produced by PAM-5-treated cells were insignificantly different from the RFUs generated by the untreated

cells, indicating no distinguishable number of viable cells between the peptide-treated and untreated cells. Most importantly, the range of peptide concentrations that was not toxic to the cell lines encompassed the peptide MBCs against the spectrum of bacteria, which included *S. anginosus*, *S. pyogenes*, *E. coli*, *P. aeruginosa*, *A. baumannii*, *A. junii*, *K. pneumoniae*, *S. flexneri*, *S.* Typhi and *S. aureus* (4 µg/mL to 128 µg/mL).

Interestingly, PAM-5 was found less toxic to Vero cells as compared to polymyxin B in PrestoBlue assays, as indicated by the overall significantly higher RFU values from the former than the latter. Polymyxin B, a colistin group peptide antibiotic, was restricted for its clinical usage due to nephrotoxicity (Azad et al., 2013; Eadon et al., 2013; Kelesidis and Falagas, 2015) despite its high potency against many bacteria, as shown in this study. Since Vero cell is a cell line that is commonly used to study for nephrotoxic effect of a compound (Lincopan et al., 2005; Negrette-Guzmán et al., 2013; Zhu et al., 2017), the overall insignificant toxicity of PAM-5 towards Vero cells as compared to polymyxin B can provide an *in vitro* prediction on the better safety profile of PAM-5 than polymyxin B in terms of nephrotoxicity.

5.8 *In vitro* Haemolytic Effect of PAM-5 to Human Erythrocytes

In order to evaluate its potential systemic application, the haemolytic effect of PAM-5 was screened on human erythrocytes via *in vitro* haemolytic assay. If the red blood cells are lysed by a lytic agent, the intracellular haemoglobin would be released into the PBS and a red coloured supernatant could be observed after

separation from the cell suspension. In contrast, absence of haemolysis was indicated by a clear and colourless supernatant. The absorbance of the supernatants reflected the amount of haemoglobin released from the erythrocytes, which in turn indicated the degree of haemolysis of the erythrocytes by the agent, which was PAM-5 in this study.

Correspondingly, the non-cytotoxicity of PAM-5 as demonstrated by PrestoBlue cell viability assay was also accompanied by the non-haemolytic effect of this peptide on human erythrocytes via *in vitro* haemolysis assay. Interestingly, the haemolytic effect of PAM-5 was not even apparent as compared to polymyxin B, in which the latter exhibited significantly higher haemolytic effect to hRBCs. This finding preliminarily potentiates the clinical application of PAM-5 against systemic bacterial infections without causing harmful effect to RBCs.

5.9   Association between physiological properties and peptide toxicity

In view of the findings on the cytotoxicity and haemolytic effect of PAM-5, coupled with the antibacterial potency of the peptide on various bacteria screened in this study, one can tentatively predict that PAM-5 may selectively act on bacteria instead of mammalian cells. The non-toxicity of the peptide towards mammalian cells and high selectivity towards bacteria might be attributed to several aspects that encompass physiochemical properties of the peptide as well as the differences in the build-up of membranes between prokaryotic (bacteria) and eukaryotic (mammalian) cells.

It is well documented that the physiochemical properties of an ABP may have certain impacts on the antibacterial potency of the peptide. These properties include peptide length, amino acid makeup, peptide cationicity and hydrophobicity (Bahar and Ren, 2013; Zhu et al., 2014; Malmsten, 2016; Haney et al., 2019). Nevertheless, the same features are also associated with the peptide toxicity on eukaryotic cells. Alteration in any of these features would affect the range of bacterial targets as well as their potential toxicity to mammalian cells (Bahar and Ren, 2013). Therefore, these properties should be taken into consideration in order to design an ABP with minimize toxicity without reducing their antibacterial efficacy.

As reported earlier in **Section 4.15**, PAM-5 is a cationic ABP with the net positive charge of +7. The peptide cationicity may be the main factor contributing to the selective action towards bacteria but not mammalian cell. As described earlier in Chapter 2, cationic ABPs with membrane-active action come with higher propensity to interact with bacterial membrane which possess many negatively charged constituents. In contrast, mammalian cell membranes are generally zwiterrionic, in which strong electrostatic interactions between the membranes and cationic ABPs are unlikely to be formed. Without these initial contact, further downstream actions on the membranes would not occur. This notion can be supported by the findings on SYTOX Green uptake by PAM-5-treated Vero cells in this study, where very low fluorescent emissions were produced by the peptide-treated cells as compared to cells with membranes that were completely permeabilized by melittin, which is a strong membrane-permeabilizing ABP (Raghuraman and Chattopadhyay, 2007; Wimley, 2018).

The trace amount of fluorescence present in the cells treated with PAM-5 was most probably emitted from the scanty number of dead cells that were present in the wells even before the treatment, which were also present in the untreated cells (DPBS-suspended cells). Therefore, this fluorescence did not reflect the toxicity of PAM-5 on the cells. By excluding these background signals, it can be concluded that PAM-5 did not permeabilize the membrane of Vero cells. In contrast to the much higher amount of SYTOX Green fluorescence emitted from PAM-treated bacteria as reported in **Section 4.5.2** (refer to **Figure 4.20**), the extremely low fluorescent intensities from the PAM-5-treated Vero cells further indicated the selective action of the peptide to bacteria instead of mammalian cells.

Besides, the range of cationicity may also influence the haemolytic effect of an ABP. In a study by Ma et al. (2014), ABPs with cationicity that range from +6 to +8 did not show remarkable sign of haemolysis to RBCs. However, when the net charge was reduced to a range that was lower than +6, the haemolytic effect of the peptide became apparent. On the other hand, increasing the net charge to above +8 did not further contribute to better antibacterial potency of the peptides. These findings suggested that +6 to +8 is the ideal range of cationicity for an ABP with optimized therapeutic index. Concordantly, the cationicity of PAM-5 falls within this optimal range, which may explain its non-haemolytic effect to human erythrocytes as demonstrated in this study.

Apart from cationicity, the hydrophobicity of an ABP was found as another determining factor contributing to peptide toxicity. Structural-functional studies have demonstrated that the balance between peptide hydrophobicity and hydrophilicity may serve as the critical factor that influence the peptide selectivity between bacterial and mammalian cell membranes (Matsuzaki, 2009; Edwards et al., 2016). In another study, it was found that increment of peptide hydrophobicity exceeding its optimal value would significantly promote its binding to mammalian cell membranes, thus leading to cell toxicity (Glukhov, Burrows and Deber 2008). The non-cytotoxic and non-haemolytic effect of PAM-5 towards the cell lines and human erythrocytes might be associated with its moderate hydrophobicity which may not sufficiently promote its interaction to the membrane phospholipid bilayer of mammalian cells.

Last but not least, the length of an ABP is also another key feature for peptide toxicity. A longer ABP may harbour higher number of hydrophobic residues and thus may increase the propensity of hydrophobic surface interaction between the peptide and mammalian cell membrane, followed by pore formation across the outer and inner membrane which resulted cell lysis (Bahar and Ren, 2013). Melittin, a 26-amino acid ABP, represents an example of ABP with poor cell selectivity as it is able to exert strong haemolytic effect towards bacteria and erythrocytes (Sharon et al., 1999). Experimental evidence showed that melittin could form pores or channels across the two zwiterrionic layers of membranes via toroidal model (Park et al., 2006; Manna and Mukhopadhyay, 2009). This explained the strong haemolytic effect of melittin to human erythrocytes in other studies, as well as its strong permeabilization to the Vero cells as reported in

Section 4.8 of this study. However, shortening of melittin from 26 residues to 15 residues was found to reduce its haemolytic effect by 300 times due to the reduction of large hydrophobic surfaces (Subbalakshmi, Nagaraj and Sitaram, 1999). In contrast to the original longer melittin, PAM-5 is relatively shorter with 15 amino acids and moderate hydrophobic surfaces. As the result, it may not able to form sufficient hydrophobic interaction with the lipid head groups in the membrane of erythrocyte, thus depriving its ability to induce pore formation across the cell membrane. As proposed earlier, due to its shorter length, PAM-5 may exert its action on the membrane via carpet and detergent-like models instead of toroidal or barrel-stave models which require longer peptide length.

In summary, ABPs may come with diverse structural and physiochemical properties that allow them to act on different target cells which may include mammalian cells. The key features for an ideal ABP to act selectively on bacterial target with minimized toxicity to mammalian cells should be taken into consideration in the rational design of a potent ABP with high therapeutic index, which is reflected by PAM-5 generated in this study.

5.10   Implications of This Study

Clearly indicated from this study, the combination of phage display selection and computer-assisted peptide modification is an ideal strategy to develop an ABP with potent antibacterial activity but minimal toxicity to mammalian cells. The former could select peptide/s that harbor/s certain motif/s with binding preference to bacterial conserved surface molecules or structures if the

bacterium is used as the target of biopanning, while the latter could be used to enhance the antibacterial features of the selected peptide by adjusting the peptide cationicity and hydrophobicity.

Findings from the antibacterial assays indicated that PAM-5 is a strong bactericidal ABP towards Gram-negative bacteria rather than Gram-positive bacteria. As the target bacterium used in the affinity selection was *P. aeruginosa*, a Gram-negative bacterium, the stronger action of this peptide towards Gram-negative bacteria could be possibly due to the affinity selection process that might have selected peptides that bound to surface structure/s that is/are mainly present on Gram-negative bacteria. Thus, PAM-5 could be considered as a potential alternative treatment against Gram-negative bacteria if more promising pre-clinical and clinical data are observed in the future. Besides, as PAM-5 was shown able to kill drug- and multi-drug resistant bacteria, along with its rapid killing kinetic as found in this study, it is expected to be able to overcome the issue of drug-resistance that compromises many conventional antibiotics currently.

The ability of PAM-5 to retain its antibacterial activity despite the presence of human plasma suggested that this peptide might be able to resist *in vivo* degradative factors which are the main obstacles to many ABPs. This peptide stability is essential for its future clinical application, particularly against bacteria that cause bloodstream infections. Nevertheless, more studies are required to support this implication.

The ability of PAM-5 to disrupt outer membrane, permeabilize cytoplasmic membrane as well as binding to bacterial DNA shows that this peptide acts in such a novel mechanism that is distinct from the conventional antibiotics. Similarly, these findings strongly suggest the potential of the peptide to overcome bacterial resistance as it possesses alternative mechanisms of action towards the bacteria if one of the above-mentioned bacterial structure is altered via adaptive mutation, which is unlikely.

Finally, the non-toxic effects towards HeLa cells and Vero cells, as well as the non-hemolytic effect of PAM-5 towards human erythrocytes imposed a very significant implication on the peptide safety to future clinical application in humant body. The range of peptide concentrations that showed no significant toxicity towards the mammalian cells encompassed those high MBCs against certain bacteria tested in this study, indicating the flexibility in dosage adjustment that is available for PAM-5 to kill these bacteria. Collectively, these findings indicate that PAM-5 may possess good therapeutic index against bacterial infections.

5.11   Limitation of This Study and Proposed Future Studies

As described earlier, PAM-5 was shown to possess potent antibacterial effects towards a spectrum of bacterial targets, particularly Gram-negative bacteria. However, its potency against Gram-positive bacteria is still yet to be concluded in consideration of its heterogeneous effects towards different Gram-positive bacteria which were tested in this study. Furthermore, only three genera and four species of Gram-positive bacteria were tested for the antibacterial effect of PAM-5 due to the unavailability of other bacterial species in the current research laboratory. Therefore, this might not overall reflect its poor potency towards Gram-positive bacteria tentatively found in this study. Therefore, additional genera or species of Gram-positive bacteria such as *Bacillus spp*., *Corynebacterium spp*., *Clostridium spp*. and *Listeria spp*. can be added into the list of antibacterial screening before making a strong conclusion on its potency against this bacterial category.

Next, even though PAM-5 was shown relatively stable in human plasma, a conclusion on its stability *in vivo* could not be made at this stage of study due to two major reasons. Firstly, only one bacterium (*P. aeruginosa* ATCC 27853) was tested in this *ex vivo* antibacterial assay, which might not reflect the overall susceptibility of other bacteria to PAM-5 in this condition. Secondly, other indigenous factors *in vivo* such as pH and salinity might have certain impact towards the peptide potency. If the peptide is subjected to animal studies in the future, the stability of the peptide *in vivo* will determine its potency against pathogenic bacteria that cause infections in different parts of the body with

different pH and salinities. Thus, in future studies, it is essential to include further *ex vivo* antibacterial assays which are set up in different pH conditions and salinities against the list of bacteria which were screened in this study. If the MBCs derived from these studies are very similar to the MBCs as reported from the *in vitro* studies, a more justifiable conclusion on its stability can be made before proceeding to animal studies.

If the above-mentioned *ex vivo* assays come with promising preliminary findings, *in vivo* antibacterial experiments could be proposed on animal model to determine whether PAM-5 could maintain its antibacterial potency in the whole body. Host body microenvironment may present with different degradative factors that may reduce the efficacy of the peptide, such as peptidase, proteinase, gastric hydrolytic enzymes, and acid. Data from these *in vivo* antibacterial experiments could provide important clues on further modification of the peptide to sustain these *in vivo* impairing factors. One of the bacterial examples that could be employed for this *in vivo* study is *Helicobacter pylori* (*H. pylori*), the agent that causes gastritis, gastric ulcer, and stomach cancer. Since this bacterium could inhabit host stomach, where low pH and degradative enzymes may be challenging factors to the efficacy of PAM-5, an *in vivo* antibacterial experiment by feeding PAM-5 to an animal model in which its stomach is infested with this bacterium is worthly to be carried out to justify the clinical application in the future.

In terms of killing kinetic, although the time-kill assays in this study had demonstrated that PAM-5 exerted rapid killing kinetics towards *P. aeruginosa* ATCC 27853 and *E. coli* ATCC 35218, but it is not justifiable to conclude that this peptide is an ABP with rapid killing based on the limited findings on these two bacteria only. Furthermore, the bacterial strains chosen for this study were mainly reference strains from American Type Culture Collection (ATCC), which might not reflect its similar killing kinetic on clinically isolated strains. Therefore, future studies on the killing kinetic of this peptide should consider adding in more bacterial strains from various species and strains both from ATCC reference strains as well as clinically isolated strains.

As described earlier, the rapid killing of PAM-5 on the selected bacteria could be attributed to its multiple antibacterial mechanisms as found in this study, which encompassed outer membrane disruption, inner membrane permeabilization and DNA-binding. However, PAM-5 may possess other possible mechanism/s of action that is/are yet to be elucidated in this study. Since PAM-5 was shown as a membrane-active ABP, it is believed that the peptide might possess other mode of action/s apart from the morphological and structural disruption on the bacterial membrane as demonstrated by the SEM in this study. In future studies, additional membrane-active mechanisms might be further evaluated in order to gain better insight on how the peptide compromise the integrity of the membrane. For instance, 3,3′-dipropylthiadicarbocyanine iodide [diSC$_3$(5)] assay could be used to screen for inner membrane depolarization by PAM-5 as this membranous change is associated with destabilization of the membrane. Additionally, transmission electron

microscopy (TEM) could be used to screen for peptide-mediated internal structural alteration or damage in the bacteria. This microscopy could provide clue on the action of PAM-5 on other intracellular target besides nucleic acids.

Certain ABPs were found able to kill their target bacteria by targeting protein synthesis via various mechanisms (Zanetti, 2004; Carvalho Ade and Gomes, 2011; Mardirossian et al., 2014; Mardirossian et al., 2018; Graf et al., 2019). In this study, apart from DNA-binding, the other intracellular targets, for instance, ribosome or protein synthesis, may serve as the potential target of this peptide but are yet to be elucidated. Hence, in future studies, PAM-5 shall be studied for its ability to inhibit bacterial protein synthesis via *in vitro* transcription/translation and translation assays. Alternatively, the peptide can be screened for its ability to bind to bacterial ribosomes via ribosome-peptide co-sedimentation assay.

The findings from the toxicity assays on PAM-5 as reported in this study may not provide a strong conclusion on its non-toxicity towards mammalian cells in general as only two cell lines (Vero and HeLa cell lines) and a human RBC were tested. In order to have a more thorough finding, additional cell types should be included for the toxicity screening. For instance, non-tumour epithelial cells MCF10A (ATCC® CRL-10317) and colonic fibroblast cells CCD18Co (ATCC® CRL-1459) are primary cells which can be considered for the toxicity screening for this peptide using the same colorimetric assay. Subsequently, the

peptide can be proceeded to preclinical studies on its toxicity and safety by *in vivo* testing in BALB/c mice or zebrafish embryos acute toxicity assay.

CHAPTER 6

CONCLUSION

With regards to the findings in this study, it can be concluded that the combination strategies of phage-display selection followed by rational modification of the selected peptide/s could be an ideal approach for developing antibacterial peptide/s (ABP/s) with good antibacterial potency and low toxicity. The former strategy may provide a simple and rapid high-throughput screening for peptides which bind selectively to ligand/s which is/are exclusively present on bacteria but not mammalian cells, thereby minimizing the probability of producing peptide/s that are harmful to the latter. The second strategy allows the modification of the selected phage-displayed peptides in order to render the peptides with improvised features of antibacterial characteristics. In this study, biopanning of phage-displayed peptide library against *P. aeruginosa* ATCC 27853 had initially selected phage-displayed peptides with high binding affinity towards the bacterium but lack of strong antibacterial potency. With the complementation of computational calculation and prediction, the parental peptide was modified through amino acid addition and substitution to enhance the peptide cationicity and hydrophobicity. These combinatorial strategies had successfully produced a novel ABP named PAM-5, in which it possesses a net positive charge of +7 and hydrophobicity of 46%.

With the improvised features of ABP, PAM-5 demonstrated bactericidal effect towards *P. aeruginosa* ATCC 27853 at the MBC of 8 µg/mL. Apart from that, this novel ABP also exhibited potent antibacterial effects towards a spectrum of Gram-negative bacteria and selected Gram-positive bacteria from ATCC reference strains as well as clinical isolated strains. In terms of reference strains, PAM-5 was strongly potent against *P. aeruginosa* ATCC 27853, *E. coli* ATCC 25922 and *A. baumannii* ATCC 19606 at the MBC of 8 µg/mL. For *Klebsiella pneumoniae* ATCC 138833 and *Streptococcus pyogenes* ATCC 19615, PAM-5 was moderately active against these bacteria with the MBC of 32 µg/mL and 64 µg/mL, respectively. However, it was less potent against *Staphylococcus aureus* ATCC 25923 as it was only able to kill the bacterium completely at the MBC of 128 µg/mL. Interestingly, apart from its potent effects towards the selected reference strains, PAM-5 was also active against a number of clinically isolated bacteria with different profiles of antibiotic resistance, which encompassed multidrug-resistant *P. aeruginosa*, ESBL-producing *E. coli* and *K. pneumoniae*, drug-resistant *S. flexneri* and *S.* Typhi, *A. junnii*, and *S. anginosus* at the MBCs that ranged from 4 µg/mL to 32 µg/mL. However, PAM-5 was not active against a clinical strain of *Serratia marcescens* and *Enterococcus faecalis* ATCC 19433. Conclusively, PAM-5 was more active against Gram-negative bacteria but only active against limited Gram-positive bacteria.

The stability of ABPs *in vivo* condition remains as one of the major concerns that render the peptides with potential clinical application. Using an *ex vivo* microbroth dilution assay, PAM-5 was found retaining its bactericidal effect against *P. aeruginosa* despite the presence of human plasma. This preliminary

finding suggested that PAM-5 is relatively stable in human blood or plasma, which indicate its potential systemic application against blood-borne infections.

A worthwhile finding on PAM-5 is the ability of the peptide to exert rapid killing kinetic towards its target bacteria. The complete elimination of *P. aeruginosa* and *E. coli* by PAM-5 can be achieved in 10 minutes after treating the bacteria with the peptide. More importantly, PAM-5 demonstrated faster killing kinetic than gentamicin and polymyxin B despite the better potency of the latter two against the two bacteria. Although both gentamicin and polymyxin B are able to eliminate the two bacteria at relatively lower MBCs than PAM-5, but they require longer duration than PAM-5 to kill the bacteria completely. In contrast to the slow killing kinetic of gentamicin and polymyxin B, in which their efficacies are commonly compromised by the fast-replicating and mutating bacteria, the rapid killing kinetic represents an advantage to PAM-5. This is because the peptide is able to kill the bacteria in a shorter duration before the doubling time of the bacteria, thereby depriving the bacteria of any opportunity to gain resistance via mutation. In other words, the rapid killing kinetic by PAM-5 might reduce the likelihood of inducible resistance which is a common strategy exploited by bacteria to resist those slow-acting antibiotics.

The rapid killing kinetic demonstrated by PAM-5 could be attributed to its novel antibacterial mechanisms which are distinct from the above-mentioned conventional antibiotics. PAM-5 is a membrane-active ABP which is able to cause outer membrane disruption and inner membrane permeabilization, as

revealed by scanning electron microscopy and SYTOX Green uptake assay in this study, respectively. Like many other cationic ABPs, the cationicity and hydrophobicity of PAM-5 might serve as important factors contributing to its initial electrostatic interaction with the anionic bacterial membrane. Subsequently, the peptide with its relatively shorter length (15 amino acids) might disrupt the bacterial membrane via the combination of 'carpet' and 'detergent-like' models, instead of toroidal or barrel-stave models which require longer peptide length. As demonstrated by SYTOX Green uptake assay, further increase in PAM-5 concentration may allow the peptide to permeabilize the bacterial inner membrane, follow by translocation of the peptide into the bacterial intracellular compartment. Once inside the bacteria, PAM-5 is able to bind to bacterial nucleic acids which encompass both chromosomal and plasmid DNA as shown by gel retardation assay. Therefore, these preliminary findings revealed that PAM-5 is a bactericidal ABP with more than one mechanism of action, which are tentatively determined as outer membrane disruption, inner membrane permeabilization and nucleic acid binding. Unlike gentamicin which only kill its target bacteria slowly by inhibiting protein synthesis, the multiple mechanisms of actions by PAM-5 may contribute to its rapid killing kinetic as described above.

A number of research groups have evaluated the antibacterial effects and properties of various naturally isolated or chemically synthesized ABPs. However, not every single of the peptides made it all the way to clinical application due to possible undesirable effects to mammalian cells. Encouragingly, while PAM-5 was found active against a spectrum of clinically

significant bacteria, preliminary findings from PrestoBlue cell viability assay revealed that this peptide presented insignificant toxicity to mammalian cells exemplified by Vero and HeLa cells in this study. Furthermore, the therapeutic value of PAM-5 is further enhanced by its non-haemolytic effect towards human RBCs, suggesting its potential clinical application against blood-borne infections. Most importantly, the range of peptide concentrations that produced non-cytotoxic and non-haemolytic effects to the mammalian cells encompassed the range of MBCs defined against majority of the tested bacteria in this study.

Conclusively, phage display selection accompanied by rational modification could be considered as a promising approach to yield ABP with potent antibacterial effect. The product of this combined strategies in this study, PAM-5, is a hypothetical antibacterial peptide that demonstrated bactericidal effects to a spectrum of pathogenic bacteria, including drug- and multidrug-resistant bacteria by multiple mechanisms of actions. Finally, as a result of selection by bacterial ligand via biopanning and rational adjustment of the selected peptide, PAM-5 possesses relatively high selectivity by acting exclusively against bacteria but shows no obvious toxicity to mammalian cells. Hence, PAM-5 can be proposed for further evaluation in terms of peptide stability enhancement, pre-clinical and clinical studies to justify its potential role as an alternative antibacterial agent in clinical setting.

REFERENCES/BIBLIOGRAPHY

Abi Khattar, Z. et al., 2009. The dlt operon of *Bacillus cereus* is required for resistance to cationic antimicrobial peptides and for virulence in insects. *Journal of Bacteriology*, 191, pp. 7063–7073.

Aisenbrey, C., Marquette, A. and Bechinger, B., 2019. The mechanisms of action of cationic antimicrobial peptides refined by novel concepts from biophysical investigations. *Advances in Experimental Medicine and Biology*, 1117, pp. 33–64.

Aminov, R.I., 2010. A brief history of the antibiotic era: lessons learned and challenges for the future. *Frontiers in Microbiology*, 1, p. 134.

Ammerman, N.C., Beier-Sexton, M., and Azad, A.F., 2008. Growth and maintenance of Vero cell lines. *Current Protocols in Microbiology*, Appendix 4, Appendix–4E.

Anderson, D.J. et al., 2006. Predictors of mortality in patients with bloodstream infection due to ceftazidime-resistant *Klebsiella pneumoniae*. *Antimicrobial Agents and Chemotherapy*, 50, pp. 1715–1720.

Arias, M., Hoffarth, E.R., Ishida, H., Aramini, J.M. and Vogel, H.J., 2016. Recombinant expression, antimicrobial activity and mechanism of action of tritrpticin analogs containing fluoro-tryptophan residues. *Biochimica et Biophysica Acta*, 1858(5), pp. 1012-1023.

Artun, T.F. et al., 2016. *In vitro* anticancer and cytotoxic activities of some plant extracts on HeLa and Vero cell lines. *Journal of the Balkan Union of Oncology (J. BUON)*, 21, pp. 720–725.

Aslam, B. et al., 2018. Antibiotic resistance: a rundown of a global crisis. *Infection and Drug Resistance*, 11, pp. 1645–1658.

Avci, F.G., Akbulut, B.S. and Ozkirimli, E., 2018. Membrane active peptides and their biophysical characterization. *Biomolecules*, 8(3), p. 77.

Ayaad, T.H., Shaker, G.H. and Almuhnaa, A.M., 2012. Isolation of antimicrobial peptides from *Apis florae* and *Apis carnica* in Saudi Arabia and investigation of the antimicrobial properties of natural honey samples. *Journal of King Saud University – Science*, 24(2), pp. 193–200.

Azad, M.A. et al., 2013. Polymyxin B induces apoptosis in kidney proximal tubular cells. *Antimicrobial Agents and Chemotherapy*, 57, pp. 4329–4335.

Bacalum, M. and Radu, M., 2015. Cationic antimicrobial peptides cytotoxicity on mammalian cells: An analysis using therapeutic index integrative concept. *International Journal of Peptide Research and Therapeutics*, 21, pp. 47–55.

Bagheri, M., Amininasab, M. and Dathe, M., 2018. Arginine/tryptophan-rich cyclic α/β‑antimicrobial peptides: the roles of hydrogen bonding and hydrophobic/hydrophilic solvent‑accessible surface areas upon activity and membrane selectivity. *Chemistry: A European Journal*, 24, p. 14242.

Bahar, A.A. and Ren, D., 2013. Antimicrobial peptides. *Pharmaceuticals (Basel, Switzerland)*, 6(12), pp. 1543–1575.

Baltz, R.H., 2009. Daptomycin: mechanisms of action and resistance, and biosynthetic engineering. *Current Opinion in Chemical Biology*, 13(2), pp. 144–151.

Bambeke, V.F., Balzi, E. and Tulkens, P.M., 2000. Antibiotic efflux pumps. *Biochemical Pharmacology*; 60, pp. 457–470.

Bansal, S. and Tandon, V., 2011. Contribution of mutations in DNA gyrase and topoisomerase IV genes to ciprofloxacin resistance in *Escherichia coli* clinical isolates. *International Journal of Antimicrobial Agents*, 37 (3), pp. 253-255.

Bao, Y. et al., 2012. Role of mprF1 and mprF2 in the pathogenicity of *Enterococcus faecalis*. *PLoS ONE*, 7, p. e38458.

Barbosa Pelegrini, P., Del Sarto, R.P., Silva, O.N., Franco, O.L. and Grossi-de-Sa, M.F., 2011. Antibacterial peptides from plants: what they are and how they probably work. *Biochemistry Research International*, 2011, p. 250349.

Basak, S., Singh, P. and Rajurkar, M., 2016. Multidrug resistant and extensively drug resistant bacteria: a study. *Journal of Pathogens*, 2016, p. 4065603.

Bassetti, M. and Righi, E., 2015. Development of novel antibacterial drugs to combat multiple resistant organisms. *Langenbeck's Archives of Surgery*, 400(2), pp. 153-165.

Bassetti, M., Vena, A., Croxatto, A., Righi, E. and Guery, B., 2018. How to manage *Pseudomonas aeruginosa* infections. *Drugs in Context*, 7, p. 212527.

Beatriz, E.F., Jakko van, I., Melanie, W., Dick van, S., Johan, W.M., 2015. Time–kill kinetics of antibiotics active against rapidly growing mycobacteria. *Journal of Antimicrobial Chemotherapy*, 70(3), pp.811–817.

Benjelloun‑Touimi, Z., Sansonetti, P.J. and Parsot, C., 1995. SepA, the major extracellular protein of *Shigella flexneri*: autonomous secretion and involvement in tissue invasion. *Molecular Microbiology*, 17, pp. 123-135.

Bennett, P.M., 2008. Plasmid encoded antibiotic resistance: acquisition and transfer of antibiotic resistance genes in bacteria. *British Journal of Pharmacology*, 153(1), pp. 347-357.

Berrazeg, M. et al., 2015. Mutations in β-lactamase AmpC increase resistance of *Pseudomonas aeruginosa* isolates to antipseudomonal cephalosporins. *Antimicrobial Agents and Chemotherapy*, 59, pp. 6248–6255.

Bharal, A. and Sohpal, V.K., 2013. Evaluation of antimicrobial activity of bacteriocin (*L. acidophilus*) against human pathogenic and food born microorganisms. *International Journal of Innovative Research in Science, Engineering and Technology*, 2(9), pp. 4221-4225.

Bhattacharjya, S. and Ramamoorthy, A., 2009. Multifunctional host defense peptides: functional and mechanistic insights from NMR structures of potent antimicrobial peptides. *FEBS Journal*, 276, pp. 6465–6473.

Bi, X. et al., 2014. Antimicrobial properties and interaction of two Trp-substituted cationic antimicrobial peptides with a lipid bilayer. *Journal of Antibiotics*, 67, pp. 361–368.

Bishop-Hurley, S.L., Schmidt, F.J., Erwin, A.L. and Smith, A.L., 2005. Peptides selected for binding to a virulent strain of *Haemophilus influenzae* by phage display are bactericidal. *Antimicrobial Agents and Chemotherapy*, 49, pp. 2972–2978.

Bishop-Hurley, S.L., Rea, P.J., McSweeney, C.S., 2010. Phage-displayed peptides selected for binding to *Campylobacter jejuni* are antimicrobial. *Protein Engineering Design and Selection,* 23(10), pp. 751-757.

Blair, J.M. and Piddock, L.J., 2009. Structure, function and inhibition of RND efflux pumps in Gram-negative bacteria: An update. *Current Opinion in Microbiology*, 12, pp. 512–519.

Blair, J.M., Richmond, G.E. and Piddock, L.J., 2014. Multidrug efflux pumps in Gram-negative bacteria and their role in antibiotic resistance. *Future Microbiology* 9(10), pp. 1165–1177.

Bobenchik, A.M., Hindler, J.A., Giltner, C.L., Saeki, S. and Humphries, R.M., 2014. Performance of Vitek 2 for antimicrobial susceptibility testing of *Staphylococcus* spp. and *Enterococcus* spp. *Journal of Clinical Microbiology*, 52(2), pp. 392-397.

Bommarius, B. et al., 2010. Cost-effective expression and purification of antimicrobial and host defense peptides in *Escherichia coli*. *Peptides*, 31(11), pp. 1957–1965.

Boncler, M., Różalski, M., Krajewska, U., Podsędek, A. and Watala, C., 2014. Comparison of PrestoBlue and MTT assays of cellular viability in the assessment of anti-proliferative effects of plant extracts on human endothelial cells. *Journal of Pharmacological and Toxicological Methods*, 69(1), pp. 9–16.

Boto, A., Pérez de la Lastra, J.M. and González, C.C., 2018. The road from host-defense peptides to a new generation of antimicrobial drugs. *Molecules* (Basel, Switzerland), 23(2), p. 311.

Boulanger, N., Bulet, P. and Lowenberger, C., 2006. Antimicrobial peptides in the interactions between insects and flagellate parasites. *Trends in Parasitology*, 22(6), pp. 262-268.

Braff, M.H., Jones, A., Skerett, S.J. and Rubens, C.E., 2007. *Staphylococcus aureus* exploits cathelicidin antimicrobial peptides produced during early pneumonia to promote staphylokinase-dependent fibrinolysis. *Journal of Infectious Disease,* 195 (9), pp. 1365 – 1372.

Brand, G.D. et al., 2019. Intragenic antimicrobial peptides (IAPs) from human proteins with potent antimicrobial and anti-inflammatory activity. *PLoS ONE*, 14(8), p. e0220656.

Braine, T., 2011. Race against time to develop new antibiotics. *Bulletin of the World Health Organization*, 89(2), pp. 88–89.

Breidenstein, E.B.M., de la Fuente-Nunez, C. and Hancock, R.E.W., 2011. *Pseudomonas aeruginosa*: All roads lead to resistance. *Trends in Microbiology*, 19(8), pp. 419-426.

Brogden, K.A., 2005. Antimicrobial peptides: pore formers or metabolic inhibitors in bacteria? *Nature Reviews Microbiology*, 3(3), pp. 238-250.

Brogden, K.A., Ackermann, M., Mccray, P.B. and Tack, B.F., 2003. Antimicrobial peptides in animals and their role in host defences. *International Journal of Antimicrobial Agents*, 22, pp. 465-478.

Brown, S., Santa Maria, J.P. and Walker, S., 2013. Wall teichoic acids of Gram-positive bacteria. *Annual Review of Microbiology*, 67, pp. 313-336.

Brötz, H., Bierbaum, G., Reynolds, P.E. and Sahl, H.G., 1997. The lantibiotic mersacidin inhibits peptidoglycan biosynthesis at the level of transglycosylation. *European Journal of Biochemistry*, 246, pp. 193–199.

Buchanan, J.T. et al., 2005. Streptococcus iniae phosphoglucomutase is a virulence factor and a target for vaccine development. *Infection and Immunity*, 73, pp. 6935–6944.

Butler, M.S. and Cooper, M.A., 2011. Antibiotics in the clinical pipeline in 2011. *The Journal of Antibiotics*, 64, pp. 413-425.

Cardoso, M.H. et al., 2020. Computer-aided design of antimicrobial peptides:

are we generating effective drug candidates? *Frontiers in Microbiology*, 10, 3097.

Carnazza, S., Gioffre, G., Felici, F. and Guglielmino, S., 2007. Recombinant phage probes for *Listeria monocytogenes. Journal of Physics: Condensed Matter*, 19, p. 395011.

Carryn, S. et al., 2003. Intracellular pharmacodynamics of antibiotics. *Infectious Disease Clinics of North America,* 17(3), pp. 615-634.

Carvalho Ade, O. and Gomes, V.M., 2011. Plant defensins and defensin-like peptides—Biological activities and biotechnological applications. *Current Pharmaceutical Design*, 17, pp. 4270–4293.

Castelletto, V. et al., 2018. Arginine-containing surfactant-like peptides: interaction with lipid membranes and antimicrobial activity. *Biomacromolecules*, 19(7), pp. 2782–2794.

Centers for Disease Control and Prevention, Office of Infectious Disease Antibiotic resistance threats in the United States, 2013. Available at: http://www.cdc.gov/drugresistance/threat-report-2013.

Chen, Y. et al., 2007. Role of peptide hydrophobicity in the mechanism of action of alpha-helical antimicrobial peptides. *Antimicrobial Agents and Chemotherapy*, 51(4), pp. 1398-1406.

Chen, L., He, S., Li, C. and Ryu, J., 2009. Sublethal Kanamycin induced cross resistance to functionally and structurally unrelated antibiotics. *Journal of Experimental Microbiology and Immunology*, 13, pp. 53-57.

Chen, H.L. et al., 2013. Identification of a novel antimicrobial peptide from human hepatitis B virus core protein arginine-rich domain (ARD). *PLoS Pathogens*, 9(6), p. 1003425.

Chen, X. et al., 2013. Human antimicrobial peptide LL-37 modulates proinflammatory responses induced by cytokine milieus and double-stranded RNA in human keratinocytes. *Biochemical and Biophysical Research Communications*, 433(4), pp. 532-537.

Chen, X. et al., 2018. Evaluation of the bioactivity of a mastoparan peptide from wasp venom and of its analogues designed through targeted engineering. *International Journal of Biological Sciences*, 14(6), pp. 599-607.

Chesnokova, L.S., Slepenkov, S.V. and Witt, S.N., 2004. The insect antimicrobial peptide, l-pyrrhocoricin, binds to and stimulates the ATPase activity of both wild-type and lidless DnaK. *FEBS Letters*, 565, pp. 65–69.

Chevalier, S. et al., 2017. Structure, function and regulation of *Pseudomonas aeruginosa* porins. *FEMS Microbiology Reviews*, 41, pp. 698–722.

Cho, J.H. and Kim, S.C., 2010. Non-membrane targets of antimicrobial peptides: novel therapeutic opportunities? In: Wang, G. (ed.). *Antimicrobial peptides: discovery, design and novel therapeutic strategies*. CABI Publishing, Wallingford, United Kingdom.

Choi, J.H. et al., 2015. Melittin, a honeybee venom-derived antimicrobial peptide, may target methicillin-resistant *Staphylococcus aureus*. *Molecular Medicine Reports*, 12(5), pp. 6483-6490.

Chopra, I. and Roberts, M., 2001. Tetracycline antibiotics: mode of action, applications, molecular biology, and epidemiology of bacterial resistance. *Microbiology and Molecular Biology Reviews*, 65(2), pp. 232-260.

Chopra, S. and Reader, J., 2015. tRNAs as antibiotic targets. *International Journal of Molecular Sciences*, 16, pp. 321–349.

Cirioni, O. et al., 2006. *In vitro* activities of tritrpticin alone and in combination with other antimicrobial agents against *Pseudomonas aeruginosa*. *Antimicrobial Agents and Chemotherapy*, 50(11), pp. 3923-3925.

Clifton, L.A. et al., 2014. Effect of divalent cation removal on the structure of Gram-negative bacterial outer membrane models. *Langmuir: The ACS Journal of Surfaces and Colloids*, 31(1), pp. 404-412.

CLSI. *Methods for Dilution Antimicrobial Susceptibility Tests for Bacteria That Grow Aerobically; Approved Standard—Ninth Edition.* CLSI document M07-A9. Wayne, PA: Clinical and Laboratory Standards Institute; 2012.

Cockerill, F., 2012. Performance standards for antimicrobial susceptibility testing: twenty-second informational supplement. Clinical and Laboratory Standards Institute. Wayne, PA: Clinical and Laboratory Standards Institute. 2012. ISBN 978-1562387853. OCLC 795927370

Conibear, A.C. et al., 2013. The cyclic cystine ladder in θ-defensins is important for structure and stability, but not antibacterial activity. *Journal of Biological Chemistry*, 288, pp. 10830-10840.

Conly, J. and Johnston, B., 2005. Where are all the new antibiotics? The new antibiotic paradox. *The Canadian Journal of Infectious Diseases & Medical Microbiology*, 16(3), pp. 159-60.

Coskun, U. and Simons, K., 2011. Cell membranes: the lipid perspective. *Structure*,19, pp. 1543–1548.

Cotter, P.D., Ross, R.P. and Hill, C., 2013. Bacteriocins - a viable alternative to antibiotics? *Nature Reviews Microbiology*, 11(2), pp. 95-105.

Cox, K.H. et al., 2009. Inactivation of DltA modulates virulence factor expression in *Streptococcus pyogenes*. *PLoS ONE*, 4, p. e5366.

Cox, E., Michalak, A., Pagentine, S., Seaton, P. and Pokorny, A., 2014. Lysylated phospholipids stabilize models of bacterial lipid bilayers and protect against antimicrobial peptides. *Biochimica et Biophysica Acta – Biomembranes*, 1838, pp. 2198–2204.

Creative Biolabs, 2007. Premade Phage Display Peptide Libraries [Online]. Available at: https://www.creative-biolabs.com/premade-phage-display-peptide-libraries.html [Accessed: 15 February 2020]

Christensen, D.J., Gottlin, E.B., Benson, R.E. and Hamilton, P.T., 2001. Phage display for target-based antibacterial drug discovery. *Drug Discovery Today*, 6 (14), pp. 721-727.

Chrom, C.L., Renn, L.M. and Caputo, G.A., 2019. Characterization and antimicrobial activity of amphiphilic peptide AP3 and derivative sequences. *Antibiotics* (Basel, Switzerland), 8(1), p. 20.

Cullen, P., 2018. Drug-resistant superbug a factor in seven deaths in Limerick. *The Irish Times*, Tue, Oct 9.

Currie, S.M. et al., 2016. Cathelicidins have direct antiviral activity against respiratory syncytial virus *in vitro* and protective function *in vivo* in mice and humans. *Journal of Immunology*, 196(6), pp. 2699-2710.

Dathe, M., Nikolenko, H., Meyer, J., Beyermann, M. and Bienert, M., 2001. Optimization of the antimicrobial activity of magainin peptides by modification of charge. *FEBS Letters*, 501, pp. 146–150.

Dautin N., 2010. Serine protease autotransporters of enterobacteriaceae (SPATEs): biogenesis and function. *Toxins*, 2(6), pp. 1179–1206.

Dawgul, M., Maciejewska, M., Jaskiewicz, M., Karafova, A. and Kamysz, W., 2014. Antimicrobial peptides as potential tool to fight bacterial biofilm. *Acta Poloniae Pharmaceutica*, 71(1), pp. 39-47.

de Barros, E. et al., 2019. Snake venom cathelicidins as natural antimicrobial peptides. *Frontiers in Pharmacology*, 10, p. 1415.

de Sousa-Pereira, et al., 2013. An evolutionary perspective of mammal salivary peptide families: Cystatins, histatins, statherin and PRPs. *Archives of Oral Biology*, 58, pp. 451–458.

Dean, S.N., Bishop, B.M. and van Hoek, M.L., 2011. Natural and synthetic cathelicidin peptides with anti-microbial and anti-biofilm activity against *Staphylococcus aureus*. *BMC Microbiology*, 11, pp. 114-125

Delcour, A.H., 2008. Outer membrane permeability and antibiotic resistance. *Biochimica et Biophysica Acta*, 1794(5), pp. 808-816.

Demirkhanyan, L.H. et al., 2012. Multifaceted mechanisms of HIV-1 entry inhibition by human α-defensin. *The Journal of Biological Chemistry*, 287(34), pp. 28821-28838.

Deshpande, L.M., Rhomberg, P.R., Sader, H.S. and Jones, R.N., 2006. Emergence of serine carbapenemases (KPC and SME) among clinical strains of Enterobacteriaceae isolated in the United States Medical Centers: Report from

the MYSTIC Program (1999-2005). *Diagnostic Microbiology and Infectious Disease*, 56, pp. 367–372.

Deslouches, B. et al., 2013. Rational design of engineered cationic antimicrobial peptides consisting exclusively of arginine and tryptophan, and their activity against multidrug-resistant pathogens. *Antimicrobial Agents and Chemotherapy*, 57(6), pp. 2511-2521.

Di Cera, E., 2009. Serine proteases. *IUBMB Life*, 61(5), pp. 510-515.

Diamond, G., Beckloff, N., Weinberg, A. and Kisich, K.O., 2009. The roles of antimicrobial peptides in innate host defense. *Current Pharmaceutical Design*, *15*(21), pp. 2377–2392.

Dias, S.A. et al., 2017. New potent membrane-targeting antibacterial peptides from viral capsid proteins. *Frontiers in Microbiology*, 8, p. 775.

Díaz-Roa, A. et al., 2019. Sarconesin II, a new antimicrobial peptide isolated from *Sarconesiopsis magellanica* excretions and secretions. *Molecules* (Basel, Switzerland), 24(11), p. 2077.

Dijkshoorn, L. et al., 2004. The synthetic N-terminal peptide of human lactoferrin, hLF (1–11), is highly effective against experimental infection caused by multidrug-resistant *Acinetobacter baumannii*. *Antimicrobial Agents and Chemotherapy*, 48, pp. 4919–4921.

Dolejska, M. and Papagiannitsis, C.C., 2018. Plasmid-mediated resistance is going wild. *Plasmid*, 99, pp. 99–111.

Domingue, G., Costerton, J.W. and Brown, M.R.W., 1996. Bacterial doubling time modulates the effects of opsonisation and available iron upon interactions between *Staphylococcus aureus* and human neutrophils. *FEMS Immunology and Medical Microbiology,* 16 (1996), pp. 223 - 228.

Dong, N. et al., 2018. Short symmetric-end antimicrobial peptides centered on β-turn amino acids unit improve selectivity and stability. *Frontiers in Microbiology*, 9, p. 2832.

Drlica, K., Malik, M., Kerns, R.J. and Zhao, X., 2008. Quinolone-mediated bacterial death. *Antimicrobial Agents and Chemotherapy*, 52, pp. 385–392.

Dufourc, E.J., 2008. Sterols and membrane dynamics. *Journal of Chemical Biology*, 1(1-4), pp. 63–77.

Dutta, P.R., Cappello, R., Navarro-García, F. and Nataro, J.P., 2002. Functional comparison of serine protease autotransporters of enterobacteriaceae. *Infection and Immunity*, 70(12), pp. 7105–7113.

Džidic, S., Šuškovic, J. and Kos, B., 2008. Antibiotic resistance mechanisms in bacteria: Biochemical and genetic aspects. *Food Technology and Biotechnology*, 46, pp. 11–21.

Eadon, M.T. et al., 2013. Cell cycle arrest in a model of colistin nephrotoxicity. *Physiological Genomics*, 45, pp. 877–888.

Ebenhan, T., Gheysens, O., Kruger, H.G., Zeevaart, J.R. and Sathekge, M.M., 2014. Antimicrobial peptides: their role as infection-selection tracers for molecular imaging. *BioMed Research International*, 2014, pp. 1 – 15.

Edgerton, M. et al., 2000. Salivary histatin 5 and human neutrophil defensin 1 kill *Candida albicans* via shared pathways. *Antimicrobial Agents and Chemotherapy*, 44(12), pp. 3310-3316.

Edwards, I.A. et al., 2016. Contribution of amphipathicity and hydrophobicity to the antimicrobial activity and cytotoxicity of β-hairpin peptides. *ACS Infectious Diseases*, 2(6), pp. 442–450.

El-Sayed, A., Futaki, S. and Harashima, H., 2009. Delivery of macromolecules using arginine-rich cell-penetrating peptides: ways to overcome endosomal entrapment. *Journal of the American Association of Pharmaceutical Scientists* (*The AAPS Journal*), 11(1), pp. 13–22.

El-Zowalaty, M.E. et al. (2015). *Pseudomonas aeruginosa*: arsenal of resistance mechanisms, decades of changing resistance profiles, and future antimicrobial therapies. *Future Microbiology*, 10, pp. 1683–1706.

Emter, R. and Natsch, A.A., 2015. Fast resazurin-based live viability assay is equivalent to the MTT-test in the KeratinoSens assay. *Toxicology in Vitro*: an International Journal Published in Association with Bibra, 9(4), pp. 688-693.

Epand, R.F., Savage, P.B. and Epand, R.M., 2007. Bacterial lipid composition and the antimicrobial efficacy of cationic steroid compounds (Ceragenins). *Biochimica et Biophysica Acta*, 1768(10), pp. 2500-2509.

Epand, R.M., Walker, C., Epand, R.F. and Magarvey, N.A., 2016. Molecular mechanisms of membrane targeting antibiotics. *Biochimica et Biophysica Acta*, 1858(5), pp. 980-987.

Egan, K. et al., 2016. Bacteriocins: novel solutions to age old spore-related problems? *Frontiers in Microbiology*, 7, p. 461.

Etchegaray, A. and Machini, M.T., 2013. Antimicrobial lipopeptides: *in vivo* and *in vitro* synthesis. In: Mendez-vilas A, editor. Microbial pathogens and strategies for combating them, science, technology and education. *Formatex: Extremadura*, pp. 951–959.

Fair, R.J. and Tor, Y., 2014. Antibiotics and bacterial resistance in the 21st century. *Perspectives in Medicinal Chemistry*, *6*, pp. 25–64.

Falagas, M.E. and Kasiakou, S.K., 2006. Toxicity of polymyxins: a systematic review of the evidence from old and recent studies. *Critical Care*, 10, p. R27.

Farkas, A., Maróti, G., Kereszt, A., and Kondorosi, É., 2017. Comparative analysis of the bacterial membrane disruption effect of two natural plant antimicrobial peptides. *Frontiers in Microbiology*, *8*, p. 51.

Fernandez, D.I. et al., 2012. The antimicrobial peptide aurein 1.2 disrupts model membranes via the carpet mechanism. *Physical Chemistry Chemical Physics*, 14, p.15739.

Fjell, C.D., Hiss, J.A., Hancock, R.E. and Schneider, G., 2012. Designing antimicrobial peptides: form follows function. *Nature Reviews Drug Discovery*, 11, pp. 37–51.

Flachbartova, Z. et al., 2016. Inhibition of multidrug resistant *Listeria monocytogenes* by peptides isolated from combinatorial phage display libraries. *Microbiological Research*, 188, pp. 34–41.

Florin, T. et al., 2017. An antimicrobial peptide that inhibits translation by trapping release factors on the ribosome. *Nature Structural and Molecular Biology*, 24(9), pp. 752–757.

Floss, H.G. and Yu, T.W., 2005. Rifamycin-mode of action, resistance, and biosynthesis. *Chemical Reviews*, 105, pp. 621–632.

Frick, I.M. et al., 2011. Constitutive and inflammation-dependent antimicrobial peptides produced by epithelium are differentially processed and inactivated by the commensal *Finegoldia magna* and the pathogen *Streptococcus pyogenes*. *Journal of Immunology*, 187, pp. 4300 – 4309.

Friedman, N.D., Temkin, E. and Carmeli, Y., 2016. The negative impact of antibiotic resistance. *Clinical Microbiology and Infection*, 22, pp. 416–422.

Friedrich, C.L., Rozek, A., Patrzykat, A. and Hancock, R.E.W., 2001. Structure and mechanism of action of an indolicidin peptide derivative with improved activity against gram-positive bacteria. *Journal of Biological Chemistry*, 276, pp. 24015–24022.

Furci, L. et al., 2015. New role for human α-defensin 5 in the fight against hypervirulent *Clostridium difficile* strains. *Infection and Immunity*, 83(3), pp. 986-995.

Gagnon, M.G. et al., 2016. Structures of proline-rich peptides bound to the ribosome reveal a common mechanism of protein synthesis inhibition. *Nucleic Acids Research*, 44(5), pp. 2439-2450.

Gagnon, M.C. et al., 2017. Influence of the length and charge on the activity of α-helical amphipathic antimicrobial peptides. *Biochemistry*, 56, pp. 1680–1695.

Galvan, E.M., Lasaro, M.A. and Schifferli, D.M., 2008. Capsular antigen fraction 1 and Pla modulate the susceptibility of *Yersinia pestis* to pulmonary antimicrobial peptides such as cathelicidin. *Infection and Immunity*, 76, pp. 1456–1464.

Ganz, T. et al., (1985) Defensins. Natural peptide antibiotics of human neutrophils. *Journal of Clinical Investigation*, 76, pp. 1427-1435.

Ganz, T. (2003) The role of antimicrobial peptides in innate immunity. *Integrative and Comparative Biology*, 43(2), pp. 300-304.

Gasanov, U., Koina, C., Beagley, K.W., Aitken, R.J. and Hansbro, P.M., 2006. Identification of the insulin-like growth factor II receptor as a novel receptor for binding and invasion by *Listeria monocytogenes*. *Infection and Immunity*, 74, pp. 566–577.

Gera, K. and Mclver, K.S., 2014. Laboratory growth and maintenance of *Streptococcus pyogenes* (The Group A Streptococcus, GAS). *Current Protocols in Microbiology*, 30, pp. 1 – 14.

Ghosh, A. et al., 2014. Indolicidin targets duplex DNA: structural and mechanistic insight through a combination of spectroscopy and microscopy. *ChemMedChem*, 9, pp. 2052–2058.

Ghosh, P., 2011. The nonideal coiled coil of M protein and its multifarious functions in pathogenesis. *Advances in Experimental Medicine and Biology*, 715, pp. 197–211.

Giangaspero, A., Sandri, L. and Tossi, A., 2001. Amphipathic helical antimicrobial peptides. *European Journal of Biochemistry*, 268, pp. 5589–5600.

Gibson, B., Wilson, D.J., Feil, E. and Eyre-Walker, A., 2018. The distribution of bacterial doubling times in the wild. *Proceedings. Biological Sciences*, 285(1880), p. 20180789.

Gifford, J.L. et al., 2005. Lactoferricin: a lactoferrin-derived peptide with antimicrobial, antiviral, antitumor and immunological properties. *Cellular and Molecular Life Sciences*, 62, pp. 2588–2598.

Giuliani, A., Pirri, G. and Nicoletto, S., 2007. Antimicrobial peptides: an overview of a promising class of therapeutics. *Central European Journal of Biology*, 2, pp. 1–33.

Giulio, A.D. and Zhao, H.X., 2006. Antimicrobial peptides: basic mechanisms of action and emerging pharmacological interest. *Asian Journal of Biochemistry*, 1(1), pp. 28 – 40.

Glukhov, E., Stark, M., Burrows, L.L. and Deber, C.M., 2005. Basis for selectivity of cationic antimicrobial peptides for bacterial versus mammalian membranes. *Journal of Biological Chemistry*, 280, pp. 33960–33967.

Glukhov, E., Burrows, L.L. and Deber, C.M., 2008. Membrane interactions of designed cationic antimicrobial peptides: the two thresholds, *Biopolymers*, 89, pp. 360–371

Gomarasca, M. et al., 2017. Bacterium-derived cell-penetrating peptides deliver gentamicin to kill intracellular pathogens. *Antimicrobial Agents and Chemotherapy*, 61(4), pp. e02545-16.

Goodwin, D., Simerska, P. and Toth, I., 2012. Peptides as therapeutics with enhanced bioactivity. *Current Medicinal Chemistry*, 19, pp. 4451–4461.

Gordon, Y.J., Romanowski, E.G. and McDermott, A.M., 2005. A review of antimicrobial peptides and their therapeutic potential as anti-infective drugs. *Current Eye Research*, 30(7), pp. 505–515.

Gould, I.M. and Bal, A.M., 2013. New antibiotic agents in the pipeline and how they can help overcome microbial resistance. *Virulence*, 4(2), pp. 185-191.

Graf, M. et al., 2017. Proline-rich antimicrobial peptides targeting protein synthesis. *Natural Product Reports*, 34(7), pp. 702-711.

Grigat, J., Soruri, A., Forssmann, U., Riggert, J. and Zwirner, J., 2007. Chemoattraction of macrophages, T lymphocytes, and mast cells is evolutionarily conserved within the human alpha-defensin family. *Journal of Immunology*, 179(6), pp. 3958-3965.

Groisman, E.A., Kayser, J. and Soncini, F.C., 1997. Regulation of polymyxin resistance and adaptation to low-Mg^{2+} environments. *Journal of Bacteriology*, 179, pp. 7040–7045.

Gross, M., 2013. Antibiotics in crisis. *Current Biology*, 23(24), pp. R1063–R1065.

Grundmann, H., Aires-de-Sousa, M., Boyce, J. and Tiemersma, E., 2006. Emergence and resurgence of meticillin-resistant *Staphylococcus aureus* as a public-health threat. *Lancet*, 368, pp. 874–885.

Guilhelmelli, F. et al., 2013. Antibiotic development challenges: the various mechanisms of action of antimicrobial peptides and of bacterial resistance. *Frontiers in Microbiology*, 4, pp. 353.

Gulland, A., 2018. Typhoid superbug spreads throughout Pakistan. *The Telegraph*; 18 April (https://www.telegraph.co.uk/news/0/typhoid-superbug-spreads-throughout-pakistan/)

Gupta, S. et al., 2015. *In vitro* antibiotic susceptibility of *Pseudomonas aeruginosa* corneal ulcer isolates. *Ocular Immunology and Inflammation*, 23(3), pp. 252-255.

Gupte, V. and Luthra, U., 2017. Analytical techniques for Serratiopeptidase: a review. *Journal of Pharmaceutical Analysis*, 7, pp. 203-207.

Hachmann, A.B., Angert, E.R. and Helmann, J.D., 2009. Genetic analysis of factors affecting susceptibility of *Bacillus subtilis* to daptomycin. *Antimicrobial Agents and Chemotherapy*, 53, pp. 1598–1609.

Hädicke, A. and Blume, A., 2017. Binding of cationic model peptides (KX)4K to anionic lipid bilayers: Lipid headgroup size influences secondary structure of bound peptides. *Biochimica et Biophysica Acta - Biomembranes*, 1859(3), pp. 415-424.

Hancock, R., 1997. Peptide antibiotics. *The Lancet,* 349(9049), pp.418-422.

Hancock, R.E. and Chapple, D.S., 1999. Peptide antibiotics. *Antimicrobial Agents and Chemotherapy*, 43(6), pp. 1317–1323.

Hancock, R.E., 2001. Cationic peptides: effectors in innate immunity and novel antimicrobials. *Lancet Infectious Diseases*, 1(3), pp. 156–164.

Hancock, R.E., Haney, E.F. and Gill, E.E., 2016. The immunology of host defence peptides: beyond antimicrobial activity. *Nature Review Immunology*, 16, pp. 321–334.

Haney, E.F. et al., 2009. Solution NMR studies of amphibian antimicrobial peptides: linking structure to function? *Biochimica et Biophysica Acta*, 1788, pp. 1639–1655.

Haney, E.F., Straus, S.K. and Hancock, R., 2019. Reassessing the host defense peptide landscape. *Frontiers in Chemistry*, 7, p. 43.

Hao, G., Shi, Y.H., Tang, Y.L. and Le, G.W., 2013. The intracellular mechanism of action on *Escherichia coli* of BF2-A/C, two analogues of the antimicrobial peptide Buforin 2. *Journal of Microbiology*, 51, pp. 200–206.

Harris, F., Dennison, S.R. and Phoenix, D.A., 2009. Anionic antimicrobial peptides from eukaryotic organisms. *Current Protein and Peptide Science*, 10(6), pp. 585-606.

Hartmann, M. et al., 2010. Damage of the bacterial cell envelope by antimicrobial peptides gramicidin S and PGLa as revealed by transmission and scanning electron microscopy. *Antimicrobial Agents and Chemotherapy*, 54(8), pp. 3132–3142.

Hasper, H.E. et al., 2006. An alternative bactericidal mechanism of action for lantibiotic peptides that target lipid II. *Science*, 313, pp. 1636–1637.

Hassan, M., Kjos, M., Nes, I.F., Diep, D.B. and Lotfipour, F., 2006. Antimicrobial peptides in the interactions between insects and flagellate parasites. *Trends in Parasitology*, 22(6), pp. 262-268.

Haukland, H., Ulvatne, H., Sandvik, K. and Vorland, L., 2001. The antimicrobial peptides lactoferricin B and magainin 2 cross over the bacterial cytoplasmic membrane and reside in the cytoplasm. *FEBS Letters*, 508, pp. 389–393.

Hazrati, E. et al., 2006. Human alpha- and beta-defensins block multiple steps in herpes simplex virus infection. *Journal of Immunology*, 177(12), pp. 8658-8666.

He, J., Krauson, A.J. and Wimley, W.C., 2014. Toward the *de novo* design of antimicrobial peptides: Lack of correlation between peptide permeabilization of lipid vesicles and antimicrobial, cytolytic, or cytotoxic activity in living cells. *Biopolymers*, 102(1), pp. 1-6.

Heddle, J.G. et al., 2001. The antibiotic microcin B17 is a DNA gyrase poison: characterisation of the mode of inhibition. *Journal of Molecular Biology*, 307, pp. 1223–1234.

Hell, E., Giske, C.G., Nelson, A., Römling, U. and Marchini, G., 2010. Human cathelicidin peptide LL-37 inhibits both attachment capability and biofilm formation of *Staphylococcus epidermidis*. *Letters in Applied Microbiology*, 50, pp. 211-215.

Hetian, L. et al., 2002. A novel peptide isolated from a phage display library inhibits tumor growth and metastasis by blocking the binding of vascular endothelial growth factor to its kinase domain receptor. *Journal of Biological Chemistry*, 277(45), pp. 43137–43142.

Higgins, P.G., Fluit, A.C. and Schmitz, F.J., 2003. Fluoroquinolones: Structure and target sites. *Current Drug Targets*, 4, pp. 181–190.

Hilchie, A.L. et al., 2011. Pleurocidin-family cationic antimicrobial peptides are cytolytic for breast carcinoma cells and prevent growth of tumor xenografts. *Breast Cancer Research*, 13, R102.

Hilchie, A.L., Wuerth, K. and Hancock, R.E.W., 2013. Immune modulation by multifaceted cationic host defense (antimicrobial) peptides. *Nature Chemical Biology*, 9(12), pp. 761–768.

Hirsch, E.B. et al., 2012. A model to predict mortality following *Pseudomonas aeruginosa* bacteremia. *Diagnostic Microbiology and Infectious Disease*, 72(1), pp. 97-102.

Ho, Y.H., Shah, P., Chen, Y.W. and Chen, C.S., 2016. Systematic analysis of intracellular-targeting antimicrobial peptides, bactenecin 7, hybrid of pleurocidin and dermaseptin, proline-arginine-rich peptide, and lactoferricin B, by using *Escherichia coli* proteome microarrays. *Molecular & Cellular Proteomics*, 15, pp. 1837–1847.

Hoess, R.H., 2001. Protein design and phage display. *Chemical Reviews*, 101, pp. 3205–3218.

Hollmann, A. et al., 2016. Role of amphipathicity and hydrophobicity in the balance between hemolysis and peptide–membrane interactions of three related antimicrobial peptides. *Colloids and Surfaces B: Biointerfaces*, 141, pp. 528–536.

Hollmann, A., Martinez, M., Maturana, P., Semorile, L.C. and Maffia, P.C., 2018. Antimicrobial peptides: Interaction with model and biological membranes and synergism with chemical antibiotics. *Frontiers in Chemistry*, 6, p. 204.

Housseini, B., Issa, K., Phan, G. and Broutin, I., 2018. Functional mechanism of the efflux pumps transcription regulators from *Pseudomonas aeruginosa* based on 3D structures. *Frontiers in Molecular Biosciences*, 5, p. 57.

Huang, Y., Huang, J. and Chen, Y., 2010. α-helical cationic antimicrobial peptides: relationships of structure and function. *Protein and Cell*, 1(2), pp. 143–152.

Ibrahim, E.H., Sherman, G., Ward, S., Fraser, V.J. and Kollef, M.H., 2000. The influence of inadequate antimicrobial treatment of bloodstream infections on patient outcomes in the ICU setting. *Chest*, 118, pp. 146–155.

Infectious Diseases Society of America, 2010. *Clinical Infectious Diseases*, 50, p. 1081.

Inui Kishi, R.N. et al., 2018. Evaluation of cytotoxicity features of antimicrobial peptides with potential to control bacterial diseases of citrus. *PLoS ONE*, 13(9), e0203451.

Jang, S.A. et al., 2012. Mechanism of action and specificity of antimicrobial peptides designed based on buforin IIb. *Peptides*, 34, pp. 283–289.

Jean-François, F., Elezgaray, J., Berson, P., Vacher, P. and Dufourc, E.J., 2008. Pore formation induced by an antimicrobial peptide: electrostatic effects. *Biophysical Journal*, 95(12), pp. 5748-5756.

Jenssen, H., Hamill, P. and Hancock, R.E., 2006. Peptide antimicrobial agents. *Clinical Microbiology Reviews*, 19, pp. 491–511.

Jeong, J.H., Kim, J.S., Choi, S.S. and Kim, Y., 2016. NMR structural studies of antimicrobial peptides: LPcin analogs. *Biophysical Journal*, 110(2), pp. 423-430.

Jiang, Z. et al., 2008. Effects of net charge and the number of positively charged residues on the biological activity of amphipathic alpha-helical cationic antimicrobial peptides. *Biopolymers*, 90(3), pp. 369-383.

Jiang, Z. et al., 2009. Effects of net charge and the number of positively charged residues on the biological activity of amphipathic alpha-helical cationic antimicrobial peptides. *Advances in Experimental Medicine and Biology*, 611, pp. 561-562.

Jin, T. et al., 2004. *Staphylococcus aureus* resists human defensins by production of staphylokinase, a novel bacterial evasion mechanism. *Journal of Immunology*, 172, pp. 1169–1176.

Jindal, H.M. et al., 2015. Antimicrobial activity of novel synthetic peptides derived from Indolicidin and Ranalexin against *Streptococcus pneumoniae*. *PloS ONE*, 10(6), p. e0128532.

Jing, W., Demcoe, A.R. and Vogel, H.J., 2003. Conformation of a bactericidal domain of puroindoline a: structure and mechanism of action of a 13-residue antimicrobial peptide. *Journal of Bacteriology*, 185(16), pp. 4938–4947.

Johnson, P.J.T. and Levin, B.R., 2013. Pharmacodynamics, population dynamics, and the evolution of persistence in *Staphylococcus aureus*. *PLoS Genetics*, 9(1), e1003123.

Jorth, P. et al., 2017. Evolved aztreonam resistance is multifactorial and can produce hypervirulence in *Pseudomonas aeruginosa*. *mBio*, 8(5), pp. e00517-17.

Joyanes, P., del Carmen Conejo, M., Martínez-Martínez, L. and Perea, E.J., 2001. Evaluation of the VITEK 2 system for the identification and susceptibility testing of three species of non-fermenting Gram-negative rods frequently

isolated from clinical samples. *Journal of Clinical Microbiology*, 39(9), pp. 3247-3253.

Kacprzyk, L. et al., 2007. Antimicrobial activity of histidine-rich peptides is dependent on acidic conditions. *Biochimica et Biophysica Acta*, 1768(11), pp. 2667-2680.

Kahne, D., Leimkuhler, C., Lu, W. and Walsh, C., 2005. Glycopeptide and lipoglycopeptide antibiotics. *Chemical Reviews*, 105(2), pp. 425-448.

Kanamori, S., Kusano, N., Shinzato, T. and Saito, A., 2004. The role of capsule of the *Streptococcus milleri* group in its pathogenicity. *Journal of Infections and Chemotherapy,* 2004 (10), pp. 105 – 109.

Katz, L. and Ashley, G.W., 2005. Translation and protein synthesis: macrolides. *Chemical Reviews*, 105, pp. 499–528.

Kelesidis, T. and Falagas, M.E., 2015. The safety of polymyxin antibiotics. *Expert Opinion on Drug Safety*, 14, pp. 1687–1701.

Kelly, A.M., Mathema, B. and Larson, E.L., 2017. Carbapenem-resistant *Enterobacteriaceae* in the community: a scoping review. *International Journal of Antimicrobial Agents*, 50(2), pp. 127-134.

Keogh, B., 2018. CRO outbreak at Middlemore Hospital burns unit sparks review of Ministry of Health's emergency management plan. *New Zealand Herald*, 15 Apr.

Khan, F., 2018. Antibiotics classification and visual target sites for bacterial inhibition. *Advances in Pharmacology and Clinical Trials*, 3(3), p. 000137.

Kim, Y.J. et al., 2014. Risk factors for mortality in patients with *Pseudomonas aeruginosa* bacteremia; retrospective study of impact of combination antimicrobial therapy. *BMC Infectious Diseases*, 14, p. 161.

Kimura, M. et al., 2014. Salusin-β, an antimicrobially active peptide against Gram-positive bacteria. *Chemical and Pharmaceutical Bulletin*, 62(6), pp.586-590.

Klein, S. et al., 2009. Adaptation of *Pseudomonas aeruginosa* to various conditions includes tRNA-dependent formation of alanyl-phosphatidylglycerol *Molecular Microbiology*, 71, pp. 551-565.

Kmietowicz, Z., 2018. One in five GP prescriptions for antibiotics is inappropriate. *The British Medical Journal*, 360, p. k936.

Koehbach, J., 2017. Structure–activity relationships of insect defensins. *Frontiers in Chemistry*, 5, p. 45.

Kohanski, M.A., Dwyer, D.J. and Collins, J.J., 2010. How antibiotics kill bacteria: from targets to networks. *Nature Reviews Microbiology*, 8(6), pp. 423–435.

Koo, H.B. and Seo, J., 2019. Review: Antimicrobial peptides under clinical investigation. *Peptide Science*; 111(5), e24122.

Kragol, G. et al., 2001. The antibacterial peptide pyrrhocoricin inhibits the ATPase actions of DnaK and prevents chaperone-assisted protein folding. *Biochemistry*, 40, pp. 3016–3026.

Krause, K.M., Serio, A.W., Kane, T.R. and Connolly, L.E., 2016. Aminoglycosides: An Overview. *Cold Spring Harbor Perspectives in Medicine*, 6(6), a027029.

Kristian, S.A., Durr, M., van Strijp, J.A., Neumeister, B. and Peschel, A., 2003. MprF-mediated lysinylation of phospholipids in *Staphylococcus aureus* leads to protection against oxygen-independent neutrophil killing. *Infection and Immunity*, 71, pp. 546–549.

Kumar, P., Kizhakkedathu, J.N. and Straus, S.K., 2018. Antimicrobial peptides: diversity, mechanism of action and strategies to improve the activity and biocompatibility *in vivo*. *Biomolecules*, 8(1), p. 4.

Lam, K.L.H. et al., 2012. Mechanism of structural transformations induced by antimicrobial peptides in lipid membranes. *Biochimica et Biophysica Acta – Biomembranes*, 1818, pp. 194–204.

Lambert, P.A. 2002. Mechanisms of antibiotic resistance in *Pseudomonas aeruginosa*. *Journal of the Royal Society of Medicine*, 95(Suppl 41), pp. 22–26.

Larimer, B.M., Quinn, J.M., Kramer, K., Komissarov, A. and Deutscher, S.L., 2015. Multiple bacteriophage selection strategies for improved affinity of a peptide targeting ERBB2. *International Journal of Peptide Research and Therapeutics*, 21(4), pp. 383–392.

LaRock, C.N. and Nizet, V., 2015. Cationic antimicrobial peptide resistance mechanisms of streptococcal pathogens. *Biochimica et Biophysica Acta*, 1848(11 Pt B), 3047–3054.

Lauth, X. et al., 2009. M1 protein allows group A streptococcal survival in phagocyte extracellular traps through cathelicidin inhibition. *Journal of Innate Immunity*, 1, pp. 202–214.

Laverty, G. and Gilmore, B., 2014. Cationic antimicrobial peptide cytotoxicity. *SOJ Microbiology & Infectious Diseases,* 2(1), pp. 1-8.

Le, C.F. et al., 2015. *In vivo* efficacy and molecular docking of designed peptide that exhibits potent antipneumococcal activity and synergises in combination with penicillin. *Scientific Reports*, 5, pp. 11886.

Le, C.F., Fang, C.M. and Sekaran, S.D., 2017. Intracellular targeting mechanisms by antimicrobial peptides. *Antimicrobial Agents and Chemotherapy*, 61(4), pp. e02340-16.

Le-Jeune, A. et al., 2010. The extracytoplasmic function sigma factor SigV plays a key role in the original model of lysozyme resistance and virulence of *Enterococcus faecalis*. *PLoS ONE*, 5, p. e9658.

Lee, I.H., Cho, Y., and Lehrer, R.I., 1997. Effects of pH and salinity on the antimicrobial properties of clavanins. *Infection and Immunity*, 65(7), pp. 2898–2903.

Lee, C.R., Cho, I.H., Jeong, B.C. and Lee, S.H., 2013. Strategies to minimize antibiotic resistance. *International Journal of Environmental Research and Public Health*, 10(9), pp. 4274–4305.

Lee, T.H., Hall, K.N. and Aguilar, M.I., 2016. Antimicrobial peptide structure and mechanism of action: A focus on the role of membrane structure. *Current Topics in Medicinal Chemistry*, 16(1), pp. 25-39.

Leekha, S., Terrell, C.L. and Edson, R.S., 2011. General principles of antimicrobial therapy. *Mayo Clinic Proceedings*, 86(2), pp. 156–167.

Lehrer, R.I. et al., 1989. Interaction of human defensins with *Escherichia coli*. Mechanism of bactericidal activity. *The Journal of Clinical Investigation*, 84(2), pp. 553-561.

Lei, J. et al., 2019. The antimicrobial peptides and their potential clinical applications. *American Journal of Translational Research*, 11(7), pp. 3919–3931.

Li, C., Haug, T., Styrvold, O.B., Jorgensen, T.O. and Stensvag, K., 2008. Strongylocins, novel antimicrobial peptides from the green sea urchin, *Strongylocentrotus droebachiensis*. *Developmental & Comparative Immunology*, 32, pp. 1430–1440.

Li, M., Yu, D.H. and Cai, H., 2008. The synthetic antimicrobial peptide KLKL5KLK enhances the protection and efficacy of the combined DNA vaccine against *Mycobacterium tuberculosis*. *DNA and Cell Biology*, 27(8), pp. 405-413.

Li, J. et al., 2017. Membrane active antimicrobial peptides: Translating mechanistic insights to design. *Frontiers in Neuroscience*, 11, p. 73.

Lincopan, N., Mamizuka, E.M. and Carmona-Ribeiro, A.M., 2005. Low nephrotoxicity of an effective amphotericin B formulation with cationic bilayer fragments. *Journal of Antimicrobial Chemotherapy*, 55, pp. 727–734.

Liu, S. et al., 2012. Novel antibacterial polypeptide laparaxin produced by *Lactobacillus paracasei* strain NRRL B-50314 via fermentation. *Journal of Petroleum and Environmental Biotechnology*, 3, p. 3.

Liu, H. et al., 2015. Identification of a novel antimicrobial peptide from amphioxus *Branchiostoma japonicum* by *in silico* and functional analyses. *Scientific Reports*, 5, p. 18355.

Liu, W.P., Chen, Y.H., Ming, X. and Kong, Y., 2015. Design and synthesis of a novel cationic peptide with potent and broad-spectrum antimicrobial activity. *BioMed Research International*, 2015, p. 578764.

Llobet, E., Tomas, J.M. and Bengoechea, J.A., 2008. Capsule polysaccharide is a bacterial decoy for antimicrobial peptides. *Microbiology*, 154, pp. 3877–3886.

Lomakin, I.B., Gagnon, M.G. and Steitz, T.A., 2015. Antimicrobial peptides targeting bacterial ribosome. *Oncotarget*, 6(22), pp. 18744-18745.

Lopatkin, A.J. et al., 2017. Persistence and reversal of plasmid-mediated antibiotic resistance. *Nature Communications*, 8, p. 1689.

Lowy, F.D., 2003. Antimicrobial resistance: the example of *Staphylococcus aureus*. *The Journal of Clinical Investigation*, 111(9), pp. 1265–1273.

Lu, L., Zhang, L., Wai, M.S., Yew, D.T. and Xu, J., 2012. Exocytosis of MTT formazan could exacerbate cell injury. *Toxicology in Vitro*, 26(4), pp. 636–44.

Lushniak, B.D., 2014. Antibiotic resistance: a public health crisis. *Public Health Reports*, 129(4), pp. 314–316.

Luyt, C.E., Brechot, N., Trouillet, J.L. and Chastre, J., 2014. Antibiotic stewardship in the intensive care unit. *Journal of Critical Care*, 18(5), p. 480.

Lyu, Y., Yang, Y., Lyu, X., Dong, N. and Shan, A., 2016. Antimicrobial activity, improved cell selectivity and mode of action of short PMAP-36-derived peptides against bacteria and Candida. *Scientific Reports*, 6, p. 27258.

Ma, Q. et al., 2014. Structure-function relationship of Val/Arg-rich peptides: Effects of net charge and pro on activity. *Chemical Biology & Drug Design*, 84(3), pp. 348–353.

Macfarlane, E.L., Kwasnicka, A., Ochs, M.M. and Hancock, R.E., 1999. PhoP-PhoQ homologue in *Pseudomonas aeruginosa* regulate expression of the outer-membrane protein OprH and polymyxin B resistance. *Molecular Microbiology*, 34, pp. 305–316.

Marchand, C. et al., 2006. Covalent binding of the natural antimicrobial peptide indolicidin to DNA abasic sites. *Nucleic Acids Research*, 34, pp. 5157–5165.

Macfarlane, E.L., Kwasnicka, A. and Hancock, R.E., 2000. Role of *Pseudomonas aeruginosa* PhoP-phoQ in resistance to antimicrobial cationic peptides and aminoglycosides. *Microbiology*, 146, pp. 2543–2554.

Madani, F., Lindberg, S., Langel, U., Futaki, S. and Graslund, A., 2011. Mechanisms of cellular uptake of cell-penetrating peptides. *Biophysical Journal*, 2011, p. 414729.

Magiorakos, A.P. et al., 2012. Multidrug-resistant, extensively drug-resistant and pandrug-resistant bacteria: an international expert proposal for interim standard definitions for acquired resistance. *Clinical Microbiology and Infection*, 18(3), pp. 268-281.

Mahlapuu, M., Håkansson, J., Ringstad, L. and Björn, C., 2016. Antimicrobial peptides: An emerging category of therapeutic agents. *Frontiers in Cellular and Infection Microbiology*, 6, p. 194.

Mahmoud, H.A., Melake, N.A. and El-Semary, M.T., 2012. Bactericidal activity of various antibiotics versus tetracycline-loaded chitosan microspheres against *Pseudomonas aeruginosa* biofilms. *Pharmaceutica Analytica Acta*, p. S15.

Maisetta, G. et al., 2016. Anti-biofilm properties of the antimicrobial peptide temporin 1Tb and its ability, in combination with EDTA, to eradicate *Staphylococcus epidermidis* biofilms on silicone catheters. *Biofouling*, 32(7), pp. 787-800.

Makinen, P.L. and Makinen, K.K., 1994. The *Enterococcus faecalis* extracellular metalloendopeptidase (EC 3.4.24.30; coccolysin) inactivates human endothelin at bonds involving hydrophobic amino acids residues. *Biochemical and Biophysical Research Communications,* 200 (2), pp. 981 – 985.

Malanovic, N. and Lohner, K., 2016. Antimicrobial peptides targeting Gram-positive bacteria. *Pharmaceuticals* (Basel, Switzerland), 9(3), p. 59.

Malmsten, M., 2016. Interactions of antimicrobial peptides with bacterial membranes and membrane components. *Current Topics in Medicinal*

Chemistry, 16, pp. 16–24.

Manna, M. and Mukhopadhyay, C., 2009. Cause and effect of melittin-induced pore formation: a computational approach. *Langmuir*, 25, pp. 12235–12242.

Marchand, C. et al., 2006. Covalent binding of the natural antimicrobial peptide indolicidin to DNA abasic sites. *Nucleic Acids Research*, 34, pp. 5157–5165.

Mardirossian, M. et al., 2014. The host antimicrobial peptide Bac71–35 binds to bacterial ribosomal proteins and inhibits protein synthesis. *Chemistry and Biology*, 21, pp. 1639–1647.

Mardirossian, M. et al., 2018. The Dolphin proline-rich antimicrobial peptide Tur1A inhibits protein synthesis by targeting the bacterial ribosome. *Cell Chemical Biology*, 25, pp. 530.e7–539.e7.

Marshall, S.H. and Arenas, G., 2003. Antimicrobial peptides: A natural alternative to chemical antibiotics and a potential for applied biotechnology. *Electronic Journal of Biotechnology*, 6, pp. 271-284.

Martin, A., Fahrbach, K., Zhao, Q. and Lodise, T., 2018. Association between carbapenem resistance and mortality among adult, hospitalized patients with serious infections due to enterobacteriaceae: results of a systematic literature review and meta-analysis. *Open Forum Infectious Diseases*, 5(7), ofy150.

Martinez, J.L. and Baquero, F., 2000. Mutation frequencies and antibiotic resistance. *Antimicrobial Agents and Chemotherapy*, 44(7), pp. 1771-1777.

Martinez, J.L. et al., 2009. Functional role of bacterial multidrug efflux pumps in microbial natural ecosystems. *FEMS Microbiology Reviews*, 33, pp. 430–449.

Matsuzaki, K., 2009. Control of cell selectivity of antimicrobial peptides. *Biochimica et Biophysica Acta*, 1788, pp. 1687–1692.

McCormick, M.H., McGuire, J.M., Pittenger, G.E., Pittenger, R.C. and Stark, W.M., 1955. Vancomycin, a new antibiotic. I. Chemical and biologic properties. *Antibiotics Annual*, 3, pp. 606-611.

Meincken, M., Holroyd, D.L. and Rautenbach, M., 2005. Atomic force microscopy study of the effect of antimicrobial peptides on the cell envelope of *Escherichia coli*. *Antimicrobial Agents and Chemotherapy*, 49, pp. 4085–4092.

Melo, M.N., Ferro, R. and Castanho, M.A.R.B., 2009. Antimicrobial peptides: linking partition, activity and high membrane-bound concentrations. *Nature Reviews Microbiology*, 7, pp. 245–250.

Méndez-Samperio, P., 2013. Recent advances in the field of antimicrobial peptides in inflammatory diseases. *Advanced Biomedical Research*, 2, p. 50.

Mihajlovic, M. and Lazaridis, T., 2012. Charge distribution and imperfect amphipathicity affect pore formation by antimicrobial peptides. *Biochimica et Biophysica Acta (BBA) - Biomembranes*, 1818, pp. 1274–1283.

Miles, K. et al., 2009. Dying and necrotic neutrophils are anti-inflammatory secondary to the release of alpha-defensins. *Journal of Immunology*, 183, pp. 2122–2132.

Ming, L.J. and Epperson, J.D., 2002. Metal binding and structure-activity relationship of the metalloantibiotic peptide bacitracin. *Journal of Inorganic Biochemistry*, 91(1), pp. 46–58.

Mingeot-Leclercq, M.P., Glupczynski, Y. and Tulkens, P.M., 1999. Aminoglycosides: activity and resistance. *Antimicrobial Agents and Chemotherapy*, 43(4), pp. 727-737.

Mirski, T., Niemcewicz, M., Bartoszcze, M., Gryko, R. and Michalski, A., 2017. Utilisation of peptides against microbial infections - a review. *Annals of Agricultural and Environmental Medicine*, 25, pp. 205–210.

Mishra, A.K., Choi, J., Moon, E. and Baek, K.H., 2018. Tryptophan-rich and proline-rich antimicrobial peptides. *Molecules*, 23(4), p. 815.

Mitchell, J., 2011. *Streptococcus mitis*: walking the line between commensalism and pathogenesis. *Molecular Oral Microbiology*, 26, pp. 89-98.

Miyata, T. et al., 1989. Antimicrobial peptides, isolated from horseshoe crab hemocytes, tachyplesin II, and polyphemusins I and II: chemical structures and biological activity. *Journal of Biochemistry*, 106, pp. 663–668.

Mohamed, M.F., Abdelkhalek, A. and Seleem, M.N., 2016. Evaluation of short synthetic antimicrobial peptides for treatment of drug-resistant and intracellular *Staphylococcus aureus*. *Scientific Reports*, 6, p. 29707.

Mortimer, P.G. and Piddock, L.J., 1993. The accumulation of five antibacterial agents in porin-deficient mutants of *Escherichia coli*. *Journal of Antimicrobial Chemotherapy*, 32, pp. 195–213.

Mp, N. and Bv, N., 2019. Inducible Amp C beta-lactamase producing *Pseudomonas aeruginosa*: Predominant resistance mechanism and a threat in a tertiary care teaching hospital. *The Journal of the Association of Physicians of India*, 67(4), pp. 63-66.

Mukhtar, T.A. and Wright, G.D., 2005. Streptogramins, oxazolidinones, and other inhibitors of bacterial protein synthesis. *Chemical Reviews*, 105, pp. 529–542.

Münch, D. and Sahl, H.G., 2015. Structural variations of the cell wall precursor lipid II in Gram-positive bacteria - Impact on binding and efficacy of antimicrobial peptides. *Biochimica et Biophysica Acta*,1848(11 Pt B), pp. 3062-3071.

Munita, J.M. and Arias, C.A., 2016. Mechanisms of antibiotic resistance. *Microbiology Spectrum*, 4(2), 10.1128/microbiolspec.VMBF-0016-2015.

Muthuirulan, P., Paramasamy, G. and Jeyaprakash, R., 2013. Antimicrobial peptides: versatile biological properties. *International Journal of Peptides*, p. 675391.

Nagaoka, I., Tamura, H. and Hirata, M. (2006) An antimicrobial cathelicidin peptide, human CAP18/LL-37, suppresses neutrophil apoptosis via the activation of formyl-peptide receptor-like 1 and P2X7. *Journal of Immunology*, 176(5), pp. 3044-3052.

Nagaoka, I. et al., 2010. Evaluation of the effect of α-defensin human neutrophil peptides on neutrophil apoptosis. *International Journal of Molecular Medicine*, 26(6), pp. 925-934.

Nagaoka, I., Suzuki, K., Niyonsaba, F., Tamura, H., and Hirata, M., 2012. Modulation of neutrophil apoptosis by antimicrobial peptides. *International Scholarly Research Notices: Microbiology*, 2012, p. 345791.

Narayana, J.L. and Chen, J., 2015. Antimicrobial peptides: Possible anti-infective agents. *Peptides*, 72, pp. 88-94.

Nawrot, R. et al., 2014. Plant antimicrobial peptides. *Folia Microbiologica*, 59(3), pp. 181–196.

Negrette-Guzmán, M. et al., 2013. Sulforaphane attenuates gentamicin-induced nephrotoxicity: role of mitochondrial protection. *Evidence-based Complementary and Alternative Medicine: eCAM*.

Neuhaus, F.C. and Baddiley, J., 2003. A continuum of anionic charge: Structures and functions of D-alanyl-teichoic acids in Gram-positive bacteria. *Microbiology and Molecular Biology Reviews*, 67, pp. 686–723.

Nesuta, O. et al., 2017. How proteases from *Enterococcus faecalis* contribute to its resistance to short α-helical antimicrobial peptides. *Pathogen and Disease,* 75 (7), pp. 1 – 12.

New England Biolabs, 2020. Applications of the Ph.D. Phage Display Peptide Libraries [Online]. Available at: https://international.neb.com/tools-and-resources/feature-articles/applications-of-the-phd-phage-display-peptide libraries [Accessed: 15 February 2020].

Nguyen, L.T. et al., 2010. Serum stabilities of short tryptophan- and arginine-rich antimicrobial peptide analogs. *PLoS ONE*, 5(9), e12684.

Nguyen, L.T., Haney, E.F. and Vogel, H.J., 2011. The expanding scope of antimicrobial peptide structures and their modes of action. *Trends in Biotechnology*, 29, pp. 464–472.

Nikaido, H. 2009. Multidrug resistance in bacteria. *Annual Review of Biochemistry*, 78, pp. 119–146.

Nikaido, H. and Takatsuka, Y., 2009. Mechanisms of RND multidrug efflux pumps. *Biochimica et Biophysica Acta*, 1794, pp. 769–781.

Nikaido, H. and Page`s, J.M., 2012. Broad-specificity efflux pumps and their role in multidrug resistance of Gram-negative bacteria, *FEMS Microbiology Reviews*, 36(2), pp. 340–363.

Nijnik, A. and Hancock, R.E., 2009. The roles of cathelicidin LL-37 in immune defences and novel clinical applications. *Current Opinion on Haematology*, 16, pp. 41–47.

Niyonsaba, F. and Ogawa, H., 2005. Protective roles of the skin against infection: Implication of naturally occurring human antimicrobial agents beta-defensins, cathelicidin LL-37 and lysozyme. *Journal of Dermatological Science*, 40, pp. 157–168.

Niyonsaba, F., Nagaoka, I., Ogawa, H. and Okumura, K., 2009. Multifunctional antimicrobial proteins and peptides: natural activators of immune systems. *Current Pharmaceutical Design*, 15(21), pp. 2393-2413.

Niyonsaba, F. et al., 2010. Antimicrobial peptides human beta-defensins and cathelicidin LL-37 induce the secretion of a pruritogenic cytokine IL-31 by human mast cells. *Journal of Immunology*, 184(7), pp. 3526-3534.

Nordmann, P., Dortet, L. and Poirel, L., 2012. Carbapenem resistance in Enterobacteriaceae: here is the storm! *Trends in Molecular Medicine*, 18, pp. 263–272.

O'Brien-Simpson, N.M., Pantarat, N., Attard, T.J., Walsh, K.A. and Reynolds, E.C., 2016. A rapid and quantitative flow cytometry method for the analysis of membrane disruptive antimicrobial activity. *PLoS ONE*, 11(3), p. e0151694.

Oizumi, et al., 2001. Relationship between mutations in the DNA gyrase and topoisomerase IV genes and nadifloxacin resistance in clinically isolated quinolone-resistant *Staphylococcus aureus*. *Journal of Infection and Chemotherapy*, 7(3), pp. 191-194.

Olson, M.W. et al., 2006. Functional, biophysical, and structural bases for antibacterial activity of Tigecycline. *Antimicrobial Agents and Chemotherapy*, 50, pp. 2156–2166.

Omardien, S. et al., 2018. Synthetic antimicrobial peptides delocalize membrane bound proteins thereby inducing a cell envelope stress response. *Biochimica et Biophysica Acta – Biomembranes*, 1860, pp. 2416–2427.

Oppedijk, S.F., Martin, N.I. and Breukink, E., 2016. Hit 'em where it hurts: The growing and structurally diverse family of peptides that target lipid-II. *Biochimica et Biophysica Acta*, 1858(5), pp. 947-957.

Osaki, Y. et al., 2005. Genetic approach to study the relationship between penicillin-binding protein 3 mutations and *Haemophilus influenzae* β-lactam resistance by using site-directed mutagenesis and gene recombinants. *Antimicrobial Agents and Chemotherapy*, 49(7), pp. 2834-2839.

Overhage, J. et al., 2008. Human host defense peptide LL-37 prevents bacterial biofilm formation. *Infection and Immunity*, 76, pp. 4176-4182.

Özgenç, O., 2016. Methodology in improving antibiotic implementation policies. *World Journal of Methodology*, 6(2), pp. 143-153.

Pachón-Ibáñez, M.E., Smani, Y., Pachón, J. and Sánchez-Céspedes, J., 2017. Perspectives for clinical use of engineered human host defense antimicrobial peptides. *FEMS Microbiology Reviews*, 41(3), pp. 323-342.

Pachori, P., Gothalwal, R. and Gandhi, P., 2019. Emergence of antibiotic resistance *Pseudomonas aeruginosa* in intensive care unit; a critical review. *Genes and Diseases*, 6(2), pp. 109–119.

Pag, U. et al., 2008. Analysis of *in vitro* activities and modes of action of synthetic antimicrobial peptides derived from an α-helical 'sequence template'. *Journal of Antimicrobial Chemotherapy*, 61, pp. 341–352.

Paiva, A.D. et al., 2012. Toxicity of bovicin HC5 against mammalian cell lines and the role of cholesterol in bacteriocin activity. *Microbiology*, 158, pp. 2851–2858.

Papanastasiou, et al. 2009. Role of acetylation and charge in antimicrobial peptides based on human β-defensin-3. *Acta Pathologica, Microbiologica, et Immunologica Scandinavica* (*APMIS*), 117, pp. 492–499.

Papo, N. and Shai, Y., 2002. Exploring peptide membrane interaction using surface plasmon resonance: differentiation between pore formation versus membrane disruption by lytic peptides. *Biochemistry*, 42, pp. 458–466.

Papp-Wallace, K.M., Endimiani, A., Taracila, M.A. and Bonomo, R.A., 2011. Carbapenems: past, present, and future. *Antimicrobial Agents and Chemotherapy*, 55(11), pp. 4943–4960.

Parachin, N.S. and Franco, O.L., 2014. New edge of antibiotic development: antimicrobial peptides and corresponding resistance. *Frontiers in Microbiology*, 5, p. 147.

Park, C.B., Kim, H.S. and Kim, S.C., 1998. Mechanism of action of the antimicrobial peptide buforin II: buforin II kills microorganisms by penetrating the cell membrane and inhibiting cellular functions. *Biochemical and Biophysical Research Communications*, 244, pp. 253–257.

Park, S.C., et al., 2006. Investigation of toroidal pore and oligomerization by melittin using transmission electron microscopy. *Biochemical and Biophysical Research Communications*, 343, pp. 222–228.

Pasupuleti, M., Schmidtchen, A. and Malmsten, M., 2012. Antimicrobial peptides: key components of the innate immune system. *Critical Reviews in Biotechnology,* 32, pp. 143–171.

Patrzykat, A., Friedrich, C.L., Zhang, L., Mendoza, V. and Hancock, R.E., 2002. Sublethal concentrations of pleurocidin-derived antimicrobial peptides inhibit macromolecular synthesis in *Escherichia coli*. *Antimicrobial Agents and Chemotherapy*, 46(3), pp. 605-614.

Payne, E., 2018. The Ottawa Hospital is reporting outbreaks of the superbug Methicillin-resistant *Staphylococcus aureus* (MRSA) in two units at its General campus. *Ottawa Citizen*, March 28.

Peach, K.C., Bray, W.M., Winslow, D., Linington, P.F., and Linington, R.G., 2013. Mechanism of action-based classification of antibiotics using high-content bacterial image analysis. *Molecular BioSystems*, 9(7), pp. 1837–1848.

Pechere, J.C., Hughes, D., Kardas, P., Cornaglia, G., 2007. Non-compliance with antibiotic therapy for acute community infections: a global survey. *International Journal of Antimicrobial Agents*, 29, pp. 245–253.

Pendleton, J.N., Gorman, S.P. and Gilmore, B.F., 2013. Clinical relevance of the ESKAPE pathogens. *Expert Review of Anti-infective Therapy*, 11(3), pp. 297-308.

Perego, M. et al., 1995. Incorporation of D-alanine into lipoteichoic acid and wall teichoic acid in *Bacillus subtilis*. Identification of genes and regulation. *Journal of Biological Chemistry*, 270, pp. 15598–15606.

Peschel, A. et al., 1999. Inactivation of the dlt operon in *Staphylococcus aureus* confers sensitivity to defensins, protegrins, and other antimicrobial peptides. *Journal of Biological Chemistry*, 274, pp. 8405–8410.

Peschel, A. et al., 2001. *Staphylococcus aureus* resistance to human defensins and evasion of neutrophil killing via the novel virulence factor MprF is based on modification of membrane lipids with l-lysine. *Journal of Experimental Medicine*, 193, pp. 1067–1076.

Peschel, A. and Sahl, H.G., 2006. The co-evolution of host cationic antimicrobial peptides and microbial resistance. *Nature Reviews Microbiology*, 4, pp. 529-536.

Peterson, A.A., Hancock, R.E. and McGroarty, E.J., 1985. Binding of polycationic antibiotics and polyamines to lipopolysaccharides of *Pseudomonas aeruginosa*. *Journal of Bacteriology*, 164, pp. 1256–1261.

Phillips, I., 2001. Prudent use of antibiotics: Are our expectations justified? *Clinical Infectious Diseases*, 33(3), pp. S130–S132.

Piddock, L.J., 2012. The crisis of no new antibiotics—what is the way forward? *The Lancet Infectious Diseases*, 12(3), pp. 249–253.

Pincus, D.H., 2014. *Microbial identification using the bioMérieux VITEK® System*. Encyclopedia of Rapid Microbiological Methods. bioMérieux, Inc. Hazelwood, MO, USA.

Pini, A. et al., 2005. Antimicrobial activity of novel dendrimeric peptides obtained by phage display selection and rational modification. *Antimicrobial Agents and Chemotherapy*, 49(7), pp. 2665–2672.

Poirel, L., Jayol, A. and Nordmann, P., 2017. Polymyxins: antibacterial activity, susceptibility testing, and resistance mechanisms encoded by plasmids or chromosomes. *Clinical Microbiology Reviews*, 30(2), pp. 557–596.

Poole, K., 2000. Efflux-mediated resistance to fluoroquinolones in Gram-negative bacteria. *Antimicrobial Agents and Chemotherapy*; 44, pp. 2233–2241.

Poole, K., 2011. *Pseudomonas aeruginosa*: resistance to the max. *Front. Microbiol*, 2, p. 65.

Poole, K., Lau, C.H-F., Gilmour, C., Hao, Y. and Lam, J.S., 2015. Polymyxin susceptibility in *Pseudomonas aeruginosa* linked to the MexXY-OprM multidrug efflux system. *Antimicrobial Agents and Chemotherapy*, 59, pp. 7276–7289.

Potron, A., Poirel, L. and Nordmann, P., 2015. Emerging broad-spectrum resistance in *Pseudomonas aeruginosa* and *Acinetobacter baumannii*: mechanisms and epidemiology. *International Journal of Antimicrobial Agents*, 45(6), pp. 568–585.

Powers, J.P., Rozek, A. and Hancock, R.E., 2004. Structure–activity relationships for the β-hairpin cationic antimicrobial peptide polyphemusin I. *Biochimica et Biophysica Acta*, 1698, pp. 239–250.

Poyart, C., et al., 2003. Attenuated virulence of *Streptococcus agalactiae* deficient in D-alanyl-lipoteichoic acid is due to an increased susceptibility to defensins and phagocytic cells. *Molecular Microbiology*, 49, pp. 1615–1625.

Pöyry, S. and Vattulainen, I., 2016. Role of charged lipids in membrane structures - Insight given by simulations. *Biochimica et Biophysica Acta*, 1858(10), pp. 2322-2333.

Pray, L., 2008. Antibiotic resistance, mutation rates and MRSA. *Nature Education*, 1(1), p. 30.

Raghuraman, H. and Chattopadhyay, A., 2007. Melittin: a membrane-active peptide with diverse functions. *Bioscience Reports*, 27(4-5), pp. 189-223.

Rahnamaeian, M. et al., 2015. Insect antimicrobial peptides show potentiating functional interactions against Gram-negative bacteria. *Proceedings of the Royal Society B: Biological Sciences*, 282, p. 20150293.

Ramamoorthy, A. et al., 2006. Deletion of all cysteines in tachyplesin I abolishes hemolytic activity and retains antimicrobial activity and lipopolysaccharide selective binding. *Biochemistry*, 45, pp. 6529–6654.

Rao, A.G., 1999. Conformation and antimicrobial activity of linear derivatives of tachyplesin lacking disulfide bonds. *Archives of Biochemistry and Biophysics*, 361, pp. 127–134.

Rapaport, D. and Shai, Y., 1991. Interaction of fluorescently labeled pardaxin and its analogues with lipid bilayers. *Journal of Biological Chemistry*, 266(35), pp. 23769-23775.

Rathinakumar, R., Walkenhorst, W.F., and Wimley, W.C., 2009. Broad-spectrum antimicrobial peptides by rational combinatorial design and high-throughput screening: the importance of interfacial activity. *Journal of the American Chemical Society*, 131(22), pp. 7609–7617.

Read, A.F. and Woods, R.J., 2014. Antibiotic resistance management. *Evolution, Medicine, and Public Health*, 2014(1), p. 147.

Rehaume, L.M. and Hancock, R.E., 2008. Neutrophil-derived defensins as modulators of innate immune function. *Critical Reviews in Immunology*, 28(3), pp. 185-200.

Reinhardt, A. and Neundorf, I., 2016. Design and application of antimicrobial peptide conjugates. *International Journal of Molecular Sciences*, 17(5), p. 701

Reinholz, M., Ruzicka, T. and Schauber, J., 2012. Cathelicidin LL-37: an antimicrobial peptide with a role in inflammatory skin disease. *Annals of Dermatology*, 24(2), pp. 126-135.

Rice, L.B., 2010. Progress and challenges in implementing the research on ESKAPE pathogens. *Infection Control & Hospital Epidemiology*, 31(1), pp. S7–10.

Rice, L.B., 2012. Mechanisms of resistance and clinical relevance of resistance to β-lactams, glycopeptides, and fluoroquinolones. *Mayo Clinic Proceedings*, 87(2), pp. 198–208.

Rice, A. and Wereszczynski, J., 2017. Probing the disparate effects of arginine and lysine residues on antimicrobial peptide/bilayer association. *Biochimica et Biophysica Acta - Biomembranes*, 1859(10), pp. 1941–1950.

Richard, J.P. et al., 2005. Cellular uptake of unconjugated TAT peptide involves clathrin-dependent endocytosis and heparan sulfate receptors. *Journal of Biological Chemistry*, 280, pp. 15300–11536.

Rimbara, E., Noguchi, N., Kawai, T. and Sasatsu, M., 2008. Mutations in penicillin-binding proteins 1, 2 and 3 are responsible for amoxicillin resistance in *Helicobacter pylori*. *Journal of Antimicrobial Chemotherapy*, 61 (5), pp. 995-998.

Riss, T.L. et al., 2013. Cell Viability Assays. *In: Sittampalam GS, Coussens NP, Nelson H, et al., editors. Assay Guidance Manual [Internet]. Bethesda (MD): Eli Lilly & Company and the National Center for Advancing Translational Sciences.*

Riss, T., 2014. Is Your MTT Assay Really the Best Choice? Promega Corporation, pp. 1-6.

Roberts, K.D. et al., 2015. Antimicrobial activity and toxicity of the major lipopeptide components of polymyxin B and colistin: Last-line antibiotics against multidrug-resistant Gram-negative bacteria. *ACS Infectious Diseases*, 1(11), pp. 568-575.

Robinson, J.A., 2011. Protein epitope mimetics as antiinfectives. *Current Opinion in Chemical Biology*, 15, pp. 379–386.

Rokitskaya, T.I., Kolodkin, N.I., Kotova, E.A. and Antonenko, Y.N., 2011. Indolicidin action on membrane permeability: Carrier mechanism versus pore formation. *Biochimica et Biophysica Acta - Biomembranes*, 1808 (1), pp. 91-97.

Rončević, T., Puizina, J. and Tossi, A., 2019. Antimicrobial peptides as anti-infective agents in pre-post-antibiotic era? *International Journal of Molecular Sciences*, 20(22), p. 5713.

Rosenfeld, Y. and Shai, Y., 2006. Lipopolysaccharide (endotoxin)-host defense antibacterial peptides interactions: role in bacterial resistance and prevention of sepsis. *Biochimica et Biophysica Acta*, 1758, pp. 1513–1522.

Rossolini, G.M., Arena, F., Pecile, P. and Pollini, S., 2014. Update on the antibiotic resistance crisis. *Current Opinion in Pharmacology*, 18, pp. 56–60.

Roy, R.N., Lomakin, I.B., Gagnon, M.G. and Steitz, T.A., 2015. The mechanism of inhibition of protein synthesis by the proline-rich peptide oncocin. *Nature Structural & Molecular Biology*, 22(6), pp. 466-469.

Rozek, A., Friedrich, C.L. and Hancock. R.E., 2000. Structure of the bovine antimicrobial peptide indolicidin bound to dodecylphosphocholine and sodium dodecyl sulfate micelles. *Biochemistry*, 39, pp. 15765–15774.

Saiman, L. et al., 2001. Cathelicidin peptides inhibit multiply antibiotic-resistant pathogens from patients with cystic fibrosis. *Antimicrobial Agents and Chemotherapy*, 45, pp. 2838–2844.

Sainath Rao, S., Mohan, K.V.K. and Atreya, C.D., 2013. A peptide derived from phage display library exhibits antibacterial activity against *E. coli* and *Pseudomonas aeruginosa*. *PLoS ONE*, 8(2), e56081.

Salarizadeh, N., Hasannia, S., Akbari Noghabi, K. and Hassan Sajedi, R., 2014. Purification and characterization of 50 kDa extracellular metalloprotease from *Serratia sp.* ZF03. *Iranian Journal of Biotechnology*, 12(3), pp. 18-27.

Salas, C.E., Badillo-Corona, J.A., Ramírez-Sotelo, G., and Oliver-Salvador, C., 2015. Biologically active and antimicrobial peptides from plants. *BioMed Research International*, 2015, p. 102129.

Salditt, T., Li, C. and Spaar, A., 2006. Structure of antimicrobial peptides and lipid membranes probed by interface-sensitive X-ray scattering. *Biochimica et Biophysica Acta*, 1758(9), pp. 1483-1498.

Salvatore, M. et al., 2007. Alpha-Defensin inhibits influenza virus replication by cell-mediated mechanism(s). *Journal of Infectious Diseases*, 196(6), pp. 835-843.

Samant, S., Hsu, F.F., Neyfakh, A.A. and Lee, H., 2009. The *Bacillus anthracis* protein MprF is required for synthesis of lysylphosphatidylglycerols and for resistance to cationic antimicrobial peptides. *Journal of Bacteriology*, 191, pp. 1311–1319.

San Millan, A., 2018. Evolution of plasmid-mediated antibiotic resistance in the clinical context. *Trends in Microbiology*, 26, pp. 978–985.

Sani, M.A., Whitwell, T.C. and Separovic, F., 2012. Lipid composition regulates the conformation and insertion of the antimicrobial peptide maculatin 1.1. *Biochimica et Biophysica Acta*, 1818(2), pp. 205-211.

Santajit, S. and Indrawattana, N., 2016. Mechanisms of antimicrobial resistance in ESKAPE pathogens. *BioMed Research International*, 2016, p. 2475067.

Sanz-García, F., Hernando-Amado, S. and Martínez, J.L., 2018. Mutational evolution of *Pseudomonas aeruginosa* resistance to ribosome-targeting antibiotics. *Frontiers in Genetics*, 9, p. 451.

Sarı, A.N., Biçmen, M. and Gülay, Z., 2013. The first report on the outbreak of OXA-24/40-like carbapenemase-producing *Acinetobacter baumannii* in Turkey. *Japanese Journal of Infectious Diseases*, 66(5), pp. 439–442.

Sato, H. and Feix, J.B., 2006. Peptide-membrane interactions and mechanisms of membrane destruction by amphipathic alpha-helical antimicrobial peptides. *Biochimica et Biophysica Acta,* 1758, pp. 1245-1256.

Schibli, D.J., Nguyen, L.T., Kernaghan, S.D., Rekdal, Ø. and Vogel, H.J., 2006. Structure-function analysis of tritrpticin analogs: potential relationships between antimicrobial activities, model membrane interactions, and their micelle-bound NMR structures. *Biophysical Journal*, 91(12), pp. 4413-26.

Schmidtchen, A., Frick, I.M., Andersson, E., Tapper, H. and Bjorck, L., 2002. Proteinases of common pathogenic bacteria degrade and inactivate the antibacterial peptide LL-37. *Molecular Microbiology*, 46(1), pp. 157 – 168.

Schmitt, P., Rosa, R.D. and Destoumieux-Garzón, D., 2016. An intimate link between antimicrobial peptide sequence diversity and binding to essential components of bacterial membranes. *Biochimica et Biophysica Acta*, 1858(5), pp. 958-970.

Schroeder, B.O. et al., 2014. Paneth cell α-defensin 6 (HD-6) is an antimicrobial peptide. *Mucosal Immunology*, 8(3), pp. 661-671.

Scott, V., Clark, A.R. and Docherty, K., 1994. The gel retardation assay. *In Protocols for Gene Analysis* pp. 339-347.

Scott, M.G. et al., 2007. An anti-infective peptide that selectively modulates the innate immune response. *Nature Biotechnology*, 25, pp. 465–472.

Sengupta, S., Chattopadhyay, M.K. and Grossart, H.P., 2013. The multifaceted roles of antibiotics and antibiotic resistance in nature. *Frontiers in Microbiology*, 4, p. 47.

Seo, M.D., Won, H.S., Kim, J.H., Mishig-Ochir, T. and Lee, B.J., 2012. Antimicrobial peptides for therapeutic applications: a review. *Molecules (Basel, Switzerland)*, 17(10), pp. 12276–12286.

Shaheen, M., Li, J., Ross, A.C., Vederas, J.C. and Jensen, S.E., 2011. *Paenibacillus polymyxa* PKB1 produces variants of polymyxin B-type antibiotics. *Chemistry and Biology*, 18(12), pp. 1640-1648.

Shahmiri, M., Enciso, M. and Mechler, A., 2015. Controls and constrains of the membrane disrupting action of Aurein 1.2. *Scientific Reports*, 5, p.16378.

Shai, Y., 2002. Mode of action of membrane active antimicrobial peptides. *Biopolymers*, 66, pp. 236–248.

Sharon, M., Oren, Z., Shai, Y. and Anglister, J., 1999. 2D-NMR and ATR-FTIR study of the structure of a cell-selective diastereomer of melittin and its orientation in phospholipids. *Biochemistry*, 38(46), pp. 15305-15316.

Shelton, C.L., Raffel, F.K., Beatty, W.L., Johnson, S.M. and Mason, K.M., 2011. Sap transporter mediated import and subsequent degradation of antimicrobial peptides in *Haemophilus*. *PLOS Pathogens*. 7, p. e1002360.

Shenkarev, et al., 2002. Spatial structure of zervamicin IIB bound to DPC micelles: implications for voltage-gating. *Biophysical Journal*, 82, pp. 762–771.

Shepherd, C.M., Vogel, H.J. and Tieleman, D.P., 2003. Interactions of the designed antimicrobial peptide MB21 and truncated dermaseptin S3 with lipid bilayers: molecular-dynamics simulations. *The Biochemical Journal*, 370(Pt 1), pp. 233–243.

Shruti, S. et al., 2016. Antimicrobial peptides and their pore/ion channel properties in neutralization of pathogenic microbes. *Current Topics in Medicinal Chemistry*, 16, pp. 46–53.

Sieprawska-Lupa, M. et al., 2004. Degradation of human antimicrobial peptide LL-37 by *Staphylococcus aureus*-derived proteinases. *Antimicrobial Agents and Chemotherapy*, 48, pp. 4673–4679.

Sigurdardottir, et al., 2006. *In silico* identification and biological evaluation of antimicrobial peptides based on human cathelicidin LL-37. *Antimicrobial Agents and Chemotherapy*, 50(9), pp. 2983-2989.

Silhavy, T.J., Kahne, D. and Walker, S., 2010. The bacterial cell envelope. *Cold Spring Harbor Perspectives in Biology*, 2(5), p. a000414.

Simpkin, V.L., Renwick, M.J., Kelly, R. and Mossialos, E., 2017. Incentivising innovation in antibiotic drug discovery and development: progress, challenges and next steps. *The Journal of Antibiotics*, 70(12), pp. 1087-1096.

Sinha, R. and Shukla, P., 2019. Antimicrobial peptides: recent insights on biotechnological interventions and future perspectives. *Protein and Peptide Letters*, 26(2), pp. 79–87.

Sitaram, N. and Nagaraj, R., 1999. Interaction of antimicrobial peptides with biological and model membranes: Structural and charge requirements for activity. *Biochimica et Biophysica Acta*, 1462, pp. 29–54.

Smirnova, M.P., Afonin, V.G., Shpen', V.M., Tyagotin, Y.V. and Kolodkin, N.I., 2004. Structure–function relationship between analogues of the antibacterial peptide indolicidin. I. synthesis and biological activity of analogues with increased amphipathicity and elevated net positive charge of the molecule. *Russian Journal of Bioorganic Chemistry*, 30, pp. 409–416.

Smith, G.P. and Petrenko, V.A., 1997. Phage display. *Chemical Reviews*, 97(2), pp. 391–410.

Smith, J.G. et al., 2010. Insight into the mechanisms of adenovirus capsid disassembly from studies of defensin neutralization. *PLoS Pathogens*, 6(6), p. e1000959.

Soehnlein, O. et al., 2008. Neutrophil secretion products pave the way for inflammatory monocytes. *Blood*, 112(4), pp. 1461–1471.

Sohlenkamp, C. and Geiger, O., 2016. Bacterial membrane lipids: diversity in structures and pathways. *FEMS Microbiology Reviews*, 40, pp. 133–159.

Song, R., Wei, R.-B., Luo, H.-Y. and Wang, D.-F., 2012. Isolation and characterization of an antibacterial peptide fraction from the Pepsin Hydrolysate of Half-Fin anchovy (*Setipinna taty*). *Molecules*, 17(12), pp. 2980–2991.

Soruri, A., Grigat, J., Forssmann, U., Riggert, J. and Zwirner, J., 2007. beta-Defensins chemoattract macrophages and mast cells but not lymphocytes and dendritic cells: CCR6 is not involved. *European Journal of Immunology*, 37(9), pp. 2474-2486.

Soundrarajan, N. et al., 2019. Protegrin-1 cytotoxicity towards mammalian cells positively correlates with the magnitude of conformational changes of the unfolded form upon cell interaction. *Scientific Reports*, 9, p. 11569.

Sousa, D.A., Mulder, K.C.L., Nobre, K.S., Parachin, N.S. and Franco, O.L., 2016. Production of a polar fish antimicrobial peptide in *Escherichia coli* using an ELP-intein tag. *Journal of Biotechnology*, 234, pp. 83-89.

Spellberg, B. and Gilbert, D.N., 2014. The future of antibiotics and resistance: a tribute to a career of leadership by John Bartlett. *Clinical Infectious Diseases*, 59(2), pp. S71–S75.

Srinivas, N. et al., 2010. Peptidomimetic antibiotics target outer membrane biogenesis in *Pseudomonas aeruginosa*. *Science*, 327, pp. 1010–1013.

Starr, C.G. and Wimley, W.C., 2017. Antimicrobial peptides are degraded by the cytosolic proteases of human erythrocytes. *Biochimica et Biophysica Acta – Biomembranes*, 1859, pp. 2319–2326.

Stefani, S. et al., 2017. Relevance of multidrug-resistant *Pseudomonas aeruginosa* infections in cystic fibrosis. *International Journal of Medical Microbiology*, 307, pp. 353–362.

Steiner, H., Hultmark, D., Engstrom, A., Bennich, H. and Boman, H.G., 1981. Sequence and specificity of two antibacterial proteins involved in insect immunity. *Nature*, 292, pp. 246–248.

Stinson, M.W., Alder, S. and Kumar, S., 2003. Invasion and killing of human endothelial cells by viridans group streptococci. *Infections and Immunity,* 71 (5), pp. 2365 – 2372.

Su, J.L. et al., 2005. A novel peptide specifically binding to interleukin-6 receptor (gp80) inhibits angiogenesis and tumor growth. *Cancer Research*, 65(11), pp. 4827–4835.

Subbalakshmi, C., Nagaraj, R. and Sitaram, N., 1999. Biological activities of C-terminal 15-residue synthetic fragment of melittin: design of an analog with improved antibacterial activity. *FEBS Letters*, 448, pp. 62–66.

Sudheendra, U.S. et al., 2015. Membrane disruptive antimicrobial activities of human β-defensin-3 analogs. *European Journal of Medicinal Chemistry*, 91, pp. 91–99.

Sugiarto, H. and Yu, P.L., 2007. Mechanisms of action of ostrich β-defensins against *Escherichia coli*. *FEMS Microbiology Letters*, 270(2), pp. 195-200.

Sun, E., Belanger, C.R., Haney, E.F. and Hancock, R.E.W., 2018. Host defense (antimicrobial) peptides. *Peptide Applications in Biomedicine, Biotechnology and Bioengineering*, pp. 253-285.

Sun, J., Deng, Z. and Yan, A., 2014. Bacterial multidrug efflux pumps: mechanisms, physiology and pharmacological exploitations. *Biochemical and Biophysical Research Communications*. 453, pp. 254–267.

Sun, S., Selmer, M. and Andersson, D.I., 2014. Resistance to β-lactam antibiotics conferred by point mutations in penicillin-binding proteins PBP3, PBP4 and PBP6 in *Salmonella enterica*. *PLoS ONE*, 9(5), art. no. e97202.

Takahashi, D., Shukla, S.K., Prakash, O. and Zhang, G., 2010. Structural determinants of host defense peptides for antimicrobial activity and target cell selectivity. *Biochimie*. 92, pp. 1236–1241.

Tally, F.P. and DeBruin, M.F., 2000. Development of daptomycin for Gram-positive infections. *The Journal of Antimicrobial Chemotherapy*, 46(4), pp. 523–526.

Tam, V.H. et al., 2005. Pharmacodynamics of polymyxin B against *Pseudomonas aeruginosa*. *Antimicrobial Agents and Chemotherapy*, 49(9), pp. 3624–3630.

Tan, Y. et al., 2018. Biological activities of cationicity-enhanced and hydrophobicity-pptimized analogues of an antimicrobial peptide, Dermaseptin-PS3, from the skin secretion of *Phyllomedusa sauvagii*. *Toxins*, 10(8), p. 320.

Tanaka, T., Kokuryu, Y. and Matsunaga, T., 2008. Novel method for selection of antimicrobial peptides from a phage display library by use of bacterial magnetic particles. *Applied and Environmental Microbiology*, 74(24), pp.7600–7606.

Tang, S.S., Prodhan, Z.H., Biswas, S.K., Le, C.F. and Sekaran, S.D., 2018. Antimicrobial peptides from different plant sources: Isolation, characterisation, and purification. *Phytochemistry*, 154, pp. 94-105.

Tang, Y.L., Shi, Y.H., Zhao, W., Hao, G. and Le, G.W., 2008. Interaction of MDpep9, a novel antimicrobial peptide from Chinese traditional edible larvae of housefly, with *Escherichia coli* genomic DNA. *Food Chemistry,* 115(2009), pp. 867-872.

Taute, H., Bester, M.J., Neitz, A.W.H. and Gaspar, A.R.M., 2015. Investigation into the mechanism of action of the antimicrobial peptides Os and Os-C derived from a tick defensin. *Peptides*, 71, pp. 179–187.

Tecle, T., Tripathi, S. and Hartshorn, K.L., 2010. Review: Defensins and cathelicidins in lung immunity. *Innate Immunity*, 16, pp. 151–159.

Thakur, S., Cattoni, D.I. and Nöllmann, M., 2015. The fluorescence properties and binding mechanism of SYTOX green, a bright, low photo-damage DNA intercalating agent. *European Biophysics Journal*, 44**,** pp**.** 337–348.

The Antimicrobial Peptide Database, 2020. [Online] Available at: <http://www. http://aps.unmc.edu/AP/main.php> [Accessed on 15 February 2020]

Tjabringa, G.S., Ninaber, D.K., Drijfhout, J.W., Rabe, K.F. and Hiemstra, P.S., 2006. Human cathelicidin LL-37 is a chemoattractant for eosinophils and neutrophils that acts via formyl-peptide receptors. *International Archives of Allergy and Immunology*, 140(2), pp. 103-112.

Todar, K., 2013, *The growth of bacterial populations* [Online]. Available at : http://textbookofbacteriology.net/growth_3.html [Accessed: 17 August 2018].

Tomasinsig, L. and Zanetti, M., 2005. The cathelicidins – structure, function and evolution. *Current Protein & Peptide Science*, 6, pp. 23–34.

Torcato, I.M. et al., 2013. Design and characterization of novel antimicrobial peptides, R-BP100 and RW-BP100, with activity against Gram-negative and Gram-positive bacteria. *Biochimica et Biophysica Acta - Biomembranes*, 1828, pp. 944-955.

Trevor, A., Katzung, B., Masters, S. and Knuidering-Hall, M., 2013. "Chapter 2: Pharmacodynamics". *Pharmacology Examination & Board Review* (10th ed.). New York: McGraw-Hill Medical. p. 17.

Trimble, M.J., Mlynárčik, P., Kolář, M. and Hancock, R.E., 2016. Polymyxin: alternative mechanisms of action and resistance. *Cold Spring Harbor Perspectives in Medicine*, 6(10), p. a025288.

Tripathi, S. et al., 2013. The human cathelicidin LL-37 inhibits influenza A viruses through a mechanism distinct from that of surfactant protein D or defensins. *The Journal of General Virology*, 94(1), pp. 40-49.

Trotti, A. et al., 2004. A multinational, randomized Phase III trial of iseganan HCl oral solution for reducing the severity of oral mucositis in patients receiving radiotherapy for head-and-neck malignancy. *International Journal of Radiation Oncology, Biology, Physic*s, 58, pp. 674–681.

van Duin, D., Kaye, K.S., Neuner, E.A. and Bonomo, R.A., 2013. Carbapenem-resistant Enterobacteriaceae: a review of treatment and outcomes. *Diagnostic Microbiology and Infectious Disease*, 75(2), pp. 115-120.

van Eijk, E., Wittekoek, B., Kuijper, E.J. and Smits, W.K., 2017. DNA replication proteins as potential targets for antimicrobials in drug-resistant bacterial pathogens. *Journal of Antimicrobial Chemotherapy*, 72(5), pp.1275-1284.

Van Epps H.L., 2006. René Dubos: unearthing antibiotics. *The Journal of Experimental Medicine*, 203(2), p. 259.

Varney, K.M. et al., 2013. Turning defense into offense: defensin mimetics as novel antibiotics targeting lipid II. *PLoS Pathogens*, 9(11), p. e1003732.

Vaucher, R.A., da Motta, A., de, S. and Brandelli, A., 2010. Evaluation of the *in vitro* cytotoxicity of the antimicrobial peptide P34. *Cell Biology International*, 34, pp. 317–323.

Vebo, H.C., Solheim, M., Snipen, L., Nes, I. and Brede, D.A., 2010. Comparative genomic analysis of pathogenic and probiotic *Enterococcus faecalis* isolates, and their transcriptional responses to growth in human urine.

PLoS ONE, 5 (8), pp. 1 – 14.

Vega-Chaparro, S.C., Valencia Salguero, J.T., Martínez Baquero, D.A. and Rosas Pérez, J.E., 2018. Effect of polyvalence on the antibacterial activity of a synthetic peptide derived from bovine lactoferricin against healthcare-associated infectious pathogens. *BioMed Research International*, 2018, p. 5252891.

Veldhuizen, E.J. et al., 2014. Antimicrobial and immunomodulatory activities of PR-39 derived peptides. *PloS ONE*, 9(4), p. e95939.

Vélez-Gómez, J.M., Melchor-Moncada, J.J., Veloza, L.A. and Sepúlveda-Arias, J.C., 2019. Purification and characterization of a metalloprotease produced by the C8 isolate of *Serratia marcescens* using silkworm pupae or casein as a protein source. *International Journal of Biological Macromolecules*, 135, pp. 97-105.

Velkov, T., Thompson, P.E., Nation, R.L. and Li, J., 2010. Structure-activity relationships of polymyxin antibiotics. *Journal of Medicinal Chemistry*, 53(5), 1898–1916.

Ventola, C. L., 2015. The antibiotic resistance crisis: part 1: causes and threats. *P & T*: *a peer-reviewed journal for formulary management*, 40(4), pp. 277-283.

Vergalli, J. et al., 2017. Fluoroquinolone structure and translocation flux across bacterial membrane. *Scientific Reports*, 7, p. 9821.

Verly, R. et al., 2017. Structure and membrane interactions of the homodimeric antibiotic peptide homotarsinin. *Scientific Reports*, 7, p. 40854.

Verraes, C. et al., 2013. Antimicrobial resistance in the food chain: a review. International Journal of Environmental Research and Public Health, 10(7), pp. 2643–2669.

Viswanathan, V.K., 2014. Off-label abuse of antibiotics by bacteria. *Gut Microbes*, 5(1), pp. 3–4.

Vylkova, S., Nayyar, N., Li, W. and Edgerton, M., 2006. Human beta-defensins kill *Candida albicans* in an energy-dependent and salt-sensitive manner without

causing membrane disruption. *Antimicrobial Agents and Chemotherapy*, 51(1), pp. 154-161.

Walter, J. et al., 2007. D-alanyl ester depletion of teichoic acids in *Lactobacillus reuteri* 100-23 results in impaired colonization of the mouse gastrointestinal tract. *Environmental Microbiology*, 9, pp. 1750–1760.

Wang, G., 2010. Database-aided prediction and design of novel antimicrobial peptides. *CAB International*, pp. 72-86.

Wang, G., 2014. Human antimicrobial peptides and proteins. *Pharmaceuticals* (Basel, Switzerland), 7(5), pp. 545–594.

Wang, S., Zeng, X., Yang, Q. and Qiao, S., 2016. Antimicrobial peptides as potential alternatives to antibiotics in food animal industry. *International Journal of Molecular Sciences*, 17(5), p. 603.

Watkins, R.R. and Bonomo, R.A., 2016. Overview: global and local impact of antibiotic resistance. *Infectious Disease Clinics of North America*, 30, pp. 313–322.

Weigel, L.M., Anderson, G.J. and Tenover, F.C., 2002. DNA gyrase and topoisomerase IV mutations associated with fluoroquinolone resistance in *Proteus mirabilis*. *Antimicrobial Agents and Chemotherapy*, 46(8), pp. 2582-2587.

Werth, B.J., 2018. Overview of Antibacterial Drugs. Merck Manual [Online]. Available at: https://www.merckmanuals.com/professional/infectious-diseases/bacteria-and-antibacterial-drugs/overview-of-antibacterial-drugs

WHO, 2014. Antimicrobial resistance: global report on surveillance 2014.

Wibowo, D. and Zhao, C.X., 2019. Recent achievements and perspectives for large-scale recombinant production of antimicrobial peptides. *Applied Microbiology and Biotechnology*, 103(2), pp. 659–671.

Wieczorek, M. et al., 2010. Structural studies of a peptide with immune modulating and direct antimicrobial activity. *Chemistry and Biology*, 17(9), pp. 970-980.

Wikler M.A. et al., 2009. Methods for dilution antimicrobial susceptibility tests for bacteria that grow aerobically; Approved Standard, 8th ed., CLSI document M07 – A8, Vol. 29, Number 2, v – xi, pp. 1 – 65. Clinical and Laboratory Standards Institute, Wayne, PA, USA.

Wilmes, M., Cammue, B.P., Sahl, H.G. and Thevissen, K., 2011. Antibiotic activities of host defense peptides: more to it than lipid bilayer perturbation. *Natural Product Reports*, 28(8), pp. 1350-1358.

Wimley, W.C., 2010. Describing the mechanism of antimicrobial peptide action with the interfacial activity model. *ACS Chemical Biology*, 5(10), pp. 905-917.

Wimley, W.C., 2018. How does melittin permeabilize membranes? *Biophysical Journal*, 114(2), pp. 251–253.

Wiradharma, N. et al., 2011. Synthetic cationic amphiphilic α-helical peptides as antimicrobial agents. *Biomaterials*, 32, pp. 2204–2212.

Wright, G.D., 2014. Something new: revisiting natural products in antibiotic drug discovery. *Canadian Journal of Microbiology*, 60(3), pp. 147–154.

Wu, C. et al., 2016. Advancement and applications of peptide phage display technology in biomedical science. *Journal of Biomedical Science*, 23, p. 8.

Wu, G. et al., 2007. Effects of cations and pH on antimicrobial activity of thanatin and s-thanatin against *Escherichia coli* ATCC25922 and *B. subtilis* ATCC 21332. *Current Microbiology*, 57(6), pp. 552-557.

Xhindoli, D. et al., 2016. The human cathelicidin LL-37 - a pore-forming antibacterial peptide and host-cell modulator. *Biochimica et Biophysica Acta*, 1858, pp. 546–566.

Xiao, Y., Liu, C. and Lai, R., 2011. Antimicrobial peptides from amphibians. *BioMolecular Concepts*, 2(1-2), pp. 27-38.

Xie, Y., Fleming, E., Chen, J.L. and Elmore, D.E., 2011. Effect of proline position on the antimicrobial mechanism of buforin II. *Peptides*, 32(4), pp. 677-682.

Xu, M., McCanna, D.J. and Sivak, J.G., 2015. Use of the viability reagent PrestoBlue in comparison with alamarBlue and MTT to assess the viability of human corneal epithelial cells. *Journal of Pharmacological and Toxicological Methods*, 71, pp. 1–7.

Yacoby, I., Shamis, M., Bar, H., Shabat, D. and Benhar, I., 2006. Targeting antibacterial agents by using drug-carrying filamentous bacteriophages. *Antimicrobial Agents and Chemotherapy*, 50, pp. 2087–2097.

Yacoby, I., Bar, H. and Benhar, I., 2007. Targeted drug-carrying bacteriophages as antibacterial nanomedicines. *Antimicrobial Agents and Chemotherapy*, 51, pp. 2156–2163.

Yamachika, S., Sugihara, C., Kamai, Y. and Yamashita, M., 2013. Correlation between penicillin-binding protein 2 mutations and carbapenem resistance in *Escherichia coli*. *Journal of Medical Microbiology*, 62 (3), pp. 429-436.

Yamaguchi, et al., 2001. Orientation and dynamics of an antimicrobial peptide in the lipid bilayer by solid-state NMR spectroscopy. *Biophysical Journal*, 81(4), pp. 2203-2214.

Yan, J. et al., 2013. Two hits are better than one: membrane-active and DNA binding-related double-action mechanism of NK-18, a novel antimicrobial peptide derived from mammalian NK-lysin. *Antimicrobial Agents and Chemotherapy*, 57(1), pp. 220–228.

Yang, D., Biragyn, A., Hoover, D.M., Lubkowski, J. and Oppenheim, J.J., 2004. Multiple roles of antimicrobial defensins, cathelicidins, and eosinophil-derived neurotoxin in host defense. *Annual Review of Immunology*, 22, pp. 181–215.

Yasir, M., Dutta, D. and Willcox, M., 2019. Comparative mode of action of the antimicrobial peptide melimine and its derivative Mel4 against *Pseudomonas aeruginosa*. *Scientific Reports*, 9(1), p. 7063.

Yeaman, M.R. and Yount, N.Y., 2003. Mechanisms of antimicrobial peptide action and resistance. *Pharmacological Reviews*, 55, pp. 27–55.

Yenugu, S. et al., 2004. Antimicrobial actions of the human epididymis 2 (HE2) protein isoforms, HE2alpha, HE2beta1 and HE2beta2. *Journal of Reproductive Biology and Endocrinology*, 2, p. 61.

Yeung, A.T., Gellatly, S.L. and Hancock, R.E., 2011. Multifunctional cationic host defence peptides and their clinical applications. *Cellular and Molecular Life Sciences,* 68, pp. 2161–2176.

Yin, L.M., Edwards, M.A., Li, J., Yip, C.M. and Deber, C.M., 2012. Roles of hydrophobicity and charge distribution of cationic antimicrobial peptides in peptide-membrane interactions. *The Journal of Biological Chemistry*, 287(10), pp. 7738-7745.

Yoneyama, F. et al., 2009. Peptide-lipid huge toroidal pore, a new antimicrobial mechanism mediated by a lactococcal bacteriocin, lacticin Q. *Antimicrobial Agents and Chemotherapy*, 53, pp. 3211–3217.

Yoshino, M. and Murakami, K., 2015. Analysis of the substrate inhibition of complete and partial types. *SpringerPlus*, 4, p. 292.

Zanetti, M., 2004. Cathelicidins, multifunctional peptides of the innate immunity. *Journal of Leukocyte Biology*, 75, pp. 39–38.

Zasloff, M., 2002. Antimicrobial peptides of multicellular organisms. *Nature*, 415, pp. 389-395.

Zeng, D. et al., 2016. Approved glycopeptide antibacterial drugs: mechanism of action and resistance. *Cold Spring Harbor Perspectives in Medicine*, 6(12), a026989.

Zhang, J. et al., 2014. A novel Omp25-binding peptide screened by phage display can inhibit *Brucella abortus* 2308 infection *in vitro* and *in vivo*. *Journal of Medical Microbiology*, 63 (6), pp. 780-787.

Zhang, J. et al., 2015. Molecular structure, chemical synthesis, and antibacterial activity of ABP-dHC-cecropin A from drury (*Hyphantria cunea*), *Peptides*, 68, pp. 197–204.

Zhang, L. et al., 2000. Interaction of polyphemusin I and structural analogs with bacterial membranes, lipopolysaccharide, and lipid monolayers. *Biochemistry*, 39, pp. 14504–14514.

Zhang, L., Rozek, A. and Hancock, R.E., 2001. Interaction of cationic antimicrobial peptides with model membranes. *Journal of Biological Chemistry*, 276(38), pp. 35714-35722.

Zhang, L.J. and Gallo, R.L., 2016. Antimicrobial peptides. *Current Biology*, 26, pp. R14-R19.

Zhao, C., Liu, L. and Lehrer, R.I., 1994. Identification of a new member of the protegrin family by cDNA cloning. *FEBS Letters*, 346, pp. 285–288.

Zhu, X., Ma, Z., Wang, J., Chou, S. and Shan, A., 2014. Importance of tryptophan in transforming an amphipathic peptide into a *Pseudomonas aeruginosa*-targeted antimicrobial peptide. *PLoS ONE*, 9(12), p. e114605.

Zhu, X. et al., 2015. Bactericidal efficiency and modes of action of the novel antimicrobial peptide T9W against *Pseudomonas aeruginosa*. *Antimicrobial Agents and Chemotherapy*, 59(6), pp. 3008-3017.

Zhu, L., Zhang, B., Dai, Y., Li, H. and Xu, W., 2017. A review: epigenetic mechanism in Ochratoxin A toxicity studies. *Toxins*, 9(4), p.113.

APPENDIX A

LIST OF LABWARE AND EQUIPMENTS

Lab-ware/Equipment	Manufacturers
15 mL centrifuge tube	Greiner, Germany
50 mL centrifuge tube	Axygen® Scientific, USA
250 mL- Erlenmeyer flask	DWK Life Sciences, Germany
1000 mL-sized media bottle	Schott Duran®, Germany
500 mL-sized media bottle	Schott Duran®, Germany
250 mL-sized media bottle	Schott Duran®, Germany
100 mL-sized media bottle	Schott Duran®, Germany
96-well microtiter plate, transparent, flat-bottomed	Greiner CELLSTAR®, Germany
White-opaque, flat-bottomed 96 well-microtiter plate	Thermo Fisher Scientific, USA
Class II A1 Biosafety-Cabinet	TELSTAR, Philipines
Fume hood	ESCO, USA
Bunsen burner	Champingaz, France
Eppendorf 5430 R Centrifuge machine, refrigerated	Eppendorf, Germany
Velocity 14R centrifuge	Dynamica, UK

Avanti J-E Centrifuge	Beckman Coulter, USA
37°C microbiological incubator	Memmert, Germany
CO_2 37°C incubator	Memmert, Germany
Shaking incubator	Yihder, Taiwan
LST 3016R shaking incubator	LabTech
Measuring cylinder	GQ, Malaysia
1.5 mL-microcentrifuge tube	Axvgen® Scientific, USA
Syringe (10 mL)	Terumo, Japan
Syringe filter (0.2 μm)	Pall corporation, USA
Micropipette set (10 μL, 200 μL and 1000 μL)	Eppendorf Research® plus, Germany
Multichannel pipettor, 200 μL	Pipetman®, USA
Micropipette tip	Axvgen® Scientific, USA
Petri dish	NEST® Biotechnology, China
Spectrophotometer	Thermo Scientific Genesys 20, Malaysia
Nanophotometer	Implen, Germany
Nanodrop 2000 spectrophotometer	Thermo Scientific, USA
Vortex mixer	VELP® Scientific, Europe
Freeze dryer	Scanvac COOLSAFE™, Denmark
Auto Fine Coater, JFC-1600	JEOL, USA
Inverted fluorescent microscope, Nikon Eclipse E200	Nikon, Japan
Olympus CKX31 inverted microscope	Olympus Microscopy Europa, Germany
Mini gel electrophoresis system	Thermo Scientific, USA
Gel cast set	Major Science, USA

Field emission scanning electron microscope, JSM 6701F	JEOL, Japan
Gel imaging system	Syngene, UK
pH meter	Sartorius Intec® Technologies, Germany
Sartorius CPA225D competence analytical balance	Sartorius Intec® Technologies, Germany
Weighing scale	Kern®, Germany
Tecan Infinite M200 microplate reader	Tecan, Switzerland
FLUOstar Omega	BMG Labtech, UK
GENESYS™ 20 Visible Spectrophotometer	Thermo Fisher Scientific, USA
Plastic disposable cuvette	Biosigma®, Italy
Freezer (-80 C)	Thermo Scientific, USA

APPENDIX B

PREPARATION OF SOLUTIONS, BUFFERS AND MEDIA

1. Preparation of Culture Broth

1.1 Preparation of Brain-Heart Infusion (BHI) broth

Brain-heart infusion (BHI) broth was used to grow *Streptococcus pyogenes*, *Streptococcus anginosus* and *Enterococcus faecalis* in suspension, which were three of the target bacteria listed in the screening of antibacterial effect of PAM-5 in this study. In order to prepare 200 mL of BHI broth, 7.4 g of BHI broth powder (Himedia, India) was dissolved in 200 mL of distilled water and autoclaved at 121°C, 15 psi for 15 minutes. The sterilized broth was kept in room temperature.

1.2 Preparation of Luria-Bertani (LB) broth

Luria-Bertani (LB) broth was used for the growth of ER2738, the host bacteria for the phage clones selected from the biopanning. Besides, this culture broth was also used to prepare bacterial glycerol stock for long-term storage. LB broth was prepared by dissolving 8 g of LB broth powder (Merck Millipore, Germany). in 200 mL of distilled water. The dissolved suspension was then autoclaved at 121°C, 15 psi for 15 minutes. The sterilized LB broth was stored at room temperature.

1.3 Preparation of Mueller-Hinton (MH) broth

Mueller-Hinton (MH) broth was used in the microbroth dilution assay for most of the target bacteria in this study except for *S. pyogenes*, *S. anginosus* and *E. faecalis*. Briefly, an amount of 4.2 g MH broth powder (Sigma Aldrich) was dissolved in 200 mL of distilled water. The dissolved suspension was then autoclaved at 121°C, 15 psi for 15 minutes. The sterilized broth was then kept in room temperature.

1.4 Preparation of Dulbecco's Modified Eagle's Medium (DMEM)

Dulbecco's Modified Eagle's Medium (DMEM) was used as the growth medium for the two cell lines in this study, Vero and HeLa cells. To prepare 1 L of DMEM, 8.3 g of formulated DMEM powder (Sigma-Aldrich, USA) was added 1 L of autoclaved, deionized water in a sterilized media bottle. After that, 3.7 g of sodium bicarbonate ($NaHCO_3$) (Merck Milipore, Germany) was added to the medium and the bottle was swirl gently to dissolve the sodium bicarbonate completely. After the solution was mixed well, 10 mL (1% v/v) of penicillin-streptomycin solution was added to the medium. The pH of the medium was adjusted to 7. Finally, the prepared medium was filter-sterilized into another sterile media bottle using a 0.22 μm sterile bottle-top vacuum filter. The sterilized medium was kept from contamination by sealing with parafilm around the bottle neck stored at 4°C when it was not in use.

2.   Preparation of Agar Media

2.1   Preparation of Mueller-Hinton (MH) Agar

Mueller-Hinton (MH) agar was used as the inoculation media for most of the bacteria after the antibacterial assay, except for *S. pyogenes*, *S. anginosus* and *E. faecalis*. Approximately 26.6 g of MH agar powder (Merck Millipore, Germany) was weighed and dissolved in 700 mL of distilled water. The broth suspension was subsequently autoclaved at 121°C, 15 psi for 15 minutes. After cooling down the sterilized agar to about 50°C, it was poured into petri dishes in the laminar flow. The agar media were allowed to solidify with half the plate opened to allow evaporation of excess water steam. The agar plates were then kept in 4°C refrigerator until use.

2.2   Preparation of MacConkey Agar

MacConkey agar was used as the master culture media for some of the Gram-negative bacteria listed in the antibacterial screening of this study, which encompassed *E. coli*, *K. pneumoniae* and *A. baumannii*. In order to prepare 300 mL of agar, 15.6 g of agar powder was weighed and added into 300 mL of distilled water. After dissolving the agar powder, the agar suspension was autoclaved at 121°C, 15 psi for 15 minutes. After the sterilization, the hot agar was cooled in room temperature to approximately 50°C before pouring into individual petri dishes in a laminar flow. The agar media were allowed to solidify with half plate opened to allow evaporation of excess water steam. The agar plates were then kept in 4°C refrigerator until use.

2.3   Preparation of Mannitol Salt Agar (MSA)

Mannitol salt agar (MSA) was used as the selective and indicator agar for *Staphylococcus aureus* in this study. Briefly, 22 g of MSA powder (Himedia, India) was dissolved in 200 mL of distilled water and autoclaved at 121°C, 15 psi for 15 minutes. The medium was poured into petri dishes and kept in 4°C refrigerator after solidification.

2.4   Preparation of Tryptic Soy Agar (TSA)

Tryptic soy agar (TSA) was used to inoculate *S. pyogenes* and *E. faecalis* for titre evaluation after peptide treatment. Briefly, 20 g of Tryptic soy agar powder was dissolved in 500 mL of distilled water. The media was then autoclaved at 121°C, 15 psi for 15 minutes. After the heat sterilization, the hot agar was cooled down in room temperature to approximately 50°C before pouring into individual petri dishes in a laminar flow. The agar media were allowed to solidify before being kept in 4°C refrigerator until use.

2.5   Preparation of Blood agar (BA)

Blood agar was used as the inoculation media for *S. pyogenes* in this study. Approximately 20 g of Tryptic soy agar powder were dissolved in 500 mL of distilled water. The media was then autoclaved at 121°C at 15 psi for 15 minutes. Once the media had cooled to ~60°C, 30 mL of human blood was added into the media and swirled to allow even distribution of blood. The media was then poured into petri dishes and then kept in refrigerator at 4°C after solidification.

2.6 Preparation of Luria-Bertani Agar Supplemented with Tetracycline (LB+Tet Agar Plates)

LB+Tet agar was used as the selective agar for the *E. coli* ER2738, which is able to grow and survive the tetracycline in the media. One litre of LB agar was prepared according to the protocol as described earlier. After autoclaving, the sterilized agar was cooled to < 70°C before adding 1 mL of tetracycline stock solution (will be described in **3.2**). The LB+Tet agar was mixed well before pouring into petri dishes. After solidifying, the agar plates were stored at 4°C in the dark.

2.7 Preparation of LB/IPTG/Xgal Agar Plates

One litre of LB agar was prepared by dissolving 40 g of LB broth powder and 15 g of agar powder into 1 L of sterile distilled water. After autoclaving at 121°C, 15 psi and 15 minutes, the agar was cooled down to < 70°C, followed by addition of 1 mL of IPTG/Xgal stock solution (as described earlier) into the agar. The agar mixture was mixed well carefully before pouring into petri dishes. After solidifying, the agar plates were stored at 4°C in the dark.

2.8 Preparation of Top Agar

Top agar, which is also commonly known as molten agar, was used in phage tittering as described in **Section 3.3.2**. For the preparation of 1 L of top agar, 10 g of Bacto-Tryptone (Thermo Fisher Scientific, USA), 5 g yeast extract (Merck Milipore, Germany), 5 g NaCl (Merck Milipore, Germany) and 7 g of agarose

310

powder (electrophoresis grade) (Merck Milipore, Germany) were added into 1 L of distilled water. After mixing and dissolving the chemical components in the water, the agar was autoclaved at 121°C, 15 psi for 15 minutes. After the heat sterilization, the top agar was dispensed into 50 mL aliquots. These aliquots were store solid in room temperature, and melted in microwave when needed.

3.   Preparation of Solutions

3.1   Preparation of IPTG/Xgal Stock Solution

IPTG/Xgal stock solution was used to prepare the LB/IPTG/Xgal agar plates (will be described later). To prepare this stock solution, 1.25 g of IPTG (isopropyl-β-D-thiogalactoside) and 1 g of Xgal (5-Bromo-4-chloro-3-indolyl-β-D-galactoside) were measured and dissolved in 25 mL of DMF (dimethyl formamide). After dissolving the chemicals in the solvent completely, the stock solution was kept in dark at -20°C.

3.2   Preparation of Tetracycline Stock

An equal portion of absolute ethanol (molecular biology grade) and sterile distilled water was mixed according to the ratio 1:1. Then 20 mg of tetracycline powder was dissolved into 1 mL of the ethanol:water suspension. The tetracycline stock solution was filter-sterilized using a 0.22 μm pore filter and the filtrate was stored at -20°C.

3.3   Preparation of Alsever's solution

Alsever's solution was added to blood suspension as an anticoagulant and blood preservative. In order to make 100 mL of Alsever's solution, 2.0 g of D-glucose ($C_6H_{12}O_6$), 0.8 g of sodium citrate ($Na_3C_6H_5O_7 \cdot 2H_2O$), 0.055 g of citric acid [$C(OH)(COOH)(CH_2 \cdot COOH)_2 \cdot H_2O$] and 0.42 g of sodium chloride (NaCl) were first weighed accordingly using an analytical balance (Sartorius, Germany). These chemicals were then dissolved in 100 mL of sterilized and deionized water and the solution was swirl gently to allow complete solubilisation of the chemicals. The solution was then filtered-sterilized using sterile 0.22 μm filter membrane.

3.4   Preparation of Tris-HCl Stock Solution (0.5 M, pH 7.5)

Tris-HCl 0.5 M (pH 7.5) was prepared by dissolving 30.29 g of Tris (Bio Basic, Canada) in 500 mL of distilled water. The pH of the solution was adjusted to 7.5 with 1 M hydrochloric acid (HCl). The solution was then autoclaved at 121°C, 15 psi for 15 minutes. The sterilized solution was kept in room temperature.

3.5   Preparation of Sodium Chloride (NaCl) Stock Solution (1.5 M)

The NaCl stock solution was prepared by dissolving 43.83 g of NaCl (Merck Milipore, Germany) in 500 mL of distilled water. After autoclaving the solution at 121°C, 15 psi for 15 minutes, it was kept at room temperature.

3.6 Preparation of Polyethylene Glycol/Sodium Chloride (PEG/NaCl)

Approximately 20% (w/v) of polyethylene glycol-8000 was mixed with NaCl at the final concentration of 2.5 M in 1 litre of sterile distilled water. After autoclaving, the solution was mixed well to combine the separated layers while it was still warm. Finally, it was stored at room temperature.

3.7 Preparation of Glutaraldehyde (3%) in PBS

Glutaraldehyde (3%) was prepared by adding 6 mL of 25% glutaraldehyde (Sigma-Aldrich Co., LLC) to 12.5 mL of 0.1 M PBS. The solution was then topped with distilled water to a final volume of 50 mL.

3.8 Preparation of ABTS Substrate Solution

In this study, ABTS [2,2'-azino-bis(3-ethylbenzothiazoline-6-sulfonic acid)] was used as the substrate for detecting the binding signals between the phages and bacterial ligands in the phage-ELISA assay. The solution was prepared by dissolving 1.4705 g of sodium citrate in 100 mL of distilled water. pH of the solution was adjusted to 4.0 with 1 M of HCl. Then, the solution was added with 0.022 g of ABTS diammonium salt (Sigma-Aldrich, USA) and mixed well. Upon complete dissolution of the salt, the solution was filter-sterilized with 0.22 μm pore filter into a sterile media bottle. The solution was kept at 4°C in dark.

4. Preparation of Buffer

4.1 Preparation of Phosphate Buffer Saline (PBS)

Phosphate-buffered saline (PBS) was prepared by adding five PBS tablets (Merck Milipore, Germany) into 500 mL of distilled water. The mixture was swirled continuously until the tablets dissolved completely. The pH of the solution was adjusted to 7.4 using 1M of sodium hydroxide (NaOH) and 1M of hydrochloric acid (HCl). The solution was then autoclaved at 121°C at 15 psi for 15 minutes.

4.2 Preparation of Dulbecco's Phosphate-Buffered Saline

Dulbecco's phosphate-buffered saline (DPBS) was a specialized buffer for cell culture work. It was prepared by dissolving 9.55 g of DPBS powder (Merck Milipore, Germany) in 1 L of deionized water in a media bottle. The pH of the prepared DPBS solution was adjusted to 7.2 before being autoclaved at 121°C, 15 psi for 15 minutes. The sterilized DPBS was sealed with parafilm to reduce the risk of contamination.

4.3 Preparation of Tris-Buffered Saline (TBS)

The TBS which was used for phage display work was prepared by mixing Tris-HCl (pH 7.5) stock solution (described in **3.4**) and NaCl stock solution (described in **3.5**) at the final concentrations of 50 mM and 150 mM, respectively, in 1 L of distilled water. The buffer was autoclaved at 121°C, 15 psi for 15 minutes. The sterilized buffer was kept as room temperature.

4.4 Preparation of Tris-Buffered Saline Supplemented with TWEEN-20 (TBST)

TBST, the detergent solution used for the washing steps during biopanning procedure and phage-ELISA, was prepared by adding TWEEN-20 to the TBS which was described earlier. The concentration of TWEEN-20 in the TBST corresponded to the cycle of biopanning. For the first round of biopanning, 0.1% (v/v) of TWEEN-20 was used for the preparation of TBST, where 1 mL of TWEEN-20 was mixed with 1 L of sterile TBS (pH 7.5). As the affinity selection in the subsequent rounds of biopanning aimed to select phage clones with higher binding specificity and affinity to the bacterial ligand, higher washing stringency was required to exclude any weak binders which were selected from the preceding rounds of biopanning. Therefore, the concentrations of TWEEN-20 in TBST were increased stepwise to 0.2%, 0.3% and 0.5% for the washing steps in the second, third and fourth round of biopanning, respectively. These were achieved by adding 2 mL, 3 mL and 5 mL of TWEEN-20 to the same volume of TBS.

4.5 Preparation of Coating Buffer

The coating buffer used in the biopanning and phage-ELISA was prepared by dissolving 0.84 g of $NaHCO_3$ (Bendosen Laboratory Chemicals, Malaysia) in 100 mL of distilled water. The pH of the solution was adjusted to 8.6 with 1M NaOH. The buffer was autoclaved at 121°C, 15 psi for 15 minutes. After sterilization, the buffer was kept in room temperature.

4.6   Preparation of Blocking Buffer

The blocking buffer which was used for phage-ELISA was prepared freshly according to the required volume by mixing 5 mg/ml bovine serum albumin (BSA) and 0.02% NaN_3 into 0.1 M $NaHCO_3$ (pH 8.6). The buffer was then filter-sterilized using a 0.2 μm nitrocellulose membrane filter into a sterile container, followed by storage at 4°C in the dark.

4.7   Preparation of Elution Buffer (Glycine-HCl)

The elution buffer which was used to separate the bound phage from the bacterial ligand as described in **Section 3.3.1** was prepared by dissolving 0.1501 g of glycine powder (Fisher Scientific, USA) in 10 mL of sterilized distilled water. The pH of the solution was adjusted to 2.2 with 1 M HCl. Then, the solution was added with 10 mg of bovine serum albumin (BSA) (Merck Milipore, Germany). After thorough mixing, the solution was filter-sterilized using a 0.22 μm pore filter. The filtered elution buffer was kept in 4°C.

4.8   Preparation of Neutralization Buffer

Neutralization buffer, which was used for neutralizing the eluted phages after biopanning (as described in **Section 3.3.1**), was prepared by dissolving 1.211 g of Tris (Bio Basic, Canada) in 10 mL of distilled water. Then, the pH of the solution was adjusted to 9.1 with 1 M NaOH. After that, the solution was autoclaved at 121°C, 15 psi for 15 minutes. The sterilized solution was kept in room temperature.

4.9   Preparation of Iodide Buffer

Iodide buffer was prepared freshly prior to use for phage DNA extraction, and the volume was prepared according to the need of the extraction. The preparation of this buffer involved the mixing of Tris-HCl (pH 8.0), EDTA and sodium iodide in which their final concentrations in the solution were 10 mM, 1 mM and 4 M, respectively.

APPENDIX C

LIST OF BACTERIA USED IN THIS STUDY

Bacterial species and strains	Relevant features
Pseudomonas aeruginosa ATCC 27853	Reference strain
Pseudomonas aeruginosa 1320026	C.I. CFZ^R
Pseudomonas aeruginosa 12594264	C.I. LVX^R MXF^R DOR^R ETP^R MEM^R CAZ^R CRO^R FEP^R (MDR)
Escherichia coli ATCC 25922	Reference strain
Escherichia coli 1160702	C.I. AMC^I CFZ^R CXM^R CTX^R CRO^R GEN^R CIP^R (ESBL)
Acinetobacter baumannii ATCC 19606	Reference strain
Acinetobacter junii 1191828	C.I. CFZ^R CRO^R CAZ^R
Klebsiella pneumoniae ATCC 138833	Reference strain
Klebsiella pneumoniae 1139142	C.I. AMP^R CFZ^R CXM^R CTX^R CAZ^R CRO^R ATM^R GEN^R CIP^R NIT^I SAM^I (ESBL)
Klebsiella pneumoniae 1208398	C.I. AMP^R AMC^R SAM^R TZP^R CFZ^R CXM^R FOX^R CTX^R CAZ^R CRO^R FEP^R ATM^R MEM^R AMK^R GEN^R CIP^R NIT^R (CRE)
Salmonella Typhi 1238912	C.I. CAZ^R CTX^R GEN^R
Shigella flexneri 1109563	C.I. CFX^R CFZ^R CXM^R AMK^R CIP^R
Serratia marcescens 1191741	C.I. AMX^R CFZ^R CXM^R FOX^R
Staphylococcus aureus ATCC 25923	Reference strain
Enterococcus faecalis ATCC 19433	Reference strain
Streptococcus pyogenes ATCC 19615	Reference strain
Streptococcus anginosus 1360589	C.I.

C.I.　　: Clinical isolate

CFZR　: resistance to cefazolin

LVXR　: resistance to levofloxacin

MXFR : resistance to moxifloxacin

DORR　: resistance to doripenem

PBR　　: resistance to polymyxin B

ETPR　: resistance to ertapenem

MEMR: resistance to meropenem

CAZR　: resistance to ceftazidime

CROR　: resistance to ceftriaxone

FEPR　: resistance to cefepime

MDR　: multi-drug resistance

AMCI　: reduced susceptibility to amoxicillin/clavulanic acid

CXMR: resistance to cefuroxime

CTXR : resistance to cefotaxime

GENR : resistance to gentamicin

CIPR　: resistance to ciprofloxacin

ATMR: resistance to aztreonam

NITI　: reduced susceptibility to nitrofurantoin

AMXR: resistance to amoxicillin

AMPR: resistance to ampicillin

SAMI　: reduced susceptibility to ampicillin/Sulbactam

TZPR　: resistance to piperacillin/Tazobactam

FOXR : resistance to cefoxitin

AMKR: resistance to amikacin

ESBL　: extended spectrum beta-lactamases

CRE　: Carbapenem-resistant Enterobacteriaceae

APPENDIX D

**GROSS VIEW OF BACTERIA INOCULATION AND TITER
CHANGES AFTER ANTIBACTERIAL ASSAY**
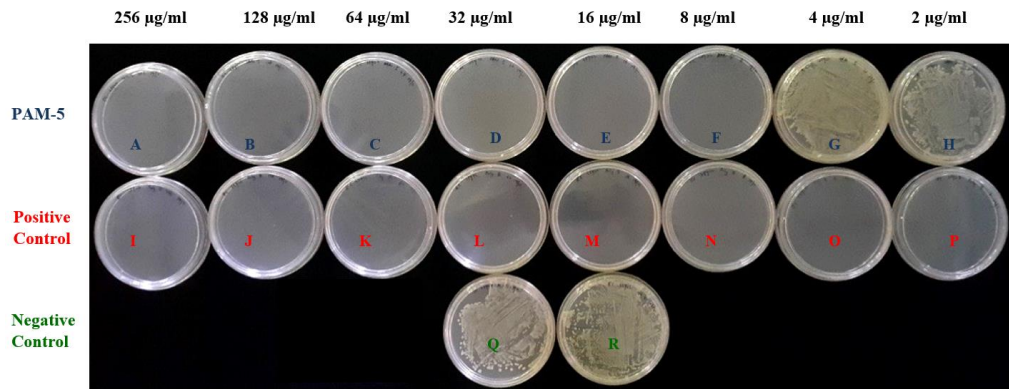
Figure I(a): Gross view of *E. coli* ATCC 25922 after PAM-5 treatment. The MBC of PAM-5 against *E. coli* ATCC 25922 was determined as 8 µg/ml as indicated by the absence of bacterial growth on Plate F. Plate I to Plate P served as the positive control plates while Plate Q and Plate R were the negative controls.
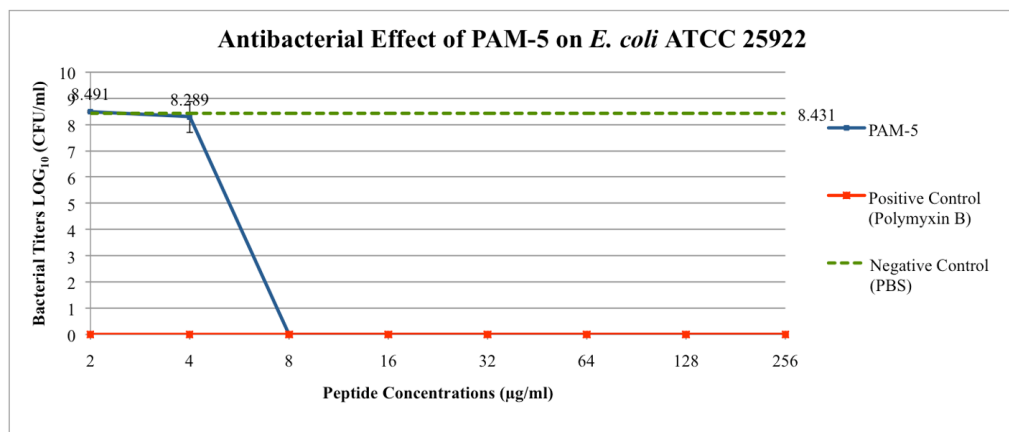
Figure I(b): Changes in titres of *E. coli* ATCC 25922 after treatment with different peptide concentrations. Bacteria were treated with different concentrations of PAM-5 and polymyxin B. Complete killing of bacteria was achieved by PAM-5 at concentrations of 8 µg/ml and above, while polymyxin B killed the bacterium at all tested concentrations. Untreated bacterium consistently grew heavily.
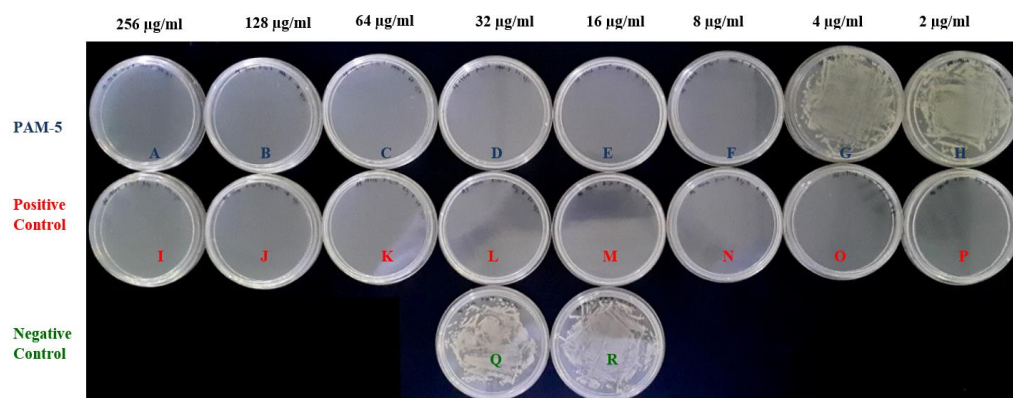
Figure II (a): Gross view of *A. baumannii* ATCC 19606 after PAM-5 treatment. Reference strain of *A. baumannii* was completely killed at PAM-5 concentrations of 8 µg/ml and above (Plate A to Plate F) where 8 µg/ml was determined as the peptide MBC. Plate I to Plate P served as the positive controls while Plate Q and Plate R were the negative controls.
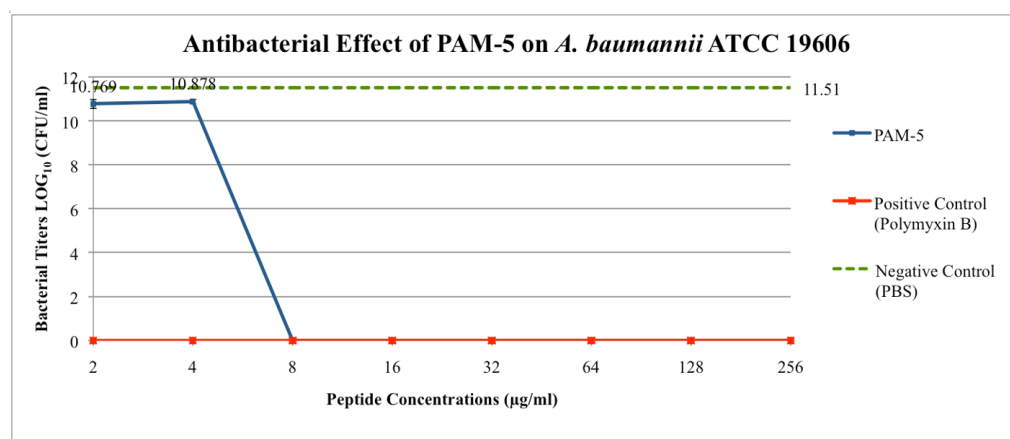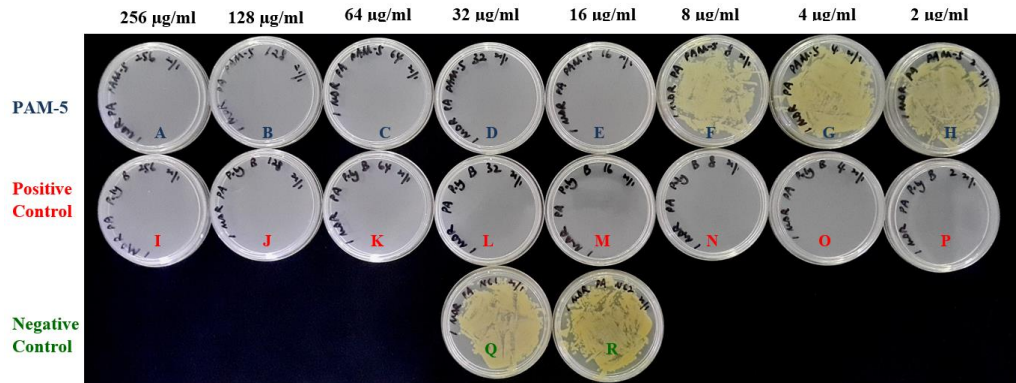

Figure II(b): Changes in titres of *A. baumannii* ATCC 19606 after treatment with different peptide concentrations. Bacteria were treated with different concentrations of PAM-5 and polymyxin B. Complete killing of bacteria was achieved by PAM-5 at concentrations of 8 µg/ml and above, while polymyxin B killed the bacterium at all tested concentrations. Untreated bacterium consistently grew heavily.
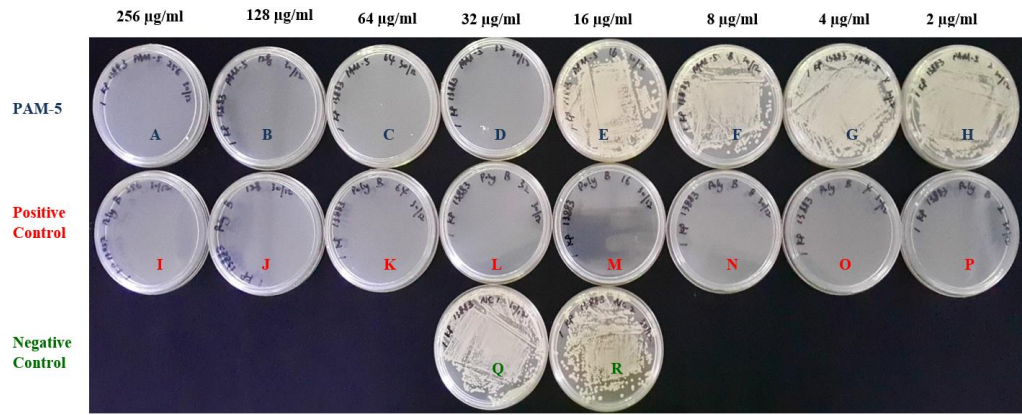
Figure III(a): Gross view of *K. pneumoniae* ATCC 138833 after treatment with PAM-5. Plate A to H were bacterial cultures treated with PAM-5 at concentrations ranging from 256 µg/ml to 2 µg/ml while Plate I to Plate P were culture treated with polymyxin B of the same concentrations as PAM-5. Plate Q and Plate R were the untreated cultures that served as the negative control.
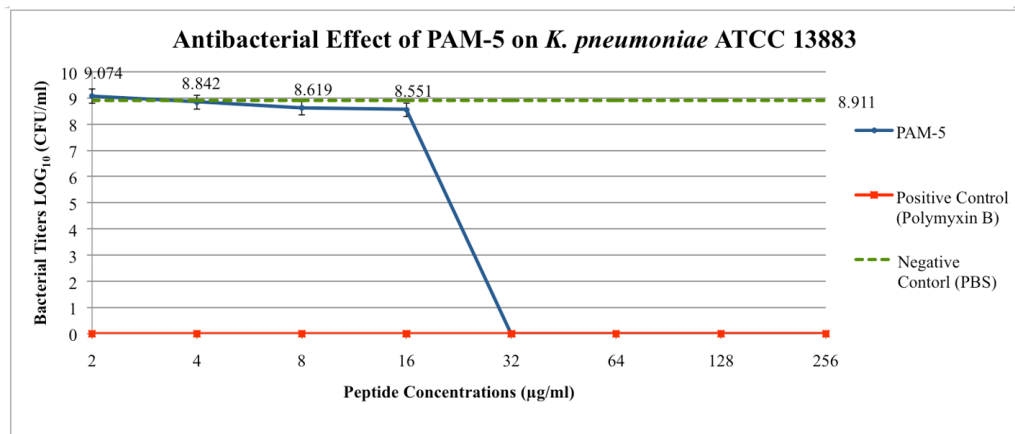
Figure III(b): Changes in titres of *K. pneumoniae* ATCC 13883 after treatment with different peptide concentrations. Bacteria were treated with different concentrations of PAM-5 and polymyxin B. Complete killing of bacteria was achieved by PAM-5 at concentrations of 32 µg/ml and above, while polymyxin B killed the bacterium at all tested concentrations. Untreated bacterium consistently grew heavily.
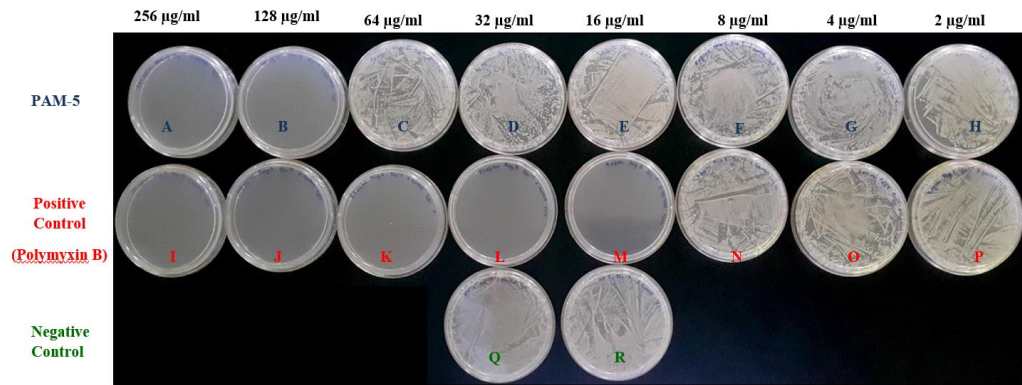
Figure IV(a): Gross view of *S. aureus* ATCC 25923 after PAM-5 treatment (Plate A to Plate H). A high MBC of 128 µg/ml was required for PAM-5 to be completely bactericidal against the reference strain of *S. aureus*. Bacterial growth was also observed on the plates inoculated with culture treated with the lowest three concentrations of polymyxin B (Plate N to Plate P). Plate Q and Plate R were the negative controls.
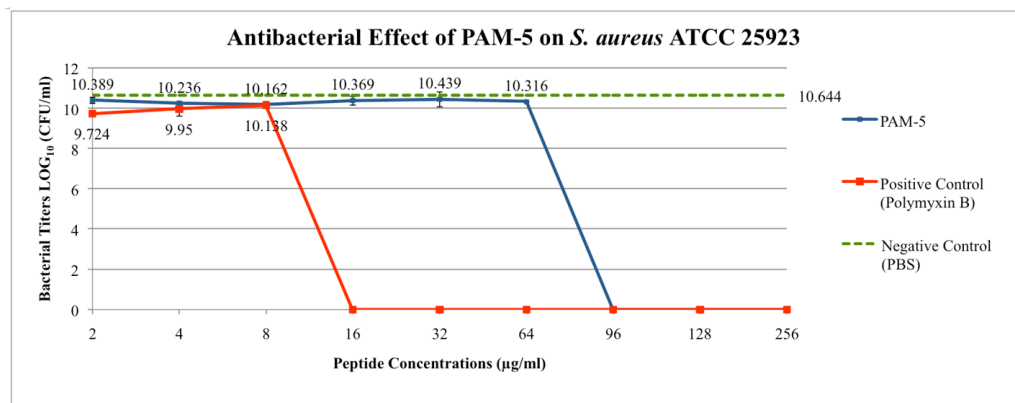
Figure IV(b): Changes in titres of *S. aureus* ATCC 25923 after treatment with different peptide concentrations. Bacteria were treated with different concentrations of PAM-5 and polymyxin B. Complete killing of bacteria was achieved by PAM-5 at concentrations of 96 µg/ml and above, while polymyxin B killed the bacterium at all tested concentrations. Untreated bacterium consistently grew heavily.
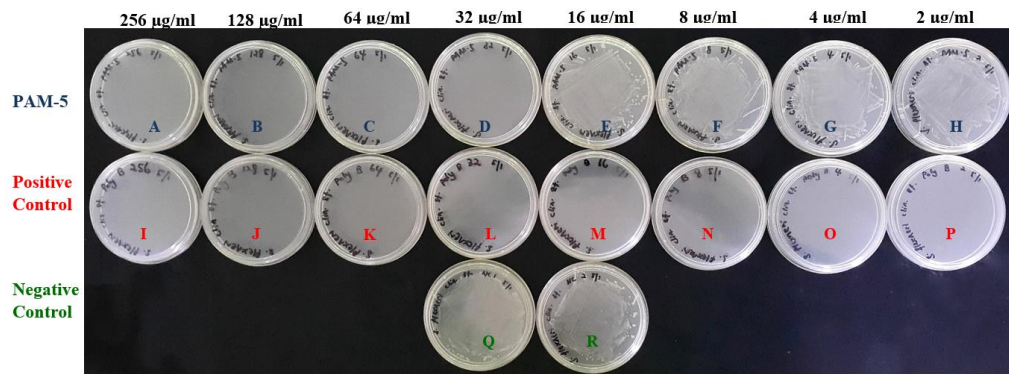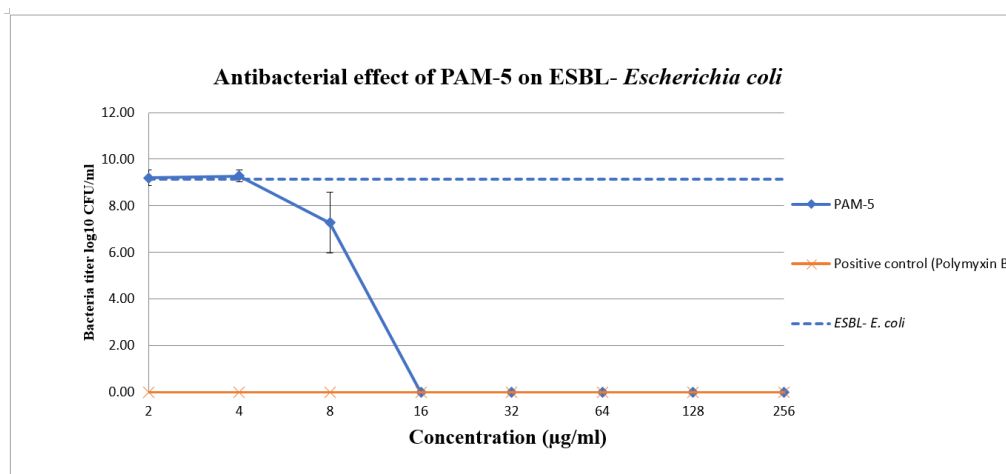
Figure V(a): Gross view of *S. flexneri* clinical isolate 1109563 after PAM-5 treatment. Plate A to Plate H were inoculated with bacterial cultures treated with different concentrations of PAM-5 while Plate I to Plate P were bacterial cultures treated with polymyxin B (positive control). Plate Q and Plate R served as the negative control. The MBC of PAM-5 against this clinical isolate was determined as 32 µg/ml.
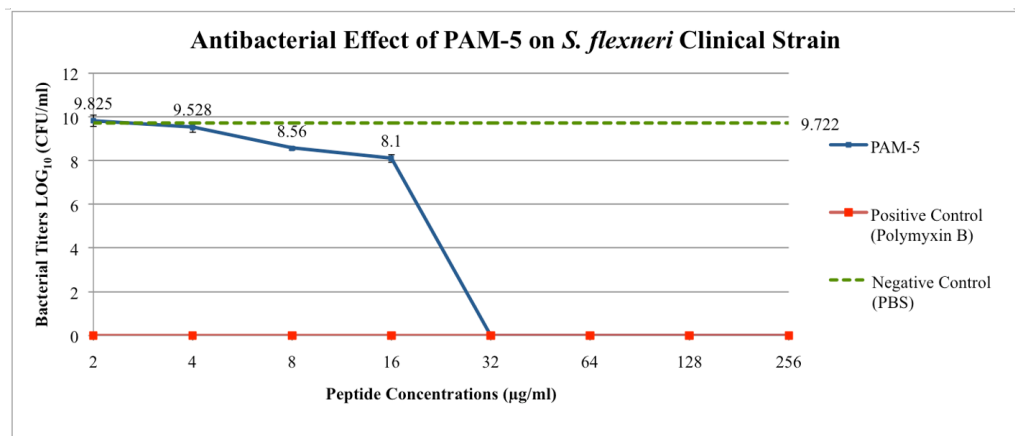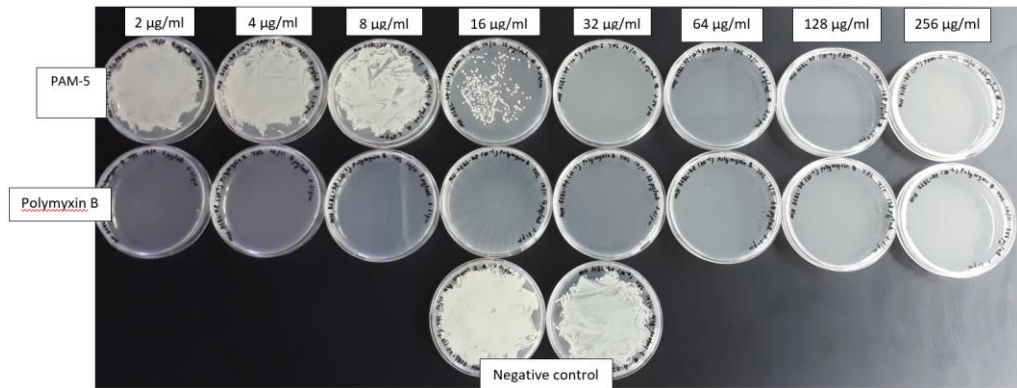

Figure V(b): Changes in titres of *S. flexneri* clinical isolate 1109563 after treatment with different peptide concentrations. Bacteria were treated with different concentrations of PAM-5 and polymyxin B. Complete killing of bacteria was achieved by PAM-5 at concentrations of 32 µg/ml and above, while polymyxin B killed the bacterium at all tested concentrations. Untreated bacterium consistently grew heavily.
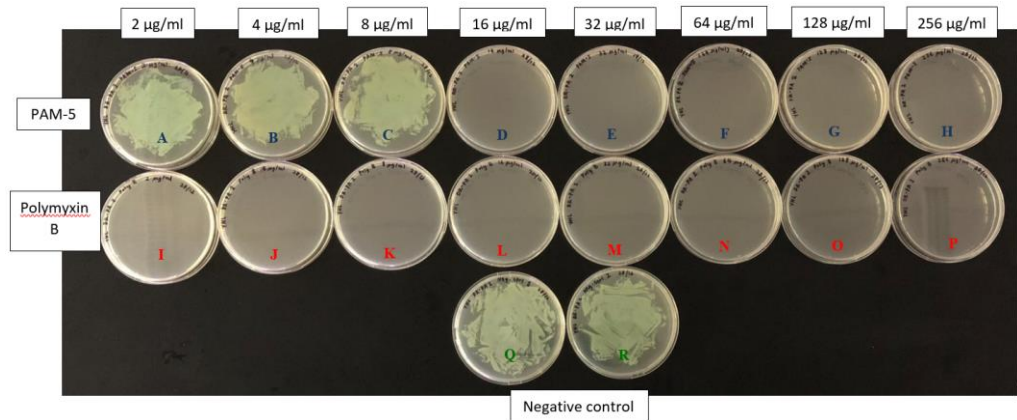
**Figure VI(a)**: Gross view of CFZ-resistant *P. aeruginosa* clinical isolate 1320026 after treatment. Plate A to Plate H were inoculated with bacterial cultures treated with different concentrations of PAM-5 while Plate I to Plate P were bacterial cultures treated with polymyxin B (positive control). Plate Q and Plate R served as the negative control. The MBC of PAM-5 against this clinical isolate was determined as 16 µg/ml.
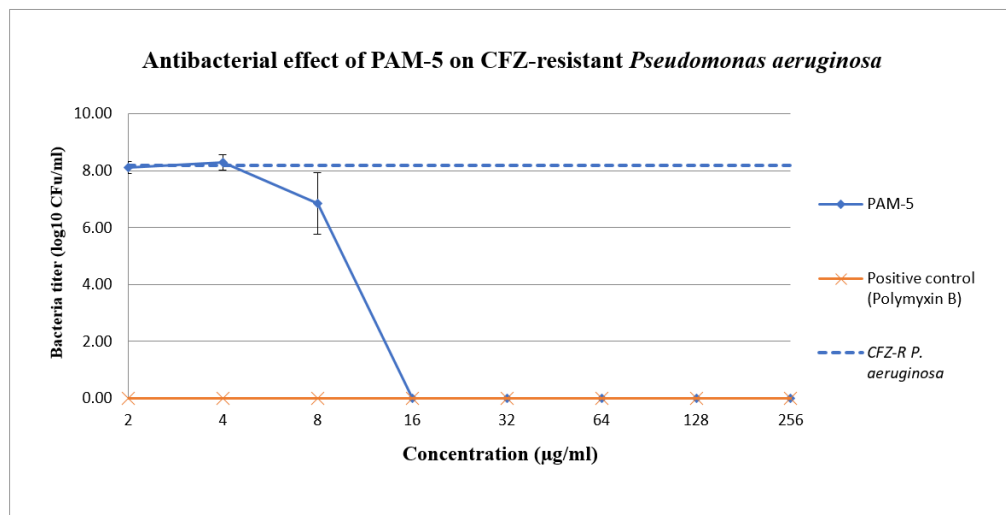
Figure VI(b): Changes in titres of CFZ-resistant *P. aeruginosa* clinical isolate 1320026 after treatment with different peptide concentrations. Bacteria were treated with different concentrations of PAM-5 and polymyxin B. Complete killing of bacteria was achieved by PAM-5 at concentrations of 16 µg/ml and above, while polymyxin B killed the bacterium at all tested concentrations. Untreated bacterium consistently grew heavily.

Figure VII(a): Gross view of MDR *P. aeruginosa* clinical isolate 12594264 after PAM-5 treatment. Plate A to Plate H were cultures treated with two-fold serially diluted PAM-5 while Plate I to Plate P were cultures treated with Polymyxin B of the same serial dilutions that served as the positive control. Plate Q and Plate R were the negative control plates. The MBC of PAM-5 against this multidrug-resistant strain was 16 µg/ml.
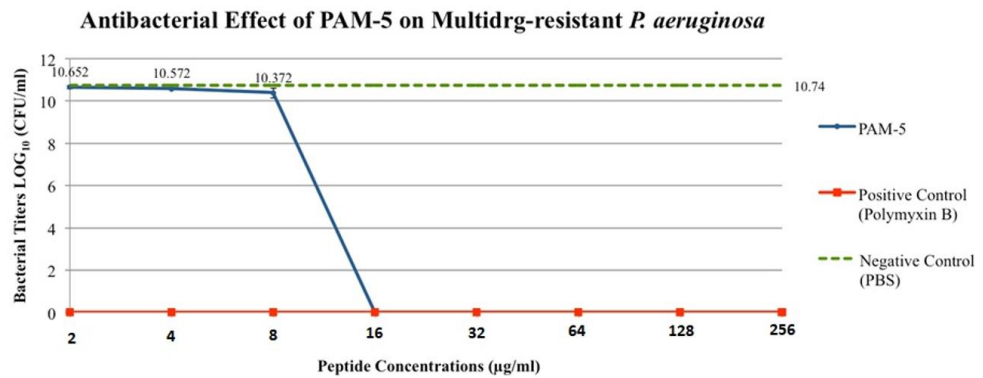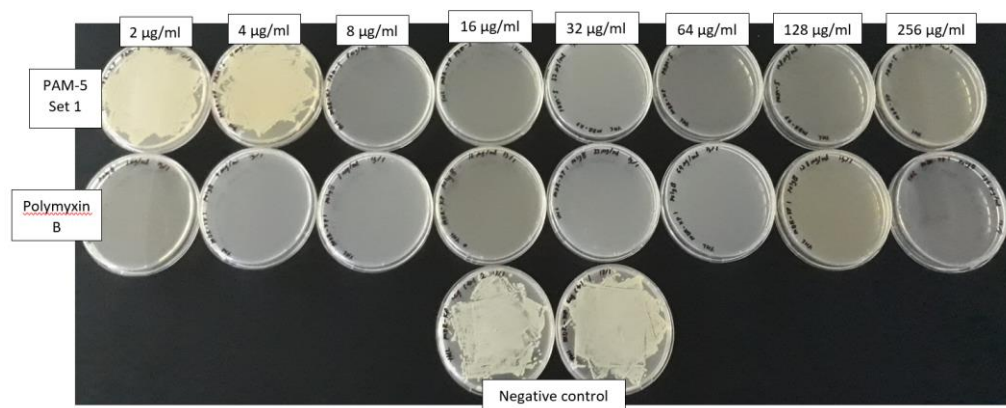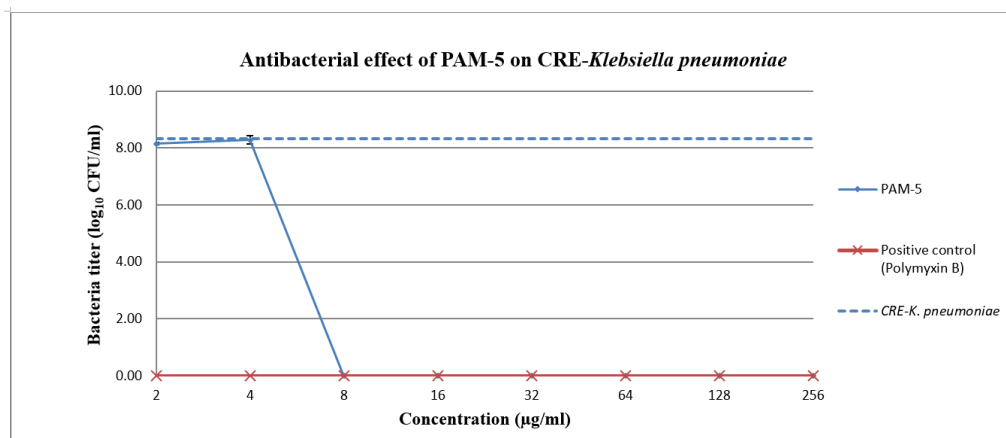

Figure VII(b): Changes in titres of MDR *P. aeruginosa* clinical isolate 12594264 after treatment with different peptide concentrations. Bacteria were treated with different concentrations of PAM-5 and polymyxin B. Complete killing of bacteria was achieved by PAM-5 at concentrations of 16 µg/ml and above, while polymyxin B killed the bacterium at all tested concentrations. Untreated bacterium consistently grew heavily.
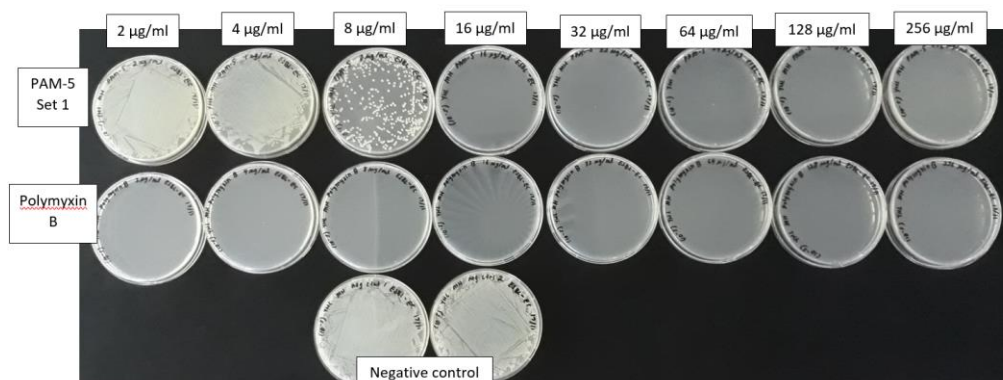
Figure VIII (a): Gross view of ESBL-producing *E. coli* clinical isolate 1160702 after PAM-5 treatment. Plate A to Plate H were cultures treated with two-fold serially diluted PAM-5 while Plate I to Plate P were cultures treated with Polymyxin B of the same serial dilutions that served as the positive control. Plate Q and Plate R were the negative control plates. The MBC of PAM-5 against this multidrug-resistant strain was 16 µg/ml.
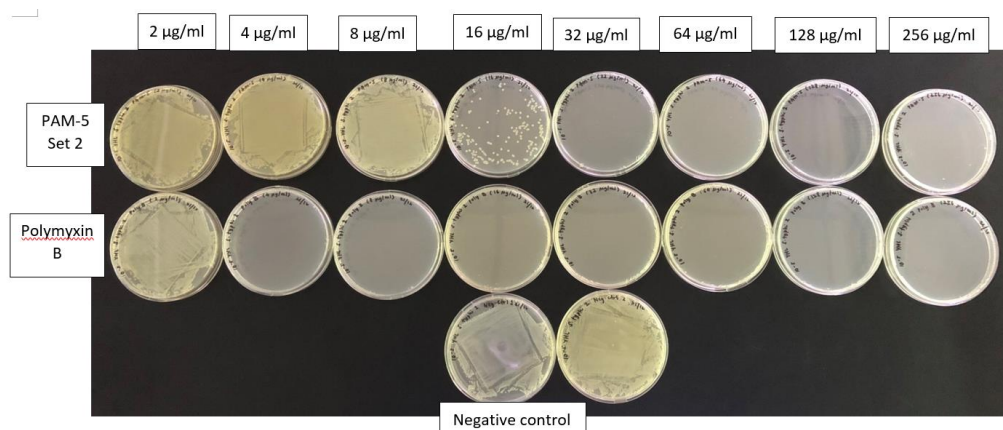

Figure VIII(b): Changes in titres of ESBL-producing *E. coli* clinical isolate 1160702 after treatment with different peptide concentrations. Bacteria were treated with different concentrations of PAM-5 and polymyxin B. Complete killing of bacteria was achieved by PAM-5 at concentrations of 16 µg/ml and above, while polymyxin B killed the bacterium at all tested concentrations. Untreated bacterium consistently grew heavily.
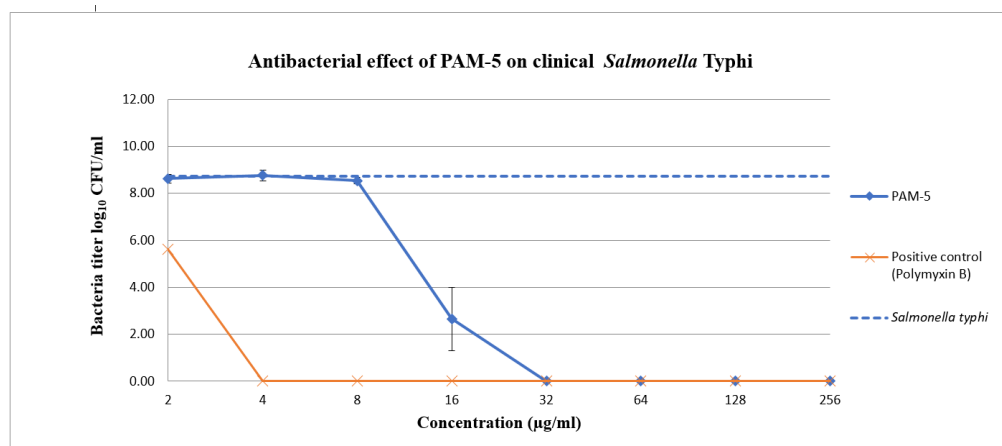
Figure IX (a): Gross view of ESBL-producing *K. pneumoniae* clinical isolate 1139142 after PAM-5 treatment. Plate A to Plate H were cultures treated with two-fold serially diluted PAM-5 while Plate I to Plate P were cultures treated with polymyxin B of the same serial dilutions that served as the positive control. Plate Q and Plate R were the negative control plates. The MBC of PAM-5 against this multidrug-resistant strain was 32 µg/ml.
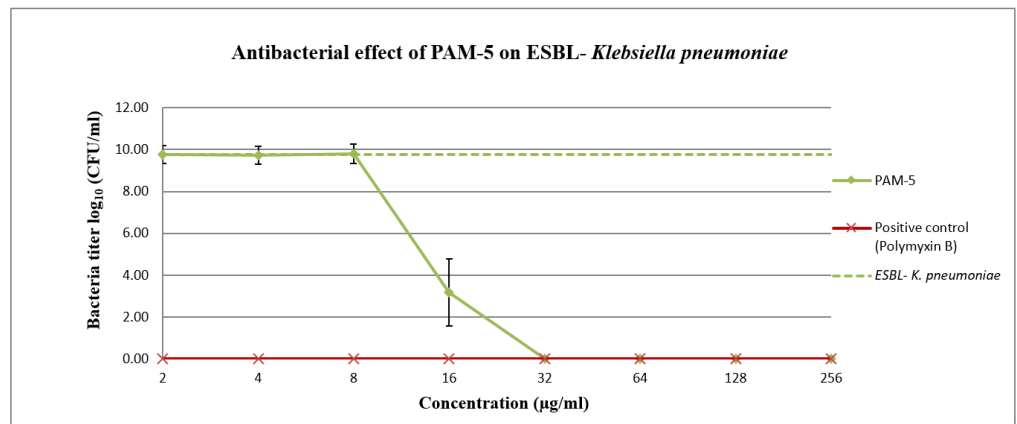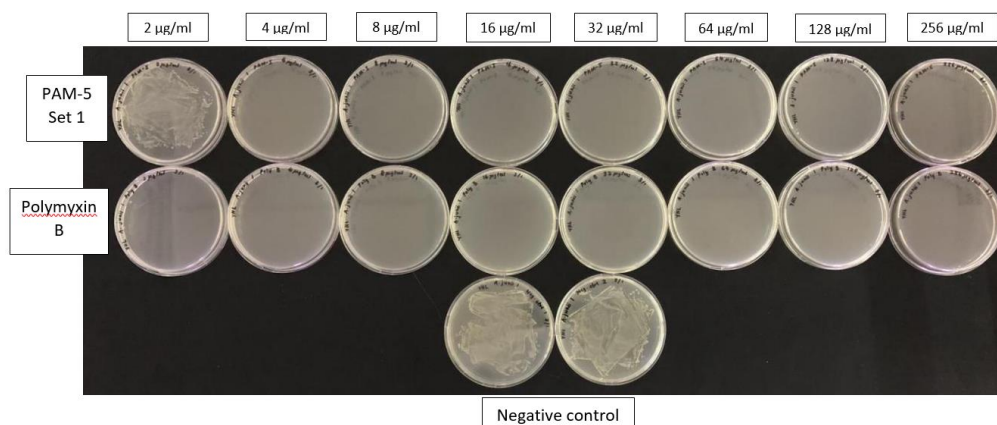

Figure IX(b): Changes in titres of ESBL-producing *K. pneumoniae* clinical isolate 1139142 after treatment with different peptide concentrations. Bacteria were treated with different concentrations of PAM-5 and polymyxin B. Complete killing of bacteria was achieved by PAM-5 at concentrations of 32 µg/ml and above, while polymyxin B killed the bacterium at all tested concentrations. Untreated bacterium consistently grew heavily.

Figure X(a): Gross view of carbapenem-resistant *K. pneumoniae* clinical isolate 1208398 after treatment with PAM-5. Plate A to Plate H were cultures treated with two-fold serially diluted PAM-5 while Plate I to Plate P were cultures treated with polymyxin B of the same serial dilutions that served as the positive control. Plate Q and Plate R were the negative control plates. The MBC of PAM-5 against this multidrug-resistant strain was 8 µg/ml.

Figure X(b): Changes in titres of carbapenem-resistant *K. pneumoniae* clinical isolate 1208398 after treatment with different peptide concentrations. Bacteria were treated with different concentrations of PAM-5 and polymyxin B. Complete killing of bacteria was achieved by PAM-5 at concentrations of 8 µg/ml and above, while polymyxin B killed the bacterium at all tested concentrations. Untreated bacterium consistently grew heavily.

Figure XI(a): Gross view of *S*. Typhi clinical isolate 1238912 after treatment with PAM-5 for one of the first two antibacterial assays. Plate A to Plate H were cultures treated with two-fold serially diluted PAM-5 while Plate I to Plate P were cultures treated with polymyxin B of the same serial dilutions that served as the positive control. Plate Q and Plate R were the negative control plates. The MBCs of PAM-5 against *S*. Typhi in these first two assays were 32 µg/ml.

Figure XI(b): Changes in titres of *S*. Typhi clinical isolate 1238912 after treatment with different peptide concentrations. Bacteria were treated with different concentrations of PAM-5 and polymyxin B. Complete killing of bacteria was achieved by PAM-5 at concentrations of 32 µg/ml and above, while polymyxin B killed the bacterium at all tested concentrations. Untreated bacterium consistently grew heavily.

Figure XII(a): Gross view of cefazolin -, ceftriaxone- and ceftazidime-resistant *A. junii* clinical isolate 1191828 after treatment with PAM-5. Plate A to Plate H were cultures treated with two-fold serially diluted PAM-5 while Plate I to Plate P were cultures treated with polymyxin B of the same serial dilutions that served as the positive control. Plate Q and Plate R were the negative control plates. The MBC of PAM-5 against this drug-resistant bacterium was 4 µg/ml.
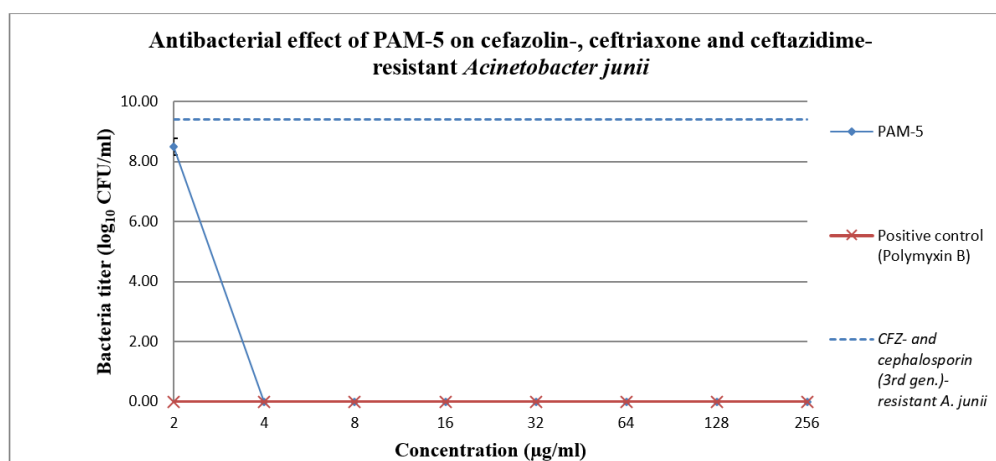
Figure XII(b): Changes in titres of cefazolin -, ceftriaxone- and ceftazidime-resistant *A. junii* clinical isolate 1191828 after treatment with different peptide concentrations. Bacteria were treated with different concentrations of PAM-5 and polymyxin B. Complete killing of bacteria was achieved by PAM-5 at concentrations of 4 µg/ml and above, while polymyxin B killed the bacterium at all tested concentrations. Untreated bacterium consistently grew heavily.
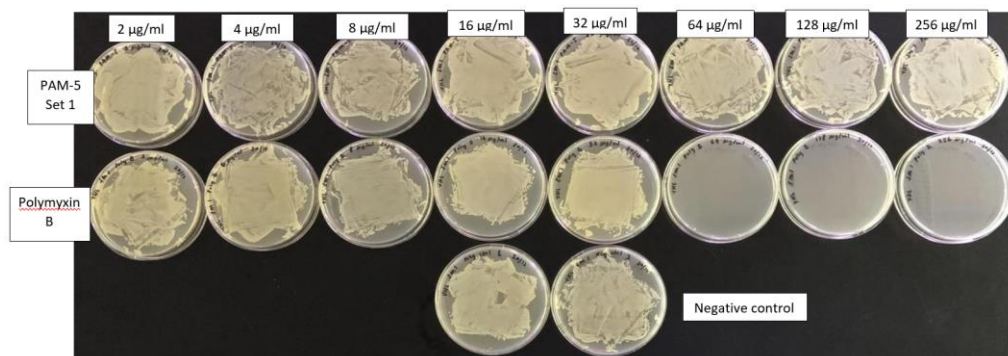
Figure XIII(a): Gross view of amoxicillin-, cefazolin-, cefuroxime- and cefoxitin-resistant *Serratia marcescens* clinical isolate 1191741 after treatment with PAM-5. Plate A to Plate H were cultures treated with two-fold serially diluted PAM-5 while Plate I to Plate P were cultures treated with polymyxin B of the same serial dilutions that served as the positive control. Plate Q and Plate R were the negative control plates. PAM-5 failed to kill the bacteria at all tested concentrations.
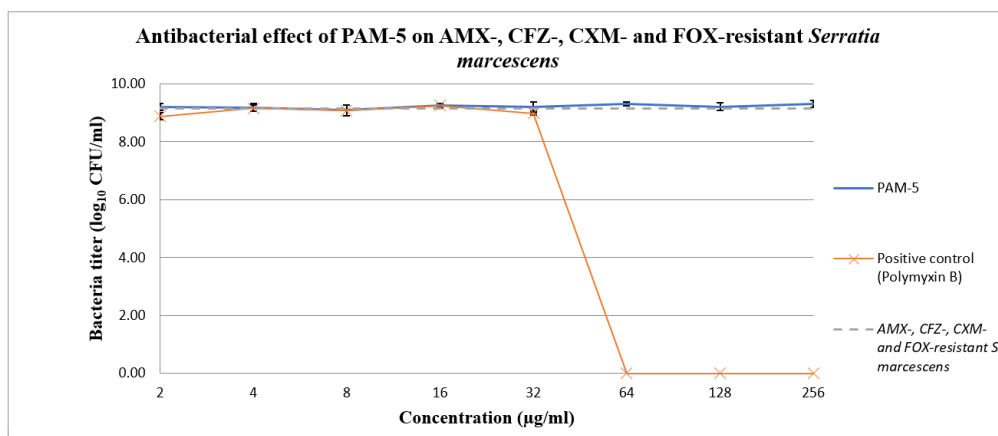

Figure XIII(b): Changes in titres of amoxicillin-, cefazolin-, cefuroxime- and cefoxitin-resistant *Serratia marcescens* clinical isolate 1191741 after treatment with different peptide concentrations. Bacteria were treated with different concentrations of PAM-5 and polymyxin B. After three independent assays, PAM-5 was found not active against this resistant bacterium at all tested concentrations. In addition, polymyxin B only killed the bacteria completely at 64 µg/ml and other higher concentrations.
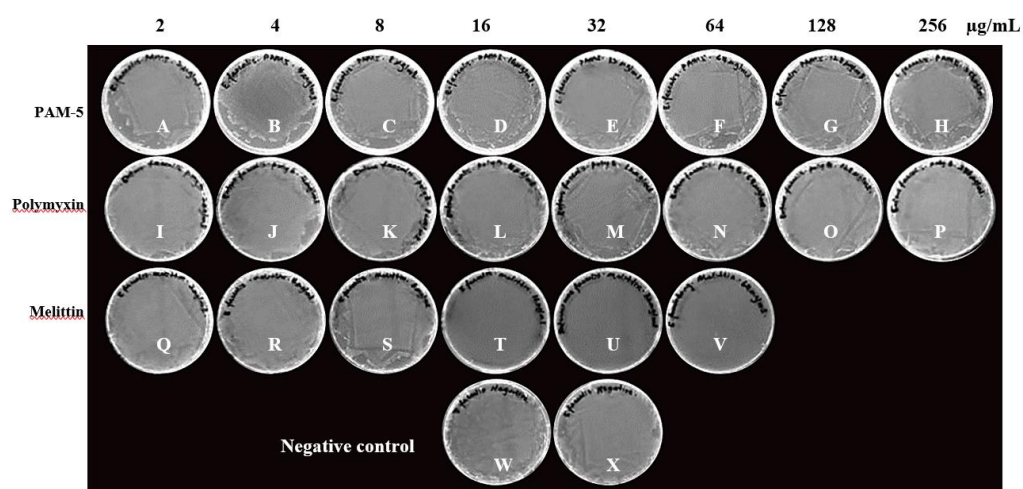
Figure XIV(a): Gross view on the culture agar inoculated with *E. faecalis* ATCC 19433 after treatment with PAM-5 (first row Plate A to Plate H), polymyxin B (second row Plate I to Plate P) and melittin (third row Plate Q to Plate V) at increasing concentrations from left to right. Plate W and X were inoculated with untreated bacteria which served as the negative control. Both MBCs of PAM-5 and polymyxin B against *E. faecalis* were > 256 µg/mL, while MBC for melittin was determined as 16 µg/mL.
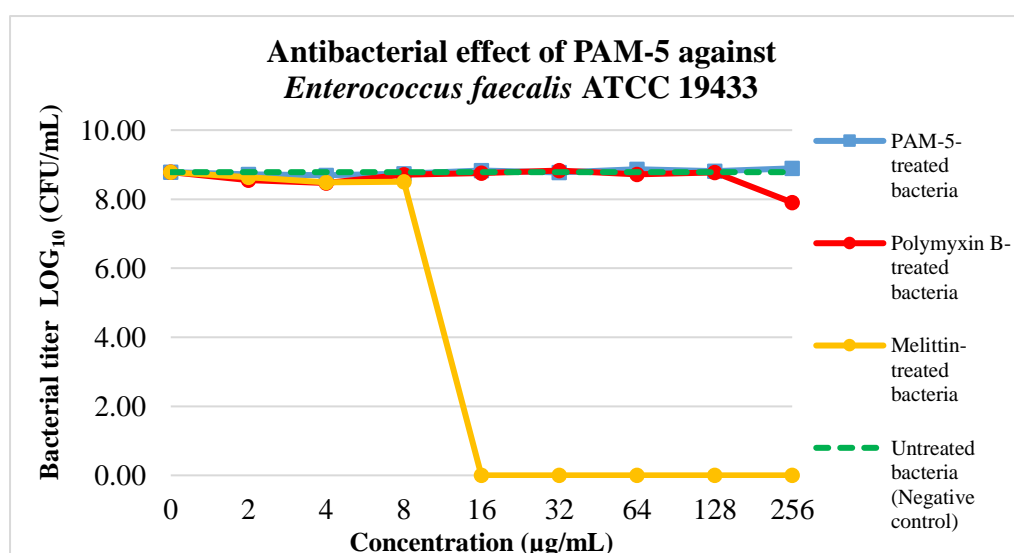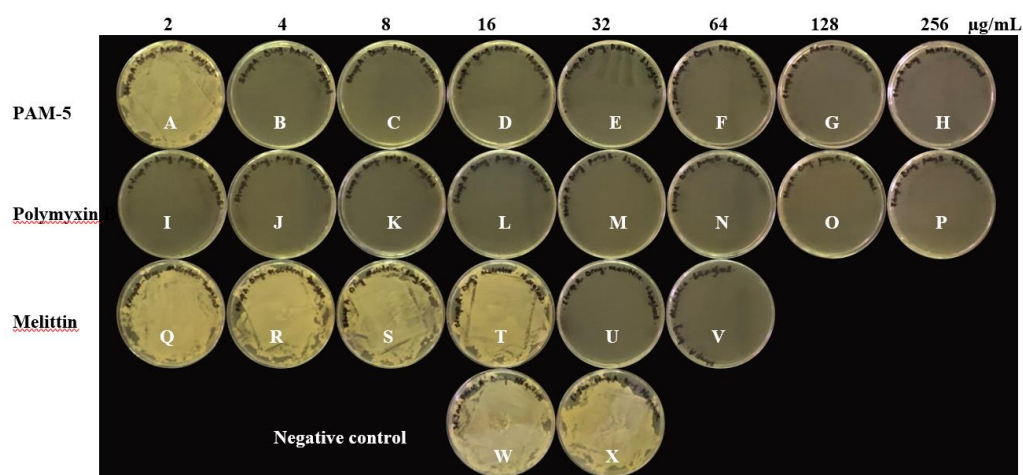

Figure XIV(b): Degree of bacterial viability after treatment with PAM-5, polymyxin B and melittin. *Enterococcus faecalis* ATCC 19433 was incubated with increasing concentrations of ABPs followed by inoculation on media for titre determination. Untreated bacteria were set up as the negative control. The MBC for melittin against *E. faecalis* was 16 µg/mL while PAM-5 and polymyxin B were not active against this bacterium.

333
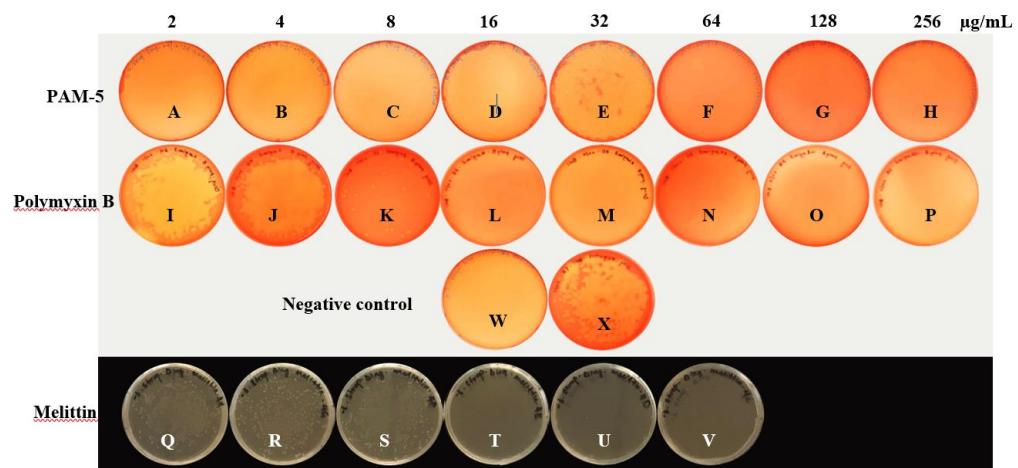
Figure XV(a): Gross view on the culture agar inoculated with *S. pyogenes* ATCC 19615. Plate A to H were inoculated with PAM-5-treated bacteria, Plate I to P were inoculated with polymyxin B-treated bacteria, while Plate Q to Plate V were inoculated with melittin-treated bacteria. The bacteria were treated with increasing concentrations of peptide from left to right (2 µg/mL to 256 µg/mL) for PAM-5 and polymyxin B. The concentrations of melittin used for the treatment range from 2 µg/mL to 64 µg/mL. Plate W and X are negative control inoculated with untreated bacteria. MBCs of PAM-5, polymyxin B and melittin against *S. pyogenes* were determined as 64 µg/mL, 8 µg/mL and 16 µg/mL, respectively.
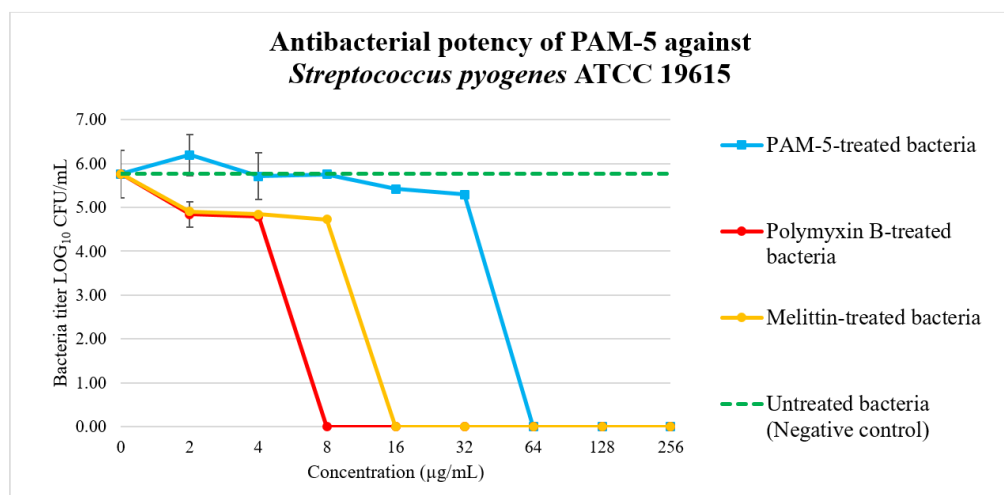
Figure XV(b): Degree of bacterial viability after treatment with PAM-5, polymyxin B and melittin. *Streptococcus pyogenes* ATCC 19615 was incubated with increasing concentrations of ABPs followed by inoculation on media for titre determination. Untreated bacteria were set up as negative control. The MBCs for PAM-5, polymyxin B and melittin against *E. faecalis* were 64 µg/mL, 16 µg/mL and 8 µg/mL, respectively.

Figure XVI(a): Culture agar inoculated with *S. anginosus* clinical isolate 1360589 after treatment with different ABPs of different concentrations. The bacteria were treated with 2-fold increasing concentrations of the ABPs. Plate A to H were inoculated with PAM-5-treated bacteria, Plate I to P were inoculated with polymyxin B-treated bacteria, whereas Plate Q to V were inoculated with melittin-treated bacteria. Plate W and X are negative control inoculated with untreated bacteria. MBC of PAM-5, polymyxin B and melittin were determined as 4 µg/mL, ≤ 2 µg/mL and 32 µg/mL, respectively.
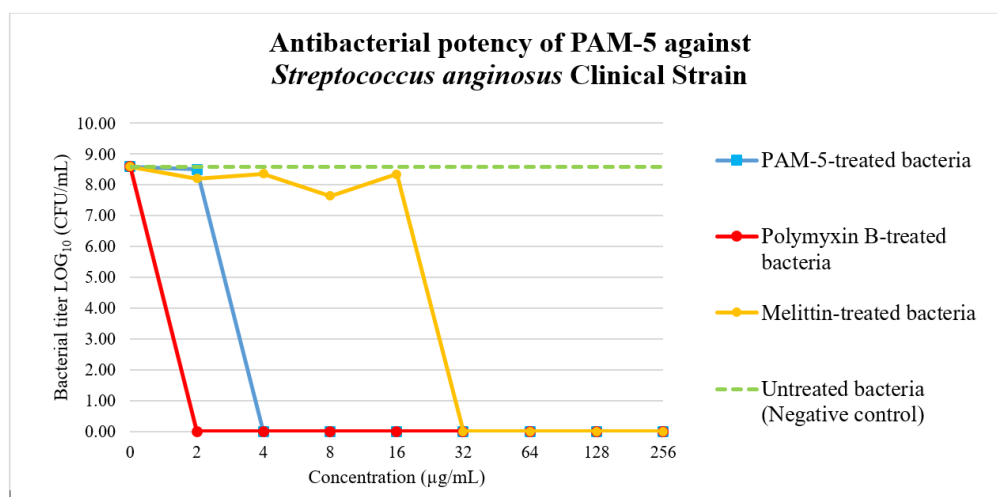
Figure XVI(b): Degree of bacterial viability after treatment with PAM-5, polymyxin B and melittin. *Streptococcus anginosus* clinical isolate 1360589 was incubated with increasing concentrations of ABPs followed by inoculation on media for titre determination. Untreated bacteria were set up as the negative control. The MBC for PAM-5, polymyxin B and melittin against E. faecalis were 4 µg/mL, ≤ 2 µg/mL and 32 µg/mL, respectively.